The Development of Bovine Fetal Ovary and Its Relationship with Reproductive Disease

Monica Dwi Hartanti

A thesis submitted in the fulfilment of
the requirement of a Doctor of Philosophy

Faculty of Health Sciences
School of Medicine
The University of Adelaide
Australia

October 2019

Table of Contents

List of Figures

Page

Chapter V

List of Tables

Chapter V

Abstract

The development of fetal ovary is a complex process involving the communication between primordial germ cells (PGCs), Gonadal Ridge Epithelial-Like (GREL) cells and stroma. Many studies in ovarian development have focused on follicles, making other features, such as stroma and ovarian surface the least studied. Additionally, perturbation of ovarian development has been suggested to lead to many reproductive diseases, such as Polycystic Ovary Syndrome (PCOS) and ovarian cancer. Studies have shown that prenatally androgenised female mammals had ovaries with PCOS features, such as small follicles and increased ovarian stromal volume. Similarly, ovarian cancer has been suggested to be able to arise from non-ovarian tissue, such as fallopian tubes and endometrium. This thesis discussed the changes of ovarian stroma (chapter II) and linked the changes to PCOS (chapter III). Furthermore, this thesis quantitated changes of non-stromal areas containing GREL cells and follicles (chapter IV) as well as identified the changes in ovarian surface during fetal development (chapter V).

Early in ovarian development, the surface epithelium of the mesonephros differentiates into GREL cells and proliferates, forming the ovarian primordium into which PGCs migrate. The stroma from the mesonephros penetrates the developing ovary and then branches. At this time, a true surface epithelium is located only at the base of the developing ovary. When the stroma reaches just underneath the surface of the developing ovary, it spreads laterally. The branching and spreading of the stroma encloses some GREL cells and PGCs into ovigerous cords. At this point, the ovigerous cords are still open to the ovarian surface. The stroma keeps on spreading, dividing the ovigerous cords into smaller units and eventually into primordial follicles. GREL cells located on the ovarian surface then start to differentiate into surface epithelium. At the last stage of development, a single layer of surface epithelium is formed and the stroma underneath the surface epithelium changes its phenotype into tunica albuginea, a collagen rich layer.

In this thesis, I analysed the stromal and non-stromal areas morphometrically and linked ovarian development with expression of a number of extracellular matrix genes. My results show that the volume of the ovarian cortex and medulla increased throughout gestation. The stromal proportion and total volume in the cortex were significantly increased ($p>0.05$), whereas the proliferation index and numerical density of proliferating cells in the

stroma decreased significantly ($p>0.05$). There was no change in numerical density of stromal cells in the cortex. Twelve extracellular matrix genes were highly expressed later in the development and positively correlated with each other and with gestational age. The total volume of non-stromal areas in the ovarian cortex significantly increased and then levelled off. The proportion of non-stromal areas in the cortex decreased significantly. The proliferation index of the non-stromal area peaked in early gestation and then decreased significantly and then remained low. The numerical density of the stromal area remained constant throughout ovarian development. My morphometric data of the stromal area as well as the gene expression have been published in Reproduction Fertility and Development. The data of the non-stromal area have been combined with other data and published in PLoS ONE.

Since many reproductive diseases might have a fetal origin, we studied the linkage between fetal ovarian development and PCOS. Recent studies have recognised 18 PCOS candidate genes identified by genome wide associated study (GWAS) analyses. Using qRT-PCR, I analysed the expression of these genes, as well as three other genes (androgen receptor *(AR)*, Transforming Growth Factor Beta 1 induced transcript 1 *(TGFB1I1)*, fibrillin3 *(FBN3)*) in the bovine fetal ovaries across gestation. To assess the regulation of these genes in the bovine fetal ovary, I analysed the expression of these genes in bovine fetal fibroblasts which had been treated with cAMP regulators, growth factors and hormones in vitro (24 treatments in total) during a previous honour project. *FBN3*, *GATA4*, *HMGA2*, *TOX3*, *DENND1A* and *LHCGR* were highly expressed in the early development, whereas *INSR*, *FSHR* and *LHCGR*, including 3 PCOS-related genes *(AMH*, *AR* and *TGFB1I1)* were highly expressed in the late development. These eleven genes were strongly correlated to each other, although some of them expressed in different cell types. Treatment of fetal stromal cells with TGFβ induced the expression of *INSR*, *AR*, *C8H9orf3* and *RAD50* and inhibited expression of *TGFB1I1*. The data have been submitted to Scientific Reports.

In the attempt of investigating the changes of ovarian surface, I analysed Scanning Electron Microscope (SEM) images and compared them with immunohistochemistry images, as well as determined the proportions of different types of cells in the ovarian surface epithelium. Early in development, the cells at the base of the developing ovary were cuboidal whereas the remaining surface appeared more irregular. Around 10 weeks of gestation until 5 months of gestation, the surface was covered by a stratified or simple epithelium of cuboidal cells. During mid-gestation clefts could be observed on the surface coinciding below with open ovigerous cords. Later in development, most of the ovary was covered by a simple surface epithelium. There appear to be two origins of ovarian surface epithelium – at the

base/hilum originating from the mesonephros and on the remainder from the GREL cells.. The data have been submitted to Journal of Histology and Cytochemistry.

Together, this work has shown the behavioural and structural changes of stroma and ovarian surface during fetal development. Since some of the PCOS candidate genes are expressed during fetal ovarian development, any potential disruption during ovarian development might have implications for the development of PCOS phenotype in the adult life.

Thesis Declaration

I certify that this work contains no material which has been accepted for the award of any other degree or diploma in my name, in any university or other tertiary institution and, to the best of my knowledge and belief, contains no material previously published or written by another person, except where due reference has been made in the text. In addition, I certify that no part of this work will, in the future, be used in a submission in my name, for any other degree or diploma in any university or other tertiary institution without the prior approval of the University of Adelaide and where applicable, any partner institution responsible for the joint-award of this degree.

I acknowledge that copyright of published works contained within this thesis resides with the copyright holder(s) of those works.

I also give permission for the digital version of my thesis to be made available on the web, via the University's digital research repository, the Library Search and also through web search engines, unless permission has been granted by the University to restrict access for a period of time.

25/06/2019

_____

Monica Dwi Hartanti Date

Acknowledgement

I would like to thank all who contributed in the completion of this thesis. First, I give thanks to God for everything that He has given me and always be by my side throughout my life. My sincere gratitude to my principal supervisor Prof. Raymond J. Rodgers and co-supervisors Dr. Katja Hummitzsch and Dr. Helen Irving-Rodgers, Ms Wendy Bonner and Mr. Nicholas Hatzirodos, who have supported me throughout my PhD studies with patience, motivation, enthusiasm, and knowledge. Your guidance helped me in all the time of research and writing of this thesis.

My sincere thanks also goes to Prof Richard Anderson and Dr. Roseanne, who provided me an opportunity to collaborate with their team in PCOS study. Without their precious support it would not be possible to achieve this PCOS manuscript.

For my friends in Adelaide (Thao, Qianhui, Jean, Zoe, Tannith, Jasmine, Kathryn, Fr. Anthoni, Sr. Sheela, Ritu, Hectorville Parish Choir), I am so grateful to have you all. Special thanks to Ms Nicole Bastian for helping me making this thesis possible. Your assistance, friendship and company made my stay in Adelaide enjoyable and memorable.

I thank my friends at Trisakti University, Indonesia; Suriyani and Rina K Kusumaratna, for their endless support, help and friendships.

I would like to acknowledge the Australia Awards for their financial support and Robinson Research Institute, The University of Adelaide for allowing me studying there, as well as Adelaide Microscopy, especially Ms Ruth Williams and Ms Lisa O'Donovan, for their guidance and supports.

Last but not least, I also thank my husband, my children, especially my dad back in Indonesia, who encouraged me and prayed for me throughout the time of my research. For my mum in Heaven, thank you for watching over me and my family. This thesis is especially for papa and mama. May the Almighty God richly bless you all.

List of Publication

Published:

1. Morphometric and gene expression analyses of stromal expansion during development of the bovine fetal ovary; **M. D. Hartanti**, K. Hummitzsch, H. F. Irving-Rodgers, W. M. Bonner, K. J. Copping, R. A. Anderson, I. C. McMillen, V. E. A. Perry and R. J. Rodgers; *Reproduction, Fertility and Development*; 2019, 31(3), 482-295. doi: 10.1071/RD18218.

2. Morphometric analyses and gene expression related to germ cells, gonodal ridge epithelial-like cells and granulosa cells during development of the bovine fetal ovary; Hummitzsch K, Hatzirodos N, Irving-Rodgers HF, **Hartanti MD**, Perry VEA, Anderson RA, Rodgers RJ.; PLoS One; 2019, 14(3):e0214130. doi: 10.1371/journal.pone.0214130.

3. Regulation of fibrillins and modulators of TGFB in fetal bovine and human ovaries; Bastian NA, Bayne RA, Hummitzsch K, Hatzirodos N, Bonner WM, **Hartanti MD**, Irving-Rodgers HF, Anderson RA, Rodgers RJ; *Reproduction*, 2016, 52(2):127-37. doi: 10.1530/REP-16-0172.

Submitted:

1. Could polysyctic ovary syndrome in women be due to perturbed fetal development of the ovary?; **Monica D Hartanti**, Roseanne Rosario, Katja Hummitzsch, Nicole A Bastian, Nicholas Hatzirodos, Wendy M Bonner, Rosemary A Bayne, Helen F Irving-Rodgers, Richard A Anderson and Raymond J Rodgers (Scientific Report)
2. Ultrastructural changes of ovarian surface during fetal bovine development; **Monica D. Hartanti**, Katja Hummitzsch, Helen F. Irving-Rodgers, Wendy M. Bonner, Nicola A. Bastian and Raymond J. Rodgers (Journal of Histochemistry and Cytochemistry)

Poster presentations

1. Stromal development in bovine fetal ovary; **Monica D Hartanti**, Katja Hummitzsch, Helen F Irving-Rodgers, Wendy M Bonner, Viv E A Perry, Raymond J Rodgers; Society for Reproductive Biology Annual Scientific Conference 2016
2. Development of the stroma of the bovine fetal ovary; **Monica D Hartanti**, Katja Hummitzsch, Helen F Irving-Rodgers, Wendy M Bonner, Viv E A Perry, Raymond J Rodgers; Androgen Excessive and PCOS Society Annual Meeting 2016
3. Stromal development of the bovine fetal ovary; **Monica D Hartanti**, Katja Hummitzsch, Helen F Irving-Rodgers, Wendy M Bonner, Viv E A Perry, Raymond J Rodgers; Florey Conference 2016
4. Stromal development in bovine fetal ovary: a morphometric analysis; **Monica D Hartanti**, Katja Hummitzsch, Helen F Irving-Rodgers, Wendy M Bonner, Viv E A Perry, Raymond J Rodgers; Robinson Research Institute Symposium 2016
5. Potential linkage between ovarian development and PCOS; **Monica D Hartanti**, Katja Hummitzsch, Helen F Irving-Rodgers, Raymond J Rodgers; Robinson Research Institute Symposium 2017
6. Connecting the fetal and genetic origins of PCOS; **Monica D Hartanti**, Katja Hummitzsch, Helen F Irving-Rodgers, Wendy M Bonner, Raymond J Rodgers; Society for Reproductive Biology Annual Scientific Conference 2018

Abbreviation

PGC	Primordial germ cell
GREL	Gonadal rich epithelial like
PCOS	Polycystic ovary syndrome
GWAS	Genome wide associated study
qRT-PCR	Quantitative real time polymerase chain reaction
AR	Androgen receptor
TGFB1I1	Transforming growth factor beta 1 induced transcript 1
FBN3	Fibrillin3
cAMP	Cyclic adenosine monophosphate
SEM	Scanning electron microscope
PRDM1	Positive regulatory domain I-biding factor 1
BLIMP1	B-lymphocyte-induced maturation protein 1
IFITM3	Interferon-induced transmembrane protein 3
TNAP	Nonspecific alkaline phosphatase
DPPA3	Developmental pluripotency associated 3
OCT3/4	Octamer-binding transcription factor 3/4
POU5F1	POU Domain, Class 5, Transcription Factor 1
SSEA	Stage-specific embryonic antigen
DAZL	Deleted In Azoospermia Like
DDX4	DEAD-Box Helicase 4
BMP	Bone morphogenic protein
TGF	Transforming growth factor
GATA	GATA Binding Protein 4
FOG2	Friend Of GATA2
WNT4	Wingless-related MMTV integrated site 4
DKK1	Dickkopf-related protein 1
FST	Follistatin
FOXL2	Orkhead box L2
GDF9	Growth differentiation factor 9
AMH	Anti-mullerian hormones
FSHR	Follicle stimulating hormone receptors
ECM	Extracellular matrix
ALK5	Activin receptor-like kinase 5

EGF	Epidermal growth factor
ALDH	Aldehyde dehydrogenase
LGR5	Leucine Rich Repeat Containing G Protein-Coupled Receptor 5
Lef-1	Lymphoid enhancer-binding factor 1
CD133	Cluster of differentiation 133
CK6B	Cytokeratin 6B
HSD3B2	3-beta-hydroxysteroid dehydrogenase type II
DHEA	Dehydroepiandrosterone
LH	Luteinising hormone
FSH	Follicle-stimulating hormone
MAP2K1	Mitogen-activated protein kinase kinase 1
PI3K	Phosphoinositide 3-kinase
IPG	Phosphoinositol glycan
LHCGR	Luteinising hormone/choriogonadotrophin receptor
THADA	Thyroid adenoma associated
ERBB4	Erb-b2 receptor tyrosine kinase 4
RAD50	RAD50 double strand break repair protein
DENND1A	DENN domain-containing protein 1A
C9orf3	Chromosome 9 open reading frame 3
FSHB	Follicle-stimulating hormone beta subunit
YAP1	Yes-associated protein 1
HMGA2	High-mobility group AT-hook 2
RAB5B	Ras-related protein Rab-5B
SUOX	Sulfite oxidase
KRR1	KRR1 small subunit processome component homolog
TOX	TOX high mobility group box family member 3
SUMO1P1	Small ubiquitin-related modifier 1 pseudogene 1
EMT	Epithelial-Mesenchymal Transition
DPC	Days post coitum
CG	Chorionic gonadotrophin
NHR	Nuclear hormone receptor
ARIP4	Androgen receptor-interacting protein 4
SRC1	Steroid receptor coactivator 1
NCoR	Nuclear receptor co-repressor 2
SMRT	Silencing mediator for retinoid or thyroid-hormone receptors

ARA55	AR-associated protein 55
LBD	Ligand Binding Domain
TGFBR3	Transforming growth factor beta receptor III
IHH	Indian hedgehog
DHH	Desert hedgehog
PKB	Proteinase kinase B
T	Testosterone
DHT	Dihydrotestosterone
IGF-1	Insulin-like growth factor 1
FBN3	Fibrillin3
OGN	Osteoglycin
LUM	Lumican
$HBSS^{+/+}$	Hank's balanced-salt solution containing Mg^{2+} and Ca^{2+}
H	High
CP	Crude protein
L	Low
CRL	Crown–rump length
EDTA	Ethylenediamine tetraacetic acid
DAPI	4',6'-diamidino-2-phenylindole dihydrochloride
CV	Coefficient of variation
DPEC	Diethyl pyrocarbonate
GAPDH	Glyceraldehyde-3-phosphate dehydrogenase
COL6	Collagen type VI
SLRP	Small leucine-rich proteoglycan
ASPN	Asporin
FN1	Fibronectin
RGS5	Regulator of G-protein signalling 5
FBLN5	Fibulin 5
FMOD	Fibromodulin
LGALS1	Lectin galactoside binding soluble 1 (galectin 1)
LCM	Laser capture micro-dissection
OCT	Optimal cutting temperature
SRY	Sex determining region Y
RQI	RNA Quality Index
RPL32	Ribosomal protein L32

PPIA	Peptidylprolyl isomerase A
ACTB	Actin beta
B2M	Beta-2-microglobulin
FGF-9	Fibroblast growth factor 9
EMX2	Empty spiracles homeobox protein 2
LHX9	LIM homeobox protein 9
WT1	Wilms Tumor 1
SF1	Steroidogenic factor 1
CTNNB1	β-catenin
Rspo1	R-spondin 1
ALDH	Aldehyde dehydrogenase
CK19	Cytokeratin 19

Chapter I:

Literature review / significance of the research

Chapter 1

Literature review / significance of the research

Understanding fetal development is critical for discovering the developmental origins of poor health and non-communicable diseases. Perturbations of ovarian development may cause a permanent alteration in ovarian functions, leading to infertility or hormonal imbalances. It is imperative to recognise all the processes involved in ovarian development in order to mitigate these perturbations. This study advances our knowledge of key aspects of ovarian development.

1.1. The formation of the mammalian fetal ovary

Observations by Hummitzsch *et al.* reveal that the formation of the bovine fetal ovary can be subdivided into six critical stages of development (Fig. 1): (1) Mesonephric stromal penetration; (2) Ovigerous cord formation; (3) Ovigerous cord breakdown; (4) Follicle formation; (5) Surface epithelium formation; and (6) Tunica albuginea formation. More recent findings in humans agree with these findings (Heeren *et al.* 2015).

1.1.1. Mesonephric stromal penetration

The formation of the ovary begins with the thickening of the surface epithelium on the ventromedial surface of the mesonephros (Sarraj & Drummond 2012, Hummitzsch *et al.* 2013, Wilhelm *et al.* 2013), the location where the genital ridge will be established at around 32 days of gestation (Ross *et al.* 2009). The mesonephros acts as a transient kidney in fetal mammals and starts to degenerate at around 40-47 days of gestation (Wrobel 2001) when the metanephros is fully functioning as a kidney. The surface epithelial cells of the mesonephric thickening will change their phenotype into Gonadal Ridge Epithelial Like (GREL) cells which start to proliferate and will form the somatic cell population of the ovary at the early stage of the ovarian primordium (Hummitzsch *et al.* 2013). After breakdown of the basal lamina underlying the mesonephric surface epithelium, the stroma from the mesonephros, which contains fibroblasts, fibres, and capillaries, commences to penetrate the ovarian primordium (Hummitzsch *et al.* 2013).

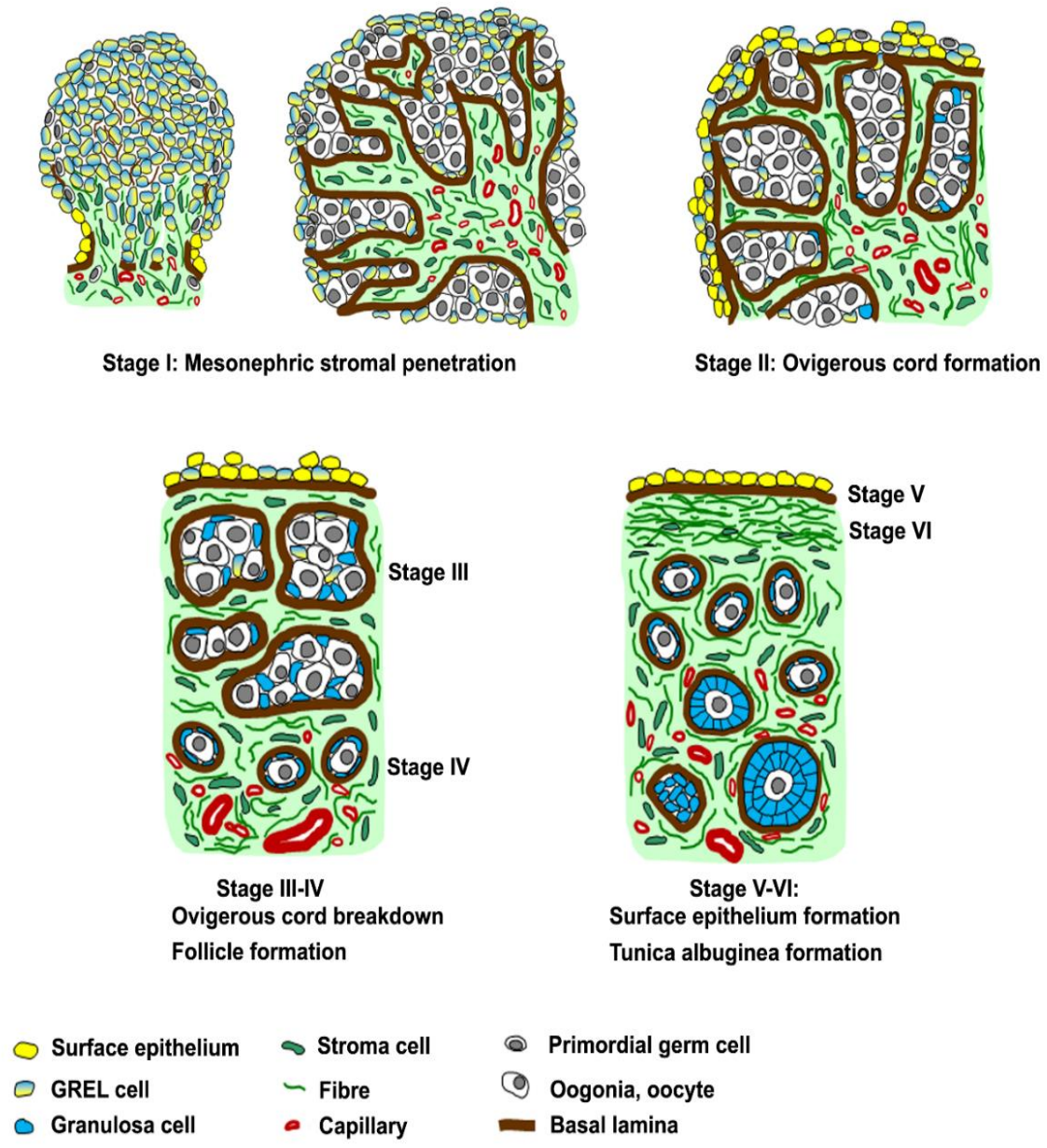

Fig. 1. Schematic diagram of the developmental stages of bovine fetal ovaries. Modified from (Hummitzsch *et al.* 2013).

1.1.2. Ovigerous cord formation

As the stroma is penetrating the developing ovary, primordial germ cells (PGCs), which have emerged from the yolk sac, start to proliferate, while migrating through the hindgut along the dorsal mesentery and into the gonadal ridges. This migration occurs at approximately days 18-31 in cows (Wrobel & Süß 1998) and at 4-14 weeks post-conception in humans (Mamsen *et al.* 2012). Once resident in the ovary, PGCs are referred to as oogonia and continue proliferating. As the stroma spread towards the ovarian surface between the GREL cells and oogonia of the primordial ovary, the stroma branches and thus corrals the

oogonia and GREL into defined areas called ovigerous cords. This occurs at day 70 in cows (Hummitzsch *et al.* 2013) and from week 15 onwards in humans (Konishi *et al.* 1986) and it results in the compartmentalisation of the ovarian primordium into the cortex, which alternates between ovigerous cords and stromal areas, and medulla, which mainly contains the mesonephros stroma containing the extracellular matrix, fibroblasts and vasculature.

The oogonia within the ovigerous cords begin to differentiate into oocytes, entering meiosis at around 75-80 days in bovines and at 11-12 weeks' gestation in humans (Cohen & Holloway 2010). At this stage, there is no defined surface epithelium on the ovarian surface and the ovigerous cords are still 'open' to the surface (Hummitzsch et al. 2013, Heeren et al. 2015). The ovigerous cords are separated from the surrounding stroma by a basal lamina (Hummitzsch *et al.* 2013, Heeren *et al.* 2015). The stromal strands between ovigerous cords also contain capillaries, each surrounded by a sub-endothelial basal lamina.

1.1.3. Ovigerous cord breakdown

Further penetration of stroma from the ovarian medulla into the cortex causes the breakdown of large ovigerous cords into smaller clusters of GREL cells and oogonia, commencing in the area closest to the medulla. The breakdown of ovigerous cords is observed at around 90 and 105 days in cattle (Garverick *et al.* 2010), and at around 112 days in humans (Motta *et al.* 1997), and 20.5-22.5 dpc in mice (Pepling & Spradling 2001). Apoptosis is observed during the breakdown of mice ovigerous cords suggesting that cell loss might have an important role in the breakdown of the ovigerous cords (Pepling & Spradling 2001, Juengel & Smith 2014).

1.1.4. Follicle formation

In bovine ovaries the breakdown of ovigerous cords by the stroma into ever smaller clusters of oogonia/oocytes and GREL cells finally results in the formation of primordial follicles, consisting of an oocyte surrounded by flattened pre-granulosa cells, which are separated from the adjacent tissue by a basal lamina (Hummitzsch *et al.* 2013). The first primordial follicles form close to the medulla at day 105 in cattle, while the more external areas of the cortex still contain ovigerous cords. Later in development, more primordial follicles are formed closer to the ovarian surface (Burkhart *et al.* 2010). Some primordial follicles are activated and develop further into primary follicles. The follicles continue to develop into preantral follicles, which contain two or more granulosa cell layers (Fortune *et al.* 2010) , and into antral follicles, which are composed of columnar-shaped granulosa cells, two theca cell layers (theca interna and externa) and the antrum (Burkhart *et al.* 2010, Rodgers & Irving-Rodgers 2010).

1.1.5. Surface epithelium formation

In bovine ovaries in late in development, stromal cells branch laterally underneath the outermost layers of cells on the ovarian surface, separating them from the ovigerous cords below, thereby 'closing' the cords. A basal lamina is located at the border of the stroma and the cells on the surface. At this stage, the ovary has a surface epithelium as classically defined, with an epithelial layer with a sub-epithelial basal lamina at the stromal interface. The early multi-layered surface epithelium differentiates into a mature single-layered epithelium later on (Hummitzsch *et al.* 2013).

1.1.6. Tunica albuginea formation

In bovine ovaries at the final stage of bovine ovarian development, the stroma below the basal lamina, underlying the ovarian surface epithelium, differentiates into the tunica albuginea (Hummitzsch *et al.* 2013); an avascular collagen-rich layer (van Wezel & Rodgers 1996).

1.2. Gene regulation during ovarian development

During ovarian development, complex processes involving crosstalk between germ cells, somatic cells and stromal cells occur. A better understanding of these early factors that regulate the cell populations in the fetal ovary will enhance our knowledge about the formation of follicles and normal ovarian development. This subchapter reviews various genes and signals involved in germ and somatic cell development in the fetal ovary.

1.2.1. The regulation of germ cells

The positive regulatory domain I-binding factor 1 (PRDM1), PRDM13 and interferon-induced transmembrane protein 3 (IFITM3/Fragilis) are expressed in PGC precursors at embryonic day (E) 6-6.5 in mice (Chuva de Sousa Lopes & Roelen 2010, Fortune *et al.* 2010, Matsui 2010). After the PGCs are located posterior to the primitive streak in the extraembryonic mesoderm, nonspecific alkaline phosphatase (TNAP) and developmental pluripotency associated 3 (DPPA3 or Stella) are expressed. During the migration process, PGCs continue to express TNAP and start to express POU Domain, Class 5, Transcription Factor 1 (POU5F1), the proto-oncogene cKIT and stage-specific embryonic antigen (SSEA) 1 and 3 [reviewed in (Hummitzsch *et al.* 2015)].

POU5F1 encodes a transcription factor containing a POU (Pit-Oct-Unc) homeodomain that plays a key role in embryonic development and stem cell pluripotency

(Yeom *et al.* 1996). POU5F1 is also known as octamer-binding transcription factor 3/4 (OCT3/4). The OCT3/4 protein is observed in bovine PGC and oogonia, as well as in the oocytes of primordial and primary follicles in cows (Hummitzsch *et al.* 2013) and women (Anderson *et al.* 2007). OCT3/4 protein is highly expressed in mouse and human oogonia that are mitotically active and it rapidly declines in the oocytes during folliculogenesis (Meyts *et al.* 2004, Stoop *et al.* 2005).

Nanog1 encodes the Nanog transcription factor that maintains the self-renewal and pluripotency of embryonic stem cells (Chambers *et al.* 2003, Mitsui *et al.* 2003). Nanog is expressed in human fetal PGC and oogonia between 7-11 weeks of gestation. At 7 weeks of gestation, it is observed in the medullary and cortical regions, however by 8 weeks of gestation its expression can mostly be observed in the cortex. After week 11, the number of Nanog positive cells decreases and most are located in the outer cortex (Kerr *et al.* 2008).

DAZL encodes an RNA binding protein and is detected in the cytoplasm of germ cells (Cooke *et al.* 1996). In the bovine fetal ovary, the DAZL protein is observed in germ cells at around 70-130 days of gestation (Hummitzsch *et al.* 2013), whereas in humans it is more commonly observed in the second trimester (Anderson *et al.* 2007). Furthermore, any knockout of DAZL in fetal mice results in infertility due to the loss of oocytes (McNeilly *et al.* 2000, Lin & Page 2005).

DDX4 encodes DEAD box proteins, which is a homolog of VASA proteins in several other species, such as Drosophila, and is involved in germ cell development (Chen *et al.* 2014). It is known as the late germ cell marker and it is detected in oogonia and oocytes in bovine and human fetal ovaries (Anderson *et al.* 2007, Albamonte *et al.* 2008, Kenngott *et al.* 2014, Heeren *et al.* 2015).

Figlα encodes factors in the germ line, a transcription factor. The expression of *Figlα* is detected from 13 dpc in mouse oocytes and this gene continues to be expressed in adulthood (Liang *et al.* 1997). It is believed that Figlα is critical for the survival of germ cells and the formation of primordial follicles (Soyal *et al.* 2000, Lei *et al.* 2006).

Stra8 encodes stimulated by retinoic acid gene 8 protein. Stra8 is believed to be required for germ cell entry into meiosis [reviewed (Feng *et al.* 2014)]. Studies in mice have shown that a deficit of *Stra8* causes impaired meiosis in fetal ovaries, leading to infertility (Baltus *et al.* 2006). *Stra8*-null mouse fetal ovaries showed hindered meiosis prior to prophase I entry (Baltus *et al.* 2006, Anderson *et al.* 2008).

Besides germ cell markers, germ cells also express some bone morphogenic proteins (BMPs). The BMP family is a member of the Transforming growth factor (TGF) superfamily

and consists of 18 members [reviewed in (Juengel & McNatty 2005)]. BMPs are believed to regulate physiological processes related to the functions of ovarian follicles at different developmental stages [reviewed in (Rossi *et al.* 2016)]. BMP-4 and -8 have been shown to facilitate the differentiation of stem cells into PGCs in humans (West *et al.* 2010) as well as the proliferation of PGCs in rodents (Ross *et al.* 2003) and humans (Childs *et al.* 2010). Some BMPs have been found to be expressed in oocytes at different follicle stages, such as BMP-2, -4, -6, -7 and -15. These BMPs are observed in the adult and fetal ovaries of humans, cattle, sheep, goats and rodents (Fatehi et al 2005; Juengel et al 2006; Glister, Kemp & Knight 2004; Frota et al 2013; Silva et al 2005; Juengel & McNatty 2005; Childs et al 2010; Miyoshi et al 2006; Erickson & Shimasaki 2003; Abir et al 2008).

1.2.2. The regulation of somatic cells

The GATA family and their co-factor FOG2 play a crucial role in the beginning of ovarian developmental processes [reviewed in (Morceau *et al.* 2004, Viger *et al.* 2008)]. GATA4 is expressed in human fetal granulosa cells at 23 weeks of gestation, then its expression decreases by week 33 (Vaskivuo *et al.* 2001a). In adult human and rat ovaries, the expression of GATA4 is observed in theca cells and in ovarian surface epithelium (Vaskivuo *et al.* 2001a, Anttonen *et al.* 2003, Capo-chichi *et al.* 2003).

The sexual development of the ovary is dramatically affected by the loss of the interaction of Gata4-Fog in mice (Manuylov *et al.* 2008). The GATA4-FOG2 complex regulates the canonical Wnt/β-catenin pathway by activating the wingless-related MMTV integrated site 4 (*WNT4*), as well as repressing the Dickkopf-related protein 1 (*DKK1*) gene (Manuylov *et al.* 2008). WNT4 is important for activating this pathway in the granulosa cells of humans (Sanchez *et al.* 2014), cattle (Abedini *et al.* 2015), pigs (Kiewisz *et al.* 2011) and mice (Hsieh *et al.* 2002, Harwood *et al.* 2008), as well as activating bone morphogenetic protein 2 (*BMP2*) and follistatin (FST) (Yao *et al.* 2004). DKK1 is a potent inhibitor of Wnt signalling (Glinka *et al.* 1998).

Follistatin (*FST)* and forkhead box L2 (*FOXL2*) are two of the first genes that can be detected early in ovarian development (Menke & Page 2002). Foxl2 is a granulosa cell marker and can be observed at embryonic day 11.5 in the developing XX gonad in mice (Wilhelm *et al.* 2009), in the human female genital ridge at around 6 weeks of gestation or before sex determination (Cocquet *et al.* 2002) and in cattle at 90 days of gestation (Hummitzsch *et al.* 2013). The cooperation of β-catenin, *FOXL2*, and *BMP2* initiates the expression of *FST*, which supports female germ cell differentiation/development.

It has been shown that the members of the TGF-β superfamily play important roles in regulating the function of the ovary (Knight & Glister 2006). TGF-β ligands bind the TGF-β type II receptor dimer, which is a serine/threonine receptor kinase, which both recruits and phosphorylates the type I receptor, forming a hetero-tetrameric complex with the ligand [reviewed in (Weiss & Attisano 2013)] . TGF-β superfamily members include TGF-β, activin, inhibin, BMPs and growth differentiation factor 9 (GDF9), anti-mullerian hormone (AMH), follicle stimulating hormone receptor (FSHR) and FST (Piek & Roberts 2001). The regulation of TGF-β family signalling depends on the recruitment of the second messengers of the Smad family. These complexes have been shown to be expressed throughout folliculogenesis (Bristol & Woodruff 2004), suggesting the importance of these pathways in ovarian development.

TGF-β1-3 isoforms are detected in the oocytes, thecal cells and granulosa cells of adult rat ovaries (Benahmed *et al.* 1993). In adult human ovaries, TGF-β1 is observed in granulosa cells and oocytes, TGF-β2 is mostly found in the granulosa cells and none of the ovarian cells express TGF-β3 (Schilling & Yeh 1999). In adult sheep ovaries, the mRNA expression of *TGFB1-2* are detected in stromal and/or thecal cells of follicles with multilayers of granulosa cells, whereas *TGFB3* is only expressed in the vascular system (Juengel 2004). In adult bovine ovaries, *TGFB1-3* are expressed in granulosa cells, theca interna, surface epithelium and stroma (Matiler 2014, Nillson 2001).

TGF-β 1-3 isoforms and the two TGF-β receptors are observed in human and bovine fetal ovaries (Schilling & Yeh 1999, Hatzirodos *et al.* 2011). Components that are involved in TGF-β signalling, such as receptors and Smads, have been identified in oocytes and granulosa cells (Schilling & Yeh 1999, Österlund & Fried 2000, Pangas *et al.* 2002). It is believed that TGF-β is involved in the proliferation of granulosa cells (Mondschein *et al.* 1988), steroidogenesis (McAllister *et al.* 1994) and the maturation of oocytes during follicular development (Feng *et al.* 1988), as well as facilitating the synthesis of FSHR in granulosa cells (Dunkel *et al.* 1994).

Activin βA or βB subunit mRNA and proteins have been shown to be expressed in the human oogonia during fetal life starting at 14 weeks of gestation (da Silva *et al.* 2004). Activin A increases oogonia proliferation *in vitro* in 14-21 week old human fetal ovaries, suggesting that activin might be involved in the regulation of germ cell proliferation (da Silva *et al.* 2004). Inhibin A mRNA and protein have been shown to be expressed in stromal and granulosa cells of fetal mice ovaries at around E13 (Weng *et al.* 2006).

BMP-1, -2, -4, -5, -6, -7 and -15 have been shown to be expressed in granulosa and/or thecal cells of primordial to antral follicles in cattle, sheep, mice, goats and humans [reviewed in (Rossi *et al.* 2016). BMP-1 has been found to regulate the formation of the extracellular matrix (ECM) during folliculogenesis in sheep (Canty-Laird *et al.* 2010). Furthermore, the changes in the composition of ECM in thecal and granulosa cells have been shown to be related to the growth of ovine ovarian follicles (Berkholtz *et al.* 2006). BMP-2, -4, -6 and -7 have been found to be involved in steroidogenesis in mice (Erickson & Shimasaki 2003), sheep (Juengel *et al.* 2006b), humans (Miyoshi *et al.* 2006), cattle (Glister *et al.* 2004), and goats (Frota *et al.* 2013) by regulating the expression StAR, P450 aromatase (CYP19A1), P450 side chain cleavage enzyme (CYP11A1), and cytochrome P450 family 17 subfamily A member 1 (CYP17A1), as well as the production of oestradiol and progesterone. BMP-5, -6 and -15 are also found to be involved in the proliferation of granulosa cells in cattle (Glister *et al.* 2004), sheep (Shimizu *et al.* 2004) and mice (Otsuka *et al.* 2000, Pierre *et al.* 2005).

BMPs signalling involves its type I (ALK-2, 3 and 6) and II receptors (BMPRII, ActR-II) (Glister *et al.* 2004, Goto *et al.* 2007, Miyagi *et al.* 2012). The interaction of type I and II BMP receptors will induce the phosphorylation of Smads, which subsequently relocate to the nucleus and regulate the expression of specific genes (Lembong *et al.* 2008, Manuylov *et al.* 2008, Ohta *et al.* 2008). These receptors and Smads have been observed in granulosa cells from primordial/primary follicles onwards in humans [reviewed in (Juengel & McNatty 2005), suggesting that BMP is critical for the development of follicles.

GDF-9 can be found in oocytes and granulosa cells in humans (Yamamoto *et al.* 2002), cattle (Bodensteiner *et al.* 1999), sheep (McNatty *et al.* 2001) and mice (Yan *et al.* 2001, Hreinsson *et al.* 2002) during folliculogenesis. In cultured human granulosa cells, GDF-9 has been shown to inhibit cAMP-induced steroid production and expression of StAR, CYP11A1 and CYP19A1, which are involved in steroidogenesis (Yamamoto *et al.* 2002). GDF-9 also enhances the development of primordial to secondary follicles in cultured human follicles (Hreinsson *et al.* 2002). Treatment of GDF-9 in rats progresses the development of follicles *in vivo* (Vitt *et al.* 2000) and *in vitro* (Nilsson & Skinner 2002). GDF-9 receptors, TGFBR1 (activin receptor-like kinase 5, ALK5) and BMPRII are expressed in ovine granulosa cells from primordial follicles onwards (Juengel & McNatty 2005). GDF-9 upregulates Kit Ligand (KL) expression in bovine granulosa cells (Nilsson & Skinner 2002). KL has been shown *in vitro* to facilitate the activation of primordial into primary follicles and the growth of oocytes in rats (Nilsson & Skinner 2002). GDF-9 null mutation mice are infertile due to arrested follicle development at the primary stage (Dong *et al.* 1996,

Carabatsos *et al.* 1998). Taken together GDF-9 is essential for further follicle progression by regulating factors that are involved in the further development of primordial follicles.

AMH is a member of the TGFβ superfamily involved in the regulation of folliculogenesis (Baarends *et al.* 1995). The AMH protein is expressed in granulosa cells after 32 weeks of gestation in humans (Meyts *et al.* 1999), as well as in granulosa cells of human (Weenen 2004), cow (Monniaux 2008), sheep (Bezard 1987) and rodent (Visser *et al.* 2006) adult ovaries. Deletion of *amh* in mice results in an increased rate of recruitment of primordial follicles (Durlinger *et al.* 1999) leading to the rapid depletion of follicle reserves. In humans (Visser 2006) and mice (Keveenar 2006), AMH is believed to be the marker of the ovarian follicular reserve, whereas in cattle AMH is shown to be a marker of the population of small antral gonadotrophin-responsive follicles (Rico 2009).

Follistatin is believed to act as an important regulatory factor in fetal ovarian development (Kashimada *et al.* 2011). Follistatin acts in the Wnt4 pathway to suppress the male pathway in XX gonads (Yao *et al.* 2004). Later in ovarian development, follistatin facilitates the survival of meiotic germ cells (Yao *et al.* 2004). Excessive follistatin in mice results in an increase in the number of germ cells within the ovigerous cords, due to a delay in ovigerous cord breakdown, as well as a decrease in the apoptosis of germ cells (Kimura *et al.* 2011), suggesting a critical role of follistatin is in regulating the breakdown of ovigerous cords.

1.3. Ovarian Surface Epithelium

The surface epithelium of the ovary has been described as an altered pelvic mesothelium composed of a single layered flat to cuboidal epithelium (Fig. 2) (Nicosia *et al.* 1991, Murdoch 1994). It expresses keratin types 7, 8, 18 and 19, as well as the mucin antigen (MUC1), 17β-hydroxysteroid dehydrogenase, and has cilia (Blaustein & Lee 1979, Auersperg *et al.* 1994, Zhang *et al.* 1998, Dubeau 1999). Simple desmosomes, tight junctions (Siemens & Auersperg 1988, Sawyer *et al.* 2002), integrins (Kruk *et al.* 1994, Cruet *et al.* 1999) and cadherins (Sundfeldt *et al.* 1997, Davies *et al.* 1998) maintain the intercellular contact and integrity of ovarian surface epithelium.

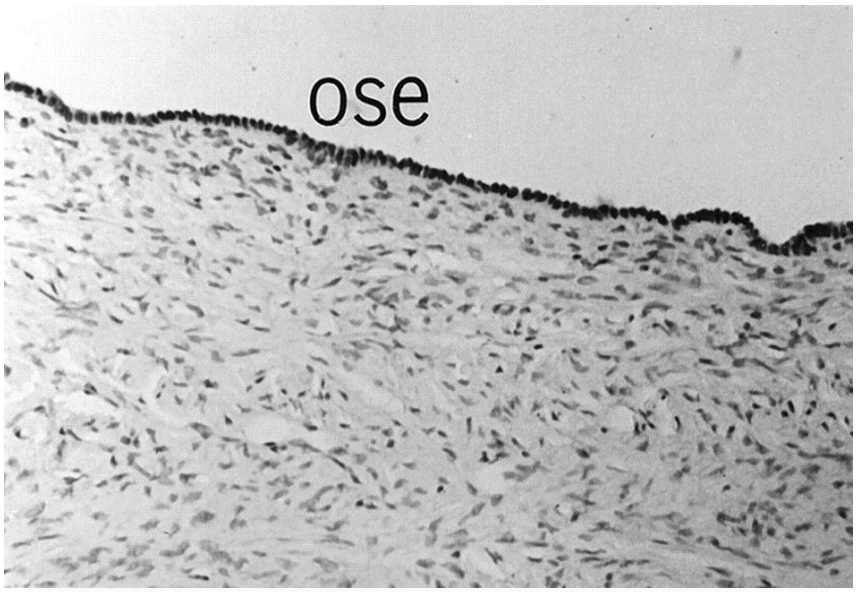

Fig. 2. Representative image of single layered cuboidal cell on the adult human ovarian surface. Modified from (Auersperg *et al.* 2001).

In early development, the future ovarian surface epithelium does not cover the presumptive gonad, except at the base (Hummitzsch *et al.* 2013, Kenngott *et al.* 2013). At around 10 weeks until 5 months of gestation, the human fetal ovarian surface epithelium changes from a flat to a cuboidal epithelium [reviewed in (Auersperg *et al.* 2001)]. The GREL cell population eventually differentiates into a surface epithelium when the stroma has penetrated to just below the superficial GREL cells (Hummitzsch *et al.* 2013). Taken together, there are two regions of ovarian surface, an established surface epithelium at the base of the ovary, derived directly from the mesonephros; and the GREL cell originated surface epithelium, covering the rest of the ovarian surface (Fig. 3).

The functions of ovarian surface epithelium are to transport material to and from the peritoneal cavity, as well as to take part in the ruptures and repair of ovulatory cycles (Nicosia *et al.* 1991, Murdoch 1994). Epidermal growth factor (EGF), collagen, ascorbate, TGF-β modulate epithelia-mesenchymal initiates epithelio-mesenchymal conversion in many epithelial cell types (Toda *et al.* 1997, Auersperg *et al.* 2001). This ability is beneficial for supporting postovulatory repair of ovarian surfaces because it enhances motility, modifies proliferative responses and capacities to alter ECM, and provides the contraction of the cells [review in (Auersperg *et al.* 2001). Aldehyde dehydrogenase (ALDH), Leucine Rich Repeat Containing G Protein-Coupled Receptor 5 (LGR5), lymphoid enhancer-binding factor 1 (Lef-1), cluster of differentiation 133 (CD133), cytokeratin 6B (CK6B) are known to be the markers of stem/progenitor cells. These genes are detected in the hilum of adult mice ovaries and believed to be responsible for the postovulatory repair of the ovarian surface epithelium

(Flesken-Nikitin *et al.* 2013). Another study of murine ovaries has shown that LGR5 is observed close to ovulating follicles and on the apical side of corpora lutea (Ng *et al.* 2014).

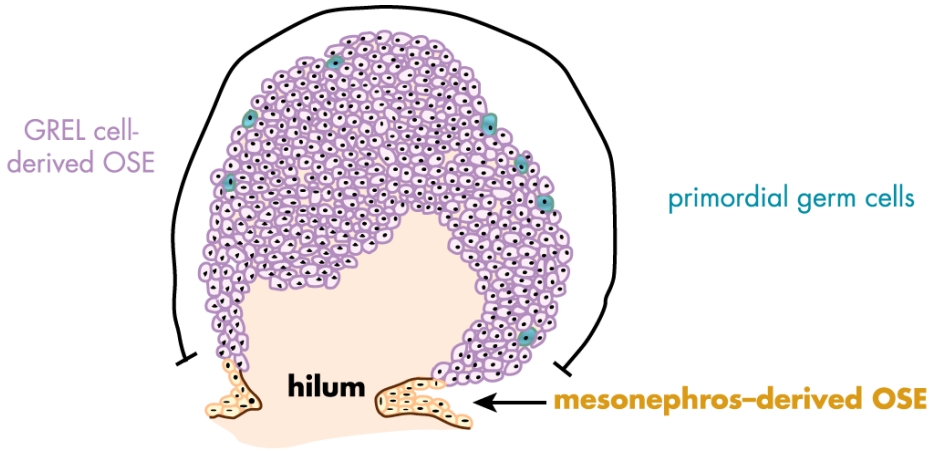

Fig. 3. The origin of the bovine ovarian surface epithelium. Modified from (Hummitzsch *et al.* 2015)

1.4. Polycystic Ovary Syndrome and its impact on reproduction

Polycystic ovary syndrome is one of the most common endocrine and metabolic disorders, affecting around 10% of women of reproductive age (Ehrmann *et al.* 2006, Bozdag *et al.* 2016). The exact underlying aetiology of PCOS is complex and still unclear. It is believed that PCOS is a multifactorial system disorder, involving abnormal steroidogenesis and regulation of ovarian function, as well as metabolic syndrome, such as insulin resistance and increased type 2 diabetes mellitus and cardiovascular disease risk factors (Teede *et al.* 2011). Dysregulation of steroidogenesis and ovarian function in PCOS is characterised by dysfunction of intrinsic thecal and granulosa cells, leading to hyperandrogenism and perturbation of folliculogenesis.

1.4.1. Dysfunction of thecal cells

The defect of steroidogenesis in PCOS thecal cells has been well studied. It has been shown that the activities of three important enzymes in androgen synthesis, CYP17A1, 3-beta-hydroxysteroid dehydrogenase type II (HSD3B2) and CYP11A1, are increased in PCOS thecal cells (Nelson *et al.* 1999, Wood *et al.* 2004). CYP11A1 converts cholesterol to pregnenolone, which is the first and rate-limiting step of the steroid biosynthesis. CYP17A1 catalyses the 17α-hydroxylation of both pregnenolone and progesterone, as well as cleaves the C17–C20 bond of 17α-hydroxypregnenolone and 17α-hydroxyprogesterone to form dehydroepiandrosterone (DHEA) and androstenedione, respectively. HSD3B2 transforms Δ5-

steroids (pregnenolone, 17α-hydroxypregnenolone and DHEA) into their Δ4-congenors. On the transcription level, it has been shown that nuclear factor 1C (NF1C) will bind to the *CYP17A1* gene promoter, leading to the repression of the *CYP17A1* promoter function. The expression levels of *NF1C* are decreased in PCOS thecal cells, suggesting its contribution to hyperandrogenemia caused by increased activity of the *CYP17A1* promoter (Wickenheisser *et al.* 2006).

The defect of thecal cell steroidogenesis in PCOS has an effect on extra-ovarian factors, such as the luteinising hormone (LH), follicle-stimulating hormone (FSH) and insulin, , as well as intra-ovarian factors, such as AMH and inhibins [reviewed in (Diamanti-Kandarakis 2008)]. Increased LH leads to the decrease of mitogen-activated protein kinase kinase 1 (MAP2K1), which is associated with increased thecal androgen biosynthesis. In the intracellular signalling of insulin, phosphoinositide 3-kinase (PI3K) and phosphoinositol glycan (IPG) activities are increased, leading to the stimulation of androgen production in thecal cells. At the same time, increased LH interacts with increased insulin and subsequently amplifies the intrinsic steroidogenic defect. In relation to increased levels of LH, FSH levels are decreased, reducing the activity of aromatase in alliance with AMH. The increase in AMH levels may have a direct effect in stimulating thecal cell androgen synthesis, leading to the inhibition of aromatase activity.

Hyperandrogenism has been linked to anovulation in PCOS women. The excessive androgen levels stimulate the growth of preantral to antral follicles as well as hinder the maturation of follicles towards the dominant stage, leading to impaired folliculogenesis (Jonard & Dewailly 2004, Maciel *et al.* 2004). Androgen receptors are required during early development of follicles, thus androgen may have an effect on the initial follicular recruitment that results in growth impairment of early follicular growth in PCOS (Vendola *et al.* 1999, Rice *et al.* 2007).

1.4.2. Details of PCOS candidate genes.

Recent genome-wide association studies (GWAS) have discovered PCOS candidate genes, such as the luteinising hormone/choriogonadotrophin receptor *(LHCGR), FSHR,* thyroid adenoma associated *(THADA),* erb-b2 receptor tyrosine kinase 4 *(ERBB4),* RAD50 double strand break repair protein *(RAD50), GATA4,* DENN domain-containing protein 1A *(DENND1A),* chromosome 9 open reading frame 3 *(C9orf3),* follicle-stimulating hormone beta subunit (*FSHB),* yes-associated protein 1 (*YAP1),* High-mobility group AT-hook 2 (*HMGA2),* Ras-related protein Rab-5B (*RAB5B),* Sulfite oxidase (*SUOX),* KRR1 **s**mall subunit processome component homolog *(KRR1),* TOX high mobility group box family

member 3 (*TOX3)*, insulin receptor *(INSR)* and Small ubiquitin-related modifier 1 SUMO1 pseudogene 1 (*SUMO1P1)* (Jones & Goodarzi 2016).

The paragraphs below summarise briefly information about the roles of PCOS candidate genes and any knowledge of their existence in ovaries. Additionally, 4 other PCOS related genes, fibrillin *(FBN3)*, anti Mullerian hormone *(AMH)*, androgen receptor *(AR)* and Transforming Growth Factor Beta 1 Induced Transcript 1 *(*TGFB1I1) will be discussed below.

A study in women has linked *DENND1A* with PCOS by showing that an overexpression of *DENND1A* isoforms in normal thecal cells resulted in a PCOS phenotype in thecal cells, such as augmented *CYP17A1* and *CYP11A1* expression and androgen biosynthesis (McAllister *et al.* 2014). Knock-down of *DENND1A.V2* in PCOS thecal cells reduced androgen biosynthesis and expression of *CYP17A1* and *CYP11A1* (McAllister *et al.* 2014).

FBN3 has been shown before to be highly expressed at the early developmental stage of human and bovine fetal ovaries *in vivo* and *in vitro* and then to decline later in gestation (Hatzirodos *et al.* 2011, Hummitzsch *et al.* 2013). *FBN3* is not expressed in the adult ovaries of women (Prodoehl *et al.* 2009a) and cows (Prodoehl *et al.* 2009b). *FBN3* encodes fibrillin 3, which is an extracellular matrix protein expressed in the stromal compartment of the bovine fetal ovary (Hatzirodos *et al.* 2011) and thought to be involved in stromal penetration during early gestation (Hummitzsch *et al.* 2013). Little is known about the regulation and action of fibrillin 3, but it is thought to bind latent Transforming Growth Factor-β (TGF-β) binding proteins (LTBPs) due to its homologous structure to fibrillins 1 and 2 [reviewed in (Davis & Summers 2012)]. Therefore, fibrillins and LTBPs sequester TGF-β in tissue and regulate its local bioavailability and action (Todorovic & Rifkin 2012). The PCOS ovary is characterised by increased thickness of the tunica albuginea, as well as increased collagen deposition and fibrous tissue of cortical and subcortical stroma (Hughesdon 1982b). It is believed that TGF-β superfamily members contribute to the phenotype of PCOS ovaries due to their role in regulating the production and deposition of collagen in normal and fibrotic tissues (Govinden & Bhoola 2003, Hetzel *et al.* 2005, Khan & Sheppard 2006, Kisseleva & Brenner 2007, LeClair & Lindner 2007, Prud'homme 2007). Taken together, changes in fibrillin 3 during ovarian development and subsequent dysregulation of TGF-β might contribute to the phenotype of the PCOS ovary.

HMGA2 and *TOX3* encode proteins which belong to the HMG-box superfamily and have a role in regulating gene expression, chromatin remodelling, genomic stability and DNA

repair [reviewed in (Cleynen & Van De Ven 2008)]. *Hmga2* is highly expressed in mouse undifferentiated cells during embryogenesis, neural stem cells and tumor cells (Nishino *et al.* 2008), as well as in human fetal tissues, including the ovary (Gattas *et al.* 1999). In adult human tissues, it is only expressed in lungs and kidneys (Gattas *et al.* 1999) and it is barely detectable in adult rat kidneys, lungs, hearts, brains, livers and intestines (Fedele *et al.* 2010). It is believed that *HMGA2* is involved in the Epithelial-Mesenchymal Transition (EMT) occurring during embryogenesis, as well as in carcinoma invasiveness and metastasis and can be provoked by TGF-β signaling via Smad transducers (Thuault *et al.* 2006). *TOX3* encodes a nuclear transcriptional factor and is a member of the thymocyte selection-associated HMG box protein (TOX) subfamily of HMG-box proteins. TOX family members share a DNA-binding domain and are believed to interact with DNA in a structure-dependent way [reviewed in (Yu & Li 2015). TOX plays an important role in the development of the immune system (Aliahmad & Kaye 2008, Aliahmad *et al.* 2010). Little is known about the function of *TOX3* in female reproduction, however, it is known to be overexpressed in breast tumors and has been linked to the fibrosis that causes an increase in mammographic density (Han *et al.* 2016). Increased breast density is related to increased epithelial and stromal tissue and fibrillary collagen deposition (Guo *et al.* 2001, Li *et al.* 2005, Hawes *et al.* 2006). In addition, *TOX3* has also been linked to bladder (Demtroder 2013), lung (Tessema *et al.* 2012) and gastric (Zhang *et al.* 2013) cancers. Collectively, *TOX3* may play an important role in regulating collagen deposition in tumors as well as other fibrotic disorders such as PCOS. Recent studies have discovered that levels of *HMGA2* mRNA were higher in PCOS (Li *et al.* 2018), whereas the TOX3 protein level was significantly lower in PCOS serum and granulosa cells, compared with normal ones (Ning *et al.* 2017).

GATA4 encodes a transcription factor regulating gonadal development and belongs to the GATA family of zinc finger proteins, having an important role in cell differentiation and organ development (Viger *et al.* 1998). Deletion of *Gata4* leads to an abnormal response of the exogenous gonadotrophins and diminished fertility in mice (Lavoie *et al.* 2004). During mouse fetal ovarian development, GATA4 protein is expressed mostly in the granulosa cells and to a lesser extent in the stroma and is detected in male and female gonads as early as 11.5 days of gestation in mice (Viger *et al.* 1998), 19 days *post coitum* (dpc) in pigs (McCoard *et al.* 2001), and 13-14 weeks of gestation in humans (Vaskivuo *et al.* 2001b). It is thought that *Gata4* is required for the breakdown of the mesonephric surface epithelium basal lamina below the surface before genital ridge formation in mice (Hu *et al.* 2013). The expression level of GATA4 protein is heavily decreased after the differentiation of the ovary at 13.5 days of gestation in mice (Viger *et al.* 1998). However, in human and porcine fetal ovaries, *GATA4*

is greatly expressed in the early stages, then decreases until the end of development (McCoard *et al.* 2001, Vaskivuo *et al.* 2001b), which is similar with our findings. In all four species, GATA4 protein is localised in the granulosa cells of the adult ovary, mainly during the time when the granulosa cells are actively proliferating and it is thought to be involved in protecting the granulosa cells from apoptosis (McCoard *et al.* 2001, Vaskivuo *et al.* 2001b, Anttonen *et al.* 2003, Lavoie *et al.* 2004). Taken together, *GATA4* might be involved in the breaking of the mesonephric surface epithelium basal lamina, which allows the penetration of mesonephric stroma during early stages of ovarian development.

LHCGR encodes the LH/CG receptor and belongs to the G protein-coupled receptor superfamily (Nogueira *et al.* 2010). It is the target receptor for the pituitary-derived luteinising hormone (LH) and the placental chorionic gonadotrophin (CG). The function of *LHCGR* has been well studied in many species, such as humans (Reshef *et al.* 1990), cattle (Nogueira *et al.* 2010), pigs (Derecka *et al.* 1995), rabbits (Jensen & Odell 1988), rats (Bonnamy *et al.* 1993) and mice (Zheng *et al.* 2001). The LHCGR is expressed in the thecal cells, granulosa cells, stromal cells and luteal cells. The activation of LHCGR by LH in the thecal cells triggers androgen production, providing the substrate for oestradiol conversion by the follicle-stimulating hormone (FSH) induced aromatase in granulosa cells [reviewed in (Richards 1994)]. In early rat ovarian development, only a truncated mRNA *Lhcgr* receptor was detected at around 13.5 days post gestation, without evidence of translation (Sokka *et al.* 1996). The full-length functional mRNA *Lhcgr* only appeared when the rat thecal layers are formed in the later stages (Sokka *et al.* 1996).

AMH has been well studied for its role in regulating male sex differentiation during gonad development. Fetal Sertoli cells produce the AMH protein to induce the regression of the Mullerian duct to avoid the default female pathway [reviewed in (Visser *et al.* 2006)]. In females, however, the AMH protein is first expressed in the granulosa cells of primary follicles and the expression is increased in pre-antral and small antral follicles but diminished in larger follicles (Durlinger *et al.* 1990). Additionally, AMH protein has a role in inhibiting the recruitment of primordial follicles and the responsiveness of developing follicles to FSH in mice ovaries (Durlinger *et al.* 1990).

FSHR, which is member of the Rhodopsin receptor family of G protein-coupled receptors (GPCRs), has an extended N-terminal extracellular domain with leucine–rich repeats (Lagerstrom & Schioth 2008). The extracellular domain of *FSHR* is first detected in embryonic rat ovaries at day 20 and the full length mRNA is observed in the granulosa cells at day 3 *post partum* (Rannikki *et al.* 1995). In sheep fetal ovaries, *FSHR* mRNA is first

detected in the granulosa cells in follicles with two or more layers of granulosa cells in 100 day old sheep fetuses (Tisdall *et al.* 1995).

INSR encodes a member of the ligand-activated receptor and the receptor tyrosine kinase family. Although this receptor is involved in regulating cell differentiation, growth and metabolism, the main function of INSR appears to be metabolic regulation (Lee & Pilch 1994). During ovarian development, INSR protein is expressed in developing oocytes of mice, rats and humans (Pitetti *et al.* 2009). In addition, a human study showed that the INSR protein is only expressed in the stroma at the beginning of follicle development, and then in the granulosa and thecal cells in the later stages. (Samoto *et al.* 1993).

The AR is a member of the nuclear hormone receptor (NHR) superfamily and located on the X chromosome at Xq11-12 and Xq26 in humans and cattle, respectively (Grosse *et al.* 2012). The AR signalling pathway is modulated by coregulatory proteins: enhancing (coactivators), such as Hic-5/TGFB1I1, androgen receptor-interacting protein 4 (ARIP4), and steroid receptor coactivator 1 (SRC1), or reducing (corepressors) AR transactivation, such as nuclear receptor co-repressor 2 (NCoR) and the silencing mediator for retinoid or thyroid-hormone receptors (SMRT) (van de Wijngaart *et al.* 2012). In the sheep fetal ovary, AR mRNA and protein were first detected in the penetrating mesonephric stroma but not in the ovigerous cords (Juengel *et al.* 2006a). It was then observed in the membrana granulosa of larger follicles, as well as in the stroma at the later stages. In adult mice and sheep ovaries, *AR* mRNA and protein are expressed in all cells of the follicles (oocyte, granulosa and thecal cells) and in stromal compartments, such as the cortical stroma (Juengel *et al.* 2006a, Sen & Hammes 2010). In developing human ovaries, the AR is expressed in the stroma (Fowler *et al.* 2011). In the current study, AR was elevated in the medulla compared with the cortex, in agreement with its expression in the stroma. Our previous study has shown that treatment of human fetal fibroblasts with TGFβ-1 caused a significant reduction in the expression level of AR (Bastian *et al.* 2016) and this could be mediated by regulating Smad3, one of the TGFβ-1 effector proteins. It is known that the interaction of Smad3 with AR supresses AR-mediated transcription (Chipuk *et al.* 2002). Thus, *AR* may be critical for regulating stromal cell functions at the later stages of gestation. This could be critical for the development of PCOS, and in particular for the animal models of PCOS, which are induced by androgens or alterations of AR expression (Walters *et al.* 2018).

TGFB1I1, a coregulatory protein of the AR, is a member of the LIM protein superfamily and also known as Hic-5, as well as AR-associated protein 55 (ARA55) (Shibanuma *et al.* 1994, Wang *et al.* 2005). As an AR coactivator, TGFB1I1 will activate the

AR promoter by binding to the Ligand Binding Domain (LBD) of the AR via the conserved LxxLL motif (Kato *et al.* 2011, Jehle *et al.* 2014). TGFB1I1 has been identified as a negative regulator of TGF-β1 via the inhibition of Smad3, which is one of the TGF-β intracellular effectors, in the rat and human prostate cell lines (Wang *et al.* 2005). The role of TGF-β in modulating the proliferation of fibroblasts, the major cell type of the stromal compartment, has been well established (Fine & Goldstein 1987, Xiao *et al.* 2012, Gao *et al.* 2016, Liu *et al.* 2016). In addition, there is an increased level of TGF-β in fibrotic diseases, such as PCOS (Raja-Khan *et al.* 2014), fibrotic lung disease (Willis & Zea Borok 2007) and hepatic fibrosis (Gressner *et al.* 2002). Since TGF-β is one of the target genes of the AR (Kanda *et al.* 2014), the increased expression of *TGFB1I1* mRNA and the elevated levels in the medulla, suggesting stromal expression, in this study suggest that *TGFB1I1* might be involved in regulating the stromal cell function at the later stage of ovarian development via the TGF-β and AR signalling pathways.

THADA, *RAB5B* and *SOUX* have been linked to type 2 diabetes (Bai *et al.* 2015, Saxena *et al.* 2015). *THADA* encodes thyroid adenoma-associated protein and was originally detected in thyroid adenomas (Rippe *et al.* 2003). *RAB5B* encodes the Ras-related proteins involved in early endosome formation (Hirota *et al.* 2007). *SUOX* encodes a sulfite oxidase enzyme located in the intermembrane space of mitochondria (Oshino & Chance 1975). *SUOX* mRNA is expressed strongly in the human and rat adult liver, kidney, skeletal muscle, heart, placenta and brain (Woo *et al.* 2003). *RAD50, C8H9orf3, YAP1* and *FSHB* are thought to be associated with follicular and oocyte development (McGee & Hsueh 2000, Franceschini *et al.* 2013, Dunaif 2016, Ji *et al.* 2017). *RAD50* encodes the Double Strand Break Repair Protein that is involved in DNA double-strand break repair (Day *et al.* 2015). Interestingly, TGF-β was observed to have a role in DNA repair by reducing the expression of genes involved in DNA repair, such as RAD50, and caused a reduction of the cells' capacity to repair the DNA double strain break (Wiegman *et al.* 2007, Liu *et al.* 2014, Pal *et al.* 2017). *C8H9orf3* (chromosome 8 open reading frame, human C9orf3) is a homolog of the human *C9orf3* gene that encodes a zinc-dependent metallopeptidase (Diaz-Perales *et al.* 2005) and has been linked to erectile dysfunction in a GWAS cohort of prostate cancer patients (Kerns *et al.* 2010). *C9orf3* is upregulated in the TGF-β1 treated human bone marrow stromal cells (Elsafadi *et al.* 2017), suggesting that TGFβ signalling has an effect on the expression of *C9orf3.* It is known that *C9orf3* is one of the target genes of the Smad4 transcription factor, which is a TGFβ inducible DNA binding protein (Yingling *et al.* 1997). *YAP1* encodes a transcriptional coactivator of the Hippo signalling pathway (Ji *et al.* 2017), which regulates the tissue growth and cell fate [reviewed in (Harvey *et al.* 2013)]. *FSHB* encodes the beta subunit of FSH, a

pituitary-secreted glycoprotein (Meduri *et al.* 2008). A study in Han Chinese women found that variants in the *FSHB* gene are related with PCOS and LH levels (Tian *et al.* 2016). *ERBB4* encodes Erb-Be Receptor Tyrosine Kinase 4 protein and belongs to the type I growth factor receptor family (Ma *et al.* 1999). A human study showed that ERBB4 protein is weakly detected in the adult ovarian surface epithelium, (Srinivasan *et al.* 1998), suggesting the *ERBB4* might be involved in the formation of surface epithelium during fetal ovarian development. *KRR1* encodes KRR1, a small subunit processome component homolog protein which has a role in assembling ribosomes (Zheng *et al.* 2014).

Table 1. PCOS-related genes

Gene name	Gene symbol	Function	Cell type in the ovary	Species
Luteinising hormone / choriogonadotrophin receptor	*LHCGR*	Triggers androgen production	Adult thecal, granulosa, stromal and luteal cells.	Humans, cattle(Nogueira *et al.* 2010), pigs, rabbits, rats and mice
Follicle stimulating hormone receptor	*FSHR*	Gonad development	Fetal granulosa cells	Sheep
Thyroid adenoma associated	*THADA*	Unknown	Unknown	Unknown
Erb-b2 receptor tyrosine kinase 4	*ERBB4*	Unknown	Adult ovarian surface epithelium	Human
RAD50 double strand break repair protein	*RAD50*	Follicular and oocyte development	Unknown	Unknown
GATA Binding Protein 4	*GATA4*	Cell differentiation and organ development	Fetal granulosa cells and stroma	Mice, pigs and humans
DENN domain-containing protein 1A	*DENND1A*	Unknown	Adult Thecal cells	Human
Chromosome 9 open reading frame 3	*C9orf3*	Follicular and oocyte development	Unknown	Unknown
follicle-stimulating hormone beta subunit	*FSHB*	Follicular and oocyte development	Unknown	Unknown
yes-associated protein 1	*YAP1*	Follicular and oocyte development	Unknown	Unknown
High-mobility group AT-hook 2	*HMGA2*	Regulating gene expression, chromatin remodelling, genomic stability and DNA repair	Fetal ovary	Human
Ras-related protein Rab-5B	*RAB5B*	Unknown	Unknown	Unknown
Sulfite oxidase	*SUOX*	Unknown	Unknown	Unknown

KRR1 small subunit processome component homolog	*KRR1*	Assembling ribosomes	Unknown	Unknown
TOX high mobility group box family member 3	*TOX3*	Regulating gene expression, chromatin remodelling, genomic stability and DNA repair	Unknown	Unknown
Insulin receptor	*INSR*	Regulating cell differentiation, growth and metabolism	Fetal oocytes, adult stroma at the beginning of follicle development, granulosa and thecal cells in the later stages	Mice, rats and humans
Small ubiquitin-related modifier 1 SUMO1 pseudogene 1	*SUMO1P1*	Unknown	Unknown	Unknown
Fibrillin3	*FBN3*	Unknown	Fetal stroma	Human and bovine
Anti Mullerian Hormone	*AMH*	Regulating male sex differentiation during gonad development	Adult granulosa cells of primary follicles	Human
Androgen Receptor	*AR*	Activate the AR promoter	Adult all cells of the follicles (oocyte, granulosa and thecal cells) and in stromal compartments, such as the cortical stroma.	Sheep, mice, human
Transforming Growth Factor Beta 1 Induced Transcript 1	*TGFB1I1*	Activate the AR promoter	Unknown	Unknown

1.4.3. Dysfunction of granulosa cells

Granulosa cells have been shown to modulate the thecal cell function. Transforming growth factor beta receptor III (TGFBR3) is produced by granulosa cells of preantral and antral follicles (Jaatinen *et al.* 1994, Roberts *et al.* 1994). TGFBR3 has been linked to thecal androgen production (Hirshfeld-Cytron *et al.* 2009). TGFBR3 has been shown to be hyper-responsive to FSH in ovarian hyperandrogenism, which occurs in two thirds of PCOS cases. In addition, the expression of TGFBR3 is upregulated in the PCOS ovary. Other granulosa cell peptides, such as the Indian hedgehog (*IHH*) and Desert hedgehog (*DHH*), have been shown to be involved in facilitating the expression of LH receptors and steroidogenic enzymes during early thecal cell development (Magarelli *et al.* 1996, Liu *et al.* 2015), suggesting the disturbance of granulosa cells has an effect on thecal cells in PCOS ovaries.

1.4.4. Metabolic features in PCOS women

PCOS has been associated with metabolic syndromes with features such as insulin resistance, dyslipidaemia and higher cardiovascular risk (Teede *et al.* 2010). *In vitro* studies have described the significant role of insulin in the production of androgen in thecal cells. This stimulation is mediated via the pathway of PI3K/proteinase kinase B (PKB), which is upregulated in PCOS thecal cells (Munir *et al.* 2004). Dyslipidaemia in PCOS is characterised by higher triglycerides and lower high-density lipoprotein cholesterol (Clark *et al.* 2014, Ladron de Guevara *et al.* 2014, Christ *et al.* 2015, Romualdi *et al.* 2016). It is believed that there are multifactorial causes of dyslipidaemia, however insulin resistance seems to be critical in mediating the stimulation of lipolysis and altering the expression of lipoprotein lipase and hepatic lipase (Ladron de Guevara *et al.* 2014). Factors of cardiovascular risk are inflammation, oxidative stress and impaired fibrinolysis (Barbieri *et al.* 1986). Moreover, higher levels of atherosclerosis markers have been observed in PCOS women, such as endothelial dysfunction, impaired pulse wave velocity, increased thickness of carotid tunica intima and media walls, the presence of carotid plaque and increased coronary artery calcification (Fauser *et al.* 2012, Clark *et al.* 2014).

1.5. Genetic linkage between ovarian development and PCOS

Recent studies indicate that there might be a fetal origin of PCOS (Abbott *et al.* 2006, Li & Huang 2008, Hatzirodos *et al.* 2011, Tata *et al.* 2018). A study in rats has found that higher levels of testosterone (T) early in intrauterine life are associated with anovulatory sterility and the polycystic ovary phenotype in offspring (Foecking *et al.* 2005). Another study in mice showed that prenatal treatment of mice with dihydrotestosterone (DHT) induced PCOS ovarian features, including irregular oestrous cycles, oligo-ovulation, reduced preantral follicle numbers, hepatic steatosis and adipocyte hypertrophy (Caldwell *et al.* 2014).

Studies in rhesus monkeys have shown that prenatally androgenised rhesus monkeys showed characteristics of the PCOS phenotype, such as irregular ovulatory menstrual cycles, ovarian hyperandrogenism, enlarged poly-follicular ovaries and LH hypersecretion, insulin resistance, diminished insulin secretion, increased incidence of type 2 diabetes, visceral adiposity, and hyperlipidaemia in adult life (Abbott *et al.* 2005). These monkeys also showed an impaired glucose-mediated β-cell secretion of insulin (Eisner *et al.* 2000) and a gluco-regulatory deficit (Abbott 2002). Additionally, an exposure carried out in early gestation resulted in female primates with enhanced male-type behaviour, diminished female-like behaviour, as well as genital masculinisation (Goy *et al.* 1988). In later gestation (100-110

days of gestation), exposure to excess androgens in female fetuses results in an adult PCOS-like phenotype, such as high blood levels of androstenedione at birth, increased numbers of primary, preantral and small antral follicles, and increased proliferation of granulosa cells (Abbott *et al.* 2005). Furthermore, mRNA expression levels of genes that are involved in the growth of primordial follicles onwards, such as FSHR, insulin-like growth factor 1 (IGF-1) and IGF-I receptors in granulosa cells were increased (Abbott *et al.* 2005). Impaired insulin action was also observed in these late exposed androgenised monkeys, but not impaired insulin secretion (Eisner *et al.* 2000). Moreover, all female offspring showed increased 5α-reductase and decreased aromatase activities, suggesting impaired follicular maturation, similar to a PCOS ovary (Dumesic *et al.* 2003).

Recently, a study of prenatally AMH treated mice (Tata et al. 2018) showed similar results to the rhesus monkey studies. The exposed mice showed maternal neuroendocrine-driven testosterone excess and diminished placental metabolism of testosterone to oestradiol, resulting in masculinisation of female fetuses and a PCOS-like phenotype in adulthood (Tata *et al.* 2018). This study suggests the important role of excess prenatal AMH exposure in developing the PCOS phenotype in adulthood.

In the bovine fetal ovary, fibrillin-3 (FBN-3) is expressed in the stromal compartment at an early stage of ovarian development (Hatzirodos *et al.* 2011). Fibrillin-3 is an extracellular matrix protein, which controls the bioactivity of TGF-β in the tissue by binding latent TGF-β binding proteins. In the ovaries of PCOS women, increased TGF-β activity has been observed [reviewed in (Raja-Khan *et al.* 2014)]. Additionally, increased amounts of fibrous tissue and collagens have been found in several parts of PCOS ovaries, such as the ovarian capsule and tunica albuginea, as well as the stroma (Hughesdon 1982a). Thus, an altered expression of fibrillin-3 might be a predisposition of having a PCOS phenotype in adulthood.

1.6. Aims of this research

Previous studies in cows and women showed the important involvement of the stroma originating from the mesonephros in the formation of ovigerous cords, follicles, surface epithelium and tunica albuginea. To date, there are limited studies dedicated to the action of the stroma, including its cells and matrices, in ovarian development (Hummitzsch *et al.* 2013, Heeren *et al.* 2015).

The first aim of my research project therefore focuses on the expansion of ovarian stroma during development and relates this to the expression of the stroma-related genes.

Additionally, non-stromal analysis is also conducted to investigate the behaviour of germ cells, GREL cells and granulosa cells during ovarian development.

Dysregulation of ovarian stromal activity has been linked to many reproductive diseases, such as PCOS (Hughesdon 1982a) and premature ovarian failure (Chen *et al.* 2014). Although a recent GWAS study about PCOS candidate genes has opened a new chance of understanding PCOS, little is known about their expression, functions and mechanisms in adult and fetal ovaries.

The second aim of my thesis is to investigate the links between PCOS-related genes and the development of bovine fetal ovaries.

The dynamics of stroma behaviour during bovine fetal development appears to be critical for the formation of surface epithelium. Microscopic studies in cows and women showed that the surface of fetal ovaries undergoes dramatic changes throughout the development of the ovary (Hummitzsch *et al.* 2013, Heeren *et al.* 2015). Firstly, the surface is covered by cells [called gonadal-ridge epithelial like cells (GREL) (Hummitzsch *et al.* 2013), which originate from the surface epithelium of the mesonephros and which change their phenotype to form the somatic cell population of the developing ovary. These GREL cells appear more tightly connected in the outermost layer of the developing surface. With the involvement of the penetrating stroma, multiple GREL cell layers become separated from the remaining underlying ovarian structures, with a basal lamina below these layers. The GREL cells on the surface change their phenotype and, at the final stage, they differentiate into a mature ovarian surface epithelium. However, no specific studies dedicated to the development of the ovarian surface have been conducted to date. It is important to understand the cellular changes in the ovarian surface during fetal development and its relationship with stromal development because their alteration might be the cause of some disorders in adult life. A Scanning Electron Microscope (SEM) has been used to describe the structure of adult and fetal human ovaries, however, these studies were carried out around 40 years ago.

The last aim of my research use a scanning electron microscopic approach to study the formation and development of the ovarian surface throughout gestation in greater detail than heretofore.

1.7. References

Abbott DH 2002 *Developmental origin of polycystic ovary syndrome - a hypothesis*.

Abbott DH, Barnett DK, Bruns CM & Dumesic DA 2005 Androgen excess fetal programming of female reproduction: a developmental aetiology for polycystic ovary syndrome? *Hum Reprod Update* **11** 357-374.

Abbott DH, Padmanabhan V & Dumesic DA 2006 Contributions of androgen and estrogen to fetal programming of ovarian dysfunction. *Reprod Biol Endocrinol* **4** 17.

Abedini A, Zamberlam G, Boerboom D & Price CA 2015 Non-canonical WNT5A is a potential regulator of granulosa cell function in cattle. *Mol Cell Endocrinol* **403** 39-45.

Albamonte MS, Willis MA, Albamonte MI, Jensen F, Espinosa MB & Vitullo AD 2008 The developing human ovary: immunohistochemical analysis of germ-cell-specific VASA protein, BCL-2/BAX expression balance and apoptosis. *Hum Reprod* **23** 1895-1901.

Aliahmad P, de la Torre B & Kaye J 2010 Shared dependence on the DNA-binding factor TOX for the development of lymphoid tissue-inducer cell and NK cell lineages. *Nat Immunol* **11** 945-952.

Aliahmad P & Kaye J 2008 Development of all CD4 T lineages requires nuclear factor TOX. *J Exp Med* **205** 245-256.

Anderson EL, Baltus AE, Roepers-Gajadien HL, Hassold TJ, de Rooij DG, van Pelt AM & Page DC 2008 Stra8 and its inducer, retinoic acid, regulate meiotic initiation in both spermatogenesis and oogenesis in mice. *Proc Natl Acad Sci U S A* **105** 14976-14980.

Anderson RA, Fulton N, Cowan G, Coutts S & Saunders PT 2007 Conserved and divergent patterns of expression of DAZL, VASA and OCT4 in the germ cells of the human fetal ovary and testis. *BMC Dev Biol* **7** 136.

Anttonen M, Ketola I, Parviainen H, Pusa AK & Heikinheimo M 2003 FOG-2 and GATA-4 Are coexpressed in the mouse ovary and can modulate mullerian-inhibiting substance expression. *Biol Reprod* **68** 1333-1340.

Auersperg N, Maines-Bandiera SL, Dyck HG & Kruk PA 1994 Characterization of cultured human ovarian surface epithelial cells: phenotypic plasticity and premalignant changes. *Lab Invest* **71** 510-518.

Auersperg N, Wong AST, Choi K-C, Kang SK & Leung PCK 2001 Ovarian surface epithelium: biology, endocrinology, and pathology. *Endocr Rev* **22** 255-288.

Baarends WM, Uilenbroek JTJ, Kramer P, Hoogerbrugge JW, van Leeuwen ECM, Themmen APN & Grootegoed JA 1995 Anti-Müllerian hormone and anti-Müllerian hormone type II receptor messenger ribonucleic acid expression in rat ovaries during postnatal development, the estrous cycle, and gonadotropin-induced follicle growth. *Endocrinology* **136** 4951-4962.

Bai H, Liu H, Suyalatu S, Guo X, Chu S, Chen Y, Lan T, Borjigin B, Orlov YL, Posukh OL, Yang X, Guilan G, Osipova LP, Wu Q & Narisu N 2015 Association analysis of genetic variants with type 2 diabetes in a mongolian population in china. *J Diabetes Res* **2015** 613236.

Baltus AE, Menke DB, Hu YC, Goodheart ML, Carpenter AE, de Rooij DG & Page DC 2006 In germ cells of mouse embryonic ovaries, the decision to enter meiosis precedes premeiotic DNA replication. *Nat Genet* **38** 1430-1434.

Barbieri RL, Makris A, Randall RW, Daniels G, Kistner RW & Ryan KJ 1986 Insulin stimulates androgen accumulation in incubations of ovarian stroma obtained from women with hyperandrogenism. *J Clin Endocrinol Metab* **62** 904-910.

Bastian NA, Bayne RA, Hummitzsch K, Hatzirodos N, Bonner WM, Hartanti MD, Irving-Rodgers HF, Anderson RA & Rodgers RJ 2016 Regulation of fibrillins and modulators of TGFβ in fetal bovie and human ovaries. *Reproduction* **152** 127-137.

Benahmed M, Morera AM, Ghiglieri C, Tabone E, Menezo Y, Hendrick JC & Franchimont P 1993 Transforming growth factor-βs in the ovary. *Ann N Y Acad Sci* **687** 13-19.

Berkholtz CB, Lai BE, Woodruff TK & Shea LD 2006 Distribution of extracellular matrix proteins type I collagen, type IV collagen, fibronectin, and laminin in mouse folliculogenesis. *Histochem Cell Biol* **126** 583-592.

Blaustein A & Lee H 1979 Surface cells of the ovary and pelvic peritoneum: a histochemical and ultrastructure comparison. *Gynecol Oncol* **8** 34-43.

Bodensteiner KJ, Clay CM, Moeller CL & Sawyer HR 1999 Molecular cloning of the ovine growth/differentiation factor-9 gene and expression of growth/differentiation factor-9 in ovine and bovine ovaries. *Biol Reprod* **60** 381-386.

Bonnamy P, Benhaim A & Leymarie P 1993 Uterine Luteinizing Hormone/Human Chorionic Gonadotropin-Binding sites in the early pregnant rat uterus: evidence for total occupancy in the periimplantation period. *Endocrinology* **132(3)** 7.

Bozdag G, Mumusoglu S, Zengin D, Karabulut E & Yildiz BO 2016 The prevalence and phenotypic features of polycystic ovary syndrome: a systematic review and meta-analysis. *Hum Reprod* **31** 2841-2855.

Bristol SK & Woodruff TK 2004 Follicle-restricted compartmentalization of transforming growth factor beta superfamily ligands in the feline ovary. *Biol Reprod* **70** 846-859.

Burkhart MN, Juengel JL, Smith PR, Heath DA, Perry GA, Smith MF & Garverick HA 2010 Morphological development and characterization of aromatase and estrogen receptors alpha and beta in fetal ovaries of cattle from days 110 to 250. *Anim Reprod Sci* **117** 43-54.

Caldwell AS, Middleton LJ, Jimenez M, Desai R, McMahon AC, Allan CM, Handelsman DJ & Walters KA 2014 Characterization of reproductive, metabolic, and endocrine features of polycystic ovary syndrome in female hyperandrogenic mouse models. *Endocrinology* **155** 3146-3159.

Canty-Laird E, Carre GA, Mandon-Pepin B, Kadler KE & Fabre S 2010 First evidence of bone morphogenetic protein 1 expression and activity in sheep ovarian follicles. *Biol Reprod* **83** 138-146.

Capo-chichi CD, Roland IH, Canderveer L, Bao R, Yamagata T, Hirai H, Cohen C, Hamilton TC, Godwin AK & Xu X-X 2003 Anomalous expresion of epithelial differentiation-determining GATA factors in ovarian tumorigenesis. *Cancer Rese* **63** 4967.

Carabatsos MJ, Elvin JA, Matzuk MM & Albertini DF 1998 Characterization of oocytes and follicle development in growth differentiation factor-9-deficient mice. *Dev Biol* **204** 373-384.

Chambers I, Colby D, Robertson M, Nichols J, Lee S, Tweedie S & Smith A 2003 Functional expression cloning of Nanog, a pluripotency sustaining factor in embryonic stem cells. *Cell* **113** 643-655.

Chen X, Gu C, Ma M, Cong Q, Guo T, Ma D & Li B 2014 A mouse model of premature ovarian insufficiency induced by tripterygium glycoside via subcutaneous injection. *Int J Clin Exp Pathol* **7** 144-151.

Childs AJ, Kinnell HL, Collins CS, Hogg K, Bayne RA, Green SJ, McNeilly AS & Anderson RA 2010 BMP signaling in the human fetal ovary is developmentally regulated and promotes primordial germ cell apoptosis. *Stem Cells* **28** 1368-1378.

Chipuk JE, Cornelius SC, Pultz NJ, Jorgensen JS, Bonham MJ, Kim SJ & Danielpour D 2002 The androgen receptor represses transforming growth factor-beta signaling through interaction with Smad3. *J Biol Chem* **277** 1240-1248.

Christ JP, Vanden Brink H, Brooks ED, Pierson RA, Chizen DR & Lujan ME 2015 Ultrasound features of polycystic ovaries relate to degree of reproductive and metabolic disturbance in polycystic ovary syndrome. *Fertil Steril* **103** 787-794.

Chuva de Sousa Lopes SM & Roelen BA 2010 On the formation of germ cells: The good, the bad and the ugly. *Differentiation* **79** 131-140.

Clark NM, Podolski AJ, Brooks ED, Chizen DR, Pierson RA, Lehotay DC & Lujan ME 2014 Prevalence of Polycystic Ovary Syndrome Phenotypes Using Updated Criteria for Polycystic Ovarian Morphology: An Assessment of Over 100 Consecutive Women Self-reporting Features of Polycystic Ovary Syndrome. *Reprod Sci* **21** 1034-1043.

Cleynen I & Van De Ven WJM 2008 The HMGA proteins: A myriad of functions (Review). *Int. J. Oncol.* **32** 17.

Cocquet J, Pailhoux E, Jaubert F, Servel N, Xia X, Pannetier M, De Baere E, Messiaen L, Cotinot C, Fellous M & Veitia RA 2002 Evoluton and expression of *FOXL2*. *J Med Genet* **39** 916-922.

Cohen PE & Holloway JK 2010 Predicting gene networks in human oocyte meiosis. *Biol Reprod* **82** 469-472.

Cooke HJ, Lee M, Kerr S & Ruggiu M 1996 A murine homologue of the human *DAZ* gene is autosomal and expressed only in male and female gonads. *Hum Mol Genet* **5** 513-516.

Cruet S, Salamanca C, Mitchell GWE & Auersperg N 1999 $\alpha v\beta 3$ and vitronectin expression by normal ovarian surface epithelial cells: role in cell adhesion and cell proliferation. *Gynecol Oncol* **75** 254-260.

da Silva SJM, Bayne RAL, Cambray N, Hartley PS, McNeilly AS & Anderson RA 2004 Expression of activin subunits and receptors in the developing human ovary: activin A promotes germ cell survival and proliferation before primordial follicle formation. *Developmental Biology* **266** 334-345.

Davies BR, Worsley SD & Ponder BAJ 1998 Expression of E-cadherin, α-catenin and β-catenin in normal ovarian surface epithelium and epithelial ovarian cancers. *Histopathology* **32** 69-80.

Davis MR & Summers KM 2012 Structure and function of the mammalian fibrillin gene family: implications for human connective tissue diseases. *Mol Genet Metab* **107** 635-647.

Day FR, Hinds DA, Tung JY, Stolk L, Styrkarsdottir U, Saxena R, Bjonnes A, Broer L, Dunger DB, Halldorsson BV, Lawlor DA, Laval G, Mathieson I, McCardle WL, Louwers Y, Meun C, Ring S, Scott RA, Sulem P, Uitterlinden AG, Wareham NJ, Thorsteinsdottir U, Welt C, Stefansson K, Laven JS, Ong KK & Perry JR 2015 Causal mechanisms and balancing selection inferred from genetic associations with polycystic ovary syndrome. *Nat Commun* **6** 8464.

Demtroder KB 2013 TOX3 (TNRC9) over expression in bladder cancer cells decreases cellular proliferation and triggers an Interferon-Like response. *Journal of Molecular Biomarkers & Diagnosis* **04**.

Derecka K, Pietila EM, Rajaniemi HJ & Ziecik AJ 1995 Cycle dependent LH/hCG receptor gene expression in porcine nongonadal reproductive tissues. *J Physiol Pharmacol* **46(1)** 9.

Diamanti-Kandarakis E 2008 Polycystic ovarian syndrome: pathophysiology, molecular aspects and clinical implications. *Expert Rev Mol Med* **10** e3.

Diaz-Perales A, Quesada V, Sanchez LM, Ugalde AP, Suarez MF, Fueyo A & Lopez-Otin C 2005 Identification of human aminopeptidase O, a novel metalloprotease with structural similarity to aminopeptidase B and leukotriene A4 hydrolase. *J Biol Chem* **280** 14310-14317.

Dong J, Albertini DF, Nishimori K, Kumar TR, Lu N & Matzuk MM 1996 Growth differentiation factor-9 is required during early ovarian folliculogenesis. *Nature* **383** 531-535.

Dubeau L 1999 The cell of origin of ovarian epithelial tumors and the ovarian surface epithelium dogma: does the emperor have no clothes? *Gynecol Oncol* **72** 437-442.

Dumesic DA, Schramm RD, Bird IM, Peterson E, Paprocki AM, Zhou R & Abbott DH 2003 Reduced intrafollicular androstenedione and estradiol levels in early-treated prenatally androgenized female rhesus monkeys receiving follicle-stimulating hormone therapy for in vitro fertilization. *Biol Reprod* **69** 1213-1219.

Dunaif A 2016 Perspectives in Polycystic Ovary Syndrome: from hair to eternity. *J Clin Endocrinol Metab* **101** 759-768.

Dunkel L, Tilly JL, Shikone T, Nishimori K & Hsueh AJW 1994 Follicle-stimulating hormone receptor expression in the rat ovary: increases during prepubertal development and regulation by the opposing actions of transforming growth factors β and α. *Biol Reprod* **50** 940-948.

Durlinger ALL, Kramer P, Karels B, De Jong FH, Uilenbroek JTJ, Grootegoed JA & Themmen APN 1990 Control of primordial follicle recruitment by Anti-Mullerian Hormone in the mouse ovary. *Endocronology* **140(12)** 8.

Durlinger ALL, Kramer P, Karels B, De Jong FH, Uilenbroek JTJ, Grootegoed JA & Themmen APN 1999 Control of primordial dollicle recruitment by anti-Müllerian hormone in the mouse ovary. *Endocrinology* **140** 5789-5796.

Ehrmann DA, Liljenquist DR, Kasza K, Azziz R, Legro RS, Ghazzi MN & Group PCTS 2006 Prevalence and predictors of the metabolic syndrome in women with polycystic ovary syndrome. *J Clin Endocrinol Metab* **91** 48-53.

Eisner JR, Dumesic DA, Kemnitz JW & Abbott DH 2000 Timing of prenatal androgen excess determines differential impairment in insulin secretion and action in adult female rhesus monkeys. *85* **3** 1206-1210.

Elsafadi M, Manikandan M, Atteya M, Abu Dawud R, Almalki S, Ali Kaimkhani Z, Aldahmash A, Alajez NM, Alfayez M, Kassem M & Mahmood A 2017 SERPINB2 is a novel TGFbeta-responsive lineage fate determinant of human bone marrow stromal cells. *Sci Rep* **7** 10797.

Erickson GF & Shimasaki S 2003 The spatiotemporal expression pattern of the bone morphogenetic protein family in rat ovary cell types during the estrous cycle. *Reprod Biol Endocrinol* **1** 1-20.

Fauser BC, Tarlatzis BC, Rebar RW, Legro RS, Balen AH, Lobo R, Carmina E, Chang J, Yildiz BO, Laven JS, Boivin J, Petraglia F, Wijeyeratne CN, Norman RJ, Dunaif A, Franks S, Wild RA, Dumesic D & Barnhart K 2012 Consensus on women's health aspects of polycystic ovary syndrome (PCOS):

the Amsterdam ESHRE/ASRM-Sponsored 3rd PCOS Consensus Workshop Group. *Fertil Steril* **97** 28-38 e25.

Fedele M, Palmieri D & Fusco A 2010 HMGA2: A pituitary tumour subtype-specific oncogene? *Mol Cell Endocrinol* **326** 19-24.

Feng CW, Bowles J & Koopman P 2014 Control of mammalian germ cell entry into meiosis. *Mol Cell Endocrinol* **382** 488-497.

Feng P, Catt KJ & Knecht M 1988 Transforming growth factor-β stimulates meiotic maturation of the rat oocyte. *Endocrinology* **122** 181-186.

Fine A & Goldstein RH 1987 The Effect of Transforming Growth Factor-β on Cell proliferation and colagen Formation by Lung Fibrobla. *J Biol Chem* **262 (8)** 6.

Flesken-Nikitin A, Hwang CI, Cheng CY, Michurina TV, Enikolopov G & Nikitin AY 2013 Ovarian surface epithelium at the junction area contains a cancer-prone stem cell niche. *Nature* **495** 241-245.

Foecking EM, Szabo M, Schwartz NB & Levine JE 2005 Neuroendocrine consequences of prenatal androgen exposure in the female rat: absence of luteinizing hormone surges, suppression of progesterone receptor gene expression, and acceleration of the gonadotropin-releasing hormone pulse generator. *Biol Reprod* **72** 1475-1483.

Fortune JE, Yang MY & Muruvi W 2010 The earliest stages of follicular development: Follicle formation and activation. *Society of Reproduction and Fertility supplement* **67** 203-216.

Fowler PA, Anderson RA, Saunders PT, Kinnell H, Mason JI, Evans DB, Bhattacharya S, Flannigan S, Franks S, Monteiro A & O'Shaughnessy PJ 2011 Development of steroid signaling pathways during primordial follicle formation in the human fetal ovary. *J Clin Endocrinol Metab* **96** 1754-1762.

Franceschini A, Szklarczyk D, Frankild S, Kuhn M, Simonovic M, Roth A, Lin J, Minguez P, Bork P, von Mering C & Jensen LJ 2013 STRING v9.1: protein-protein interaction networks, with increased coverage and integration. *Nucleic Acids Res* **41** D808-815.

Frota IM, Leitao CC, Costa JJ, van den Hurk R, Saraiva MV, Figueiredo JR & Silva JR 2013 Levels of BMP-6 mRNA in goat ovarian follicles and in vitro effects of BMP-6 on secondary follicle development. *Zygote* **21** 270-278.

Gao Y, Wang Y, Li Y, Xia X, Zhao S, Che Y, Sun Y & Lei L 2016 TGF-beta1 promotes bovine mammary fibroblast proliferation through the ERK 1/2 signalling pathway. *Cell Biol Int* **40** 750-760.

Garverick HA, Juengel JL, Smith P, Heath DA, Burkhart MN, Perry GA, Smith MF & McNatty KP 2010 Development of the ovary and ontongeny of mRNA and protein for P450 aromatase (arom) and estrogen receptors (ER) alpha and beta during early fetal life in cattle. *Anim Reprod Sci* **117** 24-33.

Gattas GJ, Quade BJ, Nowak RA & Morton CC 1999 *HMGIC* expression in human adult and fetal tissues and in uterine leiomyomata. *Gene Chrosome Canc* **25(4)** 7.

Glinka A, Wu W, Delius H, Monaghan AP, Blumenstock C & Niehrs C 1998 Dickkopf-1 is a member of a new family of secreted proteins and functions in head induction. *Nature* **391** 357-362.

Glister C, Kemp CF & Knight PG 2004 Bone morphogenetic protein (BMP) ligands and receptors in bovine ovarian follicle cells: actions of BMP-4, -6 and -7 on granulosa cells and differential modulation of Smad-1 phosphorylation by follistatin. *Reproduction* **127** 239-254.

Goto K, Kamiya Y, Imamura T, Miyazono K & Miyazawa K 2007 Selective inhibitory effects of Smad6 on bone morphogenetic protein type I receptors. *J Biol Chem* **282** 20603-20611.

Govinden R & Bhoola KD 2003 Genealogy, expression, and cellular function of transforming growth factor-β. *Pharmacology & Therapeutics* **98** 257-265.
Goy RW, Bercovitch FB & McBrair MC 1988 Behavioral masculinization is independent of genital masculinization in prenatally androgenized female rhesus macaques. *Horm Behav* **22** 552-571.
Gressner AM, Weiskirchen R, Breitkopf K & Dooley S 2002 ROLES OF TGF-beta IN HEPATIC FIBROSIS. *Frontiers in Bioscience* 7d793-807.
Grosse A, Bartsch S & Baniahmad A 2012 Androgen receptor-mediated gene repression. *Mol Cell Endocrinol* **352** 46-56.
Guo Y, Martin LJ, Hanna W, Banerjee D, Miller N, Fishell E, Khokha R & Boyd NF 2001 Growth factors and stromal matrix proteins associated with mammographic densities. **10** 6.
Han YJ, Zhang J, Zheng Y, Huo D & Olopade OI 2016 Genetic and epigenetic regulation of TOX3 expression in breast cancer. *PLoS One* **11** e0165559.
Harvey KF, Zhang X & Thomas DM 2013 The Hippo pathway and human cancer. *Nat Rev Cancer* **13** 246-257.
Harwood BN, Cross SK, Radford EE, Haac BE & De Vries WN 2008 Members of the WNT signaling pathways are widely expressed in mouse ovaries, oocytes, and cleavage stage embryos. *Dev Dyn* **237** 1099-1111.
Hatzirodos N, Bayne RA, Irving-Rodgers HF, Hummitzsch K, Sabatier L, Lee S, Bonner W, Gibson MA, Rainey WE, Carr BR, Mason HD, Reinhardt DP, Anderson RA & Rodgers RJ 2011 Linkage of regulators of TGF-beta activity in the fetal ovary to polycystic ovary syndrome. *FASEB J* **25** 2256-2265.
Hawes D, Downey S, Pearce CL, Bartow S, Wan P, Pike MC & Wu AH 2006 Dense breast stromal tissue shows greatly increased concentration of breast epithelium but no increase in its proliferative activity. *Breast Cancer Res* **8** R24.
Heeren AM, van Iperen L, Klootwijk DB, de Melo Bernardo A, Roost MS, Gomes Fernandes MM, Louwe LA, Hilders CG, Helmerhorst FM, van der Westerlaken LA & Chuva de Sousa Lopes SM 2015 Development of the follicular basement membrane during human gametogenesis and early folliculogenesis. *BMC Dev Biol* **15** 4.
Hetzel M, Bachem M, Anders D, Trischler G & Faehling M 2005 Different effects of growth factors on proliferation and matrix production of normal and fibrotic human lung fibroblasts. *Lung* **183** 225-237.
Hirota Y, Kuronita T, Fujita H & Tanaka Y 2007 A role for Rab5 activity in the biogenesis of endosomal and lysosomal compartments. *Biochem Biophys Res Commun* **364** 40-47.
Hirshfeld-Cytron J, Barnes RB, Ehrmann DA, Caruso A, Mortensen MM & Rosenfield RL 2009 Characterization of functionally typical and atypical types of polycystic ovary syndrome. *J Clin Endocrinol Metab* **94** 1587-1594.
Hreinsson JG, Scott JE, Rasmussen C, Swahn ML, Hsueh AJW & Hovatta O 2002 Growth differentiation factor-9 promotes the growth, development, and survival of human ovarian follicles in organ culture. *J Clin Endocrinol Metab* **87** 316-321.
Hsieh M, Johnson MA, Greenberg NM & Richards JS 2002 Regulated expression of Wnts and Frizzleds at specific stages of folicular development in the rodent ovary. *Endocrinology* **143** 898-908.
Hu YC, Okumura LM & Page DC 2013 *Gata4* is required for formation of the genital ridge in mice. *PLoS Genet* **9** 12.
Hughesdon PE 1982a Morphology and morphogenesis of the Stein-Leventhal ovary and of so-called "hyperthecosis". *Obstet Gynecol Surv* **37** 59-77.

Hughesdon PE 1982b Morphology and morphogenesis of the Stein-Leventhal ovary and of so-called "Hyperthecosis". *Obstet Gynecol Surv* **37(2)** 19.

Hummitzsch K, Anderson RA, Wilhelm D, Wu J, Telfer EE, Russell DL, Robertson SA & Rodgers RJ 2015 Stem cells, progenitor cells, and lineage decisions in the ovary. *Endocr Rev* **36** 65-91.

Hummitzsch K, Irving-Rodgers HF, Hatzirodos N, Bonner W, Sabatier L, Reinhardt DP, Sado Y, Ninomiya Y, Wilhelm D & Rodgers RJ 2013 A new model of development of the mammalian ovary and follicles. *PLoS One* **8** e55578.

Jaatinen T-A, Penttilä T-L, Kaipia A, Ekfors T, Parvinen M & Toppari J 1994 Expression of inhibin α, β_A and β_B messanger ribonucleic acids in the normal human ovary and in polycystic ovarian syndrome. *J Endocrinol* **143** 127-137.

Jehle K, Cato L, Neeb A, Muhle-Goll C, Jung N, Smith EW, Buzon V, Carbo LR, Estebanez-Perpina E, Schmitz K, Fruk L, Luy B, Chen Y, Cox MB, Brase S, Brown M & Cato AC 2014 Coregulator control of androgen receptor action by a novel nuclear receptor-binding motif. *J Biol Chem* **289** 8839-8851.

Jensen JD & Odell WD 1988 Identification of LH/hCG receptors in rabbit uterus. *Proc Soc Exp Biol Med* **189** 3.

Ji SY, Liu XM, Li BT, Zhang YL, Liu HB, Zhang YC, Chen ZJ, Liu J & Fan HY 2017 The polycystic ovary syndrome-associated gene Yap1 is regulated by gonadotropins and sex steroid hormones in hyperandrogenism-induced oligo-ovulation in mouse. *Mol Hum Reprod* **23** 698-707.

Jonard S & Dewailly D 2004 The follicular excess in polycystic ovaries, due to intraovarian hyperandrogenism, may be the main culprit for the follicular arrest. *Hum Reprod* **10** 107-117.

Jones MR & Goodarzi MO 2016 Genetic determinants of polycystic ovary syndrome: progress and future directions. *Fertil Steril* **106** 25-32.

Juengel JL, Heath DA, Quirke LD & McNatty KP 2006a Oestrogen receptor alpha and beta, androgen receptor and progesterone receptor mRNA and protein localisation within the developing ovary and in small growing follicles of sheep. *Reproduction* **131** 81-92.

Juengel JL & McNatty KP 2005 The role of proteins of the transforming growth factor-beta superfamily in the intraovarian regulation of follicular development. *Hum Reprod Update* **11** 143-160.

Juengel JL, Reader KL, Bibby AH, Lun S, Ross I, Haydon LJ & McNatty KP 2006b The role of bone morphogenetic proteins 2, 4, 6 and 7 during ovarian follicular development in sheep: contrast to rat. *Reproduction* **131** 501-513.

Juengel JL & Smith P. 2014. Formation of ovarian follicles in ruminants. In *Reproduction in Domestic Ruminants VIII*.

Kanda T, Jiang X & Yokosuka O 2014 Androgen receptor signaling in hepatocellular carcinoma and pancreatic cancers. *World J Gastroenterol* **20** 9229-9236.

Kashimada K, Pelosi E, Chen H, Schlessinger D, Wilhelm D & Koopman P 2011 FOXL2 and BMP2 act cooperatively to regulate follistatin gene expression during ovarian development. *Endocrinology* **152** 272-280.

Kato S, Yokoyama A & Fujiki R 2011 Nuclear receptor coregulators merge transcriptional coregulation with epigenetic regulation. *Trends Biochem Sci* **36** 272-281.

Kenngott RA, Sauer U, Vermehren M & Sinowatz F 2014 Expression of Intermediate Filaments and Germ Cell Markers in the Developing Bovine Ovary: An Immunohistochemical and Laser-Assisted Microdissection Study. *Cells Tissues Organs* **200** 153-170.

Kenngott RA, Vermehren M, Ebach K & Sinowatz F 2013 The role of ovarian surface epithelium in folliculogenesis during fetal development of the bovine ovary: a histological and immunohistochemical study. *Sex Dev* **7** 180-195.

Kerns SL, Ostrer H, Stock R, Li W, Moore J, Pearlman A, Campbell C, Shao Y, Stone N, Kusnetz L & Rosenstein BS 2010 Genome-wide association study to identify single nucleotide polymorphisms (SNPs) associated with the development of erectile dysfunction in African-American men after radiotherapy for prostate cancer. *Int J Radiat Oncol Biol Phys* **78** 1292-1300.

Kerr CL, Hill CM, Blumenthal PD & Gearhart JD 2008 Expression of pluripotent stem cell markers in the human fetal ovary. *Hum Reprod* **23** 589-599.

Khan R & Sheppard R 2006 Fibrosis in heart disease: understanding the role of transforming growth factor-beta in cardiomyopathy, valvular disease and arrhythmia. *Immunology* **118** 10-24.

Kiewisz J, Kaczmarek MM, Morawska E, Blitek A, Kapelanski W & Ziecik AJ 2011 Estrus synchronization affects WNT signaling in the porcine reproductive tract and embryos. *Theriogenology* **76** 1684-1694.

Kimura F, Bonomi LM & Schneyer AL 2011 Follistatin regulates germ cell nest breakdown and primordial follicle formation. *Endocrinology* **152** 697-706.

Kisseleva T & Brenner DA 2007 Role of hepatic stellate cells in fibrogenesis and the reversal of fibrosis. *J Gastroenterol Hepatol* **22 Suppl 1** S73-78.

Knight PG & Glister C 2006 TGF-beta superfamily members and ovarian follicle development. *Reproduction* **132** 191-206.

Konishi I, Fujii S, Okamura H, Parmley T & Mori T 1986 Development of interstitial cells and ovigerous cords in the human fetal ovary: an ultrastructural study. *J Anat* **148** 121-135.

Kruk PA, Uitto V-J, Firth JD, Dedhar S & Auersperg N 1994 Reciprocal interactions between human ovarian surface epithelial cells and adjacent extracellular matrix. *Exp Cell Res*.

Ladron de Guevara A, Fux-Otta C, Crisosto N, Szafryk de Mereshian P, Echiburu B, Iraci G, Perez-Bravo F & Sir-Petermann T 2014 Metabolic profile of the different phenotypes of polycystic ovary syndrome in two Latin American populations. *Fertil Steril* **101** 1732-1739 e1731-1732.

Lagerstrom MC & Schioth HB 2008 Structural diversity of G protein-coupled receptors and significance for drug discovery. *Nat Rev Drug Discov* **7** 339-357.

Lavoie HA, McCoy GL & Blake CA 2004 Expression of the GATA-4 and GATA-6 transcription factors in the fetal rat gonad and in the ovary during postnatal development and pregnancy. *Mol Cell Endocrinol* **227** 31-40.

LeClair R & Lindner V 2007 The role of collagen triple helix repeat containing 1 in injured arteries, collagen expression, and transforming growth factor beta signaling. *Trends Cardiovasc Med* **17** 202-205.

Lee J & Pilch PL 1994 The Insulin Receptor: structure, function, and signalling. *Am J Physiol* **266** 16.

Lei L, Zhang H, Jin S, Wang F, Fu M, Wang H & Xia G 2006 Stage-specific germ-somatic cell interaction directs the primordial folliculogenesis in mouse fetal ovaries. *J Cell Physiol* **208** 640-647.

Lembong J, Yakoby N & Shvartsman SY 2008 Spatial regulation of BMP signaling by patterned receptor expression. *Tissue Eng Part A* **14** 1469-1477.

Li M, Zhao H, Zhao S-G, Wei D-M, Zhao Y-R, Huang T, Muhammad T, Yan L, Gao F, Li L, Lu G, Chan W-Y, Leung PCK, Dunaif A, Liu H-B & Chen Z-J 2018 The HMGA2-IMP2 Pathway Promotes Granulosa Cell Proliferation in Polycystic Ovary Syndrome. *The Journal of Clinical Endocrinology & Metabolism* **104** 1049-1059.

Li T, Sun L, Miller N, Nicklee T, Woo J, Hulse-Smith L, Tsao M, Khokha R, Martin L & Boyd NF 2005 The association of measured breast tissue characteristics with mammographic density and other risk factors for breast cancer. *Cancer Epidemiol Biomarkers Prev* **14(2)** 7.

Li Z & Huang H 2008 Epigenetic abnormality: a possible mechanism underlying the fetal origin of polycystic ovary syndrome. *Med Hypotheses* **70** 638-642.

Liang L, Soyal SM & Dean J 1997 FIGα, a germ cell specific transcription factor involved in the coordinate expression of the zona pellucida genes. *Development* **124** 4939-4947.

Lin Y & Page DC 2005 Dazl deficiency leads to embryonic arrest of germ cell development in XY C57BL/6 mice. *Dev Biol* **288** 309-316.

Liu C, Peng J, Matzuk MM & Yao HH 2015 Lineage specification of ovarian theca cells requires multicellular interactions via oocyte and granulosa cells. *Nat Commun* **6** 6934.

Liu L, Zhou W, Cheng CT, Ren X, Somlo G, Fong MY, Chin AR, Li H, Yu Y, Xu Y, O'Connor ST, O'Connor TR, Ann DK, Stark JM & Wang SE 2014 TGFbeta induces "BRCAness" and sensitivity to PARP inhibition in breast cancer by regulating DNA-repair genes. *Mol Cancer Res* **12** 1597-1609.

Liu Y, Li Y, Li N, Teng W, Wang M, Zhang Y & Xiao Z 2016 TGF-beta1 promotes scar fibroblasts proliferation and transdifferentiation via up-regulating MicroRNA-21. *Sci Rep* **6** 32231.

Ma YJ, Hill DF, Creswick KE, Costa ME, Cornea A, Lioubin MN, Plowman GD & Ojeda SR 1999 Neuregulins signaling via a Glial erbB-2–erbB-4 Receptor complex contribute to the neuroendocrine control of mammalian sexual development. *J. Neurosci.* **19(22)** 15.

Maciel GA, Baracat EC, Benda JA, Markham SM, Hensinger K, Chang RJ & Erickson GF 2004 Stockpiling of transitional and classic primary follicles in ovaries of women with polycystic ovary syndrome. *J Clin Endocrinol Metab* **89** 5321-5327.

Magarelli PC, Zachow RJ & Magoffin DA 1996 Developmental and hormonal regulation of rat theca-cell differentiation factor secretion in ovarian follicles. *Biol Reprod* **55** 416-420.

Mamsen LS, Brochner CB, Byskov AG & Mollgard K 2012 The migration and loss of human primordial germ stem cells from the hind gut epithelium towards the gonadal ridge. *Int J Dev Biol* **56** 771-778.

Manuylov NL, Smagulova FO, Leach L & Tevosian SG 2008 Ovarian development in mice requires the GATA4-FOG2 transcription complex. *Development* **135** 3731-3743.

Matsui Y 2010 The molecular mechanisms regulating germ cell development and potential. *J Androl* **31** 61-65.

McAllister JM, Byrd W & Simpson ER 1994 The effect of growth factors and phorbol esters on steroid biosynthesis in isolated human theca interna and granulosa-lutein cells in long term culture. *J Clin Endocrinol Metab* **79** 106-112.

McAllister JM, Modi B, Miller BA, Biegler J, Bruggeman R, Legro RS & Strauss JF, 3rd 2014 Overexpression of a DENND1A isoform produces a polycystic ovary syndrome theca phenotype. *Proc Natl Acad Sci U S A* **111** E1519-1527.

McCoard SA, Wise TH, Fahrenkrug SC & Ford JJ 2001 Temporal and spatial localization patterns of *Gata4* during porcine gonadogenesis. *Biology of Reproduction* **65** 366-374.

McGee EA & Hsueh AJW 2000 Initial and Cyclic Recruitment of Ovarian Follicles. *Endocr Rev* **21** 15.

McNatty KP, Juengel JL, Wilson T, Galloway SM & Davis GH 2001 Genetic mutations influencing ovulation rate in sheep. *Reprod Fertil Dev* **13** 549-555.

McNeilly JR, Saunders PTK, Taggart M, Cranfield M, Cooke HJ & McNeilly AS 2000 Loss of oocytes in Dazl knockout mice results in maintained ovarian steroidogenic function but altered gonadotropin secretion in adult animals. *Endocrinology* **141** 4284-4294.

Meduri G, Bachelot A, Cocca MP, Vasseur C, Rodien P, Kuttenn F, Touraine P & Misrahi M 2008 Molecular pathology of the FSH receptor: new insights into FSH physiology. *Mol Cell Endocrinol* **282** 130-142.

Menke DB & Page DC 2002 Sexually dimorphic gene expression in the developing mouse gonad. *Gene Expression Patterns* **2** 359-367.

Meyts ER-D, Hanstein R, Jørgensne N, Graem N, Vogt PH & Skakkebaek NE 2004 Developmental expression of *POU5F1* (OCT-3/4) in normal and dysgenetic human gonads. *Hum Reprod* **19** 1338-1344.

Meyts ER, Jørgensen N, Græm N, Műller J, Cate RL & Skakkebæk NE 1999 Expression of Anti-Műllerian Hormone during normal and pathological gonadal development: association with differentiation of Sertoli and Granulosa cells. *J Clin Endocrinol Metab* **84** 3836-3844.

Mitsui K, Tokuzawa Y, Itoh H, Segawa K, Murakami M, Takahashi K, Maruyama M, Maeda M & Yamanaka S 2003 The homeprotein Nanog is required for maintenance of pluripotency in mouse epiblast and ES cells. *Cells* **113** 631-642.

Miyagi M, Mikawa S, Sato T, Hasegawa T, Kobayashi S, Matsuyama Y & Sato K 2012 BMP2, BMP4, noggin, BMPRIA, BMPRIB, and BMPRII are differentially expressed in the adult rat spinal cord. *Neuroscience* **203** 12-26.

Miyoshi T, Otsuka F, Suzuki J, Takeda M, Inagaki K, Kano Y, Otani H, Mimura Y, Ogura T & Makino H 2006 Mutual regulation of follicle-stimulating hormone signaling and bone morphogenetic protein system in human granulosa cells. *Biol Reprod* **74** 1073-1082.

Mondschein JS, Canning SF & Hammond JM 1988 Effects of transforming growth factor-β on the production of immunoreactive insulin-like growth factor I and progesterone and on [^{3}H]thymidine incorporation in porcine granulosa cell cultures. *Endocrinology* **123** 1970-1976.

Morceau F, Schnekenburger M, Dicato M & Diederich M 2004 GATA-1: friends, brothers, and coworkers. *Ann N Y Acad Sci* **1030** 537-554.

Motta PM, Makabe S & Nottola SA 1997 The ultrastructure of human reproduction. I. The natural history of the female germ cell: origin, migration and differentiation inside the developing ovary. *Hum Reprod Update* **3** 281-295.

Munir I, Yen HW, Geller DH, Torbati D, Bierden RM, Weitsman SR, Agarwal SK & Magoffin DA 2004 Insulin augmentation of 17alpha-hydroxylase activity is mediated by phosphatidyl inositol 3-kinase but not extracellular signal-regulated kinase-1/2 in human ovarian theca cells. *Endocrinology* **145** 175-183.

Murdoch WJ 1994 Ovarian surface epithelium during ovulatory and anovulatory ovine estrous cycles. *Anat Rec* **240** 322-326.

Nelson VL, Legro RS, Strauss III JF & McAllister JM 1999 Augmented Androgen Production Is a Stable Steroidogenic Phenotype of Propagated Theca Cells from Polycystic Ovaries. *Mol Endocrinol* **13** 946-957.

Ng A, Tan S, Singh G, Rizk P, Swathi Y, Tan TZ, Huang RY, Leushacke M & Barker N 2014 Lgr5 marks stem/progenitor cells in ovary and tubal epithelia. *Nat Cell Biol* **16** 745-757.

Nicosia SV, Saunders BO, Acevedo-Duncan ME, Setrakian S & Degregorio R 1991. Biopathology of ovarian mesothelium. In *Ultrastructure of the ovary*, pp. 287-310.

Nilsson EE & Skinner MK 2002 Growth and Differentiation Factor-9 Stimulates Progression of Early Primary but Not Primordial Rat Ovarian Follicle Development1. *Biology of Reproduction* **67** 1018-1024.

Ning Z, Jiayi L, Jian R & Wanli X 2017 Relationship between abnormal TOX3 gene methylation and polycystic ovarian syndrome. *Eur Rev Med Pharmacol Sci* **21** 5.

Nishino J, Kim I, Chada K & Morrison SJ 2008 Hmga2 promotes neural stem cell self-renewal in young but not old mice by reducing p16Ink4a and p19Arf Expression. *Cell* **135** 227-239.

Nogueira MFG, Fernandes P, Ereno RL, Simões RAL, Junior JB & Barros CM 2010 Luteinizing Hormone Receptor (LHR): basic concepts in cattle and other mammals. A review. *Anim. Reprod* **7(2)** 14.

Ohta Y, Nakagawa K, Imai Y, Katagiri T, Koike T & Takaoka K 2008 Cyclic AMP enhances Smad-mediated BMP signaling through PKA-CREB pathway. *J Bone Miner Metab* **26** 478-484.

Oshino N & Chance B 1975 The properties of Sulfite Oxidation in perfused rat liver; interaction of Sulfite Oxidase with the mitochondrial respiratory chain. *Arch. Biochem. Biophys.* **170** 15.

Otsuka F, Yao Z, Lee T, Yamamoto S, Erickson GF & Shimasaki S 2000 Bone morphogenetic protein-15. Identification of target cells and biological functions. *J Biol Chem* **275** 39523-39528.

Pal D, Pertot A, Shirole NH, Yao Z, Anaparthy N, Garvin T, Cox H, Chang K, Rollins F, Kendall J, Edwards L, Singh VA, Stone GC, Schatz MC, Hicks J, Hannon GJ & Sordella R 2017 TGF-beta reduces DNA ds-break repair mechanisms to heighten genetic diversity and adaptability of CD44+/CD24- cancer cells. *Elife* **6**.

Pangas SA, Rademaker AW, Fishman DA & Woodruff TK 2002 Localization of the activin signal transduction components in normal human ovarian follicles: implications for autocrine and paracrine signaling in the ovary. *J Clin Endocrinol Metab* **87** 2644-2657.

Pepling ME & Spradling AC 2001 Mouse ovarian germ cell cysts undergo programmed breakdown to form primordial follicles. *Dev Biol* **234** 339-351.

Piek E & Roberts AB 2001 Suppressor and oncogenic roles of transforming grwoth factor-β and its signalling pathways in tumorigenesis. *Adv Cancer Res* **83** 1-54.

Pierre A, Pisselet C, Dupont J, Bontoux M & Monget P 2005 Bone morphogenetic protein 5 expression in the rat ovary: biological effects on granulosa cell proliferation and steroidogenesis. *Biol Reprod* **73** 1102-1108.

Pitetti JL, Torre D, Conne B, Papaioannou MD, Cederroth CR, Xuan S, Kahn R, Parada LF, Vassalli JD, Efstratiadis A & Nef S 2009 Insulin receptor and IGF1R are not required for oocyte growth, differentiation, and maturation in mice. *Sex Dev* **3** 264-272.

Prodoehl MJ, Hatzirodos N, Irving-Rodgers HF, Zhao ZZ, Painter JN, Hickey TE, Gibson MA, Rainey WE, Carr BR, Mason HD, Norman RJ, Montgomery GW & Rodgers RJ 2009a Genetic and gene expression analyses of the polycystic ovary syndrome candidate gene fibrillin-3 and other fibrillin family members in human ovaries. *Mol Hum Reprod* **15** 829-841.

Prodoehl MJ, Irving-Rodgers HF, Bonner WM, Sullivan TM, Micke GC, Gibson MA, Perry VE & Rodgers RJ 2009b Fibrillins and latent TGFbeta binding

proteins in bovine ovaries of offspring following high or low protein diets during pregnancy of dams. *Mol Cell Endocrinol* **307** 133-141.

Prud'homme GJ 2007 Pathobiology of transforming growth factor beta in cancer, fibrosis and immunologic disease, and therapeutic considerations. *Lab Invest* **87** 1077-1091.

Raja-Khan N, Urbanek M, Rodgers RJ & Legro RS 2014 The role of TGF-beta in polycystic ovary syndrome. *Reprod Sci* **21** 20-31.

Rannikki AS, Zhang F & Huhtaniemi IT 1995 Ontogeny of follicle-stimulating hormone receptor gene expression in the rat testis and ovary. *Mol Cell Endocrinol* **107** 10.

Reshef E, Lei ZM, Rao CV, Pridham DD, Chegini G & Luborsky JL 1990 The presence of Gonadotropin Receptors in nonpregnant human uterus, human placenta, fetal membranes, and decidua. *J Clin Endocrinol Metab* **70(2)** 10.

Rice S, Ojha K, Whitehead S & Mason H 2007 Stage-specific expression of androgen receptor, follicle-stimulating hormone receptor, and anti-Mullerian hormone type II receptor in single, isolated, human preantral follicles: relevance to polycystic ovaries. *J Clin Endocrinol Metab* **92** 1034-1040.

Richards JS 1994 Hormonal control of gene expression in the ovary. *Endocrine Reviews* **15(6)** 27.

Rippe V, Drieschner N, Meiboom M, Murua Escobar H, Bonk U, Belge G & Bullerdiek J 2003 Identification of a gene rearranged by 2p21 aberrations in thyroid adenomas. *Oncogene* **22** 6111-6114.

Roberts VJ, Barth S, El-Roeiy A & Yen SSC 1994 Expression of inhibin/activin system messanger ribonucleic acids and proteins in ovarian follicles from women with polycystic ovarian syndrome. *J Clin Endocrinol Metab* **79** 1434-1439.

Rodgers RJ & Irving-Rodgers HF 2010 Morphological classification of bovine ovarian follicles. *Reproduction* **139** 309-318.

Romualdi D, Di Florio C, Tagliaferri V, De Cicco S, Gagliano D, Immediata V, Lanzone A & Guido M 2016 The Role of Anti-Mullerian Hormone in the Characterization of the Different Polycystic Ovary Syndrome Phenotypes. *Reprod Sci* **23** 655-661.

Ross AJ, Tilman C, Yao H, MacLaughlin D & Capel B 2003 AMH induces mesonephric cell migration in XX gonads. *Molecular and Cellular Endocrinology* **211** 1-7.

Ross DG, Bowles J, Hope M, Lehnert S & Koopman P 2009 Profiles of gonadal gene expression in the developing bovine embryo. *Sex Dev* **3** 273-283.

Rossi RO, Costa JJ, Silva AW, Saraiva MV, Van den Hurk R & Silva JR 2016 The bone morphogenetic protein system and the regulation of ovarian follicle development in mammals. *Zygote* **24** 1-17.

Samoto T, Maruo T, Ladines-Llave CA, Matsuo H, Deguchi J, Barnea ER & Mochizuki M 1993 Insulin receptor expression in follicular and stromal compartments of the human ovary over the course of follicular growth, regression and atresia. *Endocrine Journal* **40** 12.

Sanchez AM, Vigano P, Quattrone F, Pagliardini L, Papaleo E, Candiani M & Panina-Bordignon P 2014 The WNT/beta-catenin signaling pathway and expression of survival promoting genes in luteinized granulosa cells: endometriosis as a paradigm for a dysregulated apoptosis pathway. *Fertil Steril* **101** 1688-1696.

Sarraj MA & Drummond AE 2012 Mammalian foetal ovarian development: consequences for health and disease. *Reproduction* **143** 151-163.

Sawyer HR, Smith P, Heath DA, Juengel JL, Wakefield SJ & McNatty KP 2002 Formation of Ovarian Follicles During Fetal Development in Sheep1. *Biology of Reproduction* **66** 1134-1150.

Saxena R, Georgopoulos NA, Braaten TJ, Bjonnes AC, Koika V, Panidis D & Welt CK 2015 Han Chinese polycystic ovary syndrome risk variants in women of European ancestry: relationship to FSH levels and glucose tolerance. *Hum Reprod* **30** 1454-1459.

Schilling B & Yeh J 1999 Expression of transforming growth factor (TGF)-β1, TGF-β2, and TGF-β3 and of type I and II TGF-β receptors during the development of the human fetal ovary. *Fertil Steril* **72** 147-153.

Sen A & Hammes SR 2010 Granulosa cell-specific androgen receptors are critical regulators of ovarian development and function. *Mol Endocrinol* **24** 1393-1403.

Shibanuma M, Mashimo J, Kuroki T & Nose K 1994 Characterization of the TGFβ1-inducible *hic5* gene that encodes a putative novel Zinc Finger protein and its possible involvement in cellular senescenc. *J Biol Chem* **269(43)** 8.

Shimizu T, Yokoo M, Miyake Y, Sasada H & Sato E 2004 Differential expression of bone morphogenetic protein 4-6 (BMP-4, -5, and -6) and growth differentiation factor-9 (GDF-9) during ovarian development in neonatal pigs. *Domest Anim Endocrinol* **27** 397-405.

Siemens CH & Auersperg N 1988 Serial propagation of human ovarian surface epithelium in tissue culture. *J Cell Physiol* **134** 347-356.

Sokka TA, Hamalainen TM, Kaipia A, Warren DW & Huhtaniemi IT 1996 Development of luteinizing hormone action in the perinatal rat ovary. *Biology of Reproduction* **55** 8.

Soyal SM, Amleh A & Dean J 2000 FIGα, a germ cell-specific transcription factor required for ovarian follicle formation. *Development* **127** 4645-4654.

Srinivasan R, Poulsom R, Hurst HC & Gullick WJ 1998 Expression of the c-erbB-4/HER4 protein and mRNA in normal human fetal and adult tissues and in a survey of nine solid tumour types. *J. Pathol.* **185** 10.

Stoop H, Honecker F, Cools M, de Krijger R, Bokemeyer C & Looijenga LHJ 2005 Differentiation and development of human female germ cells during prenatal gonadogenesis: an immunohistochemical study. *Human Reproduction* **20** 1466-1476.

Sundfeldt K, Piontkewitz Y, Ivarsson K, Nilsson O, Hellberg P, Brännström M, Janson P-O, Enerbäck S & Hedin L 1997 E-cadherin expression in human epithelial ovarian cancer and normal ovary. *Int J Cancer (Pred Oncol)* **74** 275-280.

Tata B, Mimouni NEH, Barbotin AL, Malone SA, Loyens A, Pigny P, Dewailly D, Catteau-Jonard S, Sundstrom-Poromaa I, Piltonen TT, Dal Bello F, Medana C, Prevot V, Clasadonte J & Giacobini P 2018 Elevated prenatal anti-Mullerian hormone reprograms the fetus and induces polycystic ovary syndrome in adulthood. *Nat Med* **24** 834-846.

Teede H, Deeks A & Moran L 2010 Polycystic ovary syndrome: a complex condition with psychological, reproductive and metabolic manifestations that impacts on health across the lifespan. *BMC Med* **8** 1-10.

Teede HJ, Misso ML, Deeks AA, Moran LJ, Stuckey BG, Wong JL, Norman RJ, Costello MF & Groups GD 2011 Assessment and management of polycystic ovary syndrome: summary of an evidence-based guideline. *Med J Aust* **195** S65-S112.

Tessema M, Yingling CM, Grimes MJ, Thomas CL, Liu Y, Leng S, Joste N & Belinsky SA 2012 Differential epigenetic regulation of TOX subfamily high mobility group box genes in lung and breast cancers. *PLoS One* **7** e34850.

Thuault S, Valcourt U, Petersen M, Manfioletti G, Heldin CH & Moustakas A 2006 Transforming growth factor-beta employs HMGA2 to elicit epithelial-mesenchymal transition. *J Cell Biol* **174** 175-183.

Tian Y, Zhao H, Chen H, Peng Y, Cui L, Du Y, Wang Z, Xu J & Chen ZJ 2016 Variants in *FSHB a*re associated with Polycystic Ovary Syndrome and Luteinizing Hormone level in Han Chinese women. *J Clin Endocrinol Metab* **101** 2178-2184.

Tisdall DJ, Watanabe K, Hudson NL, Smith P & McNatty KP 1995 FSH receptor gene expression during ovarian follicle development in sheep. *Journal of Molecular Endocrinology* **15** 273-281.

Toda S, Matsumura S, Fujitani N, Nishimura T, Yonemitsu N & Sugihara H 1997 Transforming growth factor-β1 induces a mesenchyme-like cell shape without epithelial polarization in thyrocytes and inhibits thyroid folliculogenesis in collagen gel culture. *Endocrinology* **138** 5561-5575.

Todorovic V & Rifkin DB 2012 LTBPs, more than just an escort service. *J Cell Biochem* **113** 410-418.

van de Wijngaart DJ, Dubbink HJ, van Royen ME, Trapman J & Jenster G 2012 Androgen receptor coregulators: recruitment via the coactivator binding groove. *Mol Cell Endocrinol* **352** 57-69.

van Wezel IL & Rodgers RJ 1996 Morphological Characterization of Bovine Primordial Follicles and Their Environment In Vivo. *Biol Reprod* **55** 1003-1011.

Vaskivuo TE, Anttonen M, Herva R, Billig H, Dorland M, Te Velde ER, F. S, Heikinheimo M & Tapanainen JS 2001a Survival of human ovarian follicles from fetal to adult life: apoptosis, apoptosis-related proteins, and transcription factor GATA-4. *J Clin Endocrinol Metab* **86** 3421-3429.

Vaskivuo TE, Anttonen M, Herva R, Billig H, Dorland M, Velde ERTE, Stenback F, Heikinheimo M & Tapanainen JS 2001b Survival of human ovarian follicles from fetal to adult life: apoptosis, apoptosis-related proteins, and transcription factor GATA-4*. *J Clin Endocrinol Metab* **86** 9.

Vendola K, Zhou J, Wang J & A.Bondy C 1999 Androgens promote insulin-like growth factor-I and insulin-like growth factor-I receptor gene expression in the primate ovary. *Human Reproduction* **14** 2328-2332.

Viger RS, Guittot SM, Anttonen M, Wilson DB & Heikinheimo M 2008 Role of the GATA family of transcription factors in endocrine development, function, and disease. *Mol Endocrinol* **22** 781-798.

Viger RS, Mertineit C, Trasler JM & Nemer M 1998 Transcription factor GATA-4 is expressed in a sexually dimorphic pattern during mouse gonadal development and is a potent activator of the Müllerian inhibiting substance promoter. *Development* **125** 11.

Visser JA, de Jong FH, Laven JS & Themmen AP 2006 Anti-Mullerian hormone: a new marker for ovarian function. *Reproduction* **131** 1-9.

Vitt UA, Hayashi M, Klein C & Hsueh AJW 2000 Growth differentiation factor-9 stimulates proliferation but suppresses the follicle-stimulating hormone-induced differentiation of cultured granulosa cells from small antral and preovulatory rat follicles. *Biol Reprod* **62** 370-377.

Walters KA, Bertoldo MJ & Handelsman DJ 2018 Evidence from animal models on the pathogenesis of PCOS. *Best Pract Res Clin Endocrinol Metab* **32** 271-281.

Wang H, Song K, Sponseller TL & Danielpour D 2005 Novel function of androgen receptor-associated protein 55/Hic-5 as a negative regulator of Smad3 signaling. *J Biol Chem* **280** 5154-5162.

Weiss A & Attisano L 2013 The TGFbeta superfamily signaling pathway. *Wiley Interdiscip Rev Dev Biol* **2** 47-63.

Weng Q, Wang H, Medan MS, Jin WZ, Xia G, Watanabe G & Taya K 2006 Expression of inhibin/activin subunits in the ovaries of fetal and neonatal mice. *J Reprod Dev* **52** 607-616.

West FD, Roche-Rios MI, Abraham S, Rao RR, Natrajan MS, Bacanamwo M & Stice SL 2010 KIT ligand and bone morphogenetic protein signaling enhances human embryonic stem cell to germ-like cell differentiation. *Hum Reprod* **25** 168-178.

Wickenheisser JK, Nelson-DeGrave VL & McAllister JM 2006 Human ovarian theca cells in culture. *Trends Endocrinol Metab* **17** 65-71.

Wiegman EM, Blaese MA, Loeffler H, Coppes RP & Rodemann HP 2007 TGFbeta-1 dependent fast stimulation of ATM and p53 phosphorylation following exposure to ionizing radiation does not involve TGFbeta-receptor I signalling. *Radiother Oncol* **83** 289-295.

Wilhelm D, Washburn LL, Truong V, Fellous M, Eicher EM & Koopman P 2009 Antagonism of the testis- and ovary-determining pathways during ovotestis development in mice. *Mech Dev* **126** 324-336.

Wilhelm D, Yang JX & Thomas P 2013 Mammalian sex determination and gonad development. *Curr Top Dev Biol* **106** 89-121.

Willis BC & Zea Borok Z 2007 TGF-β-induced EMT: mechanisms and implications for fibrotic lung disease. *Am J Physiol Lung Cell Mol Physiol* **293** L525-L534.

Woo WH, Yang H, Wong KP & Halliwell B 2003 Sulphite oxidase gene expression in human brain and in other human and rat tissues. *Biochemical and Biophysical Research Communications* **305** 619-623.

Wood JR, Ho CK, Nelson-Degrave VL, McAllister JM & Strauss JF, 3rd 2004 The molecular signature of polycystic ovary syndrome (PCOS) theca cells defined by gene expression profiling. *J Reprod Immunol* **63** 51-60.

Wrobel K-H 2001 Morphogenesis of the bovine rete testis: extratesticular rete, mesonephros and establishment of the definitive urogenital junction. *Anat Embryol* **203** 293-307.

Wrobel K-H & Süß F 1998 Identification and temporospatial distribution of bovine primordial germ cells prior to gonadal sexual differentiation. *Anat Embryol* **197** 451-467.

Xiao L, Du Y, Shen Y, He Y, Zhao H & Li Z 2012 TGF-beta 1 induced fibroblast proliferation is mediated by the FGF-2/ERK pathway. *Front Biosci.* **17** 9.

Yamamoto N, Christenson LN, McAllister JM & Strauss III JF 2002 Growth differentiation factor-9 inhibits 3'5'-adenosine monophosphate-stimulated steroidogenesis in human granulosa and theca cells. *J Clin Endocrinol Metab* **87** 2849-2856.

Yan C, Wang P, DeMayo J, DeMayo FJ, Elvin JA, Carino C, Prasad SV, Skinner SS, Dunbar BS, Dube JL, Celeste AJ & Matzuk MM 2001 Synergistic Roles of Bone Morphogenetic Protein 15 and Growth Differentiation Factor 9 in Ovarian Function. *Mol Endocrinol* **15** 854-866.

Yao HH, Matzuk MM, Jorgez CJ, Menke DB, Page DC, Swain A & Capel B 2004 Follistatin operates downstream of Wnt4 in mammalian ovary organogenesis. *Dev Dyn* **230** 210-215.

Yeom YI, Fuhrmann G, Ovitt CE, Brehm A, Ohbo K, Gross M, Hübner K & Schöler HR 1996 Germline regulatory element of Oct-4 specific for the totipotent cycle of embryonal cells. *Development* **122** 881-894.

Yingling JM, Datto MB, Wong C, Frederick JP, Liberati NT & Wang X 1997 Tumor suppresor Smad4 is a tranforming growth factor β-inducible DNA binding protein. *mol Cell Biol* **17(12)** 7019-7028.

Yu X & Li Z 2015 TOX gene: a novel target for human cancer gene therapy. *Am J Cancer Res* **5(12)** 9.

Zhang S, Zhang HS, Cordon-Cardo C, Ragupathi G & Livingston PO 1998 Selection of tumor antigens as targets for immune attack using immunohistochemistry: protein antigens. *Clin Cancer Res* **4** 2669-2676.

Zhang X, Zhu H, Wu X, Wang M, Gu D, Gong W, Xu Z, Tan Y, Gong Y, Zhou J, Tang C, Tong N, Chen J & Zhang Z 2013 A genetic polymorphism in TOX3 is associated with survival of gastric cancer in a Chinese population. *PLoS One* **8** e72186.

Zheng M, Shi H, Segaloff DL & Voorhis BJV 2001 Expression and localization of Luteinizing Hormone Receptor in the female mouse reproductive tract. *Biol Reprod* **64** 9.

Zheng S, Lan P, Liu X & Ye K 2014 Interaction between ribosome assembly factors Krr1 and Faf1 is essential for formation of small ribosomal subunit in yeast. *J Biol Chem* **289** 22692-22703.

Österlund C & Fried G 2000 TGFβ receptor types I and II and the substrate proteins Smad 2 and 3 are present in human oocytes. *Mol Hum Reprod* **6** 498-503.

Chapter II:

Morphometric and gene expression analyses of stromal expansion during development of the bovine fetal ovary

Statement of Authorship

Title of Paper	Morphometric and Gene Expression Analyses of Stromal Expansion during Development of the Bovine Fetal Ovary.
Publication Status	☑ Published ☐ Accepted for Publication ☐ Submitted for Publication ☐ Unpublished and Unsubmitted work written in manuscript style
Publication Details	Hartanti, MD, Hummitzsch, K, Irving-Rodgers, HF, Bonner, WM, Copping, KJ, Anderson RA, McMillen, IC, Perry, VEA, Rodgers, RJ; Morphometric and gene expression analyses of stromal expansion during development of the bovine fetal ovary; Reproduction, Fertility and Development, 2019, 31(3), 482-295

Principal Author

Name of Principal Author (Candidate)	Monica Dwi Hartanti		
Contribution to the Paper	Planned and developed work, performed analysis on all samples, interpreted data, drafted, wrote and revised the manuscript.		
Overall percentage (%)	85 %		
Certification:	This paper reports on original research I conducted during the period of my Higher Degree by Research candidature and is not subject to any obligations or contractual agreements with a third party that would constrain its inclusion in this thesis. I am the primary author of this paper.		
Signature		Date	12/12/2018

Co-Author Contributions

By signing the Statement of Authorship, each author certifies that:

i. the candidate's stated contribution to the publication is accurate (as detailed above);

ii. permission is granted for the candidate in include the publication in the thesis; and

iii. the sum of all co-author contributions is equal to 100% less the candidate's stated contribution.

Name of Co-Author	Katja Hummitzach		
Contribution to the Paper	Supervised development of work and manuscript evaluation.		
Signature		Date	31/10/2018

Name of Co-Author	Helen F Irving-Rodgers		
Contribution to the Paper	Supervised development of work and manuscript evaluation.		
Signature		Date	12/12/2018

Name of Co-Author	Wendy M Bonner		
Contribution to the Paper	Provided experiment tissue.		
Signature		Date	9/7/19

Name of Co-Author	Katrina J Copping		
Contribution to the Paper	Development of experiment tissue and manuscript evaluation.		
Signature		Date	29/10/2018

Name of Co-Author	Richard A Anderson		
Contribution to the Paper	Manuscript evaluation.		
Signature		Date	28/11/2018

Name of Co-Author	Caroline McMillen		
Contribution to the Paper	Manuscript evaluation.		
Signature		Date	11/10/2018

Name of Co-Author	Viv E A Perry		
Contribution to the Paper	Developing of experiment tissues.		
Signature		Date	28/10/2018

Name of Co-Author	Raymond J Rodgers		
Contribution to the Paper	Supervised development of work, manuscript evaluation and acted as corresponding author.		
Signature		Date	10 July, 2019

CSIRO PUBLISHING

Reproduction, Fertility and Development
https://doi.org/10.1071/RD18218

Morphometric and gene expression analyses of stromal expansion during development of the bovine fetal ovary

M. D. Hartanti[A], *K. Hummitzsch*[A], *H. F. Irving-Rodgers*[A,B], *W. M. Bonner*[A], *K. J. Copping*[A], *R. A. Anderson*[C], *I. C. McMillen*[D], *V. E. A. Perry*[E] and *R. J. Rodgers*[A,F]

[A]Discipline of Obstetrics and Gynaecology, School of Medicine, Robinson Research Institute, The University of Adelaide, Adelaide, SA 5005, Australia.
[B]School of Medical Science, Griffith University, Gold Coast Campus, Qld 4222, Australia.
[C]Medical Research Council Centre for Reproductive Health, University of Edinburgh, Edinburgh, EH16 4TJ, UK.
[D]The Chancellery, University of Newcastle, Callaghan, NSW 2308, Australia.
[E]School of Veterinary and Medical Science, University of Nottingham, Sutton Bonington, LE12 5RD, UK.
[F]Corresponding author. Email: ray.rodgers@adelaide.edu.au

Abstract. During ovarian development stroma from the mesonephros penetrates and expands into the ovarian primordium and thus appears to be involved, at least physically, in the formation of ovigerous cords, follicles and surface epithelium. Cortical stromal development during gestation in bovine fetal ovaries ($n = 27$) was characterised by immunohistochemistry and by mRNA analyses. Stroma was identified by immunostaining of stromal matrix collagen type I and proliferating cells were identified by Ki67 expression. The cortical and medullar volume expanded across gestation, with the rate of cortical expansion slowing over time. During gestation, the proportion of stroma in the cortex and total volume in the cortex significantly increased ($P < 0.05$). The proliferation index and numerical density of proliferating cells in the stroma significantly decreased ($P < 0.05$), whereas the numerical density of cells in the stroma did not change ($P > 0.05$). The expression levels of 12 genes out of 18 examined, including osteoglycin (*OGN*) and lumican (*LUM*), were significantly increased later in development ($P < 0.05$) and the expression of many genes was positively correlated with other genes and with gestational age. Thus, the rate of cortical stromal expansion peaked in early gestation due to cell proliferation, whilst late in development expression of extracellular matrix genes increased.

Additional keywords: extracellular matrix, proliferation, stroma.

Received 9 June 2018, accepted 18 August 2018, published online 3 December 2018

Introduction

Connective tissue or stroma plays an important role in the formation of the ovary and during folliculogenesis as shown in mouse (Weng *et al.* 2006), cow (Wandji *et al.* 1996) and human (Heeren *et al.* 2015). Ovarian stroma contains fibroblasts and extracellular matrix. The matrix contains reticular fibres (Bandeira *et al.* 2015), fibrillar collagens (Iwahashi *et al.* 2000; Hummitzsch *et al.* 2013, 2015), decorin (Hummitzsch *et al.* 2013, 2015), fibronectin (Hummitzsch *et al.* 2013, 2015), versican (McArthur *et al.* 2000; Hummitzsch *et al.* 2013, 2015), fribillins (Prodoehl *et al.* 2009; Hatzirodos *et al.* 2011; Hummitzsch *et al.* 2013, 2015; Bastian *et al.* 2016), latent transforming growth factor β (TGFβ)-binding proteins (Prodoehl *et al.* 2009; Hatzirodos *et al.* 2011; Bastian *et al.* 2016) and hyaluronan (Kobayashi *et al.* 1999; Irving-Rodgers and Rodgers 2007). Stromal extracellular matrix components have been linked to the growth and maturation of follicles in sheep (Huet *et al.* 2001) by maintaining the shape of granulosa cells as well as their survival and proliferation *in vitro*.

The ovarian stroma is initially derived from the underlying mesonephros and infiltrates the genital ridge composed of the somatic gonadal ridge epithelial-like (GREL) cells and primordial germ cells–oogonia (Hummitzsch *et al.* 2013). When stroma first penetrates the ovaries, it is vascularised with capillaries. As it penetrates towards the surface of the ovary primordium the stroma branches and thus corrals the germ cells and somatic GREL cells into forming the ovigerous cords. This region containing the ovigerous cords and the branches of stroma becomes the cortex of the ovary, while the medullary area is substantially mesonephric stroma containing the rete

derived from mesonephric ducts. Later, commencing at the medullary–cortical interface, primordial follicles are formed and some become activated and develop further into primary and preantral follicles (Sarraj and Drummond 2012; Smith *et al.* 2014). As the stroma reaches to below the ovarian surface, it expands laterally below the surface sequestering a population of GREL cells underlain by a basal lamina at the interface (Hummitzsch *et al.* 2013); the hallmark of an epithelium. At the final stage of ovarian development, the stroma just below the surface develops into the avascular, collagen-rich tunica albuginea.

Many changes in gene expression occur during fetal ovarian development, such as expression of the pluripotency marker POU class 5 homeobox 1 (*POU5F1* or *Oct4*), deleted in azoospermia-like (*DAZL*), forkhead box L2 (*FOXL2*), as well as members of the TGF family including *TGFB1*, *2* and *3*, activins, inhibins and bone morphogenetic proteins (*BMP*s; reviewed in Sarraj and Drummond 2012). The ovarian stroma is potentially influenced by several factors, including members of the TGFβ pathway (Roy and Kole 1998; Bastian *et al.* 2016) and androgens and oestrogens (Abbott *et al.* 2006; Loverro *et al.* 2010). Abnormal development of ovarian stroma could potentially lead to an altered stromal volume in adulthood, as observed in polycystic ovary syndrome (PCOS; Hughesdon 1982; Fulghesu *et al.* 2001; Abbott *et al.* 2006; Li and Huang 2008). Despite the importance of stroma, it is probably the least studied compartment of the ovary. Using the bovine ovary, which is similar to the human ovary (Adams and Pierson 1995; Kagawa *et al.* 2009), including fetal ovarian development (Hatzirodos *et al.* 2011), stereometric and gene expression analyses were undertaken to evaluate stromal development and the expression of several genes respectively, in relation to major histological changes during the development of the ovary.

Materials and methods

Abattoir ovary collection

Bovine fetal ovarian pairs ($n = 27$) from different stages of development were collected from pregnant *Bos taurus* cows from a local abattoir (Thomas Foods International) and crown–rump length (CRL) was measured to estimate the gestational age (Russe 1983). All samples were transported to the laboratory on ice in Hank's balanced-salt solution containing Mg^{2+} and Ca^{2+} ($HBSS^{+/+}$; Sigma-Aldrich Pty Ltd, Australia). To determine the sex of fetuses with CRL <10 cm in order to exclude males in this study, a tail sample was taken, the DNA was extracted and a polymerase chain reaction (PCR) for sex-determining region Y (*SRY*) was performed as previously described (Hummitzsch *et al.* 2013). For histology and immunohistochemistry, one ovary from each pair was weighed and processed for further analysis, whereas for RNA analysis, the corresponding ovary was snap-frozen on dry ice and stored at −80°C for subsequent RNA extraction.

Ovaries of known gestational age

An additional group of fetal ovaries was derived from another study in which the age of the fetus was known. The experimental design of the cattle trial from which these fetal ovaries were obtained has been described previously (Copping *et al.* 2014). Briefly, the influence of diet on development *in utero* was assessed on Santa Gertrudis (*Bos taurus* × *Bos indicus*) heifers divided into four groups according to different dietary protocols based on a two-by-two factorial crossover design. The heifers were randomly assigned to either a high (H = 14% crude protein, (CP)) or low (L = 7% CP) protein diet 60 days before conception to 23 days postconception (dpc; periconception treatment). This diet was individually fed in stalls and straw (5% crude protein) was available ad libitum. The ration was as isocaloric as possible in the ruminant and supplemented with a commercial vitamin and mineral preparation (Ridley Agriproducts). The heifers were synchronously artificially inseminated to a single bull. At 23 dpc, half of each nutritional treatment group was swapped to the alternative postconception treatment, high or low. At the end of the first trimester (98 dpc), heifers were culled and the fetuses and placentae were collected. The fetuses were sexed and the fetal gonads were excised and weighed. One gonad from each fetus was processed for histology and two ovaries from each of the four groups were analysed by morphometry.

Histology

Fetal ovaries from the abattoir ($n = 27$) and the ovaries of known gestational age ($n = 8$) were fixed in 4% paraformaldehyde (Merck Pty Ltd) in 0.1 M phosphate buffer (pH 7.4) and embedded in paraffin using a Leica EG 1140H (Leica Microsystems). Serial sections of 6 µm were prepared using a CM1850 V2.2 Leica microtome (Leica Microsystems), mounted on Superfrost glass slides (HD Scientific Supplies) and stored at room temperature until used for haematoxylin–eosin staining and immunohistochemistry.

Sample grouping

Abattoir samples were sorted into five groups based on histological morphology, as follows: Stage I, ovigerous cord formation (the period when the ovigerous cords are formed ($n = 7$)); Stage II, ovigerous cord breakdown (the period when most of the ovigerous cords have broken down ($n = 4$)); Stage III, follicle formation (the period when most of primordial and primary follicles have formed but the cords are still open to the ovarian surface ($n = 3$)); Stage IV, ovarian surface epithelium formation (the time point when the ovarian surface epithelium is completely formed ($n = 8$)) and Stage V, tunica albuginea formation (the time point when tunica albuginea is formed ($n = 5$)). Additionally, the age of each fetus was estimated from the CRL ($y = -0.0103x^2 + 3.4332x + 36.08$, where y is age in days and x is CRL in cm and calculated from the method of Russe (1983)).

Immunohistochemistry

An indirect immunofluorescence method was used for dual localisation of Ki67 and collagen type I (Irving-Rodgers *et al.* 2002). Paraffin-embedded sections from different ovaries ($n = 35$ animals) were dewaxed then subjected to a pressure-cooker antigen retrieval method for 20 min (2100 retriever; Prestige Medical Ltd) in 10 mM Tris–ethylenediamine tetraacetic acid (EDTA) buffer (pH 9.0). The primary antibodies

used were mouse anti-human Ki67 (1 : 800; M7240/MIB-1; DAKO Australia Pty Ltd) to identify proliferating cells in combination with rabbit anti-human collagen type I (1 : 400; 20 μg mL^{-1}; ab34710; Abcam) to mark the stroma. Secondary antibodies were donkey anti-mouse IgG conjugated to Cy3 (1 : 100; 715 166 151) and Biotin–(SP)-conjugated AffiniPure donkey anti-rabbit IgG (1 : 100; 711 066 152) followed by dichlorotriazinylamino fluorescein (DTAF)-conjugated streptavidin (1 : 100; 016 010 084). All secondary antibodies and conjugated streptavidin were from Jackson ImmunoResearch Laboratories Inc. Cell nuclei were counterstained with 4',6'-diamidino-2-phenylindole dihydrochloride (DAPI) solution (Molecular Probes). The bovine adult ovary was used as a positive control whereas nonimmune mouse and rabbit sera (Sigma-Aldrich) were used as negative controls. All sections were photographed with an Olympus BX51 microscope with an epifluorescence attachment and a Spot RT digital camera (Diagnostic Instruments) at a magnification of 40×.

Morphometric analyses

The largest cross-section from each ovary, determined by haematoxylin–eosin staining for every 10th section, was examined using NPD.view2 software (Hamamatsu Photon). Using the ImageJ software (Schindelin *et al.* 2012), images of the cortex at 40× magnification were taken randomly with a single image dimension set at 1600 × 1200 pixels (0.06 mm^2). Each image represented a field of view that was used for morphometric analysis in this study. The total number of fields of view to be examined for each analysis was first determined by examining the coefficient of variation (CV) of 3–40 fields of view. For measuring the stromal area, the following steps were performed (Fig. 1). First, the total cortical area was identified, saved as a region of interest (tissue area) and its area measured. Next, the stromal area in the cortex was identified based on positive collagen type I staining (Fig. 2). To calculate the proportion of stroma in the cortex (volume density) and total stromal volume, the following calculations were applied and all calculations used equations that are listed in Table 1. The ovarian volume (V_{ovary}) was estimated using the ovarian weight, assuming a density of 1 g cm^{-3}. Then, the proportion of stroma in the cortex ($V_{v[stroma]}$) and the total stromal volume (V_{stroma}) were calculated using the equations shown in Table 1. The number of proliferating stromal cells (Ki67 positive) and all stromal cells (DAPI positive) in a field of view were counted using the multipoint and find maxima tool with adjusted noise tolerance (ImageJ). Nuclei, which were not detected by the threshold, were added manually using the multipoint tool. Results of proliferating cells are presented as a proliferation index (*PI*) and as a numerical density (N_{dp}/N_d) in the stromal area using the equations shown in Table 1.

RNA extraction and cDNA synthesis

RNA was extracted from the whole fetal ovary using 1 mL Trizol (Thermo Fisher Scientific) with 0.5 g of ceramic beads in homogenisation tubes using the Mo Bio Powerlyser 24 (Mo Bio Laboratories Inc.) and 200 μL chloroform (RNase-free) according to the manufacturer's instructions. The RNA concentration was determined using a Nanodrop spectrophotometer

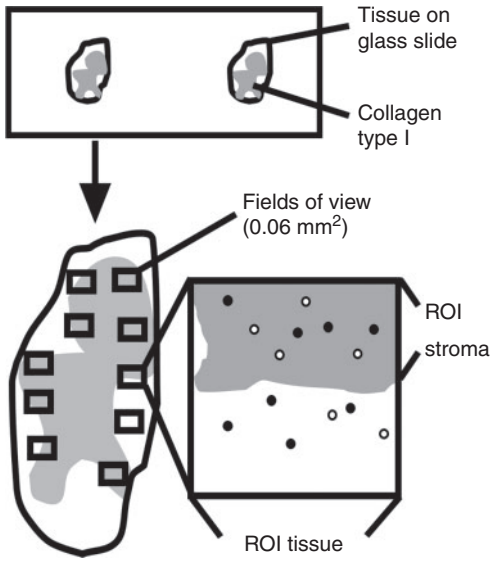

Fig. 1. Schematic diagram of the procedure for determining the stromal areas and proliferating cells in fetal ovarian tissues. For immunohistochemistry and subsequent analysis by ImageJ, the largest cross-section of each fetal ovary was used and 20–40 fields of view (each 0.06 mm^2) were randomly chosen from each section. Fluorescence staining for collagen type I was used to distinguish between stromal and non-stromal areas and Ki67 was used to mark any proliferating cells in the ovarian tissue. In each photograph the total ovarian tissue was marked as region of interest (ROI) tissue and measured. The stromal area, marked by collagen type I fibres (shaded areas), was identified as ROI stroma and measured. Ki67-positive cells (black dots) and DAPI-positive cells (white dots) were counted in stromal areas.

(NanoDrop 1000 3.7.1; Nanodrop Technologies) based on the 260λ (wavelength) absorbance. All samples which had a 260 : 280λ absorbance ratio >1.8 were used and subsequently treated with DNase I (Promega/Life Technologies Australia Pty Ltd). Complementary DNA was then synthesised from 200 ng of DNase-treated RNA using 250 ng μL^{-1} random hexamers (Geneworks) and 200 U Superscript Reverse Transcriptase III (Thermo Fisher Scientific) as previously described (Matti *et al.* 2010). For a negative control, diethyl pyrocarbonate (DEPC)-treated water instead of the Superscript Reverse Transcriptase III was added.

Quantitative real-time PCR

To conduct quantitative real-time PCR (qPCR), primers were designed against the published reference RNA sequences (Table 2) using Primer3 plus (Rozen and Skaletsky 2000) and Net primer (PREMIER Biosoft) software. To test the combination of primers, the cDNA was diluted to five different concentrations from 1 : 4 to 1 : 1000 to generate a standard curve of cycle threshold (Ct) versus concentrations. Primer combinations that showed a single sharp peak and achieved an amplification efficiency of 0.9–1.1 and an R^2 value ≥ 0.98 were used for further analysis.

Quantitative PCR was carried out using a Rotor-Gene 6000 series 1.7 thermal cycler (Qiagen GmbH) in duplicate at 95°C

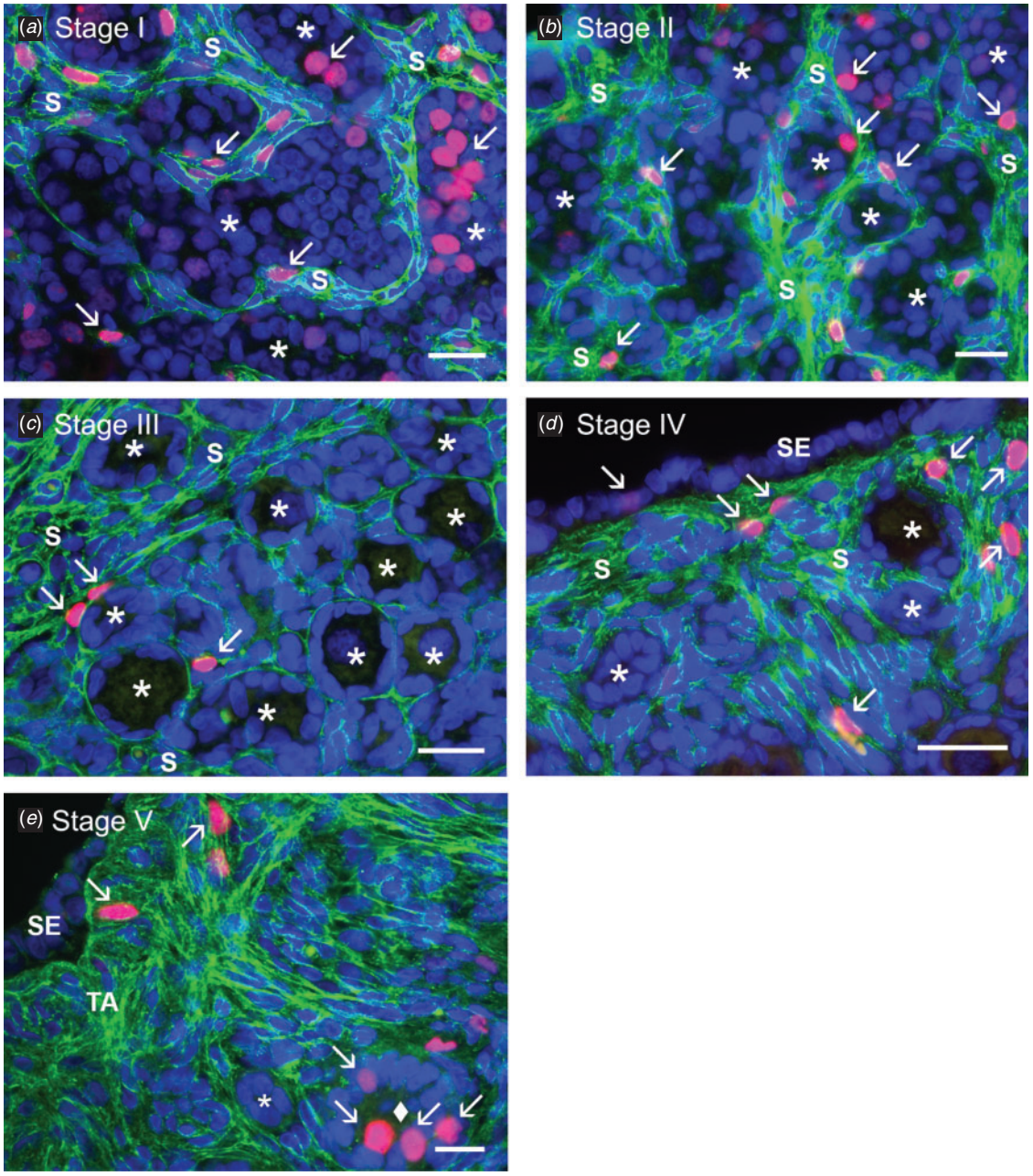

Fig. 2. Stromal distribution and proliferation in fetal ovaries from different developmental stages. Representative photographs from (*a*) Stage I (ovigerous cord formation), (*b*) Stage II (ovigerous cord breakdown), (*c*) Stage III (follicle formation), (*d*) Stage IV (ovarian surface epithelium formation) and (*e*) Stage V (tunica albuginea formation) of fetal ovarian development showing stroma (S), ovigerous cords–primordial follicles (marked with asterisks), surface epithelium (SE), tunica albuginea (TA) and a preantral follicle (marked with diamond). The stroma was identified based on the expression of collagen type I, which is a stromal marker. Collagen type I (green) is combined with the proliferation marker Ki67 (red, marked with arrows). Nuclei are counterstained with DAPI. Scale bar = 25 μm.

for 15 s then 60°C for 60 s for 40 cycles. Amplification of cDNA dilutions were prepared in 10 μL reactions containing 2 μL of the 1 : 20 cDNA dilution, 5 μL Power SYBR Green PCR Master Mix (Applied Biosystems), 0.2 μL each of forward and reserve primers (Geneworks; Table 2) for the target genes and 2.6 μL of DEPC-treated water. Ct values were determined using the Rotor-Gene 6000 software (Q series; Qiagen GmbH) at a threshold of 0.05 normalised fluorescence units. Gene expression was determined by the mean of $2^{-\Delta Ct}$, where ΔCt represents the target gene Ct – glyceraldehyde-3-phosphate dehydrogenase (*GAPDH*) Ct. *GAPDH* was used as a housekeeping gene because it is stably expressed in bovine adult ovarian tissues

Table 1. List of equations for morphometric analyses

A_{cortex}, cortical area in each image; A_{ovary}, ovarian area in each image; A_{stroma}, stromal area in each image; $A_{totalstroma}$, total analysed stromal area; $N_{pstroma}$, total number of proliferating cells in all analysed images of the stroma; N_{stroma}, total number of cells in all analysed images of the stroma; V_{ovary}, ovarian volume

Parameter	Equation	Units
Proportion of cortex in the ovary or cortical volume density ($V_{v[cortical]}$)	$V_{v[cortical]} = A_{cortex} / A_{ovary}$	%
Cortical volume (V_{cortex})	$V_{cortex} = V_{v[cortical]} \times V_{ovary}$	mm^3
Proportion of stroma in cortex or volume density of stroma in the ovarian cortex ($V_{v[stroma]}$)	$V_{v[stroma]} = A_{stroma} / A_{cortex}$	%
Cortical stromal volume (V_{stroma})	$V_{stroma} = V_{v[stroma]} \times V_{cortex}$	mm^3
Proliferation index in the cortical stroma (*PI*)	$PI = N_{pstroma} / N_{stroma}$	%
Numerical density of proliferating cells in the stroma (N_{dp})	$N_{dp} = N_{pstroma} / A_{totalstroma}$	$N\,mm^{-2}$
Numerical density of all cells in the stroma (N_d)	$N_d = N_{stroma} / A_{totalstroma}$	$N\,mm^{-2}$

Table 2. List of genes and primers used for quantitative real-time PCR

Gene name	Gene symbol	Primers (5′→3′)	Genebank accession number	Size (bp)
Glyceraldehyde-3-phosphate dehydrogenase	*GAPDH*	F: ACCACTTTGGCATCGTGGAG R: GGGCCATCCACAGTCTTCTG	NM_001034034.2	76
Osteoglycin	*OGN*	F: TGCAAGGCTAATGACACCAG R: GATGTTTTCCCAGGATGACG	NM_173946.2	85
Lumican	*LUM*	F: TTCAAAGCATTCGCCAAAATG R: CCGCCAATTAATGCCAAGAG	NM_173934.1	62
Asporin	*ASPN*	F: AAGGACATGGAAGACGAAGG R: GGGAAGAAGGGGTTAATTGG	NM_001034309.2	80
Fibromodulin	*FMOD*	F: AGGTGGGCAAGAAGGTTTTC R: TCTGGTTGTGGTCAAGATGG	NM_174058.2	129
Biglycan	*BGN*	F: CACCTTGGTGATGTTGTTGG R: TCTCGTCCGCTACTCCAAGT	NM_178318.4	202
Collagen type VI α1 chain	*COL6A1*	F: CAAGGATGTCTTTGGCTTGG R: AGAAGCTCGGCGTAGTTTTC	NM_001143865.1	120
Collagen type VI α2 chain	*COL6A2*	F: TCAAAGAGGCCGTCAAGAAC R: TGAGCTTGTTGTAGGCGAAC	NM_001075126.1	84
Collagen type VI α3 chain	*COL6A3*	F: TCAATACCTACCCCAGCAAGA R: GACCGCATCTAGGGACTTACC	XM_005197965.3	200
Collagen type I α2 chain	*COL1A2*	F: TTGAAGGAGTAACCACCAAGG R: TGTCCAAAGGTGCAATATCAA	NM_174520.2	321
Fibronectin	*FN1*	F: CGACGGCATCACTTACAATG R: CGACGGCATCACTTACAATG	NM_001163778.1	118
Fibronectin extra domain A	*FN1-EDA*	F: CCTGTTACTGGTTACAGAGTG R: AGTGAGCTGAACATTGGG	AF 260303	550
Fibronectin extra domain B	*FN1-EDB*	F: GCCGATCAGAGTTCCTGCACC R: GAGCCCAGGTGACACGCATAG	AF 260304	456
Fibronectin V region	*FN1-V*	F: CTGAAGAACAATCAGAAGAG R: CCACTATGATGTTGTAGGTG	AF 260305	600
Lectin, galactoside-binding soluble 1 (galectin 1)	*LGALS1*	F: AATCATGGCTTGTGGTCTGG R: AGGTTGTTGTCGTCTTTGCC	NM_175782.1	129
Regulator of G-protein signalling 5	*RGS5*	F: GCCATTGACCTTGTCATTCC R: TTGTTCTGCAGGAGCTTGTC	NM_001034707.2	119
Fibulin-1	*FBLN1*	F: GCAGCGCAGCCAAGTCAT R: AGATATGTCTGGGTGCTACAAACG	NM_001098029.1	66
Fibulin-2	*FBLN2*	F: TGGCACTCACGATTGTAACC R: GTTGATGTCCACGCATTTCC	XM_589271.8	130
Fibulin-5	*FBLN5*	F: TGCAACTGAGAATCCCTGTG R: GCATTCGTCCATATCACTGC	NM_001014946	121

Table 3. Characteristics of developmental stages (I to V) of bovine fetal ovaries from the abattoir collection

Data are mean ± s.e.m. One-way ANOVA with post hoc Tuckey's tests were used to analyse data. [a,b,c,d]Values within a row with different superscripts indicate significant differences ($P < 0.05$)

Parameter	Developmental stage				
	I	II	III	IV	V
Gestational age (days)[A,B]	79 ± 6^{a}	127 ± 6^{b}	173 ± 12^{c}	234 ± 9^{d}	264 ± 6^{d}
Time from previous stage (days)		48	46	61	30
Weight (mg)[B]	17.9 ± 5.1^{a}	49.2 ± 7.9^{b}	113.5 ± 33.6^{bc}	245.8 ± 62.9^{cd}	475.3 ± 22.6^{c}
Fold change in weight from previous stage		2.7	2.3	2.2	1.9
Total cortical volume (mm^3)[B]	10.3 ± 3.0^{a}	30.1 ± 4.8^{b}	70.7 ± 27.4^{bc}	65.5 ± 9.0^{bcd}	142.1 ± 37.5^{cd}
Fold change in cortical volume from previous stage		2.9	2.3	0.9	2.2
Cortical volume density (%)	56.9 ± 3.0^{a}	61.7 ± 6.7^{a}	59.7 ± 9.1^{ab}	33.2 ± 5.5^{bc}	29.5 ± 7.0^{c}
Total medullar volume (mm^3)[B,C]	7.7 ± 2.1^{a}	19.0 ± 4.5^{ab}	42.8 ± 9.5^{bc}	180.3 ± 57.9^{cd}	333.1 ± 34.8^{d}
Fold change in medullar volume from previous stage		2.5	2.5	4.2	1.8
Total cortical stromal volume (mm^3)[B]	3.3 ± 0.8^{a}	12.9 ± 1.9^{b}	43.4 ± 20.1^{bc}	49.6 ± 7.3^{cd}	112.7 ± 28.1^{cd}
Fold change in cortical stroma from previous stage		3.9	3.4	1.1	2.3

[A]Estimated from the CRL (Russe 1983).
[B]Statistical analysis was conducted using log-transformed data.
[C]Calculated from total cortical volume and percentage of medullar area.

(Berisha *et al.* 2002) and showed stable expression in our samples.

Statistical analyses

All statistical analyses were carried out using Microsoft Office Excel 2010 and GraphPad Prism Version 6.00 (GraphPad Software Inc.). All data that were not normally distributed or showed significantly different standard deviations between groups were first log-transformed. The morphometric and $2^{-\Delta Ct}$ data for each fetal ovarian sample were compared using ANOVA with Tukey's *post-hoc* test. A value of $P < 0.05$ was considered to be significant. For testing the association between expression levels of each gene throughout development, correlation coefficients were determined using the Spearman correlation coefficient. After correlation values between genes were identified, a network graph was plotted using the qgraph R package (Epskamp *et al.* 2012) and illustrated using an adjacent matrix plot.

Results

Classification of ovaries

As we have observed previously (Hummitzsch *et al.* 2013), there was variation in the developmental stage of ovaries from fetuses of the same crown–rump length, particularly at early stages. We therefore devised a classification system based upon five identifiable stages of development of the cortex commencing with ovigerous cord formation (Stage I), ovigerous cord breakdown (Stage II), follicle formation (Stage III), surface epithelium formation (Stage IV) and tunica albuginea formation (Stage V) as illustrated in Fig. 2 and subsequently analysed data from the abattoir collection using this classification system.

Determination of total number of fields of view

Using the ovaries from our abattoir collections we first determined the optimum number of total fields of view required for the morphometric measurements of the proportion of stroma in the cortex and the proportion of proliferating stromal cells in the ovarian cortex. A CV analysis was conducted from 3 up to 40 fields of view photographed at 40× magnification accounting for 0.06 mm^2 (Fig. S1, available as Supplementary Material to this paper). For fetuses with a CRL <30 cm, the CV of the volume density of stroma (Fig. S1*a–c*) and the proportion of proliferating stromal cells in the ovarian cortex (Fig. S1*g–i*) was relatively variable until nine fields of view and then remained similar until 20 fields of view. However, for fetuses with CRL of 39 cm the CV of the proportion of stroma in the cortex (Fig. S1*d*) and the proportion of proliferating stromal cells in the ovarian cortex (Fig. S1*j*) were similar for almost all numbers of fields of view. For fetuses with CRL >50 cm, the parameters were highly variable from 3 to 20 fields of view (Fig. S1*e*, *f*, *k*, *l*) and then stabilised from 20 to 40 fields of view. Thus, for morphometric quantitation of fetuses with a CRL of <50 cm we assessed 10 fields of view and for fetuses with a CRL of >50 cm we assessed 20 fields of view.

Ovary changes in Stages I to V

Details of the ovaries and fetuses of each stage from our abattoir collection are presented in Table 3. With advancing stages the fetuses were older and the ovaries became significantly heavier and they had more cortex and medulla, but proportionally less cortex relative to medulla in the last two stages of development (Table 3). We calculated the time to transit from one stage to the next and fold changes between each stage in weight, cortical volume and medullary volume (Table 3). The transition time between Stages I and II, II and III, III and IV and IV and V were 48, 46, 61 and 30 days respectively (Table 3); thus, the duration of development before Stage III was 94 (48 + 46) days and after Stage III was 91 (61 + 30) days. From Stages I to III versus Stages III to V the fold changes in weight were 6.2 and 4.2, the fold changes in cortical volume were 6.7 and 2.0 and the fold changes in medullary volume were 6.3 and 7.6 respectively

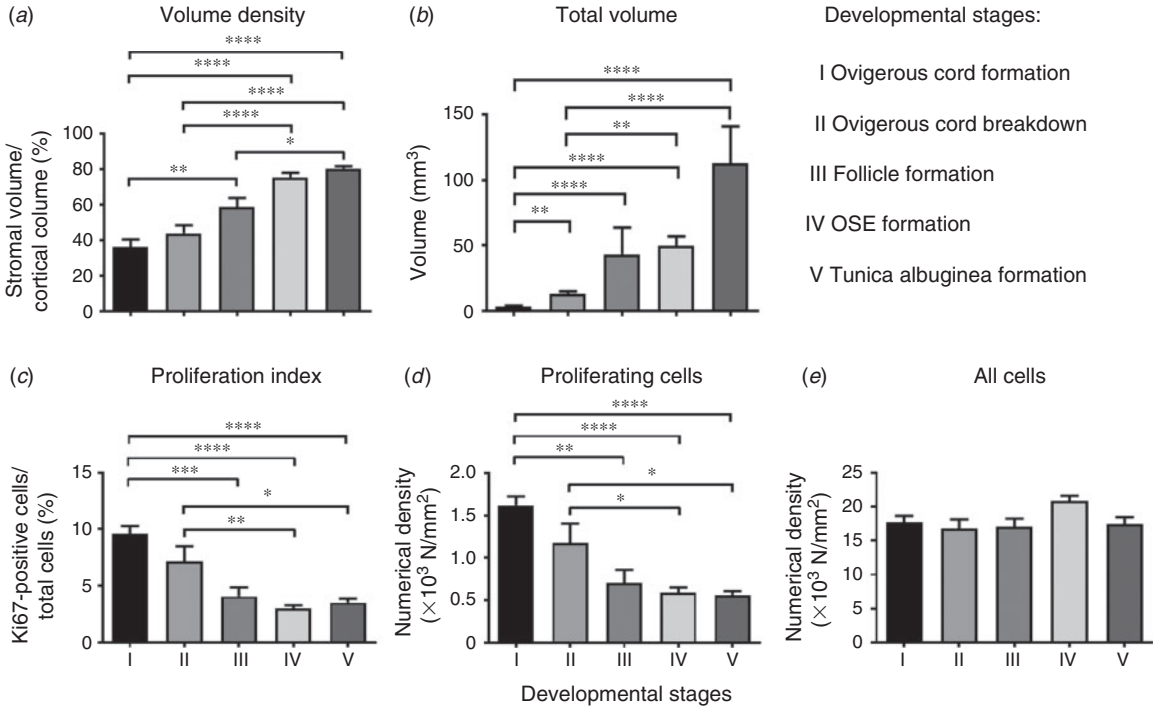

Fig. 3. Morphometric analyses of the stroma during bovine fetal ovarian development. Data are presented as mean ± s.e.m. Samples were grouped into five stages of ovarian development based on their histological morphology: ovigerous cord formation ($n = 7$, Stage I), ovigerous cord breakdown ($n = 4$, Stage II), follicle formation ($n = 3$, Stage III), ovarian surface epithelium (OSE) formation ($n = 8$, Stage IV) and tunica albuginea formation ($n = 5$, Stage V). (*a*) Volume density represents the proportion of stroma in the cortex, (*b*) total volume represents the total stromal volume in the ovarian cortex, (*c*) proliferation index represents the ratio between total proliferating and all cells in the cortical stroma, (*d*) proliferating cells represents the numerical density of proliferating cells in the cortical stroma and (*e*) all cells represents the numerical density of all cells in the cortical stroma. One-way ANOVA with post hoc Tuckey's tests were used to analyse the data. *$P < 0.05$, **$P < 0.01$, ***$P < 0.001$, ****$P < 0.0001$.

(calculated from Table 3). Thus, after Stage III when follicles formed, the expansion of the cortex slowed but the medulla continued to expand at its previous rate, leading to proportionally more medulla. From 79 to 264 days of gestation the ovarian volume increased 26.5 fold (17.9 to 475.3 mm^3), the cortex increased 13.8 fold in volume (10.3 to 142.1 mm^3) and the medulla increased 34.1 fold in volume (3.3 to 112.7 mm^3).

Morphometric characteristics of fetal ovarian stroma

During ovigerous cord formation at Stage I (Fig. 2*a*), the stroma containing many Ki67-positive cells formed branches between ovigerous cords (Fig. 3*c*, *d*). At this stage the ovigerous cords contained oogonia, undergoing mitosis as shown by colocalisation with the proliferation marker Ki67 (Fig. 2*a*). The proportion of stroma in the ovarian cortex increased during ovigerous cord breakdown at Stage II (Fig. 3*a*, *b*), although it was not statistically significant. Ki67-positive cells were observed in the stromal area and in the partitioned ovigerous cords (Fig. 2*b*). In the stromal area, the total number of Ki67-positive cells was lower than during Stage I (Fig. 3*c*, *d*); however, the difference was not statistically significant. During follicle formation at Stage III (Fig. 2*c*), the proportion of stroma in the ovarian cortex had increased further (Fig. 3*a*, *b*). The stroma now surrounded the primordial follicles, which were first formed at the inner cortex adjacent to the medulla. Proliferating cells were observed in the stroma but not in primordial follicles (Fig. 2*c*); however, the total number of Ki67-positive cells in stroma were lower than during Stage II (Fig. 3*c*, *d*), although the difference was not statistically significant. During the formation of surface epithelium at Stage IV (Fig. 2*d*), the ovary had more stroma underneath the ovarian surface. At this stage Ki67-positive cells localised in the stroma as well as the ovarian surface. Tunica albuginea formation at Stage V was characterised by bundles of thick collagen type I fibres underneath the ovarian surface epithelium (Fig. 2*e*). At this stage stromal cells and some granulosa cells in growing follicles were positive for Ki67.

We quantitatively measured the proportion of stroma in the cortex and the total volume of the stroma in the cortex (Fig. 3) and both were significantly increased during ovarian development ($P < 0.05$; Fig. 3*a*, *b*). Interestingly, the cell proliferation index of the stroma in the ovarian cortex significantly declined during ovarian development (Fig. 3*c*). The numerical density of proliferating cells also significantly declined in the cortical stroma throughout gestation (Fig. 3*d*). However, the numerical density of cortical stromal cells was stable during ovarian development (Fig. 3*e*), suggesting that the increase in stromal volume during gestation was not affected by an increase in extracellular space in the cortical stroma.

Table 4. Morphometric analyses of the cortical stroma in bovine fetal ovaries from the trial at Day 98 of gestation
Data are mean ± s.e.m. ($n = 8$)

Characteristic	Value
Weight (mg)	26.5 ± 1.1
Total volume cortical stroma (mm^3)	3.9 ± 0.2
Proportion of stroma in the cortex (%)	26.1 ± 0.1
Proliferation index of cortical stroma (%)	7.3 ± 0.5
Numerical density of proliferating cells in cortical stroma ($N\,mm^{-2}$)	1340 ± 77
Numerical density of cortical stromal cells ($N\,mm^{-2}$)	18 737 ± 607

To assess if our morphometric analyses used for the abattoir collection were adequate, we analysed fetal ovarian samples from the trial collected on Day 98 of gestation. Using the CRL, age was estimated by the method of Russe (1983) to be 95.3 ± 1.2 days, which is in very good agreement with the known age of 98 days. During this time of gestation, the stroma occupied 26.1 ± 0.1 % of the cortex and was 3.9 ± 0.2 mm^3 in total volume. The proliferation index of the cortical stroma was 7.3 ± 0.5 %, the numerical density of the proliferating stromal cells in the cortex was 1340 ± 77 cells mm^{-2} and the numerical density of all the stromal cells was 18 737 ± 607 cells mm^{-2} (Table 4).

Gene expression

We analysed the mRNA expression of genes that are specifically expressed in the stroma of many adult tissues, including the ovary. The mRNA expression of osteoglycin (*OGN*), lumican (*LUM*), asporin (*ASPN*), collagen type VI A1 (*COL6A1*), *COL6A2*, *COL6A3*, fibronectin (*FN1*), regulator of G-protein signalling 5 (*RGS5*) and fibulin 5 (*FBLN5*) in fetal ovaries significantly increased in Stages IV and V of development (Fig. 4*a–c*, *g–j*, *o*, *r*) relative to earlier stages. We also analysed the mRNA expression of another three *FN1* splice variants (FN1 extra domain A (*FN1-EDA*), FN1 extra domain B (*FN1-EDB*) and FN1 variable (*FN1-V*)), which have three different additional domains. Our results showed that *FN1-EDA*, *FN1-EDB* and *FN1-V* were also significantly increased late in development (Fig. 4*k–m*). The expression of fibromodulin (*FMOD*), biglycan (*BGN*), *COL1A2*, *FBLN1*, *FBLN2* and Lectin galactoside-binding soluble 1 (galectin 1) *(LGALS1)* did not show any significant differences across stages of ovarian development (Fig. 4*d–f*, *n*, *p*, *q*).

Correlation analyses

To analyse the correlations between the 18 genes of interest and additionally with gestational age (Table 5), we generated the Spearman correlation matrix from the Ct values of all genes. After correlation values between genes were identified, a network graph was plotted using the qgraph R package (Epskamp *et al.* 2012) to plot an adjacent matrix (Fig. 5) and some examples of these are correlations as shown in Fig. 6. *OGN*, *LUM*, *ASPN*, *BGN*, *COL6A1*, *COL6A2*, *COLA3*, *COL1A2*, *FN1*, *FN1-EDA*, *FN1-EDB*, *FN1-V*, *RGS5*, *FBLN1* and *FBLN5* were all strongly positively associated with each other ($r > 0.6$). In addition, *FMOD* had strong positive correlations ($r > 0.6$) with *BGN*, *COL6A1*, *COL6A2*, *COLA3*, *COL1A2*, *FN1*, *FN1-EDA*, *FN1-EDB*, *FN1-V* and *LGALS1*. *FBLN2* and *LGALS1* showed weaker positive relationships to other genes ($r < 0.6$). Gestational age had strong positive correlations ($r > 0.6$) with *FBLN5*, *LUM*, *RGS5*, *ASPN*, *OGN*, *FN1-EDB*, *COL6A3*, *COL6A2*, *COLA1*, *FN1-V*, *FN1-EDA*, *COL1A2* and *FBLN1*, but had weaker positive correlations ($r < 0.6$) with *FN1*, *BGN*, *LGALS1* and *FMOD* (Table 5). Interestingly, *FBLN2* had a weak negative correlation with gestational age (Table 5).

Discussion

In this study we conducted morphometric analyses of the developing bovine fetal ovary, focusing on cortical stroma. We were able to identify the stroma by immunostaining of the stromal extracellular matrix collagen type I. We optimised our morphometric sampling regime and also examined ovaries of a known stage of gestation. Across gestation we measured the total volume and relative proportions of cortex and medulla, the proportion and total volume of stroma in the cortex and the numerical and proliferation index of cells in the stroma of the cortex. We also examined the expression of 18 genes that had previously been reported as relevant to stroma in other organs. We believe this is one of the first critical studies of the development of ovarian stroma.

Collagen type I is an extracellular matrix of stroma that has been localised in the stroma of fetal bovine (Hummitzsch *et al.* 2013) and rat ovaries (Paranko 1987), as well as adult bovine (Figueiredo *et al.* 1995), mouse (Berkholtz *et al.* 2006) and human (Lind *et al.* 2006) ovaries. Collagen type I was observed at all stages of fetal bovine ovary development by immunostaining but the intensity of immunostaining increased qualitatively throughout development. This suggests that greater deposition of collagen type I occurs during fetal development, leading to a stiffer stromal matrix.

An earlier morphometric study examining the bovine fetal ovary has been conducted but over a shorter period of time than our study. From their results we calculated that the ovary volume increased 4.2 fold in volume (35 to 148 mm^3), the cortex increased 2.8 fold in volume (21.9 to 62.4 mm^3) and the medulla increased 6.5 fold (13.1 to 85.6 mm^3) from 3 to 7 months of gestation (Santos *et al.* 2013). Our measurements are in agreement with theirs where, during Stages I to III (taking 94 days) versus Stages III to V (taking 91 days) the changes in ovarian weight were 6.2 and 4.2 fold, in medullary volume were 6.3 and 7.6 fold and in cortical volume were 6.7 and 2.0 fold respectively. Our values are higher than theirs as our study was over a longer time frame. Our results also show that throughout gestation the medulla expanded substantially more (34.1 fold) than the cortex (13.8 fold) did and that the rate of expansion of the cortex declined past Stage III when follicles were formed. What drives the continued expansion of the medulla is not known, nor why this would continue.

The numerical density (cells per area or volume) of cells in the cortical stroma, however, did not change across gestation. Assuming that the sizes of the stromal cells did not change, and there was no observable evidence that they did, then the

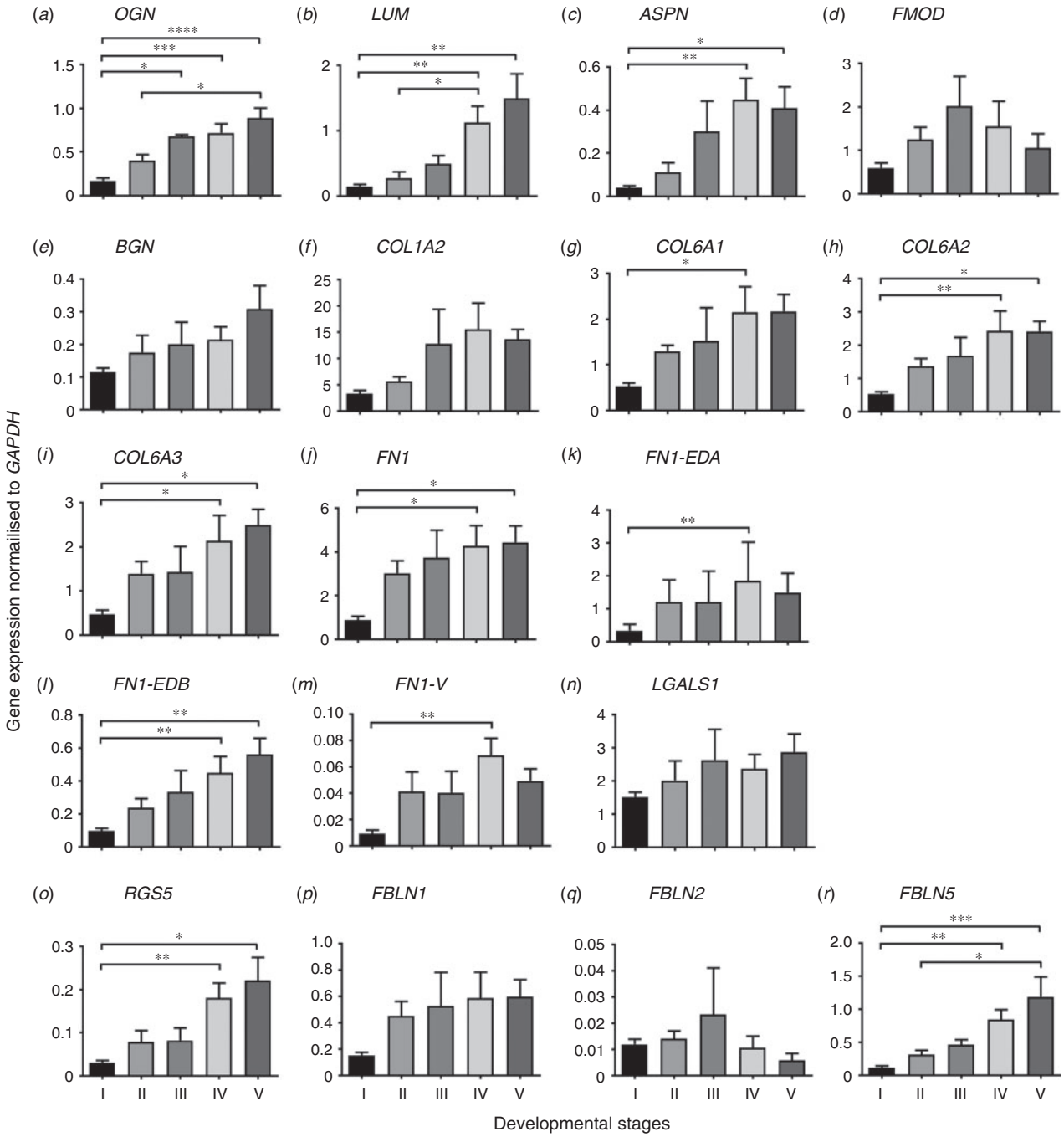

Fig. 4. Differential mRNA expression levels of genes in whole bovine fetal ovaries. One ovary from each pair was used for mRNA analysis ($n = 27$ pairs). Data are presented as mean ± s.e.m. (normalised to *GAPDH*). Samples were grouped into five stages of ovarian development based on their histological morphology: ovigerous cord formation ($n = 7$, Stage I), ovigerous cord breakdown ($n = 4$, Stage II), follicle formation ($n = 3$, Stage III), surface epithelium formation ($n = 8$, Stage IV) and tunica albuginea formation ($n = 5$, Stage V). One-way ANOVA with post hoc Tuckey's tests were used to analyse the data. *$P < 0.05$, **$P < 0.01$, ***$P < 0.001$, ****$P < 0.0001$.

proportion of extracellular space in the cortical stroma was constant across gestation. This is different from what is known to happen in the tunica albuginea, which has a significantly lower cell numerical density than cortical stroma and has proportionally more extracellular space rich in extracellular matrix containing at least collagens, versican, fibronectin, decorin (Hummitzsch *et al.* 2013), latent transforming growth factor β-binding protein 2 and fibrillin 1 (Prodoehl *et al.* 2009). Thus, as also observed in the human fetal ovary from 20 to 25 weeks of gestational age (Sforza *et al.* 1993), there was an

Table 5. Spearman correlation coefficients (*r*) of mRNA expression levels of stroma-related genes and gestational age ($n = 27$)

$^{*}P < 0.05$, $^{**}P < 0.01$, $^{***}P < 0.001$, $^{****}P < 0.0001$

	LGALS1	*OGN*	*RGS5*	*FBLN5*	*ASPN*	*COL1A2*	*COL6A1*	*COL6A2*	*COL6A3*	*FBLN1*	*FBLN2*	*FN1-EDA*	*FN1-EDB*	*FN1-V*	*FN1*	*LUM*	*FMOD*	*BGN*
LGALS1	–	–	–	–	–	–	–	–	–	–	–	–	–	–	–	–	–	–
OGN	0.646***	–	–	–	–	–	–	–	–	–	–	–	–	–	–	–	–	–
RGS5	0.587**	0.769****	–	–	–	–	–	–	–	–	–	–	–	–	–	–	–	–
FBLN5	0.522*	0.897****	0.834****	–	–	–	–	–	–	–	–	–	–	–	–	–	–	–
ASPN	0.480*	0.786****	0.898****	0.877****	–	–	–	–	–	–	–	–	–	–	–	–	–	–
COL1A2	0.515**	0.792****	0.741****	0.876****	0.859****	–	–	–	–	–	–	–	–	–	–	–	–	–
COL6A1	0.477*	0.759****	0.85****	0.845****	0.887****	0.910****	–	–	–	–	–	–	–	–	–	–	–	–
COL6A2	0.477*	0.766****	0.868****	0.853****	0.891****	0.904****	0.979****	–	–	–	–	–	–	–	–	–	–	–
COL6A3	0.585**	0.809****	0.86****	0.886****	0.856****	0.896****	0.967****	0.959****	–	–	–	–	–	–	–	–	–	–
FBLN1	0.573**	0.628***	0.801****	0.675***	0.732***	0.744****	0.847****	0.863****	0.889****	–	–	–	–	–	–	–	–	–
FBLN2	0.072	0.077	0.033	0.049	0.170	0.226	0.322	0.273	0.272	0.386*	–	–	–	–	–	–	–	–
FN1-EDA	0.574**	0.737****	0.859****	0.835****	0.881****	0.889****	0.941****	0.953****	0.950****	0.884****	0.337	–	–	–	–	–	–	–
FN1-EDB	0.582**	0.820****	0.872****	0.911****	0.869****	0.919****	0.92****	0.944****	0.949****	0.839****	0.157	0.935****	–	–	–	–	–	–
FN1-V	0.592**	0.740****	0.864****	0.831****	0.860****	0.832****	0.867****	0.889****	0.892****	0.827****	0.264	0.966****	0.905****	–	–	–	–	–
FN1	0.554**	0.781****	0.630***	0.797****	0.694****	0.775****	0.734****	0.730****	0.758****	0.634***	0.096	0.769****	0.739****	0.754****	–	–	–	–
LUM	0.436*	0.869****	0.806****	0.914****	0.877****	0.823****	0.833****	0.841****	0.856****	0.694****	0.079	0.824****	0.847****	0.813****	0.684****	–	–	–
FMOD	0.609***	0.518**	0.520**	0.491**	0.522**	0.671***	0.674***	0.708****	0.725****	0.814****	0.434	0.759****	0.698****	0.695****	0.604***	0.485*	–	–
BGN	0.594**	0.752****	0.658***	0.747****	0.697****	0.817****	0.801****	0.785****	0.817****	0.737****	0.312*	0.804****	0.828****	0.79****	0.763****	0.745****	0.699****	–
Gestational age	0.416*	0.818****	0.876****	0.895****	0.868****	0.720****	0.750****	0.765****	0.776****	0.600***	0.217	0.724****	0.808****	0.727****	0.571**	0.877****	0.321	0.563**

Fig. 5. Scatter plots showing related mRNA expression levels of (*a*) *LUM* versus *FBLN5*, (*b*) *FN1-EDB* versus *COL1A2* and (*c*) *FN1-EDA* versus *COL6A2* in whole bovine fetal ovaries. One ovary from each pair was used for mRNA analysis ($n = 27$ pairs). Data are presented as normalised gene expression to *GAPDH*. Spearman's correlation coefficient (*R*) test was used to analyse the data.

increase in stroma expansion across gestation but this rate of expansion slowed after Stage III. These rates of expansion are mirrored by the proliferation of stromal cells, but not the proportion of extracellular space, suggesting that stromal cell proliferation is largely responsible for stromal expansion during ovarian development.

Since stroma has been shown to expand significantly during ovarian development, genes that encode extracellular matrix proteins that might be involved in the expansion of the ovarian stroma were examined. Small leucine-rich proteoglycans (*SLRP*s) have a role in regulating collagen type I fibrillogenesis, which has been shown to be expressed during ovarian development in the rat (Paranko 1987) and cow (Hummitzsch *et al.* 2013). There are three classes of *SLRP*, Class I, Class II and Class III, which consist of extracellular matrix proteins, including asporin (*ASPN*) and biglycan (*BGN*), lumican (*LUM*) and

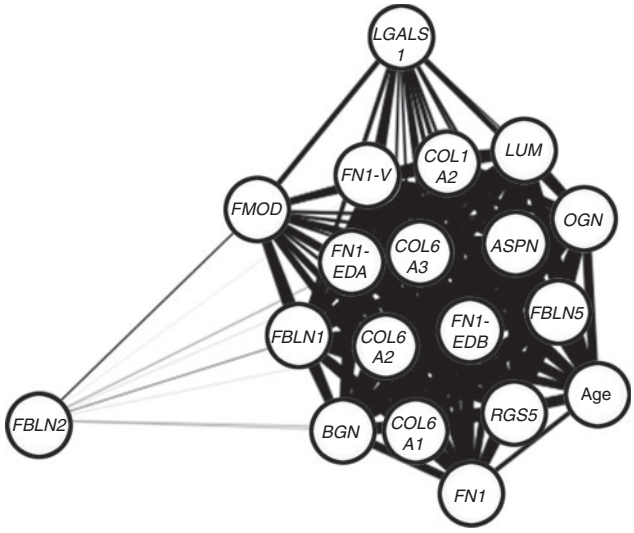

Fig. 6. An adjacent matrix network graph using correlation coefficients from Table 5. The closeness of the genes and the thickness of the interconnecting lines indicate stronger correlations between genes. Age is age of gestation.

fibromodulin (*FMOD*) and osteoglycin (*OGN*; Ameye and Young 2002). *ASPN* and *BGN* have been shown to be involved in collagen type I fibrillogenesis in human embryonic kidney cells and adult mouse ovary respectively (Oksjoki *et al.* 1999; Kalamajski *et al.* 2009). Another study showed that *LUM* and *FMOD* bind to collagen type I in an antagonistic manner during tendon development, which might be related to the formation of progressively thicker collagen fibrils (Kalamajski and Oldberg 2009). Additionally, *OGN* is involved in regulating collagen type I fibrillogenesis in mouse embryo fibroblasts (Ge *et al.* 2004). Since collagen type I also increases as the stroma expands during ovarian development, our findings indicate that *ASPN*, *LUM* and *OGN* might be involved in the deposition and assembly of extracellular matrix in stroma in bovine fetal ovary.

The establishment and the remodelling of the ovarian vascular system is required for development of the ovary (Robinson *et al.* 2009). Initially the penetration and expansion of the mesonephric stroma into the developing ovary brings with it capillaries contained therein (Hummitzsch *et al.* 2013; Smith *et al.* 2014). It has been shown that *RGS5* and *FBLN5*, which encode regulator of G-protein signalling 5 and fibulin 5 protein respectively, are involved in vascular remodelling (Berger *et al.* 2005; Spencer *et al.* 2005). RGS5 protein is a pericyte marker observed in the vasculature of mouse ovarian follicles (Berger *et al.* 2005), rat cerebral capillaries (Kirsch *et al.* 2001) and mouse embryonic pericytes (Bondjers *et al.* 2003). Pericytes have been observed in 23–24 week human fetal ovary as a part of a vascular network in the stroma (Niculescu *et al.* 2011). Additionally, a study using *FBLN5* knockout mice suggests the important role of *FBLN5* in neointima formation and vascular remodelling after an induced vascular injury (Spencer *et al.* 2005). Since the interaction between endothelial cells, pericytes and smooth muscle cells is critical for the development of the vasculature (Niculescu *et al.* 2011), the increased expression of *RGS5* and *FBLN5* suggests that these genes may play a role in expansion of the vasculature in the cortical stroma.

COL6A1, *COL6A2* and *COL6A3* encode the extracellular matrix component collagen type VI, which is predicted to help in anchoring tissues and cells to the connective tissue extracellular matrix (Cescon *et al.* 2015). In human adult ovary, collagen type VI is observed in the thecal layer, especially in the theca externa, and has a role in the interactions between the thecal cell and extracellular matrix during folliculogenesis (Iwahashi *et al.* 2000). A study using a yeast two-hybrid system showed an interaction between collagen type VI and collagen type IV (Kuo *et al.* 1997), which is localised in follicular basal lamina during ovarian development (Hummitzsch *et al.* 2013). Additionally, collagen type VI also interacts with other extracellular matrix components, such as collagen type I (Bonaldo *et al.* 1990) and fibronectin (Sabatelli *et al.* 2001). A study in the bovine fetal ovary showed that collagen type I and fibronectin were specifically expressed in the ovarian stroma (Hummitzsch *et al.* 2013), suggesting that collagen type VI might have an important role in anchoring vasculature in the stroma during the late stage of ovarian development.

FN1 encodes fibronectin, which modulates cell–cell and cell–matrix interactions (Goldberg *et al.* 2006). Fibronectin is composed of three structurally homologous types of repeated domains: Type I, II and III. Three different alternative splicing regions are located in Type III fibronectin: extra domain A (ED-A), B (ED-B) and the variable (V) region, encoded by *FN1-EDA*, *FN1-EDB* and *FN1-V*, respectively, (the variable region can have three to five alternative splicing events). The ED-A, ED-B and V regions are located between the 11th and 12th, between the 7th and 8th and between the 14th and 15th Type III repeats respectively (De Candia and Rodgers 1999). Collectively, these alternative splicing events potentially produce multiple different isoforms in humans, cows, mice and rats: ED-A+, ED-A–, ED-B+, ED-B–, V+ and V–. These have been shown to be expressed in bovine antral follicles of 0.5–9 mm diameter, in corpora lutea and in fetal bovine liver, lung and kidney but fetal ovaries were not examined in that study (De Candia and Rodgers 1999). The ED-A+ isoform has been identified in ovarian follicles and is predicted to be associated with the replication of granulosa cells (Colman-Lerner *et al.* 1999), whereas the ED-B+ and V+ isoforms have been shown to be involved in angiogenesis (Castellani *et al.* 1994; De Candia and Rodgers 1999). It is possible that the isoforms of FN1 might be involved in follicle formation and angiogenesis during ovarian development.

Many of the genes examined in the present study were highly positively correlated with gestational age and also with each other. This is not surprising as many of these genes were extracellular matrix genes associated with stroma, which also expanded during fetal development. Comparisons with earlier studies of bovine fetal ovaries (Hatzirodos *et al.* 2011) showed that fibrillin 3, another extracellular matrix gene that is familiarly linked to PCOS, is highly expressed only in the first trimester and declines in expression thereafter. This is interesting as fibrillin 3 is thus expressed in the fetal cortical stroma when it is proportionally expanding the most during fetal development. Why this particular gene should exhibit this

behaviour and not other stromal extracellular matrix genes is not known, but it does suggest that fibrillin 3 may have a unique role during ovarian cortical stroma expansion.

In summary we have shown quantitatively that the rate of expansion of cortical stroma is greatest early in development when the stroma penetrates the ovarian primordium from the mesonephros. The expansion of the cortical stroma occurs due to cell proliferation and not a change in cell size or a change in the amount of extracellular space. The mRNA expression levels of many extracellular matrix genes increased in the later stages of ovarian development and were highly correlated with each other, suggesting that they might be co-regulated. In conclusion, the behaviour of stroma changes during ovarian development and this might have consequences for its roles.

Conflicts of interest

The authors declare that there is no conflict of interest that could be perceived as prejudicing the impartiality of the research reported.

Acknowledgements

This research was funded by the Australia Awards Scholarship from the Australian Government, The University of Adelaide, the National Health and Medical Research Council (NHMRC) of Australia, the NHMRC Centre for Research Excellence in the Evaluation, Management and Health Care Needs of Polycystic Ovary Syndrome, the Society for Reproductive Biology and the Robinson Research Institute. We would like to acknowledge the Australian Research Council, Griffith University, S. Kidman and Co. and Ridley Agriproducts Pty Ltd for also funding this research. We would like to thank Thomas Food International, Murray Bridge, South Australia for providing the bovine tissues for this research.

References

Abbott, D. H., Padmanabhan, V., and Dumesic, D. A. (2006). Contributions of androgen and estrogen to fetal programming of ovarian dysfunction. *Reprod. Biol. Endocrinol.* **4**, 17. doi:10.1186/1477-7827-4-17

Adams, G. P., and Pierson, R. A. (1995). Bovine model for study of ovarian follicular dynamics in humans. *Theriogenology* **43**(1), 113–120. doi:10.1016/0093-691X(94)00015-M

Ameye, L., and Young, M. F. (2002). Mouse deficient in small leucine-rich proteoglycans novel *in vivo* models for osteoporosis, osteoarthritis, Ehlers–Danlos syndrome, muscular dystrophy, and corneal diseases. *Glycobiology* **12**(9), 107R–116R. doi:10.1093/GLYCOB/CWF065

Bandeira, F. T., Carvalho, A. A., Castro, S. V., Lima, L. F., Viana, D. A., Evangelista, J., Pereira, M., Campello, C. C., Figueiredo, J. R., and Rodrigues, A. (2015). Two methods of vitrification followed by *in vitro* culture of the ovine ovary: evaluation of the follicular development and ovarian extracellular matrix. *Reprod. Domest. Anim.* **50**(2), 177–185. doi:10.1111/RDA.12463

Bastian, N. A., Bayne, R. A., Hummitzsch, K., Hatzirodos, N., Bonner, W. M., Hartanti, M. D., Irving-Rodgers, H. F., Anderson, R. A., and Rodgers, R. J. (2016). Regulation of fibrillins and modulators of TGFβ in fetal bovine and human ovaries. *Reproduction* **152**, 127–137. doi:10.1530/REP-16-0172

Berger, M., Bergers, G., Arnold, B., Hammerling, G. J., and Ganss, R. (2005). Regulator of G-protein signaling-5 induction in pericytes coincides with active vessel remodeling during neovascularization. *Blood* **105**, 1094–1101. doi:10.1182/BLOOD-2004-06-2315

Berisha, B., Pfaffl, M. W., and Schams, D. (2002). Expression of estrogen and progesterone receptors in the bovine ovary during estrous cycle and pregnancy. *Endocrine* **17**, 207–214. doi:10.1385/ENDO:17:3:207

Berkholtz, C. B., Lai, B. E., Woodruff, T. K., and Shea, L. D. (2006). Distribution of extracellular matrix proteins type I collagen, type IV collagen, fibronectin, and laminin in mouse folliculogenesis. *Histochem. Cell Biol.* **126**(5), 583–592. doi:10.1007/S00418-006-0194-1

Bonaldo, P., Russo, V., Bucciotti, F., Doliana, R., and Colombatti, A. (1990). Structural and functional features of the alpha3 chain indicate a bridging role for chicken collagen VI in connective tissues. *Biochemistry* **29**(5), 1245–1254. doi:10.1021/BI00457A021

Bondjers, C., Kalén, M., Hellström, M., Scheidl, S. J., Abramsson, A., Renner, O., Lindahl, P., Cho, H., Kehrl, J., and Betsholtz, C. (2003). Transcription profiling of platelet-derived growth factor-B-deficient mouse embryos identifies RGS5 as a novel marker for pericytes and vascular smooth muscle cells. *Am. J. Pathol.* **162**(3), 721–729. doi:10.1016/S0002-9440(10)63868-0

Castellani, P., Viale, G., Dorcaratto, A., Nicolo, G., Kaczmarek, J., Querze, G., and Zardi, L. (1994). The fibronectin isoform containing the ED-B oncofetal domain: a marker of angiogenesis. *Int. J. Cancer* **59**, 612–618. doi:10.1002/IJC.2910590507

Cescon, M., Gattazzo, F., Chen, P., and Bonaldo, P. (2015). Collagen VI at a glance. *J. Cell Sci.* **128**(19), 3525–3531. doi:10.1242/JCS.169748

Colman-Lerner, A., Fischman, M. L., Lanuza, G. M., Bissel, D. M., Kornblihtt, A. R., and Baranao, J. L. (1999). Evidence for a role of the alternatively spliced ED-I sequence of fibronectin during ovarian follicular development. *Endocrinology* **140**(6), 2541–2548. doi:10.1210/ENDO.140.6.6708

Copping, K. J., Hoare, A., Callaghan, M., McMillen, I. C., Rodgers, R. J., and Perry, V. E. A. (2014). Fetal programming in 2-year-old calving heifers: peri-conception and first trimester protein restriction alters fetal growth in a gender-specific manner. *Anim. Prod. Sci.* **54**, 1333–1337.

De Candia, L. M., and Rodgers, R. J. (1999). Characterization of the expression of the alternative splicing of the ED-A, ED-B and V regions of fibronectin mRNA in bovine ovarian follicles and corpora lutea. *Reprod. Fertil. Dev.* **11**, 367–377. doi:10.1071/RD99087

Epskamp, S., Cramer, A. O. J., Waldorp, L. J., Schmittmann, V. D., and Borsboom, D. (2012). qgraph: network visualizations of relationships in psychometric data. *J. Stat. Softw.* **48**(4), 1–18. doi:10.18637/JSS.V048.I04

Figueiredo, J. R., Hulshof, S. C. J., Thiry, M., Van den Hurk, R., Bevers, M. M., Nusgens, B., and Beckers, J. F. (1995). Extracellular matrix proteins and basement membrane: their identification in bovine ovaries and significance for the attachment of cultured preantral follicles. *Theriogenology* **43**, 845–858. doi:10.1016/0093-691X(95)00036-8

Fulghesu, A. M., Clampelli, M., Belosi, C., Apa, R., Pavone, V., and Lanzone, A. (2001). A new ultrasound criterion for the diagnosis of polycystic ovary syndrome: the ovarian stroma/total area ratio. *Fertil. Steril.* **76**(2), 326–331. doi:10.1016/S0015-0282(01)01919-7

Ge, G., Seo, N. S., Liang, X., Hopkins, D. R., Hook, M., and Greenspan, D. S. (2004). Bone morphogenetic protein-1/tolloid-related metalloproteinases process osteoglycin and enhance its ability to regulate collagen fibrillogenesis. *J. Biol. Chem.* **279**(40), 41626–41633. doi:10.1074/JBC.M406630200

Goldberg, M., Septier, D., Oldberg, A., Young, M. F., and Ameye, L. G. (2006). Fibromodulin-deficient mice display impaired collagen fibrillogenesis in predentin as well as altered dentin mineralization and enamel formation. *J. Histochem. Cytochem.* **54**(5), 525–537. doi:10.1369/JHC.5A6650.2005

Hatzirodos, N., Bayne, R. A., Irving-Rodgers, H. F., Hummitzsch, K., Sabatier, L., Lee, S., Bonner, W., Gibson, M. A., Rainey, W. E., Carr, B. R., Mason, H. D., Reinhardt, D. P., Anderson, R. A., and Rodgers, R. J. (2011). Linkage of regulators of TGF-beta activity in the fetal ovary to polycystic ovary syndrome. *FASEB J.* **25**(7), 2256–2265. doi:10.1096/FJ.11-181099

Heeren, A. M., van Iperen, L., Klootwijk, D. B., de Melo Bernardo, A., Roost, M. S., Gomes Fernandes, M. M., Louwe, L. A., Hilders, C. G., Helmerhorst, F. M., van der Westerlaken, L. A., and Chuva de Sousa Lopes, S. M. (2015). Development of the follicular basement membrane during human gametogenesis and early folliculogenesis. *BMC Dev. Biol.* **15**, 4. doi:10.1186/S12861-015-0054-0

Huet, C., Pisselet, C., Mandon-Pépin, B., Monget, P., and Monniaux, D. (2001). Extracellular matrix regulates ovine granulosa cell survival, proliferation and steroidogenesis: relationships between cell shape and function. *J. Endocrinol.* **169**, 347–360. doi:10.1677/JOE.0.1690347

Hughesdon, P. E. (1982). Morphology and morphogenesis of the Stein–Leventhal ovary and of so-called "hyperthecosis". *Obstet. Gynecol. Surv.* **37**(2), 59–77. doi:10.1097/00006254-198202000-00001

Hummitzsch, K., Irving-Rodgers, H. F., Hatzirodos, N., Bonner, W., Sabatier, L., Reinhardt, D. P., Sado, Y., Ninomiya, Y., Wilhelm, D., and Rodgers, R. J. (2013). A new model of development of the mammalian ovary and follicles. *PLoS One* **8**(2), e55578. doi:10.1371/JOURNAL.PONE.0055578

Hummitzsch, K., Anderson, R. A., Wilhelm, D., Wu, J., Telfer, E. E., Russell, D. L., Robertson, S. A., and Rodgers, R. J. (2015). Stem cells, progenitor cells, and lineage decisions in the ovary. *Endocr. Rev.* **36**(1), 65–91. doi:10.1210/ER.2014-1079

Irving-Rodgers, H. F., and Rodgers, R. J. (2007). Extracellular matrix in ovarian follicular and luteal development. In 'Novel Concepts in Ovarian Endocrinology'. (Ed. A. Gonzalez-Bulnes.) pp. 83–112. (Transworld Research Network: Kerala, India.)

Irving-Rodgers, H. F., Bathgate, R. A. D., Ivell, R., Domagalski, R., and Rodgers, R. J. (2002). Dynamic changes in the expression of relaxin-like factor (Insl3), cholesterol side-chain cleavage cytochrome p450, and 3beta-hydroxysteroid dehydrogenase in bovine ovarian follicles during growth and atresia. *Biol. Reprod.* **66**, 934–943. doi:10.1095/BIOLREPROD66.4.934

Iwahashi, M., Muragaki, Y., Ooshima, A., and Nakano, R. (2000). Type VI collagen expression during growth of human ovarian follicles. *Fertil. Steril.* **74**(2), 343–347. doi:10.1016/S0015-0282(00)00618-X

Kagawa, N., Silber, S., and Kuwayama, M. (2009). Successful vitrification of bovine and human ovarian tussue. *Reprod. Biomed. Online* **18**, 568–577. doi:10.1016/S1472-6483(10)60136-8

Kalamajski, S., and Oldberg, A. (2009). Homologous sequence in lumican and fibromodulin leucine-rich repeat 5–7 competes for collagen binding. *J. Biol. Chem.* **284**(1), 534–539. doi:10.1074/JBC.M805721200

Kalamajski, S., Aspberg, A., Lindblom, K., Heinegard, D., and Oldberg, A. (2009). Asporin competes with decorin for collagen binding, binds calcium and promotes osteoblast collagen mineralization. *Biochem. J.* **423**(1), 53–59. doi:10.1042/BJ20090542

Kirsch, T., Wellner, M., Luft, F. C., Haller, H., and Lippoldt, A. (2001). Altered gene expression in cerebral capillaries of stroke-prone spontaneously hypertensive rats. *Brain Res.* **910**, 106–115. doi:10.1016/S0006-8993(01)02670-1

Kobayashi, H., Sun, W. G., and Terao, T. (1999). Immunolocalization of hyaluronic acid and inter-alpha-trypsin inhibitor in mice. *Cell Tissue Res.* **296**, 587–597. doi:10.1007/S004410051320

Kuo, H.-J., Maslen, C. L., Keene, D. R., and Glanville, R. W. (1997). Type VI collagen anchors endothelial basement membranes by interacting with type IV collagen. *J. Biol. Chem.* **272**(42), 26522–26529. doi:10.1074/JBC.272.42.26522

Li, Z., and Huang, H. (2008). Epigenetic abnormality: a possible mechanism underlying the fetal origin of polycystic ovary syndrome. *Med. Hypotheses* **70**(3), 638–642. doi:10.1016/J.MEHY.2006.09.076

Lind, A. K., Weijdegard, B., Dahm-Kahler, P., Molne, J., Sundfeldt, K., and Brannstrom, M. (2006). Collagens in the human ovary and their changes in the perifollicular stroma during ovulation. *Acta Obstet. Gynecol. Scand.* **85**(12), 1476–1484. doi:10.1080/00016340601033741

Loverro, G., De Pergola, G., Di Naro, E., Tartagni, M., Lavopa, C., and Caringella, A. M. (2010). Predictive value of ovarian stroma measurement for cardiovascular risk in polycyctic ovary syndrome: a case control study. *J. Ovarian Res.* **3**, 25. doi:10.1186/1757-2215-3-25

Matti, N., Irving-Rodgers, H. F., Hatzirodos, N., Sullivan, T. R., and Rodgers, R. J. (2010). Differential expression of focimatrix and steroidogenic enzymes before size deviation during waves of follicular development in bovine ovarian follicles. *Mol. Cell. Endocrinol.* **321**(2), 207–214. doi:10.1016/J.MCE.2010.02.019

McArthur, M. E., Irving-Rodgers, H. F., Byers, S., and Rodgers, R. J. (2000). Identification and immunolocalization of decorin, versican, perlecan, nidogen, and chondroitin sulfate proteoglycans in bovine small-antral ovarian follicles. *Biol. Reprod.* **63**, 913–924. doi:10.1095/BIOLREPROD63.3.913

Niculescu, M., Novac, L., Mateescu, G. O., Mihail, S. R., Neamtu, S., and Papachristu, A. (2011). Original study the vasculogenesis of the fetal ovary – morphological and immunohistochemical study. *Analele Universitatii "Dunarea De Jos" Galati Medicina* **17**(1), 5–9.

Oksjoki, S., Sallinen, S., Vuorio, E., and Anttila, L. (1999). Cyclic expression of mRNA transcripts for connective tissue components in the mouse ovary. *Mol. Hum. Reprod.* **5**(9), 803–808. doi:10.1093/MOLEHR/5.9.803

Paranko, J. (1987). Expression of type I and III collagen during morphogenesis of fetal rat testis and ovary. *Anat. Rec.* **219**, 91–101. doi:10.1002/AR.1092190115

Prodoehl, M. J., Irving-Rodgers, H. F., Bonner, W. M., Sullivan, T. M., Micke, G. C., Gibson, M. A., Perry, V. E., and Rodgers, R. J. (2009). Fibrillins and latent TGFbeta binding proteins in bovine ovaries of offspring following high or low protein diets during pregnancy of dams. *Mol. Cell. Endocrinol.* **307**(1–2), 133–141. doi:10.1016/J.MCE.2009.03.002

Robinson, R. S., Woad, K. J., Hammond, A. J., Laird, M., Hunter, M. G., and Mann, G. E. (2009). Angiogenesis and vascular function in the ovary. *Reproduction* **138**(6), 869–881. doi:10.1530/REP-09-0283

Roy, S. K., and Kole, A. R. (1998). Ovarian transforming growth factor-b (TGF-b) receptors: *in vitro* effects of follicle stimulating hormone, epidermal growth factor and TGF-b on receptor expression in human preantral follicles. *Mol. Hum. Reprod.* **4**(3), 207–214. doi:10.1093/MOLEHR/4.3.207

Rozen, S., and Skaletsky, H. J. (2000). Primer3 on the WWW for general users and for biologist programmers. In 'Bioinformatics methods and protocols: methods in molecular biology'. (Eds S. Krawetz and S. Misener.) pp. 365–386. (Humana Press: Totowa, NJ, USA.)

Russe, I. (1983). Oogenesis in cattle and sheep. *Bibl. Anat* **24**, 77–92.

Sabatelli, P., Bonaldob, P., Lattanzia, G., Braghettab, P., Bergaminb, N., Capannic, C., Mattiolid, E., Columbarod, M., Ognibenec, A., Pepee, G., Bertinif, E., Merlinid, L., Maraldia, N. M., and Squarzonia, S. (2001). Collagen VI deficiency affects the organization of fibronectin in the extracellular matrix of cultured fibroblasts. *Matrix Biol.* **20**(7), 475–486. doi:10.1016/S0945-053X(01)00160-3

Santos, S. S., Ferreira, M. A., Pinto, J. A., Sampaio, R. V., Carvalho, A. C., Silva, T. V., Costa, N. N., Cordeiro, M. S., Miranda, M. S., Ribeiro, H. F., and Ohashi, O. M. (2013). Characterization of folliculogenesis and the occurrence of apoptosis in the development of the bovine fetal ovary. *Theriogenology* **79**(2), 344–350. doi:10.1016/J.THERIOGENOLOGY.2012.09.026

Sarraj, M. A., and Drummond, A. E. (2012). Mammalian foetal ovarian development: consequences for health and disease. *Reproduction* **143**(2), 151–163. doi:10.1530/REP-11-0247

Schindelin, J., Arganda-Carreras, I., Frise, E., Kaynig, V., Longair, M., Pietzsch, T., Preibisch, S., Rueden, C., Saalfeld, S., Schmid, B., Tinevez, J.-Y., White, D. J., Hartenstein, V., Eliceiri, K., Tomancak, P., and

Cardona, A. (2012). Fiji: an open-source platform for biological-image analysis. *Nat. Methods* **9**(7), 676–682. doi:10.1038/NMETH.2019

Sforza, C., Ferrario, V. F., De Pol, A., Marzona, L., Forni, M., and Forabosco, A. (1993). Morphometric study of the human ovary during compartmentalization. *Anat. Rec.* **236**, 626–634. doi:10.1002/AR.1092360406

Smith, P., Wilhelm, D., and Rodgers, R. J. (2014). Development of mammalian ovary. *J. Endocrinol.* **221**(3), R145–R161. doi:10.1530/JOE-14-0062

Spencer, J. A., Hacker, S. L., Davis, E. C., Mecham, R. P., Knutsen, R. H., Li, D. Y., Gerard, R. D., Richardson, J. A., Olson, E. N., and Yanagisawa, H. (2005). Altered vascular remodeling in fibulin-5-deficient mice reveals a role of fibulin-5 in smooth muscle cell proliferation and migration. *Proc. Natl. Acad. Sci. USA* **102**(8), 2946–2951. doi:10.1073/PNAS.0500058102

Wandji, S. A., Sršeň, V., Voss, A. K., Eppig, J. J., and Fortune, J. E. (1996). Initiation *in vitro* of growth of bovine primordial follicles 1. *Biol. Reprod.* **55**(5), 942–948. doi:10.1095/BIOLREPROD55.5.942

Weng, Q., Wang, H., Medan, M. S., Jin, W., Xia, G., Watanabe, G., and Taya, K. (2006). Expression of inhibin-activin subunits in the ovaries of fetal and neonatal mice. *J. Reprod. Dev.* **52**(5), 607–616. doi:10.1262/JRD.18026

Supplementary Material

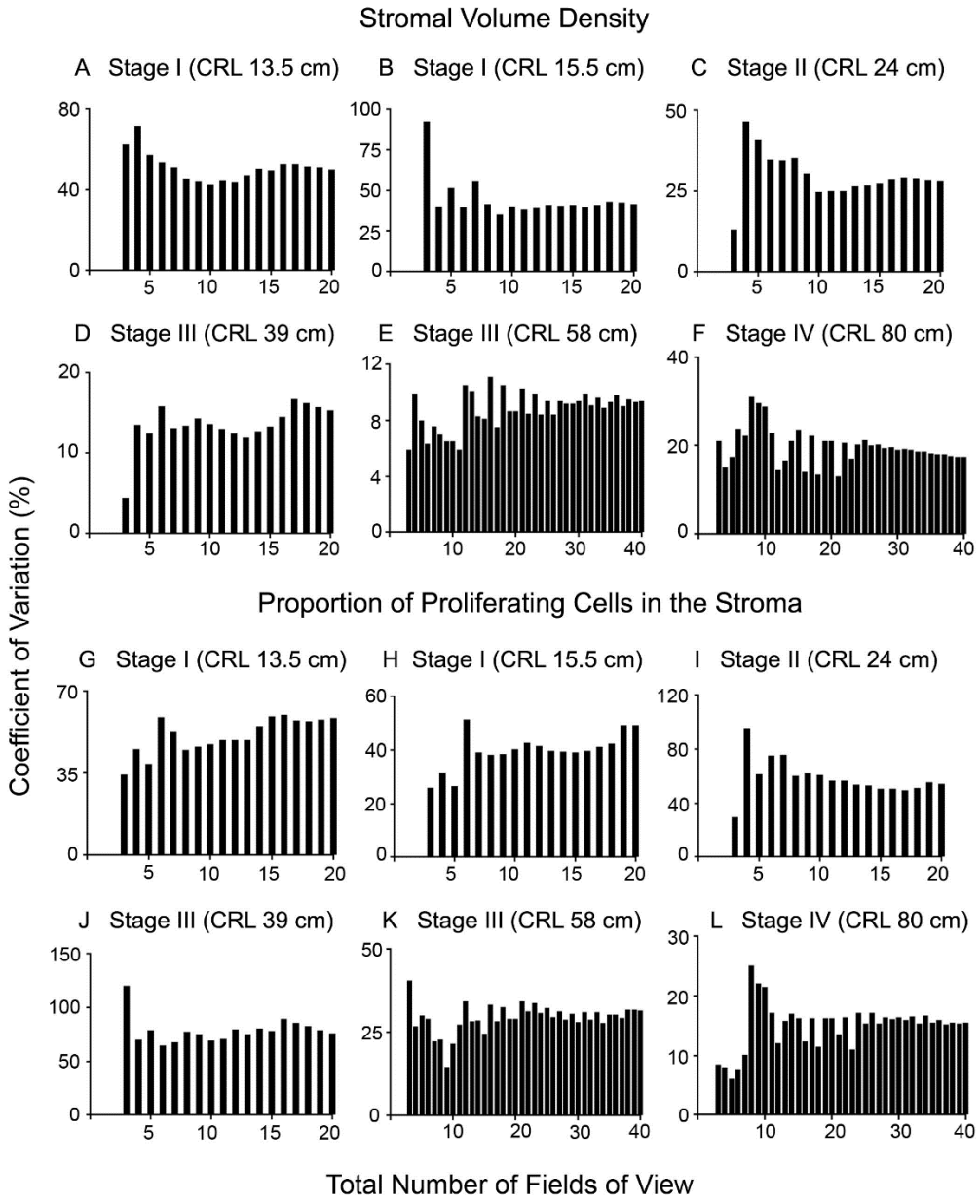

Fig. S1. Hartanti *et al.*

Fig. S1. Variation of morphometric analysis. Data are presented as percentage of 3 – 40 fields of view and was counted by dividing standard deviation by the mean from each total number of fields of view to calculate the coefficient of variation (CV). The CV of the percentage of stromal area (A-F) and the proportion of stromal cells that are proliferating (G-L) in the ovarian cortex are presented. CRL 13.5 cm or 80 days (A and G), CRL 15.5 cm or 87 days (B and H), CRL 24 cm or 112 days (C and I), CRL 39 cm of 154 days (D and J), CRL 58 cm or 200 days (E and K) and CRL 80 cm or 245 days (F and L), respectively.

Chapter III:

Could Polycystic Ovary Syndrome in Women be due to Perturbed Fetal Development of the Ovary?

This chapter is based on the following article that was submitted to Scientific Report:

Monica D Hartanti, Roseanne Rosario, Katja Hummitzsch, Nicole A Bastian, Nicholas Hatzirodos, Wendy M Bonner, Rosemary A Bayne, Helen F Irving-Rodgers, Richard A Anderson and Raymond J Rodgers, "Could polycystic ovary syndrome in women be due to perturbed fetal development of the ovary?", Scientific Report

Statement of Authorship

Title of Paper	**Could polycystic ovary syndrome in women be due to perturbed fetal development of the ovary?**
Publication Status	☐ Published ☐ Accepted for Publication ☑ Submitted for Publication ☐ Unpublished and Unsubmitted work written in manuscript style
Publication Details	**Monica D Hartanti**, Roseanne Rosario, Katja Hummitzsch, Nicole A Bastian, Nicholas Hatzirodos, Wendy M Bonner, Rosemary A Bayne, Helen F Irving-Rodgers, Richard A Anderson and Raymond J Rodgers; Could polycystic ovary syndrome in women be due to perturbed fetal development of the ovary?; Scientific Report

Principal Author

Name of Principal Author (Candidate)	**Monica Dwi Hartanti**		
Contribution to the Paper	**Planned and developed work of bovine samples, performed analysis on all samples, interpreted data, drafted, wrote and revised the manuscript.**		
Overall percentage (%)	**75 %**		
Certification:	**This paper reports on original research I conducted during the period of my Higher Degree by Research candidature and is not subject to any obligations or contractual agreements with a third party that would constrain its inclusion in this thesis. I am the primary author of this paper.**		
Signature		**Date**	**12/12/2018**

Co-Author Contributions

By signing the Statement of Authorship, each author certifies that:

i. **the candidate's stated contribution to the publication is accurate (as detailed above);**
ii. **permission is granted for the candidate in include the publication in the thesis; and**
iii. **the sum of all co-author contributions is equal to 100% less the candidate's stated contribution.**

Name of Co-Author	**Roseanne Rosario**		
Contribution to the Paper	**Planned and developed work of human samples and interpreted data.**		
Signature		**Date**	**28/11/2018**

Name of Co-Author	Nicole A Bastian		
Contribution to the Paper	Planned and developed work of cultured bovine samples.		
Signature		Date	9/7/2019

Name of Co-Author	Rosemary A Bayne		
Contribution to the Paper	Manuscript evaluation.		
Signature		Date	30/11/2018

Name of Co-Author	Katja Hummitzach		
Contribution to the Paper	Supervised development of work and manuscript evaluation.		
Signature		Date	21/12/2018

Name of Co-Author	Nicholas Hatzirodos		
Contribution to the Paper	Planned work of cultured bovine samples.		
Signature		Date	21/12/2018

Name of Co-Author	Wendy M Bonner		
Contribution to the Paper	Provided experiment tissue.		
Signature		Date	9/7/19

Name of Co-Author	Helen F Irving-Rodgers		
Contribution to the Paper	Supervised development of work and manuscript evaluation.		
Signature		Date	12/12/2018

Name of Co-Author	Richard A Anderson		
Contribution to the Paper	Manuscript evaluation.		
Signature		Date	28/11/2018

Name of Co-Author	Raymond J Rodgers		
Contribution to the Paper	Supervised development of work, manuscript evaluation and acted as corresponding author.		
Signature		Date	9/7/2019

Could Polycystic Ovary Syndrome in Women be due to Perturbed Fetal Development of the Ovary?

Monica D Hartanti[1,2], Roseanne Rosario[3], Katja Hummitzsch[1], Nicole A Bastian[1], Nicholas Hatzirodos[1], Wendy M Bonner[1], Rosemary A Bayne[3], Helen F Irving-Rodgers[1,4], Richard A Anderson[3] and Raymond J Rodgers[1]

[1] Discipline of Obstetrics and Gynaecology, School of Medicine, Robinson Research Institute, The University of Adelaide, Adelaide, SA 5005, Australia
[2] Faculty of Medicine, Trisakti University, Jakarta 11440, Indonesia
[3] Medical Research Council Centre for Reproductive Health, University of Edinburgh, Edinburgh, EH16 4TJ, United Kingdom.
[4] School of Medical Science, Griffith University, Gold Coast Campus, QLD 4222, Australia

Running title: Expression of PCOS candidate genes in the fetal ovary

Disclosure Summary: The authors of this manuscript have nothing to declare and no conflict of interest that could be perceived as prejudicing the impartiality of the research reported.

Abstract

Polycystic ovary syndrome (PCOS) affects around 10% of young women, with adverse consequences on fertility and cardiometabolic outcomes. The polycystic ovary has numerous small follicles and an expanded fibrous, collagen-rich stroma. PCOS appears to result from a sgenetic predisposition interacting with developmental events during fetal or perinatal life. We hypothesised that PCOS candidate genes might be expressed in the fetal ovary when the stroma develops; mechanistically linking the genetics, fetal origins and adult ovarian phenotype of PCOS. We examined human and bovine fetal ovaries. Of 18 PCOS candidate genes only one (*SUMO1P1*) was not expressed. Three patterns of expression were observed: early gestation (*FBN3*, *GATA4*, *HMGA2*, *TOX3*, *DENND1A* and *LHCGR*), late gestation (*INSR*, *FSHR* and *LHCGR*) and throughout gestation (*THADA*, *ERBB4*, *RAD50*, *C8H9orf3*, *YAP1*, *RAB5B*, *SUOX* and *KRR1*). Three other genes, likely to be related to the PCOS aetiology [*AMH*, *AR* and *TGFB1I1* (a TGFβ-regulated coactivator of the androgen receptor)], were also expressed late in gestation. Significantly within each of the three groups, the mRNA levels of many genes were highly correlated with each other, despite, in some instances, being expressed in different cell types. TGFβ is a well-known stimulator of stromal cell replication and collagen synthesis. TGFβ treatment of cultured fetal ovarian stromal cells increased expression of *INSR*, *AR*, *C8H9orf3* and *RAD50* and inhibited expression of *TGFB1I1*. These results have enabled the formulation of a new hypothesis that the predisposition to PCOS in adult life arises by perturbation of the expression of PCOS candidate genes during development of the ovary.

Polycystic ovary syndrome (PCOS) is an endocrine and metabolic disorder, affecting around 10 % of women of reproductive age [1]. It is characterized by the high level of androgens, ovulatory disturbances, infertility, hyperinsulinemia, insulin resistance and obesity [2, 3]. The cause(s) and aetiology of PCOS are not completely understood. PCOS appears to have a genetic origin [4, 5, 6] and a predisposition arising in fetal or perinatal life [7, 8, 9].

Recent genome-wide association cohort studies (GWAS) into PCOS discovered new susceptibility loci associated with 17 genes [reviewed by [10]]: DENN domain-containing 1A *(DENND1A)*, luteinizing hormone/chorionic gonadotropin receptor *(LHCGR)*, follicle stimulating hormone beta subunit *(FSHB)*, follicle stimulating hormone receptor *(FSHR)*, yes associated protein 1 *(YAP1)*, insulin receptor *(INSR)*, ras-related protein *RAB5B*, TOX high mobility group box family member 3 *(TOX3)*, high mobility group AT-hook 2 *(HMGA2)*, chromosome 9 open reading frame 3 *(C9orf3)*, GATA binding protein 4 *(GATA4)*, Erb-B2 receptor tyrosine kinase 4 *(ERBB4)*, DNA repair protein (*RAD50)*, thyroid adenoma associated (*THADA*), sulphite oxidase (*SUOX*), Ca2+/calmodulin-dependent protein kinase (*KRR1*) and the small ubiquitin-like modifier 1 pseudogene 1 *(SUMO1P1)* [11, 12, 13, 14]. Many human studies have been conducted in an effort to investigate these PCOS candidate genes, particularly *DENND1A* and its variants [15], *TOX3* [16], *FSHR* [17], *LHCGR* [18] and *INSR* [19]. Another PCOS susceptibility loci was identified earlier by case-cohort studies using microsatellite analyses and it is located in an intron of fibrillin 3 (*FBN3*) [20]. However, the contribution of these and other candidate gene loci in the development of the PCOS phenotype are still unclear. This is not an uncommon situation for many polygenic diseases where identifying how a SNP or loci identified from genomic studies are related to the aetiology of the disease can take considerable research effort to succeed [21].

Some of the cardinal features of the PCOS ovary are the increased production of androgens, the presence of many antral follicles (inaccurately referred to as cysts in the name PCOS) and substantially more fibrous collagen-rich stroma and tunica albuginea [22]. How or why the stroma is different are not known. However, it is known that when the ovary develops, the stroma in the mesonephros underlying the gonadal ridge migrates or penetrates into the developing ovary; this is a consistent process observed in ovine [23] bovine [24, 25] and human [26, 27] ovarian development. The existence of a relationship between the genetics and fetal origins and the fibrous ovarian phenotype received impetus when it was discovered that *FBN3* is expressed in human and bovine ovarian stroma only in the early stage of fetal development when the stroma penetrates the ovary [8]. Fibrillins regulate TGFβ activity in tissues by their ability to bind latent TGFβ binding proteins [28] and TGFβ stimulates stromal growth and collagen deposition [29]. Thus the concept was developed that increased TGFβ bioactivity during fetal development could contribute to the mechanism of the fetal origins of

a predisposition to developing PCOS in later life [8, 30]. These developmental changes might be subject to environmental modification, during development or postnatally [31].

To date the potential expression of the other PCOS candidate genes in fetal ovaries has not been investigated. Access to human fetal ovaries is relatively limited especially at later gestational ages and so we additionally chose an animal model to investigate expression of PCOS candidate genes. The histology and development of the bovine fetal ovary is similar to the human fetal ovary, as is the length of gestation [32, 33]. Therefore, we analysed the expression of PCOS candidate genes identified by GWAS and additional genes, including androgen receptor *(AR)*, transforming growth factor beta 1 induced transcript 1 *(TGFB1I1)*, *FBN3* and anti-Mullerian hormone *(AMH)*, in bovine fetal ovaries throughout gestation as well as in adult ovaries. We examined the cellular location of expression of these genes by laser capture micro-dissection and examined their expression in bovine fetal ovarian stromal cells *in vitro*. We also analysed the expression of some PCOS candidate genes in human fetal ovaries from the first half of gestation.

Materials and Methods

Ethics approvals

The human study was approved by the Lothian Research Ethics Committee (ref 08/S1101/1). For our bovine study, there were no ethical issues regarding this project since fetal bovine ovaries were collected from the local abattoir which was processing animals for the food chain.

Collection of human fetal ovaries

Human fetal ovaries (n = 15, 8-20 weeks of gestation) were obtained following medical termination of pregnancy as previously described [34]. Maternal informed consent was obtained and the study was approved by the Lothian Research Ethics Committee (ref 08/S1101/1). To determine the gestational age, an ultrasound scan was performed and the length of the fetal foot was measured [35].

Collection of bovine fetal and adult ovaries

Thirty-seven ovaries from fetuses of *Bos taurus* cows across gestation as well as five adult ovaries taken from non-pregnant animals across the estrous cycle (early and mid-luteal phases and the follicular phases) were collected from local abattoirs (Thomas Foods International, Murray Bridge, SA, Australia and Midfield Meat International, Warrnambool,

Victoria, Australia) and were either transferred on ice in Hank's Balanced-Salt solution containing Mg^{2+} and Ca^{2+} ($HBSS^{+/+}$, Sigma-Aldrich Pty Ltd, Castle Hill, NSW, Australia) to the laboratory or dissected and processed on site. To estimate the gestational age of fetal samples, the crown-rump length (CRL) was measured [36].

For laser capture micro-dissection (LCM), fetal ovaries from early (n = 5, 10 – 17 weeks of gestation) and late (n = 5, 36 – 39 weeks of gestation) stage of development were embedded into cryomolds filled with optimal cutting temperature (OCT) compound (ProSciTech, Thuringowa central, QLD, Australia) with the hilum on the side of the mould, frozen on dry ice and stored at -80^{o}C. For RNA extraction from the ovarian samples, 27 whole fetal and 1-3 pieces of cortical area containing preantral follicles and stroma from 5 adult ovaries were snap-frozen on dry ice and stored at -80°C freezer for further analysis, whereas for the laser capture micro-dissected samples the cortical and medullar area were dissected from the fetal ovary and subsequently used for qRT-PCR.

Sex determination of bovine fetuses

Genomic DNA was extracted from the tail of fetuses with a CRL less than 10 cm using the Wizard SV Genomic DNA Purification System (Promega Australia, Alexandria, NSW, Australia) according to the manufacturer's instructions and subsequently amplified. Two pairs of primers specific for a region in the SRY-determining sequence (sense primer: 5'-TCACTCCTGCAAAAGGAGCA-3', antisense primer: 5'-TTATTGTGGCCCAGGCTTG-3') and for the 18S ribosomal RNA (18S) gene sequence was used for amplifying the genomic DNA in individual reactions. Sex determining region Y (SRY) product sequences were verified using a PCR as previously described [24].

Classification of bovine fetal ovaries

Non-laser capture micro-dissected fetal ovary samples were grouped into five groups based on their histological morphology; stage I: ovigerous cord formation (n = 7, 79 ± 6 days of gestation), stage II: ovigerous cord breakdown (n = 4, 127 ± 6 days), stage III: follicle formation (n = 3, 173 ± 12 days), stage IV: ovarian surface epithelium formation (n = 8, 234 ± 9 days) and stage V: tunica albuginea formation (n = 5, 264 ± 6 days) [25].

Laser capture micro-dissection of bovine fetal ovaries

Serial frozen sections of 8 µm thickness were cut using a CM1800 cryostat (Leica Microsystems, Buffalo, IL). Cryosections were transferred onto room temperature PET (polyethylene terephthalate) membrane frame slides (Leica Microsystems, North Ryde, NSW, Australia) and stored in a RNase-free slide box. Slides were fixed in 70% ethanol in DEPC-

treated water, stained in 1% cresyl violet acetate (pH 7.75) (ProSciTech) in 70% ethanol [37], washed for 30 sec with 70%, 90%, and 100% ethanol, followed by 1 min in 100% ethanol and either dissected directly or stored overnight at -80°C in a parafilm-sealed 50 ml tube with dry desiccant. Slides were transferred to the LCM room on dry ice, then incubated for 5 min at 55°C immediately prior to LCM (LMD AS, Leica Microsystems, North Ryde, NSW, Australia). Excised cortical and medullar samples [Supplemental Fig. S1 [38]] were collected into 20 µl of Ambion lysis solution for RNA isolation (Invitrogen, Carlsbad, CA, USA). Ten sections per area collected from 5 animals for each early and late stage of development were used for RNA isolation and subsequent qRT-PCR analysis.

RNA Extraction and cDNA synthesis for human and bovine fetal ovaries

For human samples, RNA from fetal ovaries was extracted using the RNeasy Micro Kit (Qiagen, Crawley, UK) according to manufacturer's instructions. 500ng of RNA was reverse transcribed to cDNA using concentrated random primers and Superscript III reverse transcriptase (Life Technologies) according to manufacturer's instructions, and the cDNA synthesis reaction was diluted 1:20 before proceeding.

Whole fetal and adult bovine ovaries, as well as bovine fetal fibroblasts, were homogenised in 1 ml Trizol® (Thermo Fisher Scientific, Waltham, MA, USA) using the Mo Bio Powerlyser 24 (Mo Bio Laboratories Inc., Carlsbad, CA, USA) and RNA extracted according to manufacturer's instructions. The RNA concentration was then determined using a Nanodrop spectrophotometer (NanoDrop 1000 3.7.1, Nanodrop Technologies, Wilmington, DE, USA) based on the 260λ (wavelength) absorbance. Only samples which had a 260/280λ absorbance ratio > 1.8 were used and subsequently treated with DNase I (Promega/Life Technologies Australia Pty Ltd, Tullmarine, Vic, Australia) for 20 min at 37°C.

For the laser capture micro-dissected samples, total RNA from 2 tissue sections was extracted and DNase treated using the RNAqueous®-Micro Kit (Cat# AM1931, Thermo Fisher Scientific, Waltham, MA, USA) procedure for LCM according to the manufacturer's protocol. The integrity of RNA was assessed using the Experion™ automated electrophoresis system with the Experion RNA HighSens Analysis Kit (Cat# 7007105, Biorad, Hercules, California, USA). Only samples which had a RNA Quality Index (RQI) more than 4 were concentrated using 3M sodium acetate and 100% ethanol. Concentrated RNA samples were then reassessed using the Experion™ automated electrophoresis system and only those which had RQI more than 5 were used for qRT-PCR analysis.

Complementary DNA was then synthesised from 9-200 ng of DNase-treated RNA using 250 ng/µl random hexamers (Sigma, Adelaide, SA, Australia) and 200 U Superscript Reverse Transcriptase III (Thermo Fisher Scientific, Waltham, MA, USA) as previously

described [39]. To exclude genomic contamination, negative control was generated by adding DEPC-water instead of the Superscript Reverse Transcriptase III.

Quantitative real-time PCR

For each gene a standard curve of Cycle threshold (Ct) versus cDNA concentrations was then generated to test the combination of primers. The reactions were performed in duplicate using the following steps. cDNA dilutions were prepared in 10 µl reactions containing 1-2 µl of the 0.5 ng/ul cDNA dilution, 5 µl of Power SYBR™ Green PCR Master Mix (Applied Biosystems, Foster City, CA, USA), 0.1-0.3 µl each of forward and reserve primers [Sigma; Supplemental Table 1 [38]] for the target genes, and 2.6-3.6 µl of DEPC-treated water. The amplification conditions were a 95°C for 15 s, then by 60°C for 60 s for 40 cycles using a Rotor-Gene 6000 series 1.7 thermal cycler (Qiagen GmbH, Hilden, Germany). Ct values were then determined using the Rotor-Gene 6000 software (Q series, Qiagen GmbH, Hilden, Germany) at a threshold of 0.05 normalised fluorescence units. Gene expression was determined by the mean of $2^{-\Delta Ct}$, where ΔCt represents the target gene Ct – average of ribosomal protein L32 *(RPL32)* and peptidylprolyl isomerase A *(PPIA)* Ct for fetal samples and *RPL19* and *RPL32* for comparison of fetal and adult samples. These combinations of housekeeping genes were used because they were the most stable across all samples out of *RPL32, RPL19, PPIA*, actin beta *(ACTB)* and glyceraldehyde-3-phosphate dehydrogenase *(GAPDH)*.

Primers for quantitative real-time PCR

For human fetal ovary samples, qRT-PCR primers were designed to amplify all transcript variants and to span exons [Supplemental Table 1 [38]]. Primer pair efficiencies were calculated with the LinReg PCR applet [40]. Each reaction was performed in a final volume of 10 µL, with 1x Brilliant III SYBR Green qPCR Master Mix (Agilent, Santa Clara, California), 20 pmol of each primer and 2 µL of diluted cDNA. Each cDNA sample was analysed in triplicate. For expression analyses in human fetal ovaries, target genes were normalised to the geometric mean expression of beta-2-microglobulin *(B2M)* and *RPL32*. Data analysis for relative quantification of gene expression and calculation of standard deviations was performed as outlined by [41].

For bovine samples, qRT-PCR primers were designed based on the published reference RNA sequences available in NCBI [Supplemental Table 1 [38]] using Primer3 plus [42] and Net primer (PREMIER Biosoft Palo Alto, CA, USA) software. *DENND1A* is alternatively spliced and variant 1 is the full length mRNA and shares a number of exons in common with other splice variants. Primers used in the human (exons 21 and 22) detected

DENND1A.V1 but could also possibly detect variants 3 and 4 (*DENND1A.V3,4*) [Supplemental Figs 2-4 [38]] and in bovine (exon 12), the primers could also possibly detect the predicted variants 1, 2, 3 and 4 (*DENND1A.X1-4*) [Supplemental Figs. 2-4 [38]]. To attempt to detect variant 2 in the bovine primers to exon 20, and to a what is listed as intronic but corresponding to exon 21 in the human, were used [Supplemental Fig 4 [38]]. The alignment of the human and bovine *DENND1A* sequences and the primer sequences was analysed with the T-coffee method for multiple sequences alignment [43]. Gene *C8H9orf3* is the bovine homologue of the human PCOS candidate gene *C9orf3*.

Statistical analyses

All statistical analyses were carried out using Microsoft Office Excel 2013 (Microsoft Redmond, WA, USA) and GraphPad Prism version 7.00 (GraphPad Software Inc., La Jolla, CA, USA). All $2^{-\Delta Ct}$ data for each fetal ovarian sample were plotted in scatter plot and bar graphs to describe their levels of expression during ovarian development. To analyse the difference between the level of mRNA expression of each gene, one-way ANOVA with Holm-Sidak and Dunnet's *post-hoc* test were used for the whole ovary samples and fetal fibroblasts, respectively. For laser capture micro-dissected samples, unpaired t-test was applied. Pearson correlation test was used for analysing the correlation between levels of each gene with gestational age. After correlation values between genes were identified, a network graph was plotted using the qgraph R package [44] and illustrated using an adjacent matrix plot.

Screening for regulators of PCOS candidate genes

For screening of possible regulators of PCOS candidate genes in fetal ovary, RNA extracted from cultured and treated bovine fetal fibroblasts from another study was used [45]. All ovaries analysed in the current study were from the second trimester. Briefly, bovine fetal ovaries were collected, gestational ages of the fetuses were determined and all ovaries were transferred to the laboratory using the protocol previously mentioned. After removing the surrounded connective tissue, the ovaries were rinsed in 70% ethanol and $HBSS^{+/+}$, dissected and minced with a scalpel. The samples were digested in 1mg/ml collagenase type I (GIBCO/ Life Technologies Australia Pty Ltd, Mulgrave, VIC, Australia) in $HBSS^{+/+}$ at 37ºC shaking at 150 rpm and after centrifugation at 1500 rpm for 5 min, the supernatant was removed. The samples were then digested in 2 ml of 0.025% trypsin/EDTA (GIBCO/Life Technologies) in Hank's Balanced-Salt Solution without Mg^{2+} and Ca^{2+} ($HBSS^{-/-}$; Sigma-Aldrich) for 5 min at 37ºC at 150 rpm and centrifuged at 1500 rpm for 5 min. The pellet was then resuspended in DMEM/F12 medium containing 5% FCS, 1% penicillin and streptomycin sulphate, and 0.1%

fungizone (all GIBCO/Life Technologies). The cells were then dispersed and cultured in 6-well plates or 10 cm petri dishes at 38.5ºC and 5% CO_2 until confluent. The fetal fibroblast cultures were detached by treatment with 0.25% trypsin/EDTA, then the total number of viable cells was estimated with the trypan blue method and stored in liquid nitrogen for subsequent experiments. Bovine fetal fibroblasts (n = 4 from weeks 13, 14, 17 and 19 of gestation for screening of possible regulators; n = 6 for weeks 19-26 of gestation for TGFβ-1 treatment) previously stored in liquid nitrogen were thawed and 30,000 cells/well seeded in 24-well plates in DMEM/F12 medium containing 5% FCS, 1% penicillin and streptomycin sulphate and 0.1% fungizone. The cells were incubated for 24 h at 38.5ºC and 5% CO_2 until 60-70% confluent then the wells were washed with 1X PBS. Different chemical treatments at concentration previously reported in the literature [Supplemental Table 2 [38]] including 5 ng/µl or 20 ng/µl TGFβ-1 in DMEM/F12 medium containing 1% FCS, 1% penicillin and streptomycin sulphate, and 0.1% fungizone were added then after 18 h, the cells were harvested for RNA.

Results

Expression of PCOS candidate genes in the human fetal ovary

We first analysed the mRNA expression levels of *FBN3, HMGA2, TOX3, GATA4, DENND1A.V1-7, DENND1A.V1,3,4, FSHB, LHCGR* and *FSHR* in morphologically normal human fetal ovaries less than 150 days of gestation (Fig. 1). All genes, except for *FSHB,* were detected in the human fetal ovary (Fig. 1). *FBN3, HMGA2* and *DENND1A.V1,3,4* were highly expressed before 70 days of gestation (Figs 1A, C, G), then their expression levels markedly decreased. Additionally, their expression levels were strongly correlated to each other (Table 1). The expression level of *GATA4* was strongly correlated with expression levels of *FBN3* ($P < 0.001$), *HMGA2* ($P < 0.0001$) and *DENND1A* ($P < 0.0001$) (Table 1). A weaker but significant correlation was observed between the *GATA4, DENND1A.V1-7* and *FSHR* expression levels and gestational age (Figs 1B, F, H and Table 1).

Expression of PCOS candidate genes in bovine fetal and adult ovaries

The mRNA levels of PCOS candidate genes were determined in whole ovaries (n = 27) collected from bovine fetuses ranging from 8 – 39 weeks gestation and in adult ovaries. Most

of the PCOS candidate genes were expressed during the development of the bovine fetus (Figs 2 – 4). We could not detect expression of *DENND1A.V2* and *SUMO1P1* in the bovine fetal ovary, nor in the bovine adult thecal cells, ovary, heart, spleen, kidney or liver.

Of the PCOS candidate genes that were analysed in the bovine fetal ovary, *FBN3, GATA4, HMGA2, TOX3* and *DENND1A.X1,2,3,4* were expressed early during ovarian development and then declined (Figs 2A–D, G). *LHCGR* was upregulated in early development, downregulated to the lowest point around 150 days of gestation, then sharply increased in late gestation (Fig. 2E) whereas the other early genes showed no similar increase in late gestation. *FSHB* mRNA levels peaked at around 100 days of gestation then declined until the end of gestation, however, the levels were exceedingly low and may not have much biological relevance (Fig. 2F). The mRNA levels of three of the PCOS candidate genes identified by GWAS studies, *INSR, FSHR* and *AMH*, as well as *AR* and *TGFB1I1* were low early in gestation gradually increasing until the end of gestation (Figs 3A-E). The other genes, *C8H9orf3, RAB5B, ERBB4, YAP1, SUOX, RAD50, THADA,* and *KRR1* were expressed throughout development, however, their mRNA levels did not correlate with gestational age (Figs 4A-H).

We also classified the fetal ovary samples into 5 groups reflecting key stages in development as shown previously [25] and described in the Materials and Methods. We compared the mRNA levels at each stage and with those in the adult ovary. *FBN3*, *HMGA2* and *TOX3* mRNA levels were high in the early stages and decreased significantly from stage III to the lowest levels in the adult ovary (Figs 2H, J-K). *GATA4, FSHB* and *DENND1A.X1,2,3,4* (Figs 2I, M-N), as well as *C8H9orf3, RAB5B, RAD50* and *KRR1* (Figs 4I, J, N, P), mRNA levels were elevated in stages I and II declining significantly at the later stages. There was no significant difference between the mRNA levels of *YAP1* and *SUOX* in all 5 fetal stages, however, in the adult ovary, their levels were significantly decreased (Figs 4L, M). *FSHR* and *AMH* were expressed highly in the adult ovary compared to all 5 stages in the fetal ovary (Figs 3G-H). The mRNA levels of *AR* and *TGFB1I1* peaked at stage V (Figs 3I, J). Their mRNA levels were significantly lower in the adult ovary compared to stages IV and V (Figs 3I, J). No significant differences were observed in the mRNA levels of *LHCGR* (Fig. 2L), *INSR* (Fig. 3F) and *THADA* (Fig. 4O) in the fetal and adult ovaries.

Correlations between levels of mRNA

To analyse the correlation between the expression levels of PCOS candidate genes and gestational age in bovine ovaries, we generated a Pearson correlation matrix (Table 2). *FBN3* positively correlated with *HMGA2* ($P < 0.0001$), *TOX3* ($P < 0.0001$), *GATA4* ($P < 0.0001$) and *DENND1A.X1,2,3,4* ($P < 0.0001$), *HMGA2* positively correlated with *TOX3* ($P < 0.0001$),

GATA4 ($P < 0.0001$) and *DENND1A.X1,2,3,4* ($P < 0.001$), *TOX3* positively correlated with *GATA4* ($P < 0.0001$) and *DENND1A.X1,2,3,4* ($P < 0.0001$), and *GATA4* positively correlated with *DENND1A.X1,2,3,4* ($P < 0.0001$) (Table 2). In addition, *FBN3, HMGA2* and *TOX3* also negatively correlated ($r > -0.6$) with *FSHR, AMH, INSR, AR* and *TGFB1I1*. After correlation values between genes were identified, a network graph was plotted using the qgraph R package [44] to plot an adjacent matrix [Supplemental Fig. 5 [38]]. Most of the genes, except *ERBB4*, were closely and highly connected with each other as well as with gestational age, suggesting a strong correlation between all genes and gestational age.

To accommodate the bimodal expression pattern of *LHCGR*, we additionally analysed the correlations between expression levels of genes in bovine fetal ovaries using the data from fetuses less than 150 days of gestation [Supplemental Table 3 [38]]. Our results showed that there was a strong correlation ($r > 0.6$) between the expression levels of the majority of genes that were highly expressed in early development (*FBN3*, *GATA4*, *HMGA2*, *DENND1A.X1,2,3,4* and *LHCGR*) [Supplemental Table 3 [38]]. Interestingly, a strong negative correlation was observed between *LHCGR* and *INSR* ($P < 0.01$), *AR* ($P < 0.01$) and *TGFB1I1* ($P < 0.001$), which are the genes that were highly expressed in late stages of development [Supplemental Table 3 [38]]. The results also showed a strong correlation ($r > 0.6$) between *FSHB* and *GATA4* and between *HMGA2* and *LHCGR* [Supplemental Table 3 [38]].

Differential gene expression in the cortex and medulla of fetal ovary

To study the localization of cells expressing these genes, we conducted laser capture micro-dissection in the bovine ovarian cortex and medulla at early (10 – 17 weeks) and late (36 – 39 weeks) stages of gestation. We investigated the mRNA levels of PCOS candidate genes in these two areas [Supplemental Figs 6-8 [38]]. If expressed higher in the medulla we putatively interpreted this as being stromal expression and if expressed more highly in the cortex we putatively interpreted this as expression in the cortical ovigerous cords or follicles if late in gestation. Validation of this approach was confirmed by examining the expression of germ cell markers (*VASA* and *OCT4*) as well as the epithelial marker *KRT19*, which is expressed in GREL and granulosa cells of the bovine fetal ovary but not in stromal cells [24] [Supplemental Fig 9 [38]], and *FBN3* [Supplemental Fig. 6 [38]], which is expressed in the stroma [8, 24].

The level of mRNA of *FSHB* was significantly higher in the ovarian cortex compared with the medulla in the early stage [Supplemental Fig. 6 [38]], *FSHR* in the late stage [Supplemental Fig. 7 [38]] and *ERBB4* in both the early and late stage of development [Supplemental Fig. 8 [38]]. The expression levels of *FBN3* [Supplemental Fig. 6 [38]], *INSR, AR, TGFB1I1* [Supplemental Fig. 7 [38]], *YAP1* and *SUOX* [Supplemental Fig. 8 [38]] were significantly higher in the ovarian medulla compared with the cortex in early development.

Other genes did not show any significant difference between cortical and medullar expression levels.

Regulation of PCOS related genes in bovine fetal ovary

We treated bovine fetal fibroblasts (n = 4 from 13-19 weeks of gestation) with 24 growth factors and hormones [Supplemental Table 2 [38]], and observed the effect on the expression of PCOS candidate genes [Supplemental Figs 10-12 [38]]. These factors and hormones have been shown to have important physiological roles in the adult ovary, such as cell proliferation and the production of extracellular matrices. The average levels of expression (2^delta-delta-Ct) for the untreated cells are shown in Supplemental Table 4 [38], and compared with the *in vivo* RNA levels from whole ovaries from the same gestational ages as shown in Figs 2-4. Most genes were expressed at a lower level except *GATA4* and *TGFB1I1* which were >20 fold higher *in vitro* [Supplemental Table 4 [38]]. Treatment with fibroblast growth factor 9 (FGF-9) significantly increased mRNA levels of *HMGA2* in fetal fibroblasts [Supplemental Fig. 10 [38]]. Other treatments did not affect the expression level of *HMGA2* [Supplemental Figs 10-12 [38]]. Other PCOS genes, except *FSHR* and *FSHB,* were detected in the cultured bovine fetal fibroblasts, however, none were significantly affected by any of the treatments [Supplemental Figs 10-12 [38]].

Treatment with TGFβ-1 (5 or 20 ng/ml) of 19-26 weeks bovine fetal fibroblasts resulted in a significant reduction in expression levels of *INSR*, *AR*, *C8H9orf3* and *RAD50* (Fig. 5), compared to the untreated control and this reduction was enhanced by the higher TGFβ-1 concentration. We did not find any significant effect on *TGFB1I1* expression in fetal fibroblasts treated with 5 ng/ml TGFβ-1, however, a significant increase was observed with 20 ng/ml TGFβ-1 (Fig. 5). Other genes were not significantly affected (Fig. 5).

Discussion

To our knowledge, this is the first study that reports the levels of mRNA of PCOS candidate genes identified by GWAS in the developing fetal ovary. In both human and bovine ovaries we were able to identify a number of candidate genes that were expressed, whose pattern of expression changed during gestation, and whose expression levels were highly correlated with each other. Additionally in bovine ovaries we identified the region of the ovary where the genes were expressed and we examined gene expression in cultured fetal ovarian fibroblasts. This study thus identified relationships between the genetic and fetal origins of a predisposition to developing PCOS in later life.

It should be noted that this study was limited to the analyses of only 11 human fetal ovaries, which is why we additionally undertook bovine analyses. Also human fetal ovaries were not available from late gestation for analyses. No direct causality studies were conducted. It is difficult to imagine how they could be at this stage, given that ovaries cannot readily be sampled during fetal development and linked with PCOS status in later life.

For discussion we have grouped the genes into three categories based upon their expression pattern across gestation. The early genes were expressed highly in the first trimester but continued to decline in expression to reach a low at about mid gestation. The late genes were first detected midway through gestation and continued to increase in expression during the remainder of gestation. The third group of genes were expressed at relatively similar levels across all of gestation. Expression of some genes including *DENND1A.V2* and *SUMO1P1* (bovine only examined) was not detected.

The early genes

The group of bovine genes expressed early in gestation included *FBN3, GATA4, HMGA2, TOX3* and *DENND1A.X1,2,3,4*. Their mRNA levels were strongly positively correlated with each other and negatively with gestational age. *FBN3, GATA4* and *DENND1A.X1,2,3,4* were elevated in the medulla early in gestation but *HMGA2* and *TOX3* did not show any differential pattern between cortex and medulla. *LHCGR* expression was also elevated early during ovarian development declining to the lowest point around mid-gestation, before sharply increasing until the end of gestation. *LHCGR* expression was also elevated in the medulla at the early stages, like *FBN3, GATA4* and *DENND1A.X1,2,3,4*. Examining the data in the first half of gestation only, showed that *LHCGR* expression was positively but weakly correlated with most of the other early genes. This early expression of *LHCGR* precedes follicle formation and the expression in the medulla suggests that this is not associated with follicular cells at the early stage.

This same set of genes was examined in human fetal ovaries in the first half of gestation. All genes identified in the bovine were expressed in the human ovaries particularly at the earliest stages. In the human ovary *FBN3, GATA4, HMGA2* and *DENND1A* (V1-7 and V1, 3, 4) were all strongly positively correlated with each other and negatively with gestational age. *TOX3* only declined in the two oldest samples examined and *LHCGR* was only elevated in two of four youngest samples and hence whilst these genes showed a similar patterns of expression to the other early genes their expression was not correlated with them.

Two other genes were expressed early but differently between bovine and human. *FSHB*, although normally expressed in the anterior pituitary, was detected early in the bovine ovary and its expression level peaked at around 100 days of gestation then declined until the

end of gestation. However, it should be noted that the levels were very low and may not be of biological relevance. In the human *FSHB* was not detected but *FSHR* was expressed in three of the youngest four ovaries examined and it was very low in the older samples. At this stage it is not entirely clear how best to interpret these findings.

DENND1A encodes DENND1A (DENN domain containing 1A, connecdenn 1) protein which is believed to assist endocytosis [46]. Human *DENND1A* possesses 7 variants in total (DENND1A.V1-7) as well as 19 predicted variants (DENND1A.X1-19) (https://www.ncbi.nlm.nih.gov/). The function of these variants is still unclear, however, 2 variants, DENND1A.V1 and DENND1A.V2 have been linked to PCOS [47, 48]. DENND1A.V1 encodes a 1009 amino acid protein with C-terminal proline-rich domain, whereas DENND1A.V2 encodes a 559 amino acid protein containing three DENN domains and additionally a C-terminal 33 amino acid sequence [47]. A recent study has found that *DENND1A.V2* might play an important role in pathophysiology of hyperandrogenemia associated with PCOS [47] due to several reasons: significantly elevated levels of DENND1A.V2 mRNA and protein in PCOS thecal cells compared to non-PCOS thecal cells; significantly elevated levels of *DENND1A.V2* mRNA in urine of PCOS women compared to women with normal cycles; augmentation of *CYP17A1* and *CYP11A1* gene transcription, as well as increased dehydroepiandrosterone (DHEA) production in response to overexpression of *DENND1A.V2* in normal thecal cells [48]. We were unable to detect the expression of *DENND1A.V2* in bovine fetal ovaries or adult thecal cells. However, there were elevated mRNA levels of *DENND1A* in early bovine and human fetal ovaries.

Overall this group of genes expressed early has some unique characteristics. The genes are highly expressed when the ovigerous cords are forming by penetration of the stroma from the mesonephros [24, 25] and the proteins encoded by these genes have different cellular functions including extracellular matrix, transcription factors, hormone receptors and clathrin-mediated endocytosis. These genes may also be expressed in different cell types as inferred from their different expression patterns comparing the cortex and medulla of the ovary. These genes are all elevated long before the time of gestation when animal models of PCOS can be generated by treating pregnant mothers or newborns with androgens [49].

The late genes

The mRNA levels of two of the PCOS candidate genes, *INSR* and *FSHR*, as well as *AMH, AR* and *TGFB1I1* were low early in bovine gestation and then gradually increased from mid gestation until the end of gestation. The mRNA levels of these genes were highly correlated with each other and with gestational age. *INSR, AR* and *TGFB1I1* were elevated in the medulla suggesting that they are expressed in the stroma. *FSHR* was elevated in the cortex in

late gestation suggesting that it is associated, as expected, with granulosa cells of follicles, although *AMH* expression did not show the same localization. The *LHCGR* gene was also upregulated in the second half of gestation and its mRNA levels were highly correlated with *FSHR* and *AMH*, but not *INSR*, *AR* and *TGFB1I1* mRNA levels. It is intriguing that expression levels correlate with each other yet three of the genes appear to be expressed in stroma (*INSR*, *AR* and *TGFB1I1*) and three in follicles (*FSHR*, *LHCGR* and *AMH*). Expression of *TGFB1I1* and *AR* suggest that TGFβ signaling could be augmenting AR signaling and regulating stromal function during the second half of gestation.

The constantly expressed genes

The other genes, *C8H9orf3*, *RAB5B*, *ERBB4*, *YAP1*, *SUOX*, *RAD50*, *THADA* and *KRR1* were expressed throughout development of the bovine fetal ovary, however, their mRNA levels did not correlate with gestational age except for weak negative correlations with *C8H9orf3* and *RAD50*. Within this group there were a number of associations, but in particular *C8H9orf3*, *RAB5B*, *SUOX* and *YAP1* were highly positively correlated with each other and with *DENND1A.X1,2,3,4* from the early group of genes. *C8H9orf3* also showed some weaker but positive correlations with some of the other members of the early group of genes. *SUOX* and *YAP1* were elevated in the medulla and *ERBB4* was elevated in the cortex. There is little information regarding the expression and function of *SUMO1P1*, one of the eight human *SUMO1* pseudogenes in human or bovine [50]. In this study, we could not detect expression of *SUMO1P1* in the bovine fetal ovary or adult thecal cells, liver, heart, spleen and kidney, suggesting that this gene might not be expressed in bovine tissues.

Overall changes in PCOS candidate gene expression

The mRNA levels of most PCOS candidate genes were correlated with many others in bovine fetal ovaries, suggesting a degree of co-regulation or coordination of behaviours of different cells in the ovary. Genes that were highly expressed early are thought to be linked to stroma development, whereas genes that were upregulated later in the development may have an important role in follicular development. Interestingly, strong negative correlations were observed between the genes that were upregulated early and those that were upregulated later in ovarian development.

Regulation of genes

Bovine fetal fibroblasts from the second trimester were treated with growth factors and hormones and the expression of PCOS candidate genes measured. Previous examination of these cells in culture found that *FBN3* expression declined whilst *FBN1* increased [51],

suggesting that the fibroblasts were undergoing maturation similar to changes in fibrillin gene expression during fetal ovarian development [8]. Most genes were unresponsive to treatments except *HMGA2* which increased in response to fibroblast growth factor 9 (FGF-9), and *INSR*, *AR*, *C8H9orf3* and *RAD50* all decreased while *TGFB1I1* increased in response to TGFβ-1. All the components of the TGFβ pathways are expressed in the fetal ovary, changing during the course of ovarian development [8]. Since TGFβ stimulates stromal growth and collagen deposition [29] the concept was developed that increased TGFβ bioactivity during fetal development could contribute the mechanism of the fetal disposition to PCOS in later life [8, 30]. That five of the PCOS candidate genes, including AR and its co-activator TGFB1I1 could be regulated by TGFβ-1 further supports the concept that altered TGFβ signalling during fetal development could contribute to the aetiology of the predisposition to PCOS in later life.

Summary and conclusions

In summary nearly all genes in loci associated with PCOS were expressed in the developing fetal ovary. They fell into three groups of early, late and constant expression during development. Within each group, the expression levels of many genes were strongly correlated with each other, despite, in some instances, being expressed in different cell types indicating that gene expression is coordinated and linked to fetal ovarian development. Three of the PCOS candidate genes, and *AR* and its coactivator *TGFB1I1*, were regulated by TGFβ *in vitro.* This is notable as fetal or neonatal exposure to androgens can induce PCOS in later life. Additionally in stroma TGFβ stimulates expansion of the stroma and collagen deposition, both known to be elevated in the polycystic ovary. Members of the TGFβ pathway also change during development of the ovary suggesting that TGFβ signalling is multifaceted [8]. We conclude that the expression of these genes might be related to ovarian development, thus potentially holding the key to understanding the predisposition to the development of PCOS in later life.

Acknowledgements

The authors would like to thank Thomas Food International, Murray Bridge, South Australia and Midfield Meat International, Warrnambool, Victoria for providing the bovine tissues for this research. We are also grateful to Ms Ruth Williams (Adelaide Microscopy, The University of Adelaide, North Terrace, Adelaide) for providing training on the Lasercapture Micro-dissection Microscope and to Adelaide Microscopy, The University of Adelaide, North Terrace, Adelaide for the use of the Leica AS-LMD Laser Microdissection Microscope.

Financial Support: The research activities conducted in Australia were funded by the Australia Awards Scholarship from the Australian Government, The University of Adelaide, the National Health and Medical Research Council of Australia, the NHMRC Centre for Research Excellence in the Evaluation, Management and Health Care Needs of Polycystic Ovary Syndrome. The research activities conducted in the UK were supported by the UK Medical Research Council (grant no G1100357).

Author contributions: MDH, NAB, KH, NH, HFI-R and RJR designed the study on bovine samples. WMB provided bovine samples. MDH, KH, HFI-R and RJR carried out data analysis bovine samples. MDH carried out laser capture micro-dissection and gene expression assays in bovine samples. NAB and KH conducted cell culture and treatment experiments in bovine fetal fibroblasts. RR and RAB carried out gene expression assays in human samples. RR conducted data analysis in human samples. MDH drafted the manuscript. RAB, KH, HFI-R, RAA and RJR critically reviewed and approved the final version of the manuscript.

Correspondence: Raymond J Rodgers, Discipline of Obstetrics and Gynaecology, School of Medicine, Robinson Research Institute, The University of Adelaide, Adelaide, SA 5005, Australia. Email ray.rodgers@adelaide.edu.au

Disclosure Summary: The authors of this manuscript have nothing to declare and no conflict of interest that could be perceived as prejudicing the impartiality of the research reported.

References

1. Bozdag G, Mumusoglu S, Zengin D, Karabulut E, Yildiz BO. The prevalence and phenotypic features of polycystic ovary syndrome: a systematic review and meta-analysis. *Hum Reprod* **31**, 2841-2855 (2016).

2. Lim SS, Davies MJ, Norman RJ, Moran LJ. Overweight, obesity and central obesity in women with polycystic ovary syndrome: a systematic review and meta-analysis. *Hum Reprod Update* **18**, 618-637 (2012).

3. Teede H, Deeks A, Moran L. Polycystic ovary syndrome: a complex condition with psychological, reproductive and metabolic manifestations that impacts on health across the lifespan. *BMC medicine* **8**, 41 (2010).

4. Wang T*, et al.* Genetic Predisposition to Polycystic Ovary Syndrome, Postpartum Weight Reduction, and Glycemic Changes: A Longitudinal Study in Women With Prior Gestational Diabetes. *J Clin Endocrinol Metab* **100**, E1560-1567 (2015).

5. Vink JM, Sadrzadeh S, Lambalk CB, Boomsma DI. Heritability of polycystic ovary syndrome in a Dutch twin-family study. *J Clin Endocrinol Metab* **91**, 2100-2104 (2006).

6. Coviello AD, Sam S, Legro RS, Dunaif A. High prevalence of metabolic syndrome in first-degree male relatives of women with polycystic ovary syndrome is related to high rates of obesity. *J Clin Endocrinol Metab* **94**, 4361-4366 (2009).

7. Tata B*, et al.* Elevated prenatal anti-Mullerian hormone reprograms the fetus and induces polycystic ovary syndrome in adulthood. *Nature medicine* **24**, 834-846 (2018).

8. Hatzirodos N*, et al.* Linkage of regulators of TGF-beta activity in the fetal ovary to polycystic ovary syndrome. *FASEB J* **25**, 2256-2265 (2011).

9. Dumesic DA, Goodarzi MO, Chazenbalk GD, Abbott DH. Intrauterine environment and polycystic ovary syndrome. *Semin Reprod Med* **32**, 159-165 (2014).

10. Jones MR, Goodarzi MO. Genetic determinants of polycystic ovary syndrome: progress and future directions. *Fertil Steril* **106**, 25-32 (2016).

11. Chen ZJ*, et al.* Genome-wide association study identifies susceptibility loci for polycystic ovary syndrome on chromosome 2p16.3, 2p21 and 9q33.3. *Nat Genet* **43**, 55-59 (2011).

12. Shi Y*, et al.* Genome-wide association study identifies eight new risk loci for polycystic ovary syndrome. *Nat Genet* **44**, 1020-1025 (2012).

13. Hayes MG*, et al.* Genome-wide association of polycystic ovary syndrome implicates alterations in gonadotropin secretion in European ancestry populations. *Nat Commun* **6**, 7502 (2015).

14. Day FR*, et al.* Causal mechanisms and balancing selection inferred from genetic associations with polycystic ovary syndrome. *Nat Commun* **6**, 8464 (2015).

15. McAllister JM, Legro RS, Modi BP, Strauss JF, 3rd. Functional genomics of PCOS: from GWAS to molecular mechanisms. *Trends Endocrinol Metab* **26**, 118-124 (2015).

16. Ning Z, JIAYI L, JIAN R, WANLI X. Relationship between abnormal TOX3 gene methylation and polycystic ovarian syndrome. *Eur Rev Med Pharmacol Sci* **21**, 5 (2017).

17. Wu XQ, Xu SM, Liu JF, Bi XY, Wu YX, Liu J. Association between FSHR polymorphisms and polycystic ovary syndrome among Chinese women in north China. *J Assist Reprod Genet* **31**, 371-377 (2014).

18. Kanamarlapudi V, Gordon UD, Lopez Bernal A. Luteinizing hormone/chorionic gonadotrophin receptor overexpressed in granulosa cells from polycystic ovary syndrome ovaries is functionally active. *Reprod Biomed Online* **32**, 635-641 (2016).

19. Mutib MT, Hamdan FB, Anam R. Al-Salihi AR. INSR gene variation is associated with decreased insulin sensitivity in Iraqi women with PCOs. *Iran J Reprod Med* **12(7)**, 8 (2014).

20. Urbanek M, Sam S, Legro RS, Dunaif A. Identification of a polycystic ovary syndrome susceptibility variant in fibrillin-3 and association with a metabolic phenotype. *J Clin Endocrinol Metab* **92** 4191-4198 (2007).

21. Manolio TA*, et al.* Finding the missing heritability of complex diseases. *Nature* **461**, 747-753 (2009).

22. Hughesdon PE. Morphology and morphogenesis of the Stein-Leventhal ovary and of so-called "hyperthecosis". *Obstet Gynecol Surv* **37**, 59-77 (1982).

23. Juengel JL*, et al.* Origins of follicular cells and ontogeny of steroidogenesis in ovine fetal ovaries. *Mol Cell Endocrinol* **191**, 1-10 (2002).

24. Hummitzsch K*, et al.* A new model of development of the mammalian ovary and follicles. *PLoS One* **8**, e55578 (2013).

25. Hartanti MD*, et al.* Morphometric and gene expression analyses of stromal expansion during development of the bovine fetal ovary. *Reproduction, Fertility and Development* **(in press)**, (2018).

26. Konishi I, Fujii S, Okamura H, Parmley T, Mori T. Development of interstitial cells and ovigerous cords in the human fetal ovary: an ultrastructural study. *J Anat* **148**, 121-135 (1986).

27. Heeren AM*, et al.* Development of the follicular basement membrane during human gametogenesis and early folliculogenesis. *BMC Dev Biol* **15**, 4 (2015).

28. Massam-Wu T*, et al.* Assembly of fibrillin microfibrils governs extracellular deposition of latent TGF beta. *J Cell Sci* **123**, 3006-3018 (2010).

29. Stewart AG, Thomas B, Koff J. TGF-beta: Master regulator of inflammation and fibrosis. *Respirology (Carlton, Vic)*, (2018).

30. Raja-Khan N, Urbanek M, Rodgers RJ, Legro RS. The role of TGF-beta in polycystic ovary syndrome. *Reprod Sci* **21**, 20-31 (2014).

31. Rodgers RJ*, et al.* Is polycystic ovary syndrome a 20th Century phenomenon? . *Medical Hypotheses* **124**, 31–34 (2019).

32. Jimenez R. Ovarian organogenesis in mammals: mice cannot tell us everything. *Sex Dev* **3**, 291-301 (2009).

33. Adams GP, Jaiswal R, Singh J, Malhi P. Progress in understanding ovarian follicular dynamics in cattle. *Theriogenology* **69**, 72-80 (2008).

34. Coutts SM*, et al.* Activin signals via SMAD2/3 between germ and somatic cells in the human fetal ovary and regulates kit ligand expression. *Dev Biol* **314**, 189-199 (2008).

35. Mhaskar R, Agarwal N, Takkar D, Bruckshee K, Anandalakshmi, Deorari A. Fetal foot length - a new parameter for assessment of gestational age. *Int J Gynecol Obstet* **29**, 35-38 (1989).

36. Russe I. Oogenesis in cattle and sheep. *Biblthca Anat* **24**, 77-92 (1983).

37. Cummings M, McGinley CV, Wilkinson N, Field SL, Duffy SR, Orsi NM. A robust RNA integrity-preserving staining protocol for laser capture microdissection of endometrial cancer tissue. *Analytical biochemistry* **416**, 123-125 (2011).

38. Hartanti MD*, et al.* Could polycystic ovary syndrome in women could be due to perturbed fetal development of the ovary? *To be uploaded to Dryad Digital Repository*, (2019).

39. Matti N, Irving-Rodgers HF, Hatzirodos N, Sullivan TR, Rodgers RJ. Differential expression of focimatrix and steroidogenic enzymes before size deviation during waves of follicular development in bovine ovarian follicles. *Mol Cell Endocrinol* **321**, 207-214 (2010).

40. Ramakers C, Ruijter J, Deprez R, Moorman A. Assumption-free analysis of quantitative real-time polymerase chain reaction (PCR) data. *Neuroscience Letters* **339**, 62-66 (2003).

41. Vandesompele J*, et al.* Accurate normalization of real-time quantitative RT-PCR data by geometric averaging of multiple internal control genes. *Genome Biology* **3**, 1-12 (2002).

42. Rozen S, Skaletsky HJ. Primer3 on the WWW for general users and for biologist programmers. In: *Bioinformatics Methods and Protocols: Methods in Molecular Biology* (ed^(eds Krawetz S, Misener S). Humana Press (2000).

43. Notredame C, Higgins DG, Heringa J. T-Coffee: A novel method for fast and accurate multiple sequence alignment. *J Mol Biol* **302**, 205-217 (2000).

44. Epskamp S, Cramer AOJ, Waldorp LJ, Schmittmann VD, Borsboom D. qgraph: Network Visualizations of Relationships in Psychometric Data. *J Stat Softw* **48**, 1-18 (2012).

45. Bastian NA*, et al.* Regulation of fibrillins and modulators of TGFβ in fetal bovie and human ovaries. *Reproduction* **152**, 127-137 (2016).

46. Marat AL, Dokainish H, McPherson PS. DENN domain proteins: regulators of Rab GTPases. *J Biol Chem* **286**, 13791-13800 (2011).

47. Tee MK*, et al.* Alternative splicing of DENND1A, a PCOS candidate gene, generates variant 2. *Mol Cell Endocrinol* **434**, 25-35 (2016).

48. McAllister JM*, et al.* Overexpression of a DENND1A isoform produces a polycystic ovary syndrome theca phenotype. *Proc Natl Acad Sci U S A* **111**, E1519-1527 (2014).

49. Walters KA, Bertoldo MJ, Handelsman DJ. Evidence from animal models on the pathogenesis of PCOS. *Best practice & research Clinical endocrinology & metabolism* **32**, 271-281 (2018).

50. LeBlanc M*, et al.* Genome-wide study identifies PTPRO and WDR72 and FOXQ1-SUMO1P1 interaction associated with neurocognitive function. *J Psychiatr Res* **46**, 271-278 (2012).

51. Bastian NA*, et al.* Regulation of fibrillins and modulators of TGFβ in fetal bovine and human ovaries. *Reproduction* **152**, 11 (2016).

Table 1. Pearson correlation coefficients (r) of mRNA expression levels of PCOS-candidate genes and gestational age in the human fetal ovary (n = 15).

	Age	***FBN3***	***GATA4***	***HMGA2***	***TOX3***	***LHCGR***	***DENND1A. V1-7***	***DENND1A. V1,3,4***
FBN3	-0.906[b]							
GATA4	-0.593[a]	0.767[c]						
HMGA2	-0.685[b]	0.852[d]	0.934[d]					
TOX3	-0.033	-0.134	-0.078	-0.115				
LHCGR	-0.491	0.421	0.020	0.287	0.081			
DENND1A. V1-7	-0.595[a]	0.697[b]	0.782[c]	0.864[d]	0.302	0.291		
DENND1A. V1,3,4	-0.674[b]	0.790[c]	0.808[c]	0.904[d]	0.232	0.357	0.982[d]	
FSHR	-0.545[a]	0.575[a]	0.680[b]	0.606[a]	-0.185	-0.033	0.445	0.421

[a] $P < 0.05$, [b] $P < 0.01$, [c] $P < 0.001$, [d] $P < 0.0001$

Table 2. Pearson correlation coefficients (r) of mRNA expression levels of PCOS-candidate genes and gestational age in bovine fetal ovaries (n = 27).

	Age	***FBN3***	***GATA4***	***HMGA2***	***TOX3***	***LHCGR***	***FSHB***	***DENND1A.X1,2,3,4***	***C8H9orf3***	***RAB5B***	***ERBB4***	***YAP1***	***SUOX***	***RAD50***	***THADA***	***KRR1***	***INSR***	***FSHR***	***AMH***	***AR***
FBN3	-0.887[d]																			
GATA4	-0.709[d]	0.898[d]																		
HMGA2	-0.898[d]	0.959[d]	0.849[d]																	
TOX3	-0.892[d]	0.824[d]	0.670[d]	0.826[d]																
LHCGR	0.332	-0.156	-0.079	-0.177	-0.382[a]															
FSHB	-0.563[b]	0.406[a]	0.182	0.443[a]	0.678[c]	-0.403[a]							\							
DENND1A.X1,2,3,4	-0.606[c]	0.696[d]	0.777[d]	0.675[c]	0.731[d]	-0.311	0.347													
C8H9orf3	-0.393[a]	0.543[b]	0.671[c]	0.506[b]	0.511[b]	-0.256	0.295	0.841[d]												
RAB5B	-0.314	0.246	0.340	0.258	0.485[a]	-0.459[a]	0.471[a]	0.714[d]	0.644[c]											
ERBB4	0.305	-0.240	-0.161	-0.256	-0.164	0.162	0.049	0.010	0.044	0.278										
YAP1	-0.080	0.236	0.491[b]	0.217	0.225	-0.387[a]	0.064	0.637[c]	0.716[d]	0.692[d]	0.232									
SUOX	0.175	0.140	0.403[a]	0.083	-0.037	0.073	-0.250	0.505[b]	0.639[c]	0.392[a]	0.073	0.722[d]								
RAD50	-0.497[b]	0.405[a]	0.359	0.434[a]	0.600[c]	-0.577[b]	0.563[b]	0.526[b]	0.430[a]	0.690[d]	0.186	0.490[b]	0.054							
THADA	0.380	-0.264	0.001	-0.231	-0.268	0.177	-0.176	0.217	0.435[a]	0.359	0.225	0.557[b]	0.585[b]	0.059						
KRR1	-0.352	0.379	0.368	0.463[a]	0.515[b]	-0.478[a]	0.505[b]	0.663[c]	0.586[b]	0.600[c]	-0.110	0.589[b]	0.430[a]	0.591[b]	0.334					
INSR	0.775[d]	-0.601[c]	-0.312	-0.643[c]	-0.632[c]	0.248	-0.435[a]	-0.143	0.167	0.116	0.369	0.392[a]	0.572[b]	-0.283	0.756[d]	-0.070				
FSHR	0.753[d]	-0.580[b]	-0.436[a]	-0.640[c]	-0.684[d]	0.675[c]	-0.531[b]	-0.392[a]	-0.203	-0.196	0.451[a]	-0.062	0.256	-0.391[a]	0.456[a]	-0.432[a]	0.729[d]			
AMH	0.682[d]	-0.525[b]	-0.408[a]	-0.542[b]	-0.632[c]	0.846[d]	-0.427[a]	-0.476[a]	-0.310	-0.374	0.242	-0.306	0.153	-0.619[c]	0.313	-0.438[a]	0.573[b]	0.818[d]		
AR	0.765[d]	-0.669[c]	-0.420[a]	-0.654[c]	-0.648[c]	0.234	-0.452[a]	-0.258	-0.028	-0.047	0.055	0.137	0.420[a]	-0.358	0.491[b]	-0.040	0.696[d]	0.476[a]	0.568[b]	
TGFB1I1	0.853[d]	-0.664[c]	-0.413[a]	-0.695[d]	-0.676[c]	0.231	-0.444[a]	-0.188	0.034	0.024	0.432[a]	0.292	0.518[b]	-0.352	0.584[b]	-0.032	0.876[d]	0.669[c]	0.537[b]	0.772[d]

[a] $P < 0.05$, [b] $P < 0.01$, [c] $P < 0.001$, [d] $P < 0.0001$

Figures

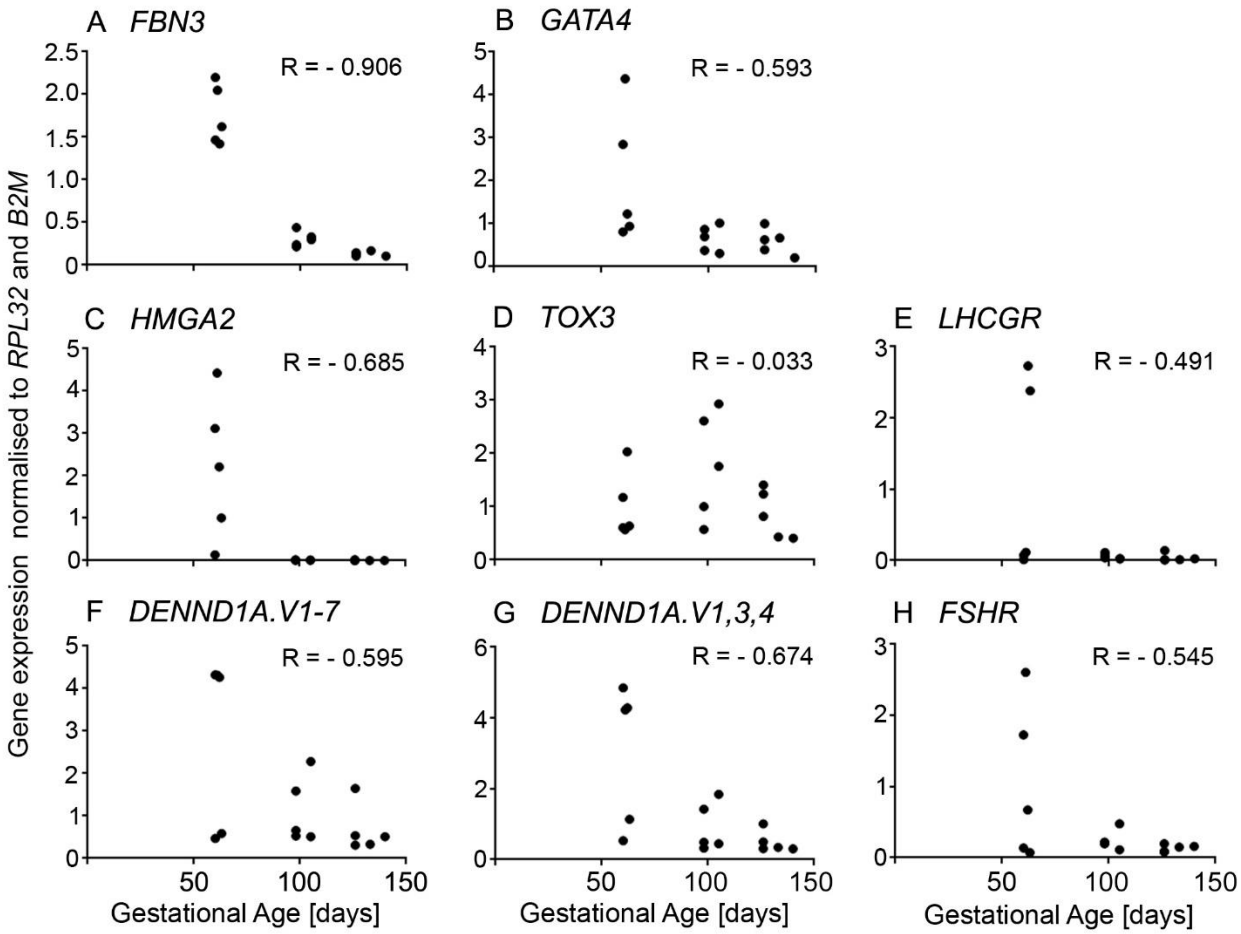

Figure 1. Scatter plot of mRNA expression levels of some PCOS candidate genes analysed in human fetal ovaries (n = 15, 8 – 20 weeks of gestation). Pearson correlation coefficient (r) test was used to analyse the data.

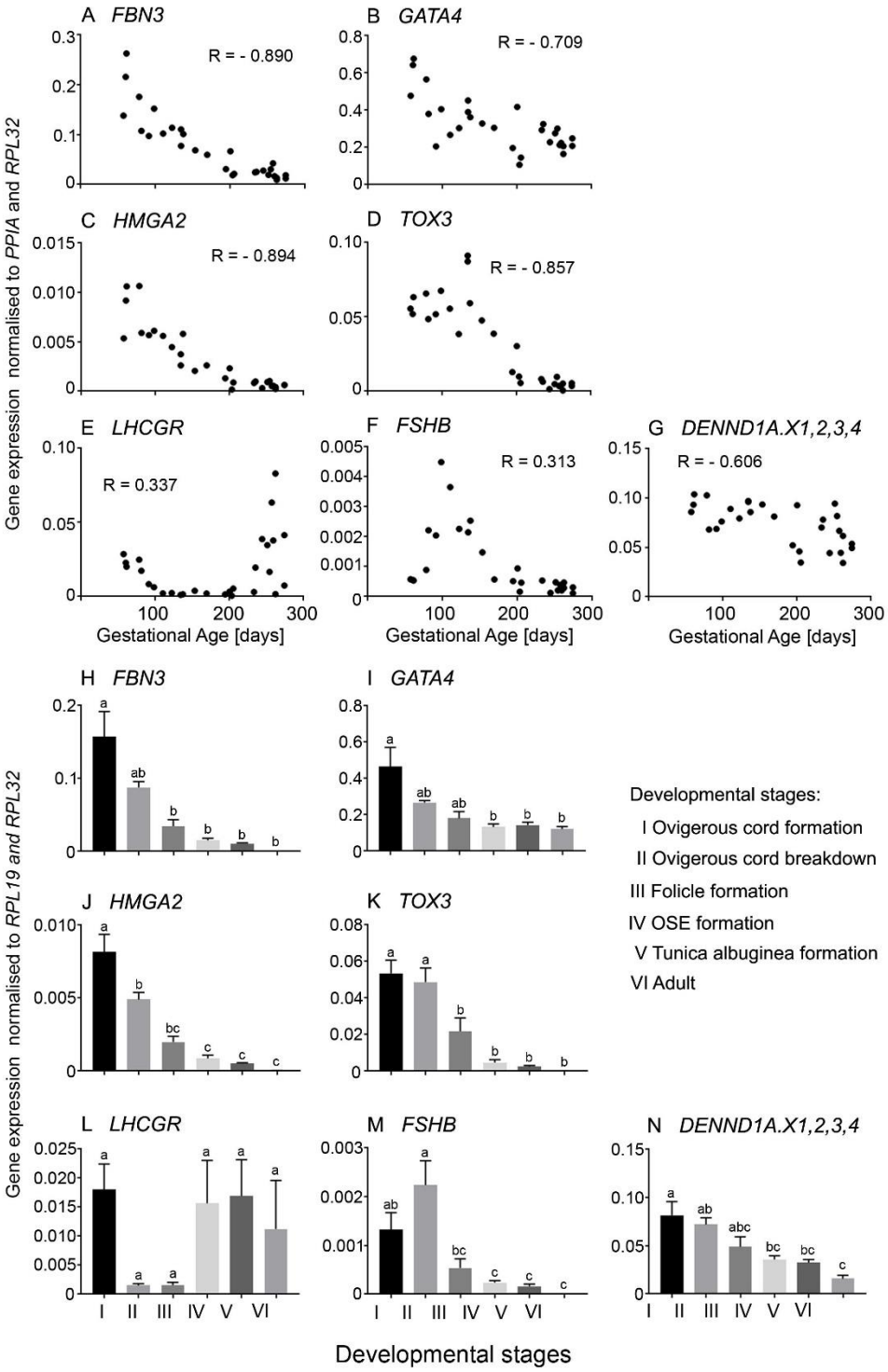

Figure 2. **A-G**. Scatter plots of mRNA expression levels of PCOS candidate genes which were highly expressed during early gestation in bovine fetal ovaries (n = 27). Pearson correlation coefficient (R) test was used to analyse data. **H-N**. Differential mRNA expression levels in ovaries grouped into six stages of ovarian development based on their histological morphology: ovigerous cord formation (n = 7, Stage I), ovigerous cord breakdown (n = 4, Stage II), follicle formation (n = 3, Stage III), surface epithelium formation (n = 8, Stage IV), tunica albuginea formation (n = 5, Stage V) and adult (n = 6, Stage VI). Data are presented as mean ± s.e.m. (normalised to *PPIA* and *RPL32* for scatter plot and *RPL19* and *RPL32* for bar graphs). One-way ANOVA with *post hoc* Holm-Sidak test were used to analyse the data. Different letters indicate statistically significant differences ($P < 0.05$).

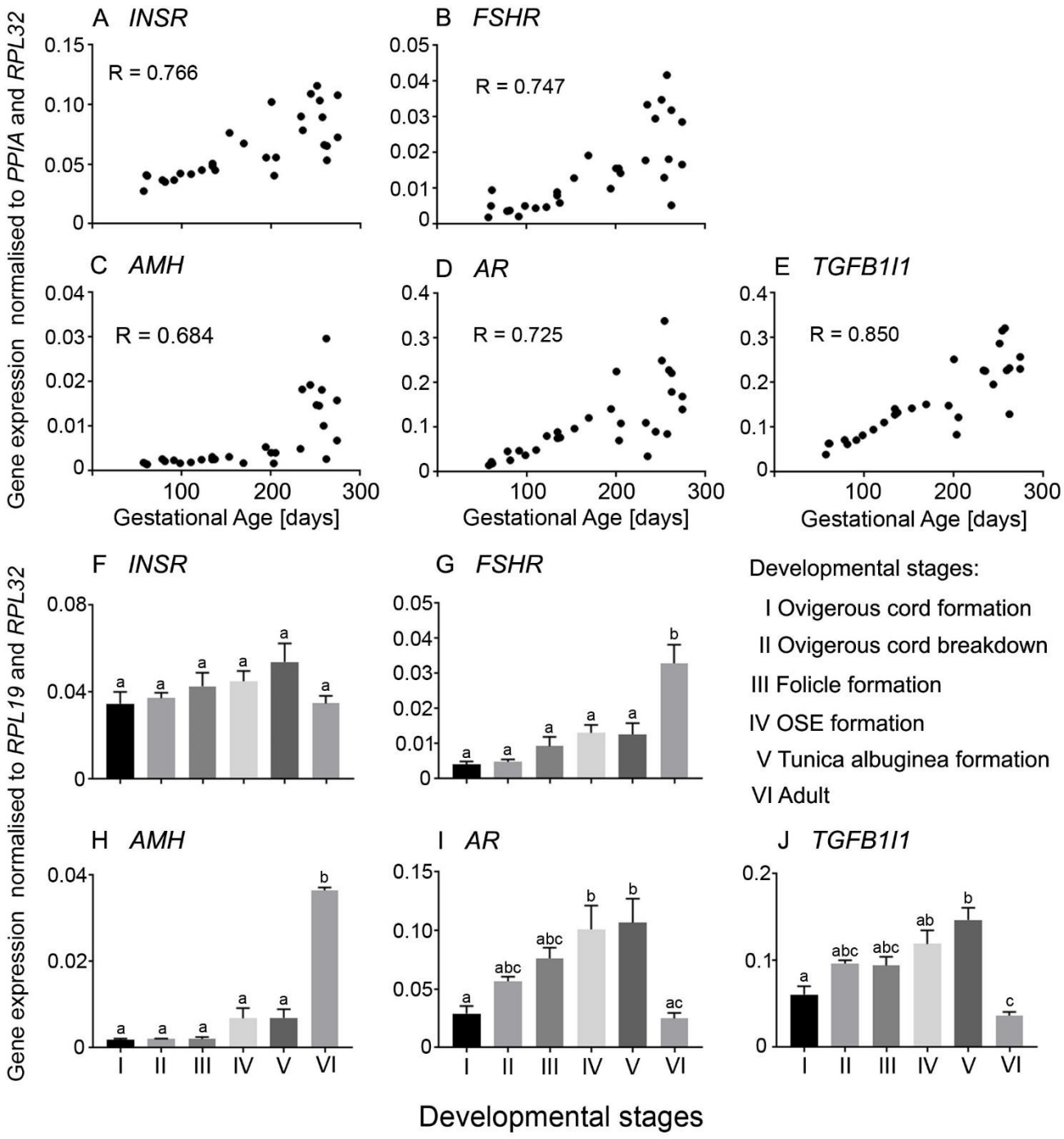

Figure 3. A-E. Scatter plots of mRNA expression levels from genes which are highly expressed late in gestation in bovine fetal ovaries (n = 27). Pearson correlation coefficient (R) test was used to analyse data. **F-J**. Differential mRNA expression levels in ovaries grouped into six stages of ovarian development based on their histological morphology: ovigerous cord formation (n = 7, Stage I), ovigerous cord breakdown (n = 4, Stage II), follicle formation (n = 3, Stage III), surface epithelium formation (n = 8, Stage IV), tunica albuginea formation (n = 5, Stage V) and adult (n = 6, Stage VI). Data are presented as mean ± s.e.m. (normalised to *PPIA* and *RPL32* for scatter plot and *RPL19* and *RPL32* for bar graphs). One-way ANOVA with *post hoc* Holm-Sidak test were used to analyse the data. Different letters indicate statistically significant differences ($P < 0.05$).

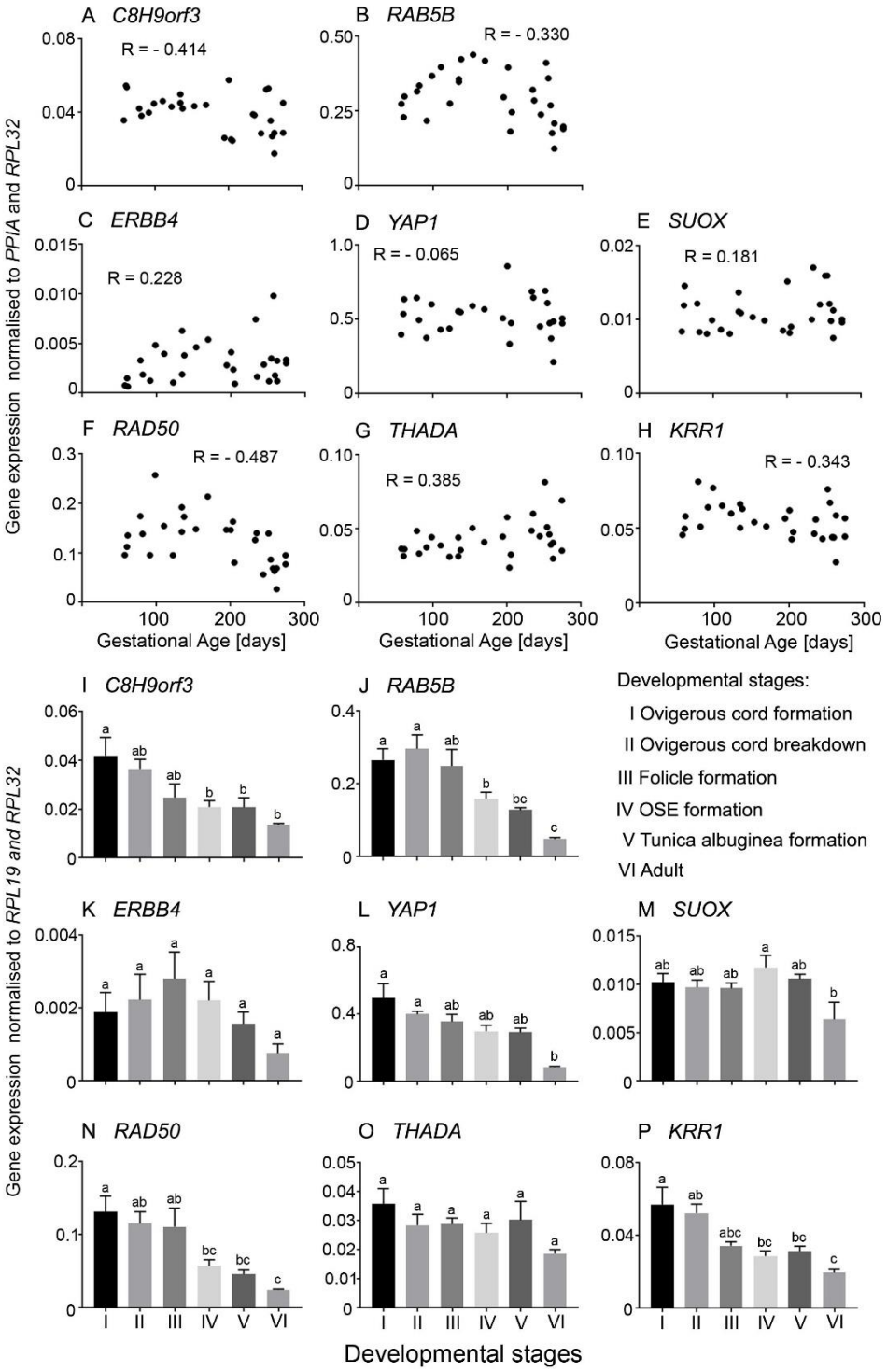

Figure 4. **A-H**. Scatter plot of mRNA expression levels of PCOS candidate genes which are constantly expressed throughout gestation in bovine fetal ovaries (n = 27). Pearson correlation coefficient (R) test was used to analyse data. **I-M**. Differential mRNA expression levels in ovaries grouped into six stages of ovarian development based on their histological morphology: ovigerous cord formation (n = 7, Stage I), ovigerous cord breakdown (n = 4, Stage II), follicle formation (n = 3, Stage III), surface epithelium formation (n = 8, Stage IV), tunica albuginea formation (n = 5, Stage V) and adult (n = 6, Stage VI). Data are presented as mean ± s.e.m. (normalised to *PPIA* and *RPL32* for scatter plot and *RPL19* and *RPL32* for bar graphs). One-way ANOVA with *post hoc* Holm-Sidak test were used to analyse the data. Different letters indicate statistically significant differences ($P < 0.05$).

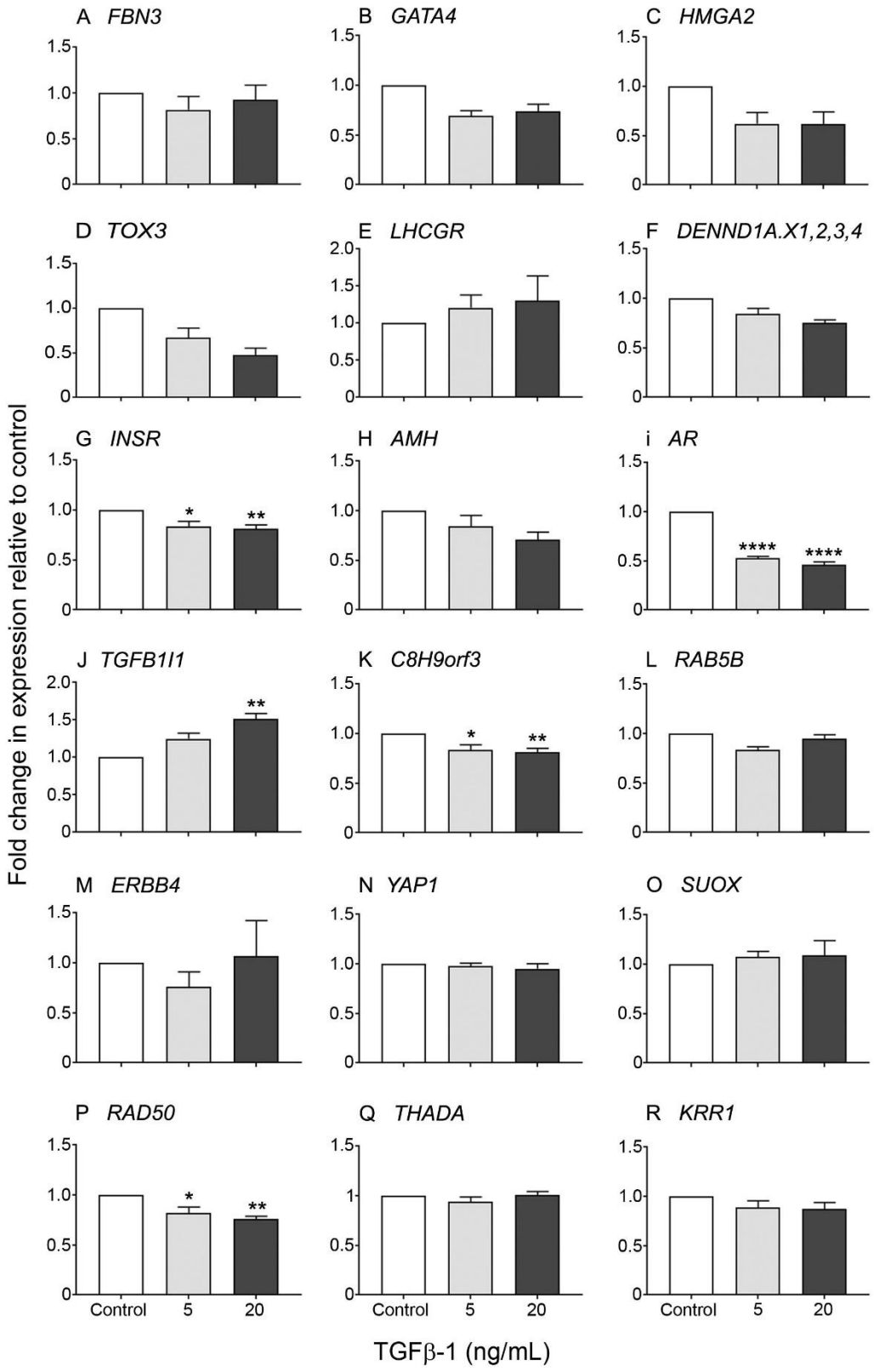

Figure 5. Expression of genes in bovine fetal fibroblasts from 19 – 26 weeks of gestation. Fibroblasts were cultured in the presence of 5 and 20 ng/mL TGFβ-1 for 18 h. Data are represented as mean ± s.e.m. of fold change in gene expression relative to the untreated control (n = 6 ovaries). One-way ANOVA with Dunnet's *post hoc* test were used to analyse the data. Asterisk symbols indicates statistically significant different form the control. ****$P < 0.0001$.

Supplemental Tables

Supplemental Table 1. List of genes and primers used for qRT-PCR.

Gene name	Gene Symbol	Species	Primers (5'→3') (F = forward, R = reverse)	Genebank Accession Number	Size (bp)
Ribosomal protein L32	*RPL32*	Bovine	F : GCCATCAGAATCACCAATCC R : AAATGTGCACACGAGCTGTC	NM_001034783.2	73
Ribosomal protein L32	*RPL32*	Human	F:CATCTCCTTCTCGGCATCA R:AACCCTGTTGTCAATGCCT	NM_000994	153
Ribosomal protein L19	*RPL19*	Bovine	F: GATCCGGAAGCTGATCAAAG R: TACCCATATGCCTGCCTTTC	NM_001040516.1	113
Peptidylprolyl isomerase A (cyclophilin A)	*PPIA*	Bovine	F : CTGGCATCTTGTCCATGGCAAA R : CCACAGTCAGCAATGGTGATCTTC	NM_178320.2	202
Beta-2-microglobulin	*B2M*	Human	F:ACTGAATTCACCCCCACTGA R:CCTCCATGATGCTGCTTACA	NM_004048	114
Fibrillin 3	*FBN3*	Bovine	F : GCCACAGCCTGCCTAGATGT R : CTGCCCTCAGTGTTTTTGCA	XM_001254849.2	82
Fibrillin 3	*FBN3*	Human	F : TGTCGTACCCATCTGTAGGC R : GCCCCCATTCATACAGCTCA	NM_032447	142
High Mobility Group AT-Hook 2	*HMGA2*	Bovine	F : TTATCCGCCCACGATTAGAG R : TTGAGTGTGTGTGTGCTTGG	XM_002704288	72
High Mobility Group AT-Hook 2	*HMGA2*	Human	F : TCAGAAGAGAGGACGCGG R : TTGAGCTGCTTTAGAGGGAC	NM_003483	124
TOX High Mobility Group Box Family Member 3	*TOX3*	Bovine	F : TATGGCTGAGGCAAACAACG R : TTCAAACTCCTCATCCCCAAGG	XM_015467340	79
TOX High Mobility Group Box Family Member 3	*TOX3*	Human	F : AGCAAATCCAGCAGCAGATG R : GAGGAGAAGGCTGAGACTGG	NM_001146188	180
GATA binding protein 4	*GATA4*	Bovine	F : CAGGAGGCAAAAATGCTAGG R : ATCACCCGTCGTCTTTCTTC	NM_001192877.1	82
GATA binding protein 4	*GATA4*	Human	F : CATCAAGACGGAGCCTGGCC R : TGACTGTCGGCCAAGACCAG	NM_002052	219

DENN Domain Containing 1A	*DENND1A.X1,2,3,4*	Bovine	F : TGTCGTGATCCTGAATGTGG R : ACATCATTTGGGAGGCTCTG	XM_005213126	71
Predicted DENN Domain Containing 1A Variant 2	*DENND1A.V2*	Bovine	F : ACCGAAGAGCAACATCACAG R : TGACGCAGCAATCTCCTATC	NM_001193014	306
DENN Domain Containing 1A Variant 1-7	*DENND1A.V1-7*	Human	F : GTCCATCTCAGCGTGCATTC R : CGGCGTTCGTACAGCATAC	NM_020946	149
DENN Domain Containing 1A Variant 1, 3, 4	*DENND1A.V1,3,4*	Human	F : CAGCCAGGGACCTTTGACTA R : CAGAGCTTGTTGTACGGGTG	NM_020946	104
Anti-Mullerian hormone	*AMH*	Bovine	F : ACACCGGCAAGCTCCTCAT R : TCTCGTCCGCTACTCCAAGT	NM_178318.4	202
Follicle stimulating hormone receptor (FSHR)	*FSHR*	Bovine	F : GACCCTGATGCCTTCCAGA R : TGGCAAGTGCTTAATACCTGTGTT	NM_174061.1	74
Follicle stimulating hormone receptor (FSHR)	*FSHR*	Human	F: GCTGCCTACTCTGGAAAAGC R: ATCTCTGACCCCTAGCCTGA	NM_000145	173
Insulin receptor	*INSR*	Bovine	F : AGGAGCTGGAGGAGTCCTCGTTCA R : CATTCCCCACGTCACCAAGGGCTC	XM_0154640	111
Androgen Receptor	*AR*	Bovine	F : TGCCCCTGACCTGGTTTTC R : TCGGACACACTGGCTGTACATC	NM_001244127.1	67
Transforming growth factor beta 1 induced transcript 1	*TFGB1I1*	Bovine	F : TCCCCTGTTCTCCCAAAGC R : GCCCTGAGGCTGGAAGATG	NM_001035313.1	109
Thyroid adenoma associated	*THADA*	Bovine	F : TGTGGTTAGGAGGCTTTTGG R : ACAGTGAGCTGGTGCATTTG	XM_015465336	117
Erb-B2 Receptor Tyrosine Kinase 4	*ERBB4*	Bovine	F : CCTGGAAATAACCAGCATCG R : CTTTGTCCCACGGATAATGC	XM_015462361	142
RAD50 Double Strand Break Repair Protein	*RAD50*	Bovine	F : GCTTTGAGCTTGGACCATTC R : AACAGTTGGCTGGCAGTTTC	NM_001206868	100
Chromosome 8 open reading frame, human C9orf3	*C8H9orf3*	Bovine	F : ACAGGGGATGAAAGTTGTGG R : AAATCTCAGAAGGGGCTTCC	NM_001206980	111
Yes Associated Protein 1	*YAP1*	Bovine	F : GATGGTGGGACTCAAAATCC R : TGAGCTATTGGTCGTCATGG	XM_015474584	75
RAB5B, Member RAS Oncogene Family	*RAB5B*	Bovine	F : AAGCGCATGGTGGAGTATG R : TTCTGGGGTTCACTCTTTGG	XM_005206651	146
Predicted SUMO Pseudogene 1	*SUMO1P1*	Bovine	F : CAGGGTTATTGGACAGGATAGC R : TGAGGGAATTCACTGGAACG	NM_001035458.1	116
Luteinising hormone/chorionic gonadotrophin receptor	*LHCGR*	Bovine	F : GCCACTGCTGTGCTTTTAGAAA R : CCAGCCACTCAGTTCACTCTCA	NM_174381.1	158

Luteinising hormone/chorionic gonadotrophin receptor	*LHCGR*	Human	F : TCAATGTGGTGGCCTTCTTCATA R : TTGGCACAAGAATTGATGGGATA	NM_000233	256
Sulphite Oxidase	*SUOX*	Bovine	F : TGGTGATAACTCCAGCACCAG R : ATCATGACAGGCCAACACTG	NM_001034366	79
KRR1, Small Subunit Processome Component Homolog	*KRR1*	Bovine	F : CCGAGATGAATCTGAACTCCTC R : TCTGGGATTGTCCTCTTTGG	NM_001037819	76
Follicle Stimulating Hormone Beta Subunit	*FSHB*	Bovine	F: GTCACCACTCAGACCTGTATTC R: GGGATTGCCTGAGAGGATTT	NM_174060.1	120
Follicle Stimulating Hormone Beta Subunit	*FSHB*	Human	F : TGAGCTGACCAACATCACCA R : TGGCTGGGTCCTTATACACC	NM_000510	122
Cytokeratin 19	*KRT19*	Bovine	F : AAGCTTTGCGCATGAGTGTG R : TCAATCTGCATCTCCAGGTCAG	NM_001015600.3	97
DEAD (Asp-Glu-Ala-Asp) box polypeptide 4	*VASA*	Bovine	F : ATGAAGCTGATCGCATGCTG R : TGACGCTGTTCCTTTGATGG	NM_001007819.1	91
POU class 5 homeobox 1	*OCT4*	Bovine	F : AGGCTTTGCAGCTCAGTTTC R : TTGTTGTCAGCTTCCTCCAC	NM_174580.2	79

Supplemental Table 2. Treatments used for bovine fetal fibroblasts.

Category	Treatments	Concentration	Distribution
Stimulators	Forskolin	4.1 μg/mL	Sigma-Aldrich
	Dibutyryladenosine cyclic monophosphate	1mM	Sigma-Aldrich
Growth factors	Basic fibroblast growth factor	100 ng/mL	Roche Australia Pty Ltd, Thebarton, SA, Australia
	Connective tissue growth factor	25 ng/mL	Invitrogen/Life Technologies
	Stem cell factor	100 ng/mL	R&D Systems
	Vascular endothelial growth factor	10 ng/mL	R&D Systems
	Transforming growth factor β1	10 ng/mL	R&D Systems
	Bone morphogenetic protein 6	100 ng/mL	R&D Systems
	Bone morphogenetic protein 15	100 ng/mL	R&D Systems
	Glial-derived factor 9	100 ng/mL	R&D Systems
	Glial-cell derived neurotrophic factor	100 ng/mL	R&D Systems
	Leukemia inhibitory factor	10^3 U/mL	Sigma-Aldrich
	Platelet-derived growth factor	10 ng/mL	R&D Systems
	Activin A	100 ng/mL	R&D Systems
	Epidermal growth factor	10 ng/mL	Boehringer Ingelheim Pty Ltd, North Ryde, NSW, Australia
	Fibroblast growth factor 7	10 ng/mL	R&D Systems
	Fibroblast growth factor 9	30 ng/mL	R&D Systems
	Retinoic acid	3 μg/mL	Sigma-Aldrich
Hormones	Dihydroxytestosterone	100 ng/mL	Sigma-Aldrich
	Testosterone	100 ng/mL	Sigma-Aldrich
	Estradiol	100 ng/mL	Sigma-Aldrich
	Insulin-like protein 3	100 ng/mL	From Dr Ross Bathgate – University of Melbourne, Australia
	Mullerian-inhibiting substance	10 ng/mL	Biogen Idec Australia Pty Ltd, North Ryde, NSW, Australia
	Insulin-like growth factor 1	30 ng/mL	GroPep Bioreagents Pty Ltd, Thebarton, SA, Australia

Supplemental Table 3. Pearson correlation coefficients (r) of mRNA expression levels of PCOS-candidate genes and gestational age in less than 150 day bovine fetal ovaries (n = 27).

	Age	*FBN3*	*GATA4*	*HMGA2*	*TOX3*	*LHCGR*	*FSHB*	*DENND1A.X12,3,4*	*C8H9orf3*	*RAB5B*	*ERBB4*	*YAP1*	*SUOX*	*RAD50*	*THADA*	*KRR1*	*INSR*	*FSHR*	*AMH*	*AR*
FBN3	-0.675[a]																			
GATA4	-0.650[a]	0.920[d]																		
HMGA2	-0.651[a]	0.850[c]	0.802[b]																	
TOX3	0.223	0.119	0.219	0.021																
LHCGR	-0.922[d]	0.609[a]	0.719[a]	0.651[a]	-0.126															
FSHB	-0.530	0.515	0.679[a]	0.688[a]	0.059	0.730[a]														
DENND1A.X1,2,3,4	-0.165	0.641[a]	0.708[a]	0.591	0.502	0.295	0.518													
C8H9orf3	-0.163	0.723[a]	0.572	0.536	0.168	0.006	0.128	0.569												
RAB5B	0.592	-0.325	-0.216	-0.231	0.375	-0.504	-0.314	0.088	-0.095											
ERBB4	0.426	-0.266	-0.237	-0.049	0.287	-0.412	-0.045	-0.047	-0.038	0.758[b]										
YAP1	-0.064	0.617[a]	0.671[a]	0.632[a]	0.553	0.159	0.448	0.607[a]	0.501	0.324	0.335									
SUOX	-0.253	0.821[b]	0.819[b]	0.761[b]	0.491	0.300	0.424	0.817[b]	0.720[a]	0.048	-0.027	0.841[b]								
RAD50	0.237	0.043	0.0510	0.118	0.473	-0.247	0.014	0.048	0.092	0.679[a]	0.872[c]	0.628[a]	0.234							
THADA	-0.189	0.139	0.104	0.436	0.242	0.222	0.420	0.172	-0.158	0.225	0.600	0.389	0.159	0.629[a]						
KRR1	0.392	-0.081	-0.155	0.146	0.460	-0.355	0.151	0.180	0.017	0.385	0.688[a]	0.489	0.192	0.695[a]	0.740[b]					
INSR	0.764[b]	-0.114	-0.165	-0.245	0.387	-0.773[b]	-0.323	0.208	0.469	0.393	0.289	0.333	0.256	0.276	-0.287	0.385				
FSHR	0.276	0.418	0.381	0.155	0.570	-0.291	-0.183	0.565	0.661[a]	0.316	-0.030	0.625a	0.708a	0.217	-0.281	0.119	0.707[a]			
AMH	0.719[a]	-0.615[a]	-0.458	-0.453	0.327	-0.470	-0.050	-0.014	-0.435	0.237	0.100	-0.034	-0.188	-0.047	-0.065	0.385	0.434	0.064		
AR	0.939[d]	-0.584	-0.561	-0.520	0.133	-0.811[b]	-0.319	-0.051	-0.139	0.377	0.266	-0.054	-0.186	0.064	-0.178	0.417	0.742[b]	0.224	0.811[b]	
TGFβ1I1	0.951[d]	-0.456	-0.411	-0.488	0.371	-0.848[c]	-0.404	0.088	0.071	0.553	0.344	0.132	0.019	0.216	-0.261	0.372	0.887[c]	0.504	0.707[a]	0.921[d]

[a] $P < 0.05$, [b] $P < 0.01$, [c] $P < 0.001$, [d] $P < 0.0001$

Supplemental Table 4. Normalized gene expression in cultured bovine fetal fibroblast (*in vitro*, n = 4) and whole bovine fetal ovaries (*in vivo*, n = 5) at 13-28 weeks of gestation.

Genes	*In vitro*	*In vivo*
FBN3	0.0009 ± 0.0002	0.008 ± 0.002
GATA4	0.136 ± 0.0212	0.004 ± 0.001
HMGA2	0.0005 ± 0.0001	0.003 ± 0.0004
TOX3	0.005 ± 0.003	0.342 ± 0.037
LHCGR	0.0005 ± 0.0003	0.040 ± 0.003
FSHB	Not detected	0.004 ± 0.001
DENND1A.X1,2,3,4	0.022 ± 0.005	0.151 ± 0.026
INSR	0.0166 ± 0.004	0.044 ± 0.002
FSHR	Not detected	0.536 ± 0.046
AMH	0.0004 ± 0.0001	0.004 ± 0.0008
AR	0.012 ± 0.004	0.315 ± 0.024
TGFB1I1	0.231 ± 0.050	0.010 ± 0.0008
C8H9orf3	0.008 ± 0.001	0.061 ± 0.004
RAB5B	0.112 ± 0.024	0.052 ± 0.008
ERBB4	0.002 ± 0.002	0.057 ± 0.013
YAP1	0.330 ± 0.063	0.081 ± 0.005
SUOX	0.007 ± 0.002	0.073 ± 0.011
RAD50	0.043 ± 0.008	0.127 ± 0.023
THADA	0.0276 ± 0.007	0.096 ± 0.017
KRR1	0.025 ± 0.007	0.002 ± 0.0006

Data are presented as mean ± s.e.m.

Supplemental Figures

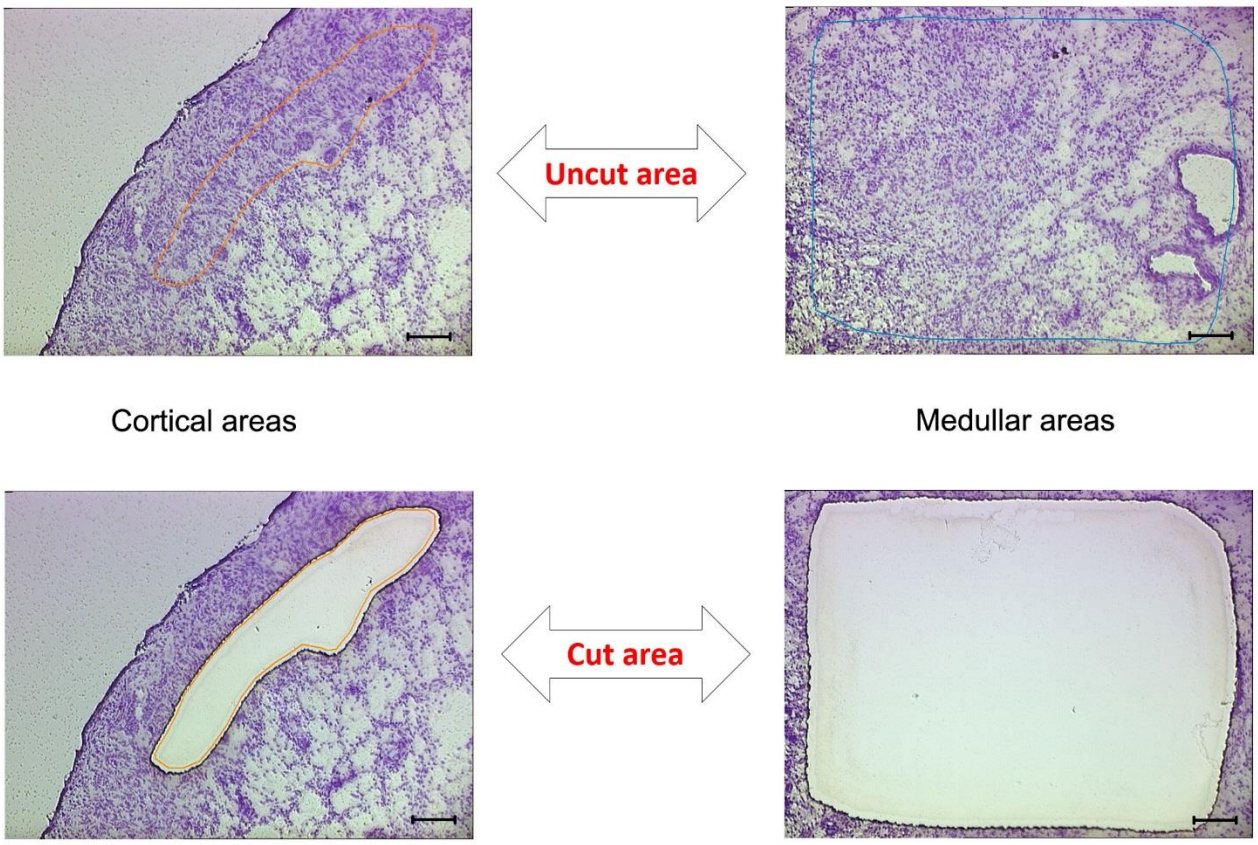

Supplemental Fig. S1
Representative images of bovine fetal ovary showing the cortical and medullar areas prior to and post LCM. The whole ovary was embedded into cryomold filled with OCT compound with the hilum on the side of the mold. For confirming the cortical and medullar areas, 5-20 section of 8 µm thickness were cut and mounted into colourfrost glass slides (HD Scientific Supplies). Slides were then fixed and stained in 1% cresyl violet acetate (pH 7.75) in 70% ethanol using the same protocol as described in this study. The cortical area was identified as the outer area lying beneath the tunica albugines, composed of connective tissue and fibers, as well as scattered ovigerous cords and/or primordial/primary follicles. The medullar area was identified as the middle area, composed of connective tissue and fibers with cvarious szes of vasculature. After those areas were identified using microscope Olympus BX-50, then 10-12 sections of 8um thickness were cut and transferred into the PET membrane frame slides. Scale bars: 50 um. LCM, laser capture microdissection. OCT, optimal cutting temperature.

Supplemental Fig. S2. Alignment of the exons of human *DENND1A.V1*; bovine *DENND1A*; predicted bovine *DENND1A.X1,2,3,4*; and *DENND1A.X1,2,3,4* primer sequences. Alignment was generated with CLUSTAL multiple sequence alignment by Kalign (2.0) based on sequences available at Ensembl Asia with transcript ID for human *DENND1A.V1* (ENST00000373624.6) and bovine *DENND1A* (ENSBTAG00000003610) and at NCBI PubMed with accession numbers: predicted bovine *DENND1A.X1* (XM_005213126.4); *DENND1A.X2* (XM_015473579.2); *DENND1A.X3* (XM_015473580.2); and *DENND1A.X4* (XM_024998568.1). The alignment was analysed with T-COFFEE (1) and colored based on the consistency: red (high), yellow (average); green and blue (poor). Consistency is estimated from CORE index. Bright aqua highlighted areas represent the primer sequences. ..... represent intronic areas not shown so as to reduce the size of this file.

1. Notredame C, Higgins DG, Heringa J. T-Coffee: A novel method for fast and accurate multiple sequence alignment. J Mol Biol. 2000;302(1):205-17. doi: 10.1006/jmbi.2000.4042.

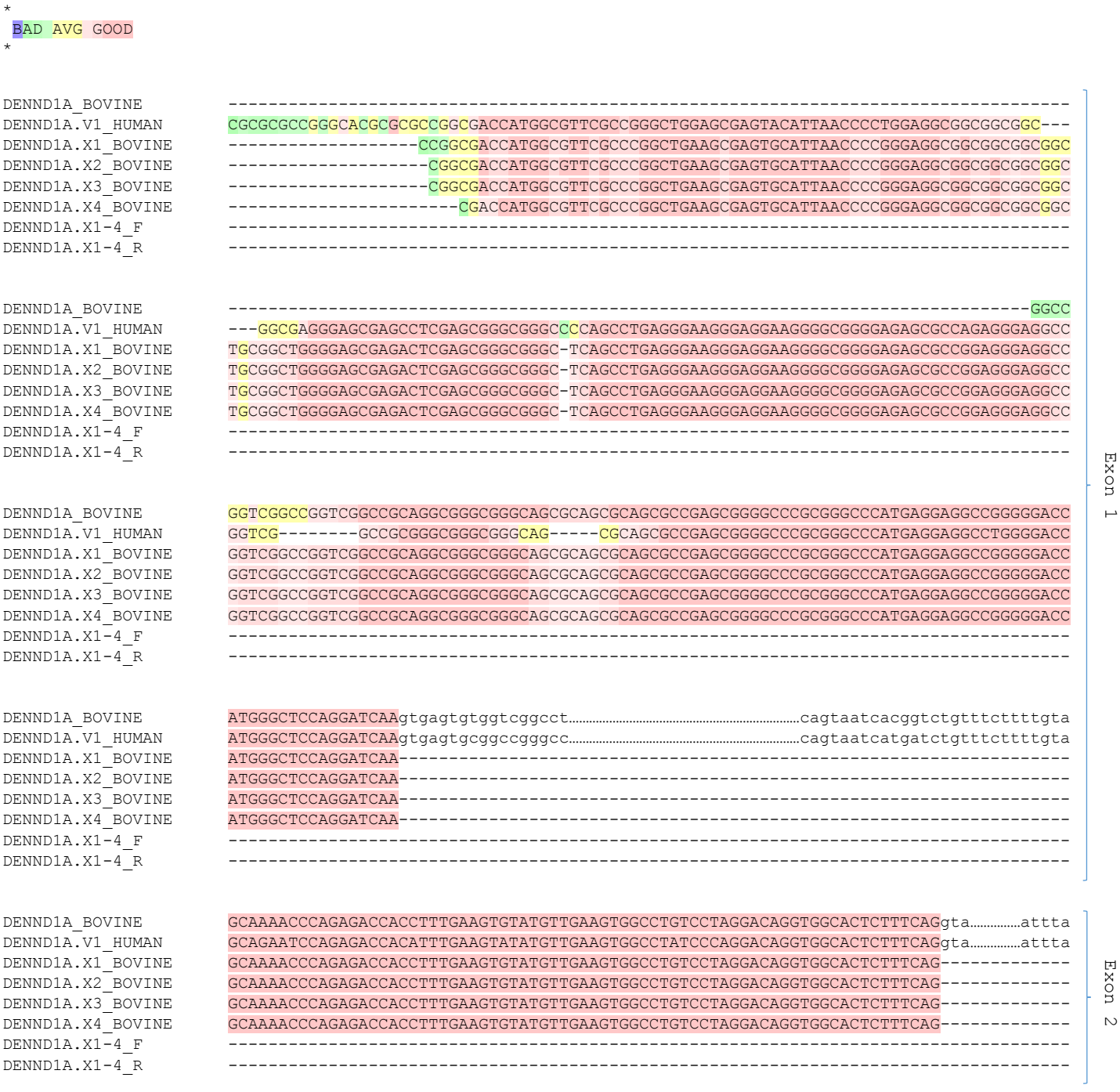

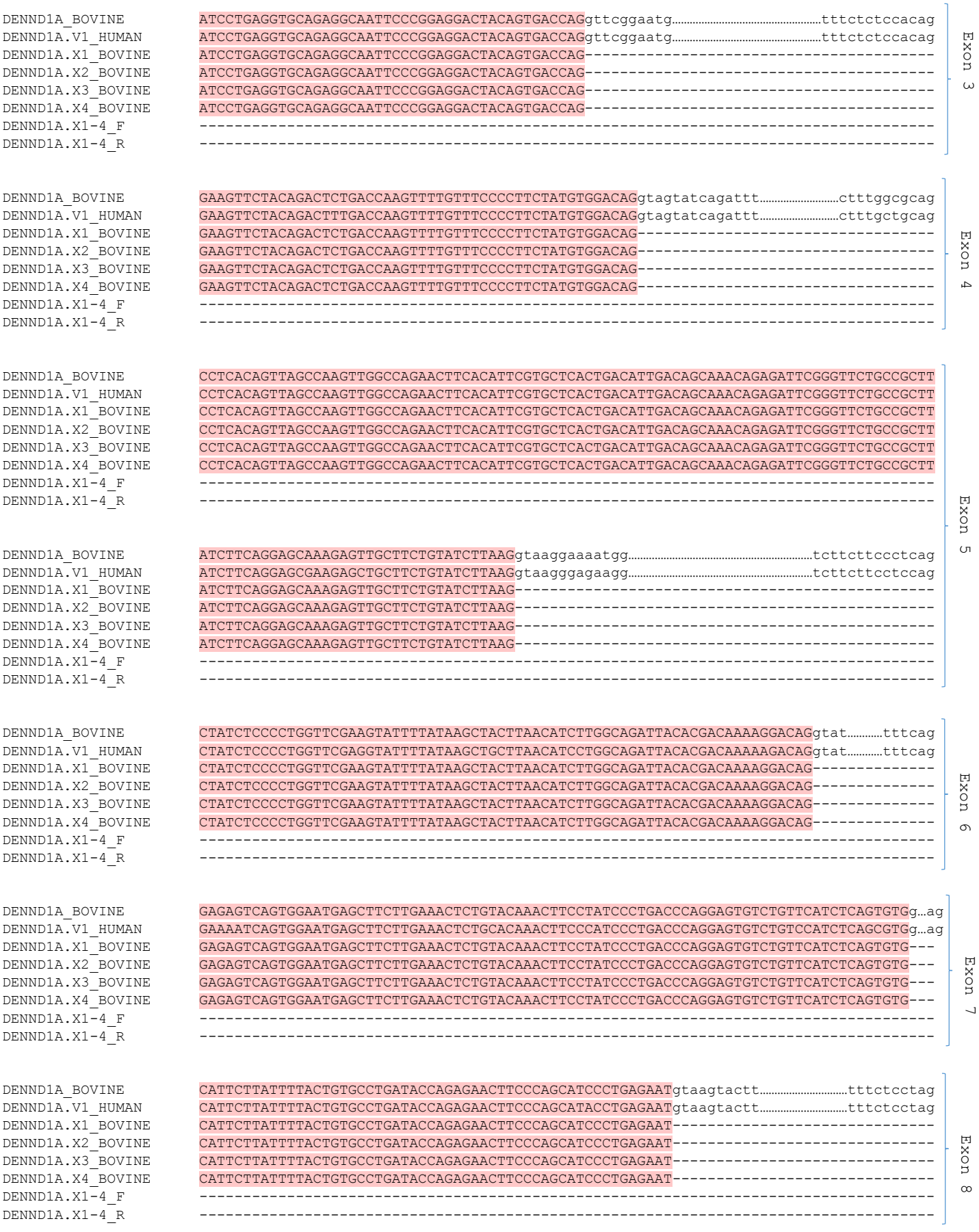
DENND1A_BOVINE ATCCTGAGGTGCAGAGGCAATTCCCGGAGGACTACAGTGACCAGgttcggaatg……tttctctccacag
DENND1A.V1_HUMAN ATCCTGAGGTGCAGAGGCAATTCCCGGAGGACTACAGTGACCAGgttcggaatg……tttctctccacag
DENND1A.X1_BOVINE ATCCTGAGGTGCAGAGGCAATTCCCGGAGGACTACAGTGACCAG----------
DENND1A.X2_BOVINE ATCCTGAGGTGCAGAGGCAATTCCCGGAGGACTACAGTGACCAG----------
DENND1A.X3_BOVINE ATCCTGAGGTGCAGAGGCAATTCCCGGAGGACTACAGTGACCAG----------
DENND1A.X4_BOVINE ATCCTGAGGTGCAGAGGCAATTCCCGGAGGACTACAGTGACCAG----------
DENND1A.X1-4_F ----------
DENND1A.X1-4_R ----------
Exon 3
DENND1A_BOVINE GAAGTTCTACAGACTCTGACCAAGTTTTGTTTCCCCTTCTATGTGGACAGgtagtatcagattt……ctttggcgcag
DENND1A.V1_HUMAN GAAGTTCTACAGACTTTGACCAAGTTTTGTTTCCCCTTCTATGTGGACAGgtagtatcagattt……ctttgctgcag
DENND1A.X1_BOVINE GAAGTTCTACAGACTCTGACCAAGTTTTGTTTCCCCTTCTATGTGGACAG----------
DENND1A.X2_BOVINE GAAGTTCTACAGACTCTGACCAAGTTTTGTTTCCCCTTCTATGTGGACAG----------
DENND1A.X3_BOVINE GAAGTTCTACAGACTCTGACCAAGTTTTGTTTCCCCTTCTATGTGGACAG----------
DENND1A.X4_BOVINE GAAGTTCTACAGACTCTGACCAAGTTTTGTTTCCCCTTCTATGTGGACAG----------
DENND1A.X1-4_F ----------
DENND1A.X1-4_R ----------
Exon 4
DENND1A_BOVINE CCTCACAGTTAGCCAAGTTGGCCAGAACTTCACATTCGTGCTCACTGACATTGACAGCAAACAGAGATTCGGGTTCTGCCGCTT
DENND1A.V1_HUMAN CCTCACAGTTAGCCAAGTTGGCCAGAACTTCACATTCGTGCTCACTGACATTGACAGCAAACAGAGATTCGGGTTCTGCCGCTT
DENND1A.X1_BOVINE CCTCACAGTTAGCCAAGTTGGCCAGAACTTCACATTCGTGCTCACTGACATTGACAGCAAACAGAGATTCGGGTTCTGCCGCTT
DENND1A.X2_BOVINE CCTCACAGTTAGCCAAGTTGGCCAGAACTTCACATTCGTGCTCACTGACATTGACAGCAAACAGAGATTCGGGTTCTGCCGCTT
DENND1A.X3_BOVINE CCTCACAGTTAGCCAAGTTGGCCAGAACTTCACATTCGTGCTCACTGACATTGACAGCAAACAGAGATTCGGGTTCTGCCGCTT
DENND1A.X4_BOVINE CCTCACAGTTAGCCAAGTTGGCCAGAACTTCACATTCGTGCTCACTGACATTGACAGCAAACAGAGATTCGGGTTCTGCCGCTT
DENND1A.X1-4_F ----------
DENND1A.X1-4_R ----------
DENND1A_BOVINE ATCTTCAGGAGCAAAGAGTTGCTTCTGTATCTTAAGgtaaggaaaatgg……tcttcttccctcag
DENND1A.V1_HUMAN ATCTTCAGGAGCGAAGAGCTGCTTCTGTATCTTAAGgtaagggagaagg……tcttcttcctccag
DENND1A.X1_BOVINE ATCTTCAGGAGCAAAGAGTTGCTTCTGTATCTTAAG----------
DENND1A.X2_BOVINE ATCTTCAGGAGCAAAGAGTTGCTTCTGTATCTTAAG----------
DENND1A.X3_BOVINE ATCTTCAGGAGCAAAGAGTTGCTTCTGTATCTTAAG----------
DENND1A.X4_BOVINE ATCTTCAGGAGCAAAGAGTTGCTTCTGTATCTTAAG----------
DENND1A.X1-4_F ----------
DENND1A.X1-4_R ----------
Exon 5
DENND1A_BOVINE CTATCTCCCCTGGTTCGAAGTATTTTATAAGCTACTTAACATCTTGGCAGATTACACGACAAAAGGACAGgtat……tttcag
DENND1A.V1_HUMAN CTATCTCCCCTGGTTCGAGGTATTTTATAAGCTGCTTAACATCCTGGCAGATTACACGACAAAAAGACAGgtat……tttcag
DENND1A.X1_BOVINE CTATCTCCCCTGGTTCGAAGTATTTTATAAGCTACTTAACATCTTGGCAGATTACACGACAAAAGGACAG----------
DENND1A.X2_BOVINE CTATCTCCCCTGGTTCGAAGTATTTTATAAGCTACTTAACATCTTGGCAGATTACACGACAAAAGGACAG----------
DENND1A.X3_BOVINE CTATCTCCCCTGGTTCGAAGTATTTTATAAGCTACTTAACATCTTGGCAGATTACACGACAAAAGGACAG----------
DENND1A.X4_BOVINE CTATCTCCCCTGGTTCGAAGTATTTTATAAGCTACTTAACATCTTGGCAGATTACACGACAAAAGGACAG----------
DENND1A.X1-4_F ----------
DENND1A.X1-4_R ----------
Exon 6
DENND1A_BOVINE GAGAGTCAGTGGAATGAGCTTCTTGAAACTCTGTACAAACTTCCTATCCCTGACCCAGGAGTGTCTGTTCATCTCAGTGTGg…ag
DENND1A.V1_HUMAN GAAAATCAGTGGAATGAGCTTCTTGAAACTCTGCACAAACTTCCCATCCCTGACCCAGGAGTGTCTGTCCATCTCAGCGTGg…ag
DENND1A.X1_BOVINE GAGAGTCAGTGGAATGAGCTTCTTGAAACTCTGTACAAACTTCCTATCCCTGACCCAGGAGTGTCTGTTCATCTCAGTGTG---
DENND1A.X2_BOVINE GAGAGTCAGTGGAATGAGCTTCTTGAAACTCTGTACAAACTTCCTATCCCTGACCCAGGAGTGTCTGTTCATCTCAGTGTG---
DENND1A.X3_BOVINE GAGAGTCAGTGGAATGAGCTTCTTGAAACTCTGTACAAACTTCCTATCCCTGACCCAGGAGTGTCTGTTCATCTCAGTGTG---
DENND1A.X4_BOVINE GAGAGTCAGTGGAATGAGCTTCTTGAAACTCTGTACAAACTTCCTATCCCTGACCCAGGAGTGTCTGTTCATCTCAGTGTG---
DENND1A.X1-4_F ----------
DENND1A.X1-4_R ----------
Exon 7
DENND1A_BOVINE CATTCTTATTTTACTGTGCCTGATACCAGAGAACTTCCCAGCATCCCTGAGAATgtaagtactt……tttctcctag
DENND1A.V1_HUMAN CATTCTTATTTTACTGTGCCTGATACCAGAGAACTTCCCAGCATACCTGAGAATgtaagtactt……tttctcctag
DENND1A.X1_BOVINE CATTCTTATTTTACTGTGCCTGATACCAGAGAACTTCCCAGCATCCCTGAGAAT----------
DENND1A.X2_BOVINE CATTCTTATTTTACTGTGCCTGATACCAGAGAACTTCCCAGCATCCCTGAGAAT----------
DENND1A.X3_BOVINE CATTCTTATTTTACTGTGCCTGATACCAGAGAACTTCCCAGCATCCCTGAGAAT----------
DENND1A.X4_BOVINE CATTCTTATTTTACTGTGCCTGATACCAGAGAACTTCCCAGCATCCCTGAGAAT----------
DENND1A.X1-4_F ----------
DENND1A.X1-4_R ----------
Exon 8


DENND1A_BOVINE AGAAATCTGACAGAATATTTTGTGGCTGTGGATGTAAACAACATGTTACATCTGTATGCCAGTATGCTCTACGAACGCCGGATA
DENND1A.V1_HUMAN AGAAATCTGACAGAATATTTTGTGGCTGTGGATGTTAACAACATGTTGCATCTGTACGCCAGTATGCTGTACGAACGCCGGATA
DENND1A.X1_BOVINE AGAAATCTGACAGAATATTTTGTGGCTGTGGATGTAAACAACATGTTACATCTGTATGCCAGTATGCTCTACGAACGCCGGATA
DENND1A.X2_BOVINE AGAAATCTGACAGAATATTTTGTGGCTGTGGATGTAAACAACATGTTACATCTGTATGCCAGTATGCTCTACGAACGCCGGATA
DENND1A.X3_BOVINE AGAAATCTGACAGAATATTTTGTGGCTGTGGATGTAAACAACATGTTACATCTGTATGCCAGTATGCTCTACGAACGCCGGATA
DENND1A.X4_BOVINE AGAAATCTGACAGAATATTTTGTGGCTGTGGATGTAAACAACATGTTACATCTGTATGCCAGTATGCTCTACGAACGCCGGATA
DENND1A.X1-4_F ----------
DENND1A.X1-4_R ----------
Exon 9
DENND1A_BOVINE CTCATCATTTGCAGCAAACTCAGCACTgtgagtagacagtctt.....aatctttaatctctgttgcag
DENND1A.V1_HUMAN CTCATCATTTGCAGCAAACTCAGCACTgtgagtagacagtctt.....ctctgctttgctctgttccag
DENND1A.X1_BOVINE CTCATCATTTGCAGCAAACTCAGCACT----------
DENND1A.X2_BOVINE CTCATCATTTGCAGCAAACTCAGCACT----------
DENND1A.X3_BOVINE CTCATCATTTGCAGCAAACTCAGCACT----------
DENND1A.X4_BOVINE CTCATCATTTGCAGCAAACTCAGCACT----------
DENND1A.X1-4_F ----------
DENND1A.X1-4_R ----------
Exon 9
DENND1A_BOVINE TTGACTGCCTGCATCCACGGGTCTGCTGCGATGCTCTACCCCATGTTCTGGCAGCACGTGTACATCCCTGTCCTGCCTCCACAT
DENND1A.V1_HUMAN CTGACTGCCTGCATCCACGGGTCTGCGGCGATGCTCTACCCCATGTACTGGCAGCACGTGTACATCCCCGTGCTGCCGCCGCAT
DENND1A.X1_BOVINE TTGACTGCCTGCATCCACGGGTCTGCTGCGATGCTCTACCCCATGTTCTGGCAGCACGTGTACATCCCTGTCCTGCCTCCACAT
DENND1A.X2_BOVINE TTGACTGCCTGCATCCACGGGTCTGCTGCGATGCTCTACCCCATGTTCTGGCAGCACGTGTACATCCCTGTCCTGCCTCCACAT
DENND1A.X3_BOVINE TTGACTGCCTGCATCCACGGGTCTGCTGCGATGCTCTACCCCATGTTCTGGCAGCACGTGTACATCCCTGTCCTGCCTCCACAT
DENND1A.X4_BOVINE TTGACTGCCTGCATCCACGGGTCTGCTGCGATGCTCTACCCCATGTTCTGGCAGCACGTGTACATCCCTGTCCTGCCTCCACAT
DENND1A.X1-4_F ----------
DENND1A.X1-4_R ----------
DENND1A_BOVINE CTGCTGGACTACTGCTGgtaaggccactg.....gtctctgtttctcttcacag
DENND1A.V1_HUMAN CTGCTGGACTACTGCTGgtaaggccactg.....gtctctgtttctcttcacag
DENND1A.X1_BOVINE CTGCTGGACTACTGCTG----------
DENND1A.X2_BOVINE CTGCTGGACTACTGCTG----------
DENND1A.X3_BOVINE CTGCTGGACTACTGCTG----------
DENND1A.X4_BOVINE CTGCTGGACTACTGCTG----------
DENND1A.X1-4_F ----------
DENND1A.X1-4_R ----------
Exon 10
DENND1A_BOVINE TGCTCCCATGCCCTACCTCATAGGAATCCATTTAAGTTTAATGGAGgtaagttgacttct.....ttttacttgcag
DENND1A.V1_HUMAN TGCTCCCATGCCCTACCTCATAGGAATCCATTTAAGTTTAATGGAGgtaagttgacttct.....ttctccttgcag
DENND1A.X1_BOVINE TGCTCCCATGCCCTACCTCATAGGAATCCATTTAAGTTTAATGGAG----------
DENND1A.X2_BOVINE TGCTCCCATGCCCTACCTCATAGGAATCCATTTAAGTTTAATGGAG----------
DENND1A.X3_BOVINE TGCTCCCATGCCCTACCTCATAGGAATCCATTTAAGTTTAATGGAG----------
DENND1A.X4_BOVINE TGCTCCCATGCCCTACCTCATAGGAATCCATTTAAGTTTAATGGAG----------
DENND1A.X1-4_F ----------
DENND1A.X1-4_R ----------
Exon 11
DENND1A_BOVINE AAAGTCAGAAGCATGGCCCTGGATGATGTCGTGATCCTGAATGTGGACACCAACACCCTGGAAACCCCCTTTGATGACCTCCAG
DENND1A.V1_HUMAN AAAGTCAGAAACATGGCCCTGGATGATGTCGTGATCCTGAATGTGGACACCAACACCCTGGAAACCCCCTTCGATGACCTCCAG
DENND1A.X1_BOVINE AAAGTCAGAAGCATGGCCCTGGATGATGTCGTGATCCTGAATGTGGACACCAACACCCTGGAAACCCCCTTTGATGACCTCCAG
DENND1A.X2_BOVINE AAAGTCAGAAGCATGGCCCTGGATGATGTCGTGATCCTGAATGTGGACACCAACACCCTGGAAACCCCCTTTGATGACCTCCAG
DENND1A.X3_BOVINE AAAGTCAGAAGCATGGCCCTGGATGATGTCGTGATCCTGAATGTGGACACCAACACCCTGGAAACCCCCTTTGATGACCTCCAG
DENND1A.X4_BOVINE AAAGTCAGAAGCATGGCCCTGGATGATGTCGTGATCCTGAATGTGGACACCAACACCCTGGAAACCCCCTTTGATGACCTCCAG
DENND1A.X1-4_F ----------TGTCGTGATCCTGAATGTGG----------
DENND1A.X1-4_R ----------CAG
DENND1A_BOVINE AGCCTCCCAAATGATGTGgtgggtaatgagctctcgagt.....ctcctttctgtcatcag
DENND1A.V1_HUMAN AGCCTCCCAAACGACGTGgtaggtaatgagcttgcgagg.....cttctctccatcaccag
DENND1A.X1_BOVINE AGCCTCCCAAATGATGTG----------
DENND1A.X2_BOVINE AGCCTCCCAAATGATGTG----------
DENND1A.X3_BOVINE AGCCTCCCAAATGATGTG----------
DENND1A.X4_BOVINE AGCCTCCCAAATGATGTG----------
DENND1A.X1-4_F ----------
DENND1A.X1-4_R AGCCTCCCAAATGATGT----------
Exon 12

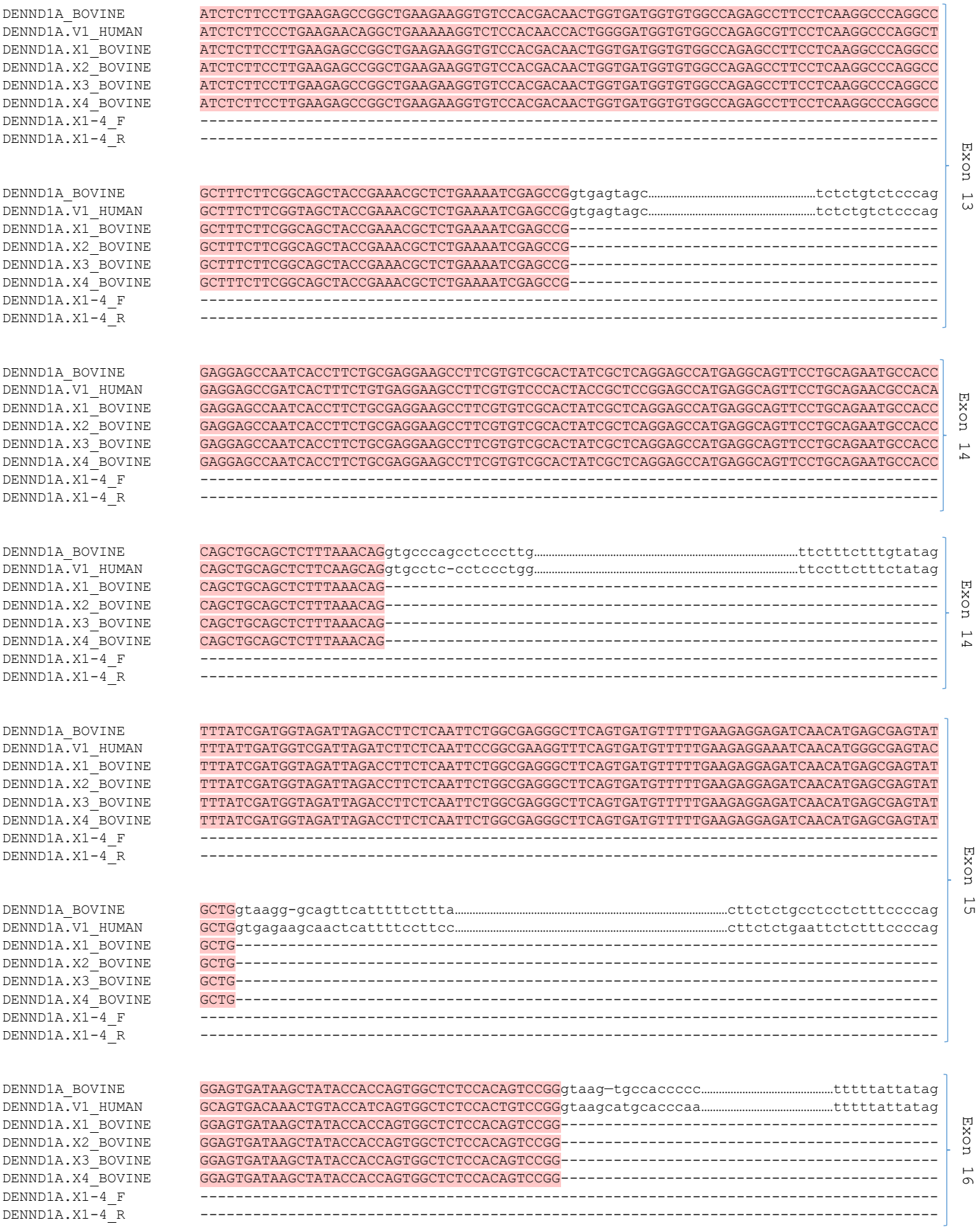
DENND1A_BOVINE ATCTCTTCCTTGAAGAGCCGGCTGAAGAAGGTGTCCACGACAACTGGTGATGGTGTGGCCAGAGCCTTCCTCAAGGCCCAGGCC
DENND1A.V1_HUMAN ATCTCTTCCCTGAAGAACAGGCTGAAAAAGGTCTCCACAACCACTGGGGATGGTGTGGCCAGAGCGTTCCTCAAGGCCCAGGCT
DENND1A.X1_BOVINE ATCTCTTCCTTGAAGAGCCGGCTGAAGAAGGTGTCCACGACAACTGGTGATGGTGTGGCCAGAGCCTTCCTCAAGGCCCAGGCC
DENND1A.X2_BOVINE ATCTCTTCCTTGAAGAGCCGGCTGAAGAAGGTGTCCACGACAACTGGTGATGGTGTGGCCAGAGCCTTCCTCAAGGCCCAGGCC
DENND1A.X3_BOVINE ATCTCTTCCTTGAAGAGCCGGCTGAAGAAGGTGTCCACGACAACTGGTGATGGTGTGGCCAGAGCCTTCCTCAAGGCCCAGGCC
DENND1A.X4_BOVINE ATCTCTTCCTTGAAGAGCCGGCTGAAGAAGGTGTCCACGACAACTGGTGATGGTGTGGCCAGAGCCTTCCTCAAGGCCCAGGCC
DENND1A.X1-4_F
DENND1A.X1-4_R
Exon 13
DENND1A_BOVINE GCTTTCTTCGGCAGCTACCGAAACGCTCTGAAAATCGAGCCGgtgagtagc tctctgtctcccag
DENND1A.V1_HUMAN GCTTTCTTCGGTAGCTACCGAAACGCTCTGAAAATCGAGCCGgtgagtagc tctctgtctcccag
DENND1A.X1_BOVINE GCTTTCTTCGGCAGCTACCGAAACGCTCTGAAAATCGAGCCG
DENND1A.X2_BOVINE GCTTTCTTCGGCAGCTACCGAAACGCTCTGAAAATCGAGCCG
DENND1A.X3_BOVINE GCTTTCTTCGGCAGCTACCGAAACGCTCTGAAAATCGAGCCG
DENND1A.X4_BOVINE GCTTTCTTCGGCAGCTACCGAAACGCTCTGAAAATCGAGCCG
DENND1A.X1-4_F
DENND1A.X1-4_R
Exon 14
DENND1A_BOVINE GAGGAGCCAATCACCTTCTGCGAGGAAGCCTTCGTGTCGCACTATCGCTCAGGAGCCATGAGGCAGTTCCTGCAGAATGCCACC
DENND1A.V1_HUMAN GAGGAGCCGATCACTTTCTGTGAGGAAGCCTTCGTGTCCCACTACCGCTCCGGAGCCATGAGGCAGTTCCTGCAGAACGCCACA
DENND1A.X1_BOVINE GAGGAGCCAATCACCTTCTGCGAGGAAGCCTTCGTGTCGCACTATCGCTCAGGAGCCATGAGGCAGTTCCTGCAGAATGCCACC
DENND1A.X2_BOVINE GAGGAGCCAATCACCTTCTGCGAGGAAGCCTTCGTGTCGCACTATCGCTCAGGAGCCATGAGGCAGTTCCTGCAGAATGCCACC
DENND1A.X3_BOVINE GAGGAGCCAATCACCTTCTGCGAGGAAGCCTTCGTGTCGCACTATCGCTCAGGAGCCATGAGGCAGTTCCTGCAGAATGCCACC
DENND1A.X4_BOVINE GAGGAGCCAATCACCTTCTGCGAGGAAGCCTTCGTGTCGCACTATCGCTCAGGAGCCATGAGGCAGTTCCTGCAGAATGCCACC
DENND1A.X1-4_F
DENND1A.X1-4_R
Exon 14
DENND1A_BOVINE CAGCTGCAGCTCTTTAAACAGgtgcccagcctcccttg ttctttctttgtatag
DENND1A.V1_HUMAN CAGCTGCAGCTCTTCAAGCAGgtgcctc-cctccctgg ttccttctttctatag
DENND1A.X1_BOVINE CAGCTGCAGCTCTTTAAACAG
DENND1A.X2_BOVINE CAGCTGCAGCTCTTTAAACAG
DENND1A.X3_BOVINE CAGCTGCAGCTCTTTAAACAG
DENND1A.X4_BOVINE CAGCTGCAGCTCTTTAAACAG
DENND1A.X1-4_F
DENND1A.X1-4_R
Exon 15
DENND1A_BOVINE TTTATCGATGGTAGATTAGACCTTCTCAATTCTGGCGAGGGCTTCAGTGATGTTTTTGAAGAGGAGATCAACATGAGCGAGTAT
DENND1A.V1_HUMAN TTTATTGATGGTCGATTAGATCTTCTCAATTCCGGCGAAGGTTTCAGTGATGTTTTTGAAGAGGAAATCAACATGGGCGAGTAC
DENND1A.X1_BOVINE TTTATCGATGGTAGATTAGACCTTCTCAATTCTGGCGAGGGCTTCAGTGATGTTTTTGAAGAGGAGATCAACATGAGCGAGTAT
DENND1A.X2_BOVINE TTTATCGATGGTAGATTAGACCTTCTCAATTCTGGCGAGGGCTTCAGTGATGTTTTTGAAGAGGAGATCAACATGAGCGAGTAT
DENND1A.X3_BOVINE TTTATCGATGGTAGATTAGACCTTCTCAATTCTGGCGAGGGCTTCAGTGATGTTTTTGAAGAGGAGATCAACATGAGCGAGTAT
DENND1A.X4_BOVINE TTTATCGATGGTAGATTAGACCTTCTCAATTCTGGCGAGGGCTTCAGTGATGTTTTTGAAGAGGAGATCAACATGAGCGAGTAT
DENND1A.X1-4_F
DENND1A.X1-4_R
DENND1A_BOVINE GCTGgtaagg-gcagttcatttttcttta cttctctgcctcctctttccccag
DENND1A.V1_HUMAN GCTGgtgagaagcaactcattttccttcc cttctctgaattctctttccccag
DENND1A.X1_BOVINE GCTG
DENND1A.X2_BOVINE GCTG
DENND1A.X3_BOVINE GCTG
DENND1A.X4_BOVINE GCTG
DENND1A.X1-4_F
DENND1A.X1-4_R
Exon 16
DENND1A_BOVINE GGAGTGATAAGCTATACCACCAGTGGCTCTCCACAGTCCGGgtaag-tgccaccccc tttttattatag
DENND1A.V1_HUMAN GCAGTGACAAACTGTACCATCAGTGGCTCTCCACTGTCCGGgtaagcatgcacccaa tttttattatag
DENND1A.X1_BOVINE GGAGTGATAAGCTATACCACCAGTGGCTCTCCACAGTCCGG
DENND1A.X2_BOVINE GGAGTGATAAGCTATACCACCAGTGGCTCTCCACAGTCCGG
DENND1A.X3_BOVINE GGAGTGATAAGCTATACCACCAGTGGCTCTCCACAGTCCGG
DENND1A.X4_BOVINE GGAGTGATAAGCTATACCACCAGTGGCTCTCCACAGTCCGG
DENND1A.X1-4_F
DENND1A.X1-4_R

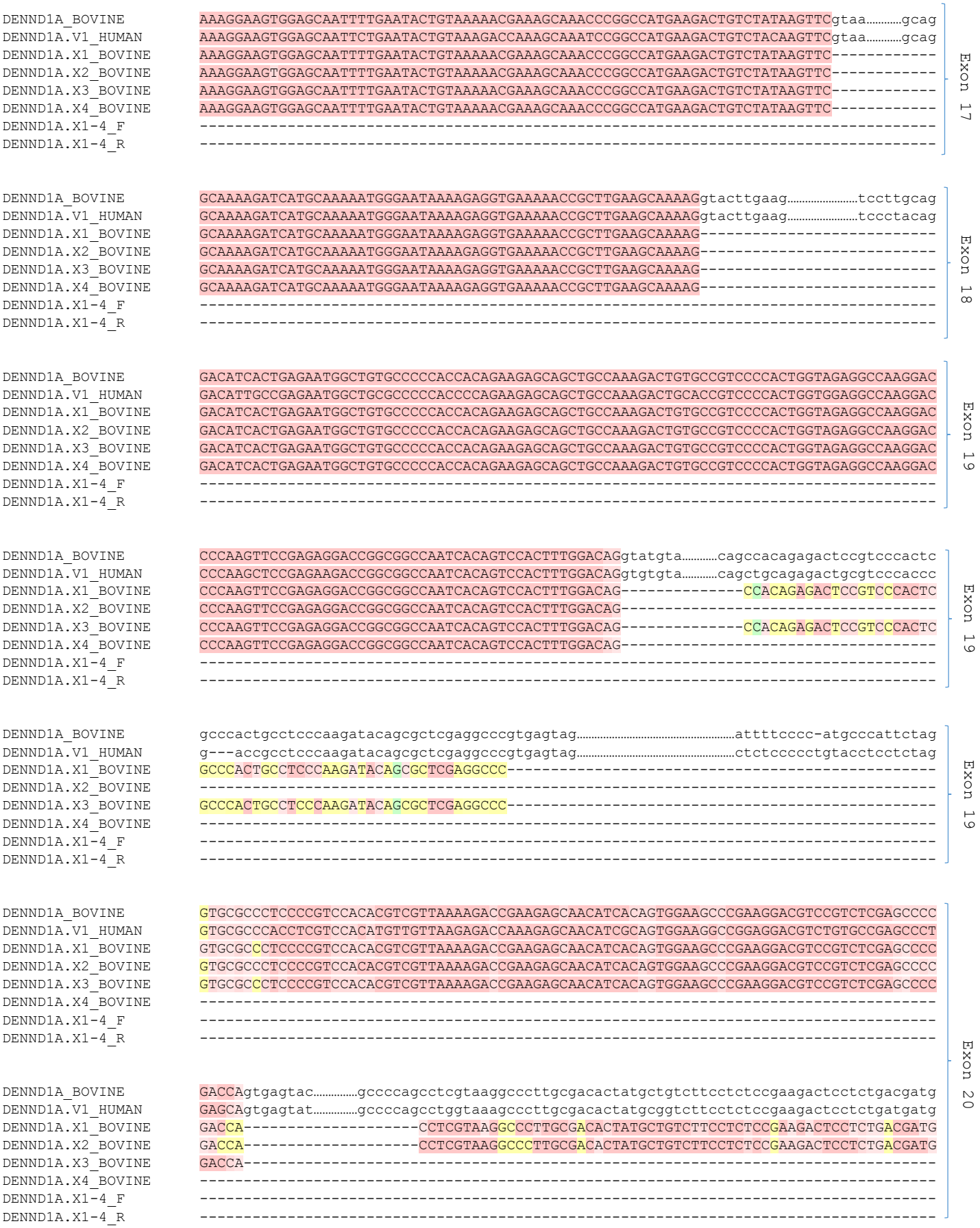
DENND1A_BOVINE
DENND1A.V1_HUMAN
DENND1A.X1_BOVINE
DENND1A.X2_BOVINE
DENND1A.X3_BOVINE
DENND1A.X4_BOVINE
DENND1A.X1-4_F
DENND1A.X1-4_R
Exon 17
Exon 18
Exon 19
Exon 19
Exon 19
Exon 20

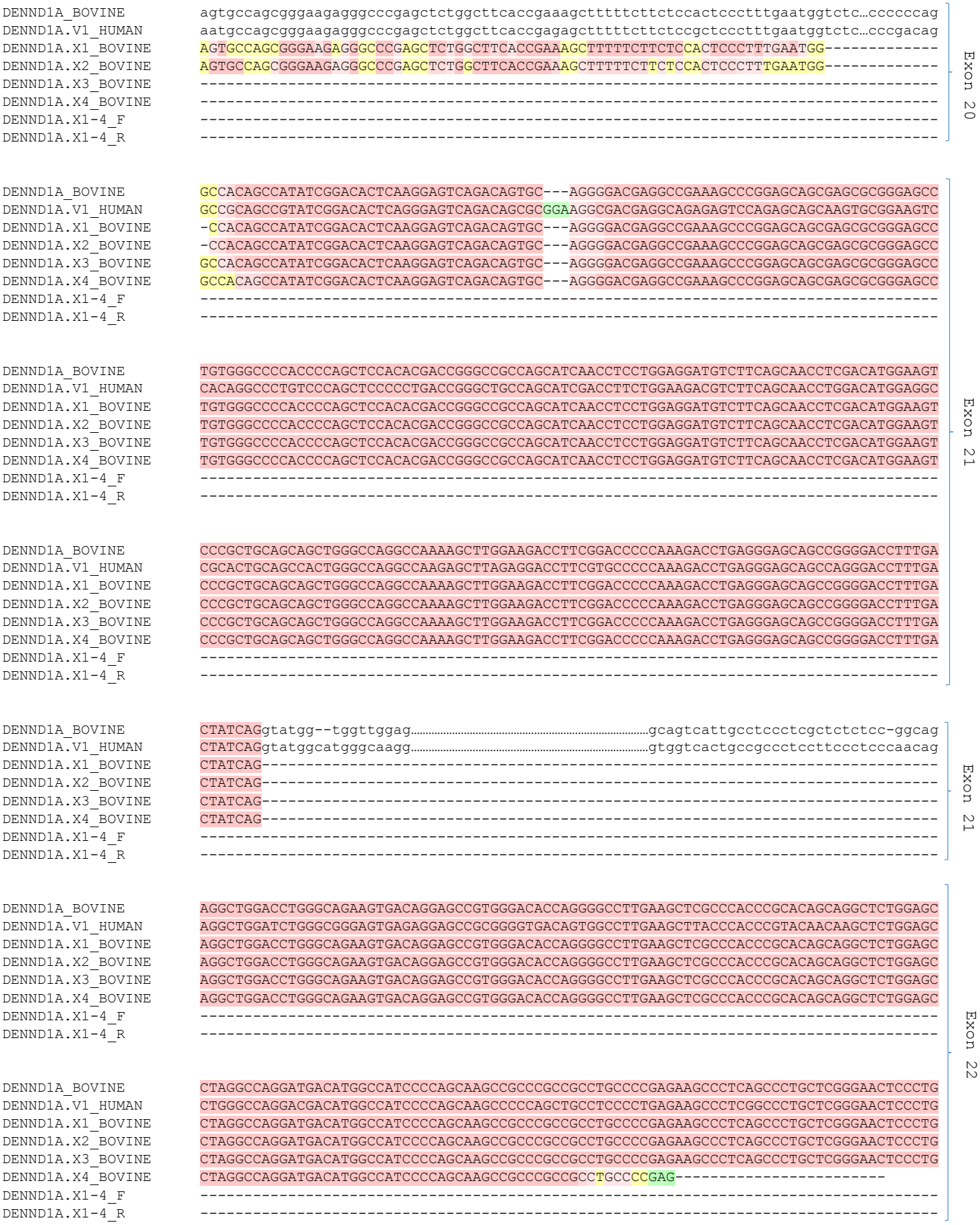
DENND1A_BOVINE agtgccagcgggaagagggcccgagctctggcttcaccgaaagctttttcttctccactccctttgaatggtctc…ccccccag
DENND1A.V1_HUMAN aatgccagcgggaagagggcccgagctctggcttcaccgagagctttttcttctccgctccctttgaatggtctc…cccgacag
DENND1A.X1_BOVINE AGTGCCAGCGGGAAGAGGGCCCGAGCTCTGGCTTCACCGAAAGCTTTTTCTTCTCCACTCCCTTTGAATGG----------
DENND1A.X2_BOVINE AGTGCCAGCGGGAAGAGGGCCCGAGCTCTGGCTTCACCGAAAGCTTTTTCTTCTCCACTCCCTTTGAATGG----------
DENND1A.X3_BOVINE ----------
DENND1A.X4_BOVINE ----------
DENND1A.X1-4_F ----------
DENND1A.X1-4_R ----------
Exon 20
DENND1A_BOVINE GCCACAGCCATATCGGACACTCAAGGAGTCAGACAGTGC---AGGGGACGAGGCCGAAAGCCCGGAGCAGCGAGCGCGGGAGCC
DENND1A.V1_HUMAN GCCGCAGCCGTATCGGACACTCAGGGAGTCAGACAGCGCGGAAGGCGACGAGGCAGAGAGTCCAGAGCAGCAAGTGCGGAAGTC
DENND1A.X1_BOVINE -CCACAGCCATATCGGACACTCAAGGAGTCAGACAGTGC---AGGGGACGAGGCCGAAAGCCCGGAGCAGCGAGCGCGGGAGCC
DENND1A.X2_BOVINE -CCACAGCCATATCGGACACTCAAGGAGTCAGACAGTGC---AGGGGACGAGGCCGAAAGCCCGGAGCAGCGAGCGCGGGAGCC
DENND1A.X3_BOVINE GCCACAGCCATATCGGACACTCAAGGAGTCAGACAGTGC---AGGGGACGAGGCCGAAAGCCCGGAGCAGCGAGCGCGGGAGCC
DENND1A.X4_BOVINE GCCACAGCCATATCGGACACTCAAGGAGTCAGACAGTGC---AGGGGACGAGGCCGAAAGCCCGGAGCAGCGAGCGCGGGAGCC
DENND1A.X1-4_F ----------
DENND1A.X1-4_R ----------
DENND1A_BOVINE TGTGGGCCCCACCCCAGCTCCACACGACCGGGCCGCCAGCATCAACCTCCTGGAGGATGTCTTCAGCAACCTCGACATGGAAGT
DENND1A.V1_HUMAN CACAGGCCCTGTCCCAGCTCCCCCTGACCGGGCTGCCAGCATCGACCTTCTGGAAGACGTCTTCAGCAACCTGGACATGGAGGC
DENND1A.X1_BOVINE TGTGGGCCCCACCCCAGCTCCACACGACCGGGCCGCCAGCATCAACCTCCTGGAGGATGTCTTCAGCAACCTCGACATGGAAGT
DENND1A.X2_BOVINE TGTGGGCCCCACCCCAGCTCCACACGACCGGGCCGCCAGCATCAACCTCCTGGAGGATGTCTTCAGCAACCTCGACATGGAAGT
DENND1A.X3_BOVINE TGTGGGCCCCACCCCAGCTCCACACGACCGGGCCGCCAGCATCAACCTCCTGGAGGATGTCTTCAGCAACCTCGACATGGAAGT
DENND1A.X4_BOVINE TGTGGGCCCCACCCCAGCTCCACACGACCGGGCCGCCAGCATCAACCTCCTGGAGGATGTCTTCAGCAACCTCGACATGGAAGT
DENND1A.X1-4_F ----------
DENND1A.X1-4_R ----------
Exon 21
DENND1A_BOVINE CCCGCTGCAGCAGCTGGGCCAGGCCAAAAGCTTGGAAGACCTTCGGACCCCCAAAGACCTGAGGGAGCAGCCGGGGACCTTTGA
DENND1A.V1_HUMAN CGCACTGCAGCCACTGGGCCAGGCCAAGAGCTTAGAGGACCTTCGTGCCCCCAAAGACCTGAGGGAGCAGCCAGGGACCTTTGA
DENND1A.X1_BOVINE CCCGCTGCAGCAGCTGGGCCAGGCCAAAAGCTTGGAAGACCTTCGGACCCCCAAAGACCTGAGGGAGCAGCCGGGGACCTTTGA
DENND1A.X2_BOVINE CCCGCTGCAGCAGCTGGGCCAGGCCAAAAGCTTGGAAGACCTTCGGACCCCCAAAGACCTGAGGGAGCAGCCGGGGACCTTTGA
DENND1A.X3_BOVINE CCCGCTGCAGCAGCTGGGCCAGGCCAAAAGCTTGGAAGACCTTCGGACCCCCAAAGACCTGAGGGAGCAGCCGGGGACCTTTGA
DENND1A.X4_BOVINE CCCGCTGCAGCAGCTGGGCCAGGCCAAAAGCTTGGAAGACCTTCGGACCCCCAAAGACCTGAGGGAGCAGCCGGGGACCTTTGA
DENND1A.X1-4_F ----------
DENND1A.X1-4_R ----------
DENND1A_BOVINE CTATCAGgtatgg--tggttggag……gcagtcattgcctccctcgctctctcc-ggcag
DENND1A.V1_HUMAN CTATCAGgtatggcatgggcaagg……gtggtcactgccgccctccttccctcccaacag
DENND1A.X1_BOVINE CTATCAG----------
DENND1A.X2_BOVINE CTATCAG----------
DENND1A.X3_BOVINE CTATCAG----------
DENND1A.X4_BOVINE CTATCAG----------
DENND1A.X1-4_F ----------
DENND1A.X1-4_R ----------
Exon 21
DENND1A_BOVINE AGGCTGGACCTGGGCAGAAGTGACAGGAGCCGTGGGACACCAGGGGCCTTGAAGCTCGCCCACCCGCACAGCAGGCTCTGGAGC
DENND1A.V1_HUMAN AGGCTGGATCTGGGCGGGAGTGAGAGGAGCCGCGGGGTGACAGTGGCCTTGAAGCTTACCCACCCGTACAACAAGCTCTGGAGC
DENND1A.X1_BOVINE AGGCTGGACCTGGGCAGAAGTGACAGGAGCCGTGGGACACCAGGGGCCTTGAAGCTCGCCCACCCGCACAGCAGGCTCTGGAGC
DENND1A.X2_BOVINE AGGCTGGACCTGGGCAGAAGTGACAGGAGCCGTGGGACACCAGGGGCCTTGAAGCTCGCCCACCCGCACAGCAGGCTCTGGAGC
DENND1A.X3_BOVINE AGGCTGGACCTGGGCAGAAGTGACAGGAGCCGTGGGACACCAGGGGCCTTGAAGCTCGCCCACCCGCACAGCAGGCTCTGGAGC
DENND1A.X4_BOVINE AGGCTGGACCTGGGCAGAAGTGACAGGAGCCGTGGGACACCAGGGGCCTTGAAGCTCGCCCACCCGCACAGCAGGCTCTGGAGC
DENND1A.X1-4_F ----------
DENND1A.X1-4_R ----------
Exon 22
DENND1A_BOVINE CTAGGCCAGGATGACATGGCCATCCCCAGCAAGCCGCCCGCCGCCTGCCCCGAGAAGCCCTCAGCCCTGCTCGGGAACTCCCTG
DENND1A.V1_HUMAN CTGGGCCAGGACGACATGGCCATCCCCAGCAAGCCCCCAGCTGCCTCCCCTGAGAAGCCCTCGGCCCTGCTCGGGAACTCCCTG
DENND1A.X1_BOVINE CTAGGCCAGGATGACATGGCCATCCCCAGCAAGCCGCCCGCCGCCTGCCCCGAGAAGCCCTCAGCCCTGCTCGGGAACTCCCTG
DENND1A.X2_BOVINE CTAGGCCAGGATGACATGGCCATCCCCAGCAAGCCGCCCGCCGCCTGCCCCGAGAAGCCCTCAGCCCTGCTCGGGAACTCCCTG
DENND1A.X3_BOVINE CTAGGCCAGGATGACATGGCCATCCCCAGCAAGCCGCCCGCCGCCTGCCCCGAGAAGCCCTCAGCCCTGCTCGGGAACTCCCTG
DENND1A.X4_BOVINE CTAGGCCAGGATGACATGGCCATCCCCAGCAAGCCGCCCGCCGCCTGCCCCGAG----------
DENND1A.X1-4_F ----------
DENND1A.X1-4_R ----------

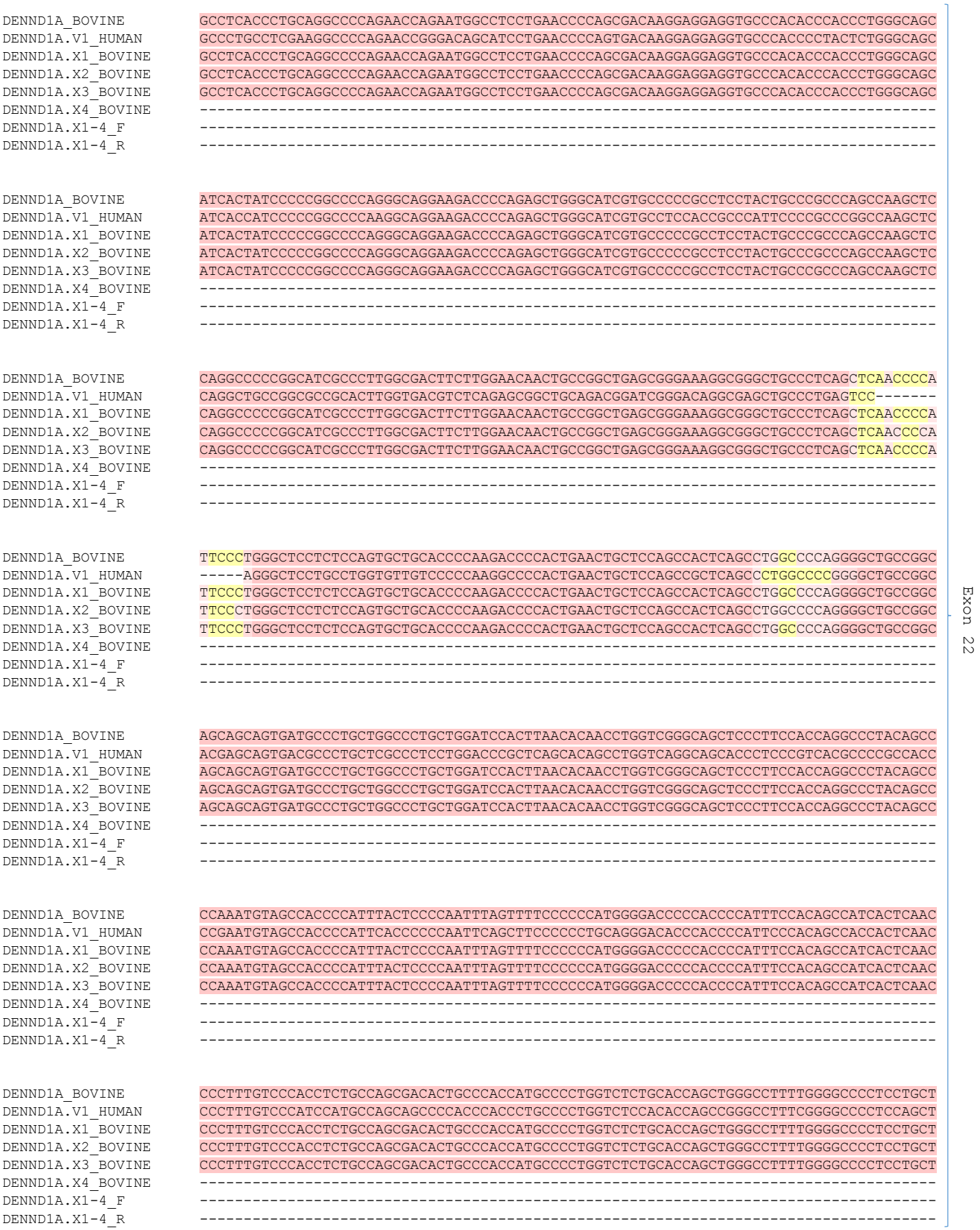
DENND1A_BOVINE GCCTCACCCTGCAGGCCCCAGAACCAGAATGGCCTCCTGAACCCCAGCGACAAGGAGGAGGTGCCCACACCCACCCTGGGCAGC
DENND1A.V1_HUMAN GCCCTGCCTCGAAGGCCCCAGAACCGGGACAGCATCCTGAACCCCAGTGACAAGGAGGAGGTGCCCACCCCTACTCTGGGCAGC
DENND1A.X1_BOVINE GCCTCACCCTGCAGGCCCCAGAACCAGAATGGCCTCCTGAACCCCAGCGACAAGGAGGAGGTGCCCACACCCACCCTGGGCAGC
DENND1A.X2_BOVINE GCCTCACCCTGCAGGCCCCAGAACCAGAATGGCCTCCTGAACCCCAGCGACAAGGAGGAGGTGCCCACACCCACCCTGGGCAGC
DENND1A.X3_BOVINE GCCTCACCCTGCAGGCCCCAGAACCAGAATGGCCTCCTGAACCCCAGCGACAAGGAGGAGGTGCCCACACCCACCCTGGGCAGC
DENND1A.X4_BOVINE ----------
DENND1A.X1-4_F ----------
DENND1A.X1-4_R ----------
DENND1A_BOVINE ATCACTATCCCCCGGCCCCAGGGCAGGAAGACCCCAGAGCTGGGCATCGTGCCCCCGCCTCCTACTGCCCGCCCAGCCAAGCTC
DENND1A.V1_HUMAN ATCACCATCCCCCGGCCCCAAGGCAGGAAGACCCCAGAGCTGGGCATCGTGCCTCCACCGCCCATTCCCCGCCCGGCCAAGCTC
DENND1A.X1_BOVINE ATCACTATCCCCCGGCCCCAGGGCAGGAAGACCCCAGAGCTGGGCATCGTGCCCCCGCCTCCTACTGCCCGCCCAGCCAAGCTC
DENND1A.X2_BOVINE ATCACTATCCCCCGGCCCCAGGGCAGGAAGACCCCAGAGCTGGGCATCGTGCCCCCGCCTCCTACTGCCCGCCCAGCCAAGCTC
DENND1A.X3_BOVINE ATCACTATCCCCCGGCCCCAGGGCAGGAAGACCCCAGAGCTGGGCATCGTGCCCCCGCCTCCTACTGCCCGCCCAGCCAAGCTC
DENND1A.X4_BOVINE ----------
DENND1A.X1-4_F ----------
DENND1A.X1-4_R ----------
DENND1A_BOVINE CAGGCCCCCGGCATCGCCCTTGGCGACTTCTTGGAACAACTGCCGGCTGAGCGGGAAAGGCGGGCTGCCCTCAGCTCAACCCCA
DENND1A.V1_HUMAN CAGGCTGCCGGCGCCGCACTTGGTGACGTCTCAGAGCGGCTGCAGACGGATCGGGACAGGCGAGCTGCCCTGAGTCC-------
DENND1A.X1_BOVINE CAGGCCCCCGGCATCGCCCTTGGCGACTTCTTGGAACAACTGCCGGCTGAGCGGGAAAGGCGGGCTGCCCTCAGCTCAACCCCA
DENND1A.X2_BOVINE CAGGCCCCCGGCATCGCCCTTGGCGACTTCTTGGAACAACTGCCGGCTGAGCGGGAAAGGCGGGCTGCCCTCAGCTCAACCCCA
DENND1A.X3_BOVINE CAGGCCCCCGGCATCGCCCTTGGCGACTTCTTGGAACAACTGCCGGCTGAGCGGGAAAGGCGGGCTGCCCTCAGCTCAACCCCA
DENND1A.X4_BOVINE ----------
DENND1A.X1-4_F ----------
DENND1A.X1-4_R ----------
DENND1A_BOVINE TTCCCTGGGCTCCTCTCCAGTGCTGCACCCCAAGACCCCACTGAACTGCTCCAGCCACTCAGCCTGGCCCCAGGGGCTGCCGGC
DENND1A.V1_HUMAN -----AGGGCTCCTGCCTGGTGTTGTCCCCCAAGGCCCCACTGAACTGCTCCAGCCGCTCAGCCCTGGCCCCGGGGCTGCCGGC
DENND1A.X1_BOVINE TTCCCTGGGCTCCTCTCCAGTGCTGCACCCCAAGACCCCACTGAACTGCTCCAGCCACTCAGCCTGGCCCCAGGGGCTGCCGGC
DENND1A.X2_BOVINE TTCCCTGGGCTCCTCTCCAGTGCTGCACCCCAAGACCCCACTGAACTGCTCCAGCCACTCAGCCTGGCCCCAGGGGCTGCCGGC
DENND1A.X3_BOVINE TTCCCTGGGCTCCTCTCCAGTGCTGCACCCCAAGACCCCACTGAACTGCTCCAGCCACTCAGCCTGGCCCCAGGGGCTGCCGGC
DENND1A.X4_BOVINE ----------
DENND1A.X1-4_F ----------
DENND1A.X1-4_R ----------
DENND1A_BOVINE AGCAGCAGTGATGCCCTGCTGGCCCTGCTGGATCCACTTAACACAACCTGGTCGGGCAGCTCCCTTCCACCAGGCCCTACAGCC
DENND1A.V1_HUMAN ACGAGCAGTGACGCCCTGCTCGCCCTCCTGGACCCGCTCAGCACAGCCTGGTCAGGCAGCACCCTCCCGTCACGCCCCGCCACC
DENND1A.X1_BOVINE AGCAGCAGTGATGCCCTGCTGGCCCTGCTGGATCCACTTAACACAACCTGGTCGGGCAGCTCCCTTCCACCAGGCCCTACAGCC
DENND1A.X2_BOVINE AGCAGCAGTGATGCCCTGCTGGCCCTGCTGGATCCACTTAACACAACCTGGTCGGGCAGCTCCCTTCCACCAGGCCCTACAGCC
DENND1A.X3_BOVINE AGCAGCAGTGATGCCCTGCTGGCCCTGCTGGATCCACTTAACACAACCTGGTCGGGCAGCTCCCTTCCACCAGGCCCTACAGCC
DENND1A.X4_BOVINE ----------
DENND1A.X1-4_F ----------
DENND1A.X1-4_R ----------
DENND1A_BOVINE CCAAATGTAGCCACCCCATTTACTCCCCAATTTAGTTTTCCCCCCATGGGGACCCCCACCCCATTTCCACAGCCATCACTCAAC
DENND1A.V1_HUMAN CCGAATGTAGCCACCCCATTCACCCCCCAATTCAGCTTCCCCCCTGCAGGGACACCCACCCCATTCCCACAGCCACCACTCAAC
DENND1A.X1_BOVINE CCAAATGTAGCCACCCCATTTACTCCCCAATTTAGTTTTCCCCCCATGGGGACCCCCACCCCATTTCCACAGCCATCACTCAAC
DENND1A.X2_BOVINE CCAAATGTAGCCACCCCATTTACTCCCCAATTTAGTTTTCCCCCCATGGGGACCCCCACCCCATTTCCACAGCCATCACTCAAC
DENND1A.X3_BOVINE CCAAATGTAGCCACCCCATTTACTCCCCAATTTAGTTTTCCCCCCATGGGGACCCCCACCCCATTTCCACAGCCATCACTCAAC
DENND1A.X4_BOVINE ----------
DENND1A.X1-4_F ----------
DENND1A.X1-4_R ----------
DENND1A_BOVINE CCCTTTGTCCCACCTCTGCCAGCGACACTGCCCACCATGCCCCTGGTCTCTGCACCAGCTGGGCCTTTTGGGGCCCCTCCTGCT
DENND1A.V1_HUMAN CCCTTTGTCCCATCCATGCCAGCAGCCCCACCCACCCTGCCCCTGGTCTCCACACCAGCCGGGCCTTTCGGGGCCCCTCCAGCT
DENND1A.X1_BOVINE CCCTTTGTCCCACCTCTGCCAGCGACACTGCCCACCATGCCCCTGGTCTCTGCACCAGCTGGGCCTTTTGGGGCCCCTCCTGCT
DENND1A.X2_BOVINE CCCTTTGTCCCACCTCTGCCAGCGACACTGCCCACCATGCCCCTGGTCTCTGCACCAGCTGGGCCTTTTGGGGCCCCTCCTGCT
DENND1A.X3_BOVINE CCCTTTGTCCCACCTCTGCCAGCGACACTGCCCACCATGCCCCTGGTCTCTGCACCAGCTGGGCCTTTTGGGGCCCCTCCTGCT
DENND1A.X4_BOVINE ----------
DENND1A.X1-4_F ----------
DENND1A.X1-4_R ----------
Exon 22


DENND1A_BOVINE TCCCTGGGGCCAGCCTTTGCCCCCAGCCTCCTGCTGTCCAATTCTGGCTTCTGTGCCCCACATCGATCTCAGCCCAACCTGTCT
DENND1A.V1_HUMAN TCCCTGGGGCCGGCTTTTGCGTCCGGCCTCCTGCTGTCCAGTGCTGGCTTCTGTGCCCCTCACAGGTCTCAGCCCAACCTCTCC
DENND1A.X1_BOVINE TCCCTGGGGCCAGCCTTTGCCCCCAGCCTCCTGCTGTCCAATTCTGGCTTCTGTGCCCCACATCGATCTCAGCCCAACCTGTCT
DENND1A.X2_BOVINE TCCCTGGGGCCAGCCTTTGCCCCCAGCCTCCTGCTGTCCAATTCTGGCTTCTGTGCCCCACATCGATCTCAGCCCAACCTGTCT
DENND1A.X3_BOVINE TCCCTGGGGCCAGCCTTTGCCCCCAGCCTCCTGCTGTCCAATTCTGGCTTCTGTGCCCCACATCGATCTCAGCCCAACCTGTCT
DENND1A.X4_BOVINE ----------
DENND1A.X1-4_F ----------
DENND1A.X1-4_R ----------
DENND1A_BOVINE GCCCTCTCCATGCCCAACCTCTTTGGCCAAGTGCCCATGGGTACCCAC------TCCCTGCAGCCTCTGGGTCCCCCAGCAGTC
DENND1A.V1_HUMAN GCCCTCTCCATGCCCAACCTCTTTGGCCAGATGCCCATGGGCACCCACACGAGCCCCCTACAGCCGCTGGGTCCCCCAGCAGTT
DENND1A.X1_BOVINE GCCCTCTCCATGCCCAACCTCTTTGGCCAAGTGCCCATGGGTACCCAC------TCCCTGCAGCCTCTGGGTCCCCCAGCAGTC
DENND1A.X2_BOVINE GCCCTCTCCATGCCCAACCTCTTTGGCCAAGTGCCCATGGGTACCCAC------TCCCTGCAGCCTCTGGGTCCCCCAGCAGTC
DENND1A.X3_BOVINE GCCCTCTCCATGCCCAACCTCTTTGGCCAAGTGCCCATGGGTACCCAC------TCCCTGCAGCCTCTGGGTCCCCCAGCAGTC
DENND1A.X4_BOVINE ----------
DENND1A.X1-4_F ----------
DENND1A.X1-4_R ----------
DENND1A_BOVINE GCCCCCTCAAGGATCCGAACATTGCCCCTGGCCCGCTCAAGTGCCAGGGCCGCCGAGGCCAAGCAAGGGCTGGCCCTGAGGCCT
DENND1A.V1_HUMAN GCCCCGTCGAGGATCCGAACGTTGCCCCTGGCCCGCTCAAGTGCCAGGGCTGCTGAGACCAAGCAGGGGCTGGCCCTGAGGCCT
DENND1A.X1_BOVINE GCCCCCTCAAGGATCCGAACATTGCCCCTGGCCCGCTCAAGTGCCAGGGCCGCCGAGGCCAAGCAAGGGCTGGCCCTGAGGCCT
DENND1A.X2_BOVINE GCCCCCTCAAGGATCCGAACATTGCCCCTGGCCCGCTCAAGTGCCAGGGCCGCCGAGGCCAAGCAAGGGCTGGCCCTGAGGCCT
DENND1A.X3_BOVINE GCCCCCTCAAGGATCCGAACATTGCCCCTGGCCCGCTCAAGTGCCAGGGCCGCCGAGGCCAAGCAAGGGCTGGCCCTGAGGCCT
DENND1A.X4_BOVINE ----------
DENND1A.X1-4_F ----------
DENND1A.X1-4_R ----------
DENND1A_BOVINE GGAGAACCCCCACTCCTCCCAGCCAGGCCCCCCCAGGGCCTGGAGCCAGCACTGCAGCCCTCTGCTCCACGAGAGGCCAGAGAC
DENND1A.V1_HUMAN GGAGACCCCCCGCTTCTGCCTCCCAGGCCCCCTCAAGGCCTGGAGCCAACACTGCAGCCCTCTGCTCCTCAACAGGCCAGAGAC
DENND1A.X1_BOVINE GGAGAACCCCCACTCCTCCCAGCCAGGCCCCCCCAGGGCCTGGAGCCAGCACTGCAGCCCTCTGCTCCACGAGAGGCCAGAGAC
DENND1A.X2_BOVINE GGAGAACCCCCACTCCTCCCAGCCAGGCCCCCCCAGGGCCTGGAGCCAGCACTGCAGCCCTCTGCTCCACGAGAGGCCAGAGAC
DENND1A.X3_BOVINE GGAGAACCCCCACTCCTCCCAGCCAGGCCCCCCCAGGGCCTGGAGCCAGCACTGCAGCCCTCTGCTCCACGAGAGGCCAGAGAC
DENND1A.X4_BOVINE ----------
DENND1A.X1-4_F ----------
DENND1A.X1-4_R ----------
DENND1A_BOVINE CCCTTTGAGGATTTGTTACGGAAAACCAAGCAAGATGTGAGCTCG----------GCCCCAGCCCCCGGCTCCGTGGAGCAG
DENND1A.V1_HUMAN CCCTTTGAGGATTTGTTACAGAAAACCAAGCAAGACGTGAGCCCGAGTCCGGCCCTGGCCCCGGCCCCAGACTCGGTGGAGCAG
DENND1A.X1_BOVINE CCCTTTGAGGATTTGTTACGGAAAACCAAGCAAGATGTGAGCTCG----------GCCCCAGCCCCCGGCTCCGTGGAGCAG
DENND1A.X2_BOVINE CCCTTTGAGGATTTGTTACGGAAAACCAAGCAAGATGTGAGCTCG----------GCCCCAGCCCCCGGCTCCGTGGAGCAG
DENND1A.X3_BOVINE CCCTTTGAGGATTTGTTACGGAAAACCAAGCAAGATGTGAGCTCG----------GCCCCAGCCCCCGGCTCCGTGGAGCAG
DENND1A.X4_BOVINE ----------
DENND1A.X1-4_F ----------
DENND1A.X1-4_R ----------
DENND1A_BOVINE CTCAGGAAGCAATGGGAGACCTTCGAGTGAGCAGC--GCTGAGGGTGGGGCGAG--CCAAGGCCGGCCGGCCCTGCTTCCCCTG
DENND1A.V1_HUMAN CTCAGGAAGCAGTGGGAGACCTTCGAGTGAGCCGGGCCCTGAGGGTGGGGGATGCACCGAGGCCCGAGGG---TCCGTCCACTG
DENND1A.X1_BOVINE CTCAGGAAGCAATGGGAGACCTTCGAGTGAGCAGC--GCTGAGGGTGGGGCGAG--CCAAGGCCGGCCGGCCCTGCTTCCCCTG
DENND1A.X2_BOVINE CTCAGGAAGCAATGGGAGACCTTCGAGTGAGCAGC--GCTGAGGGTGGGGCGAG--CCAAGGCCGGCCGGCCCTGCTTCCCCTG
DENND1A.X3_BOVINE CTCAGGAAGCAATGGGAGACCTTCGAGTGAGCAGC--GCTGAGGGTGGGGCGAG--CCAAGGCCGGCCGGCCCTGCTTCCCCTG
DENND1A.X4_BOVINE ----------
DENND1A.X1-4_F ----------
DENND1A.X1-4_R ----------
DENND1A_BOVINE CTG------------------------CTGTTTCTACCCAGGTTCTACTGGTGGGAAGGGATGGGAACCCTCTCTGCCGCC-CC
DENND1A.V1_HUMAN CTGCGGTTCCGAGGCTCCCCCGCCACTCTCTCTCTGCCCAGGTTCTGCTGGTGGGAAGGGATGGGACCCCTCTCTGCTGCCCCC
DENND1A.X1_BOVINE CTG------------------------CTGTTTCTACCCAGGTTCTACTGGTGGGAAGGGATGGGAACCCTCTCTGCCGCC-CC
DENND1A.X2_BOVINE CTG------------------------CTGTTTCTACCCAGGTTCTACTGGTGGGAAGGGATGGGAACCCTCTCTGCCGCC-CC
DENND1A.X3_BOVINE CTG------------------------CTGTTTCTACCCAGGTTCTACTGGTGGGAAGGGATGGGAACCCTCTCTGCCGCC-CC
DENND1A.X4_BOVINE ----------
DENND1A.X1-4_F ----------
DENND1A.X1-4_R ----------
Exon 22

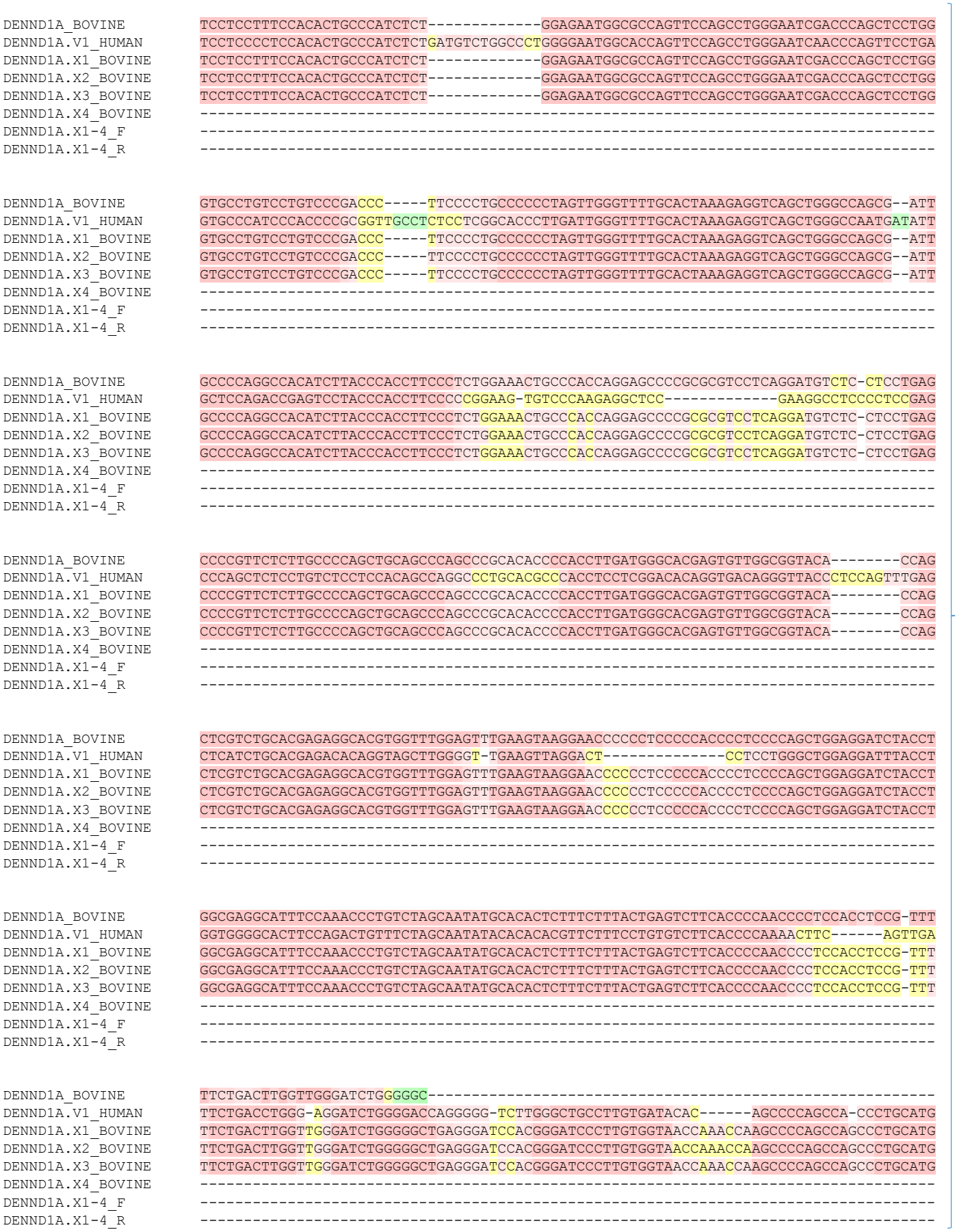
DENND1A_BOVINE TCCTCCTTTCCACACTGCCCATCTCT----------GGAGAATGGCGCCAGTTCCAGCCTGGGAATCGACCCAGCTCCTGG
DENND1A.V1_HUMAN TCCTCCCCTCCACACTGCCCATCTCTGATGTCTGGCCCTGGGGAATGGCACCAGTTCCAGCCTGGGAATCAACCCAGTTCCTGA
DENND1A.X1_BOVINE TCCTCCTTTCCACACTGCCCATCTCT----------GGAGAATGGCGCCAGTTCCAGCCTGGGAATCGACCCAGCTCCTGG
DENND1A.X2_BOVINE TCCTCCTTTCCACACTGCCCATCTCT----------GGAGAATGGCGCCAGTTCCAGCCTGGGAATCGACCCAGCTCCTGG
DENND1A.X3_BOVINE TCCTCCTTTCCACACTGCCCATCTCT----------GGAGAATGGCGCCAGTTCCAGCCTGGGAATCGACCCAGCTCCTGG
DENND1A.X4_BOVINE ----------
DENND1A.X1-4_F ----------
DENND1A.X1-4_R ----------
DENND1A_BOVINE GTGCCTGTCCTGTCCCGACCC-----TTCCCCTGCCCCCCTAGTTGGGTTTTGCACTAAAGAGGTCAGCTGGGCCAGCG--ATT
DENND1A.V1_HUMAN GTGCCCATCCCACCCCGCGGTTGCCTCTCCTCGGCACCCTTGATTGGGTTTTGCACTAAAGAGGTCAGCTGGGCCAATGATATT
DENND1A.X1_BOVINE GTGCCTGTCCTGTCCCGACCC-----TTCCCCTGCCCCCCTAGTTGGGTTTTGCACTAAAGAGGTCAGCTGGGCCAGCG--ATT
DENND1A.X2_BOVINE GTGCCTGTCCTGTCCCGACCC-----TTCCCCTGCCCCCCTAGTTGGGTTTTGCACTAAAGAGGTCAGCTGGGCCAGCG--ATT
DENND1A.X3_BOVINE GTGCCTGTCCTGTCCCGACCC-----TTCCCCTGCCCCCCTAGTTGGGTTTTGCACTAAAGAGGTCAGCTGGGCCAGCG--ATT
DENND1A.X4_BOVINE ----------
DENND1A.X1-4_F ----------
DENND1A.X1-4_R ----------
DENND1A_BOVINE GCCCCAGGCCACATCTTACCCACCTTCCCTCTGGAAACTGCCCACCAGGAGCCCCGCGCGTCCTCAGGATGTCTC-CTCCTGAG
DENND1A.V1_HUMAN GCTCCAGACCGAGTCCTACCCACCTTCCCCCGGAAG-TGTCCCAAGAGGCTCC----------GAAGGCCTCCCCTCCGAG
DENND1A.X1_BOVINE GCCCCAGGCCACATCTTACCCACCTTCCCTCTGGAAACTGCCCACCAGGAGCCCCGCGCGTCCTCAGGATGTCTC-CTCCTGAG
DENND1A.X2_BOVINE GCCCCAGGCCACATCTTACCCACCTTCCCTCTGGAAACTGCCCACCAGGAGCCCCGCGCGTCCTCAGGATGTCTC-CTCCTGAG
DENND1A.X3_BOVINE GCCCCAGGCCACATCTTACCCACCTTCCCTCTGGAAACTGCCCACCAGGAGCCCCGCGCGTCCTCAGGATGTCTC-CTCCTGAG
DENND1A.X4_BOVINE ----------
DENND1A.X1-4_F ----------
DENND1A.X1-4_R ----------
DENND1A_BOVINE CCCCGTTCTCTTGCCCCAGCTGCAGCCCAGCCCGCACACCCCACCTTGATGGGCACGAGTGTTGGCGGTACA--------CCAG
DENND1A.V1_HUMAN CCCAGCTCTCCTGTCTCCTCCACAGCCAGGCCCTGCACGCCCACCTCCTCGGACACAGGTGACAGGGTTACCCTCCAGTTTGAG
DENND1A.X1_BOVINE CCCCGTTCTCTTGCCCCAGCTGCAGCCCAGCCCGCACACCCCACCTTGATGGGCACGAGTGTTGGCGGTACA--------CCAG
DENND1A.X2_BOVINE CCCCGTTCTCTTGCCCCAGCTGCAGCCCAGCCCGCACACCCCACCTTGATGGGCACGAGTGTTGGCGGTACA--------CCAG
DENND1A.X3_BOVINE CCCCGTTCTCTTGCCCCAGCTGCAGCCCAGCCCGCACACCCCACCTTGATGGGCACGAGTGTTGGCGGTACA--------CCAG
DENND1A.X4_BOVINE ----------
DENND1A.X1-4_F ----------
DENND1A.X1-4_R ----------
DENND1A_BOVINE CTCGTCTGCACGAGAGGCACGTGGTTTGGAGTTTGAAGTAAGGAACCCCCCTCCCCCACCCCTCCCCAGCTGGAGGATCTACCT
DENND1A.V1_HUMAN CTCATCTGCACGAGACACAGGTAGCTTGGGGT-TGAAGTTAGGACT----------CCTCCTGGGCTGGAGGATTTACCT
DENND1A.X1_BOVINE CTCGTCTGCACGAGAGGCACGTGGTTTGGAGTTTGAAGTAAGGAACCCCCCTCCCCCACCCCTCCCCAGCTGGAGGATCTACCT
DENND1A.X2_BOVINE CTCGTCTGCACGAGAGGCACGTGGTTTGGAGTTTGAAGTAAGGAACCCCCCTCCCCCACCCCTCCCCAGCTGGAGGATCTACCT
DENND1A.X3_BOVINE CTCGTCTGCACGAGAGGCACGTGGTTTGGAGTTTGAAGTAAGGAACCCCCCTCCCCCACCCCTCCCCAGCTGGAGGATCTACCT
DENND1A.X4_BOVINE ----------
DENND1A.X1-4_F ----------
DENND1A.X1-4_R ----------
DENND1A_BOVINE GGCGAGGCATTTCCAAACCCTGTCTAGCAATATGCACACTCTTTCTTTACTGAGTCTTCACCCCAACCCCTCCACCTCCG-TTT
DENND1A.V1_HUMAN GGTGGGGCACTTCCAGACTGTTTCTAGCAATATACACACACGTTCTTTCCTGTGTCTTCACCCCAAAACTTC------AGTTGA
DENND1A.X1_BOVINE GGCGAGGCATTTCCAAACCCTGTCTAGCAATATGCACACTCTTTCTTTACTGAGTCTTCACCCCAACCCCTCCACCTCCG-TTT
DENND1A.X2_BOVINE GGCGAGGCATTTCCAAACCCTGTCTAGCAATATGCACACTCTTTCTTTACTGAGTCTTCACCCCAACCCCTCCACCTCCG-TTT
DENND1A.X3_BOVINE GGCGAGGCATTTCCAAACCCTGTCTAGCAATATGCACACTCTTTCTTTACTGAGTCTTCACCCCAACCCCTCCACCTCCG-TTT
DENND1A.X4_BOVINE ----------
DENND1A.X1-4_F ----------
DENND1A.X1-4_R ----------
DENND1A_BOVINE TTCTGACTTGGTTGGGATCTGGGGGC----------
DENND1A.V1_HUMAN TTCTGACCTGGG-AGGATCTGGGGACCAGGGGG-TCTTGGGCTGCCTTGTGATACAC------AGCCCCAGCCA-CCCTGCATG
DENND1A.X1_BOVINE TTCTGACTTGGTTGGGATCTGGGGGCTGAGGGATCCACGGGATCCCTTGTGGTAACCAAACCAAGCCCCAGCCAGCCCTGCATG
DENND1A.X2_BOVINE TTCTGACTTGGTTGGGATCTGGGGGCTGAGGGATCCACGGGATCCCTTGTGGTAACCAAACCAAGCCCCAGCCAGCCCTGCATG
DENND1A.X3_BOVINE TTCTGACTTGGTTGGGATCTGGGGGCTGAGGGATCCACGGGATCCCTTGTGGTAACCAAACCAAGCCCCAGCCAGCCCTGCATG
DENND1A.X4_BOVINE ----------
DENND1A.X1-4_F ----------
DENND1A.X1-4_R ----------
Exon 22

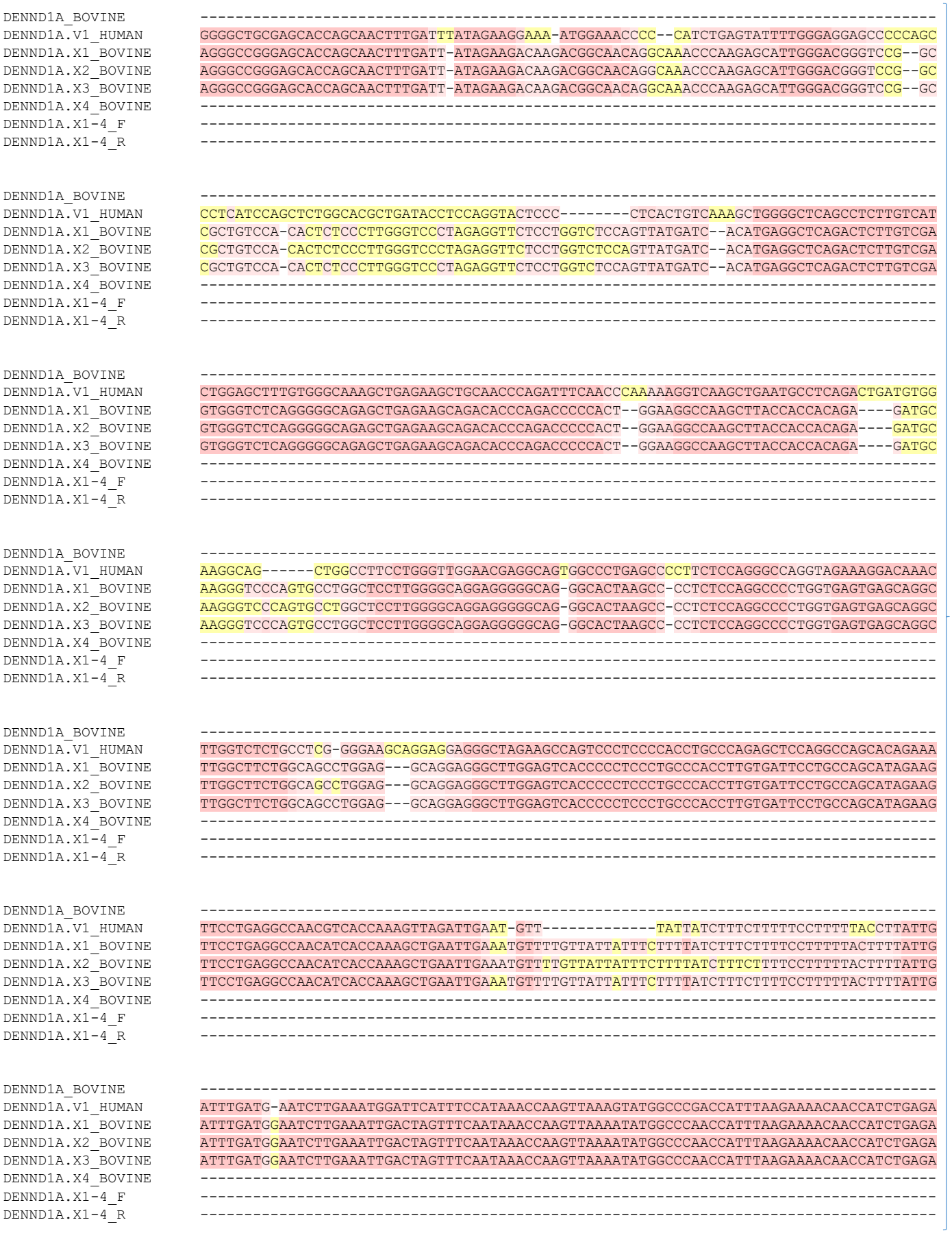
DENND1A_BOVINE
DENND1A.V1_HUMAN
DENND1A.X1_BOVINE
DENND1A.X2_BOVINE
DENND1A.X3_BOVINE
DENND1A.X4_BOVINE
DENND1A.X1-4_F
DENND1A.X1-4_R
Exon 22

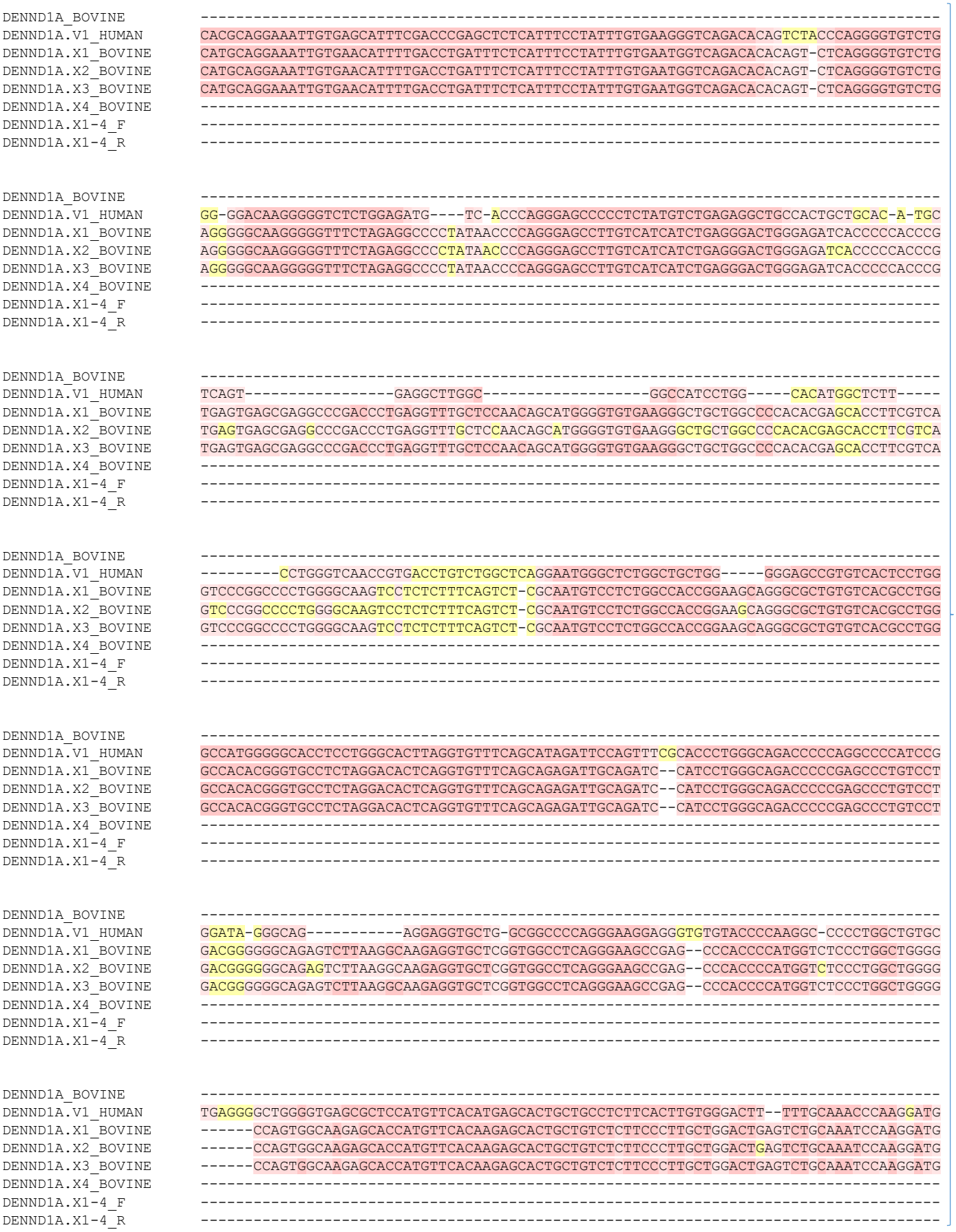
DENND1A_BOVINE
DENND1A.V1_HUMAN
DENND1A.X1_BOVINE
DENND1A.X2_BOVINE
DENND1A.X3_BOVINE
DENND1A.X4_BOVINE
DENND1A.X1-4_F
DENND1A.X1-4_R
Exon 22

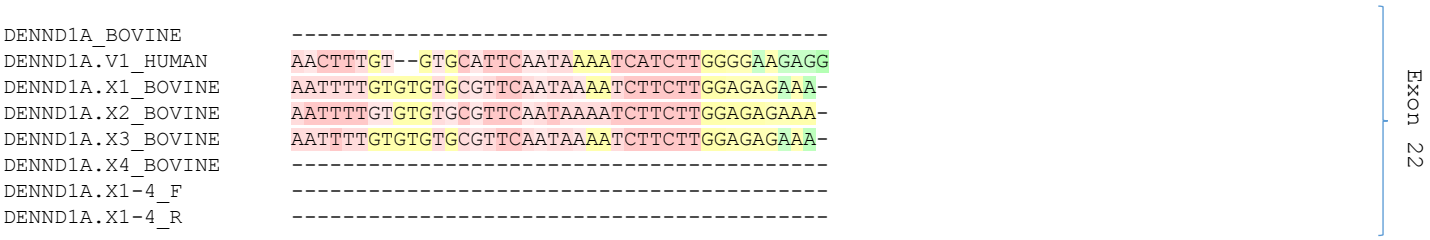
DENND1A_BOVINE ----------
DENND1A.V1_HUMAN AACTTTGT--GTGCATTCAATAAAATCATCTTGGGGAAGAGG
DENND1A.X1_BOVINE AATTTTGTGTGTGCGTTCAATAAAATCTTCTTGGAGAGAAA-
DENND1A.X2_BOVINE AATTTTGTGTGTGCGTTCAATAAAATCTTCTTGGAGAGAAA-
DENND1A.X3_BOVINE AATTTTGTGTGTGCGTTCAATAAAATCTTCTTGGAGAGAAA-
DENND1A.X4_BOVINE ----------
DENND1A.X1-4_F ----------
DENND1A.X1-4_R ----------
Exon 22

Supplemental Fig. S3. Alignment of the exons of human *DENND1A V1*, *V3* and *V4* and *DENND1A.V1,3,4* primer sequences. Alignment was generated with CLUSTAL O (1.2.4) multiple sequence alignment based on sequences available at Ensembl Asia with transcript ID: human *DENND1A.V1* (ENST00000373624.6) and at NCBI PubMed with accession numbers: *DENND1A.V3* (NM_001352964) and *DENND1A.V4* (NM_001352965). The alignment was analysed with T-COFFEE (1) and colored based on the consistency: red (high), yellow (average); green and blue (poor). Consistency is estimated from CORE index. Bright aqua highlighted areas represent the primer sequences. ..... represent intronic areas not shown so as to reduce the size of this file.

1. Notredame C, Higgins DG, Heringa J. T-Coffee: A novel method for fast and accurate multiple sequence alignment. J Mol Biol. 2000;302(1):205-17. doi: 10.1006/jmbi.2000.4042.

```
DENND1A.V1          CGCGCGCCGGGCACGCGCGCCGGCGACCATGGCGTTCGCCGGGCTGGAGCGAGTACATTAACCCCTGGAGGCGGCGGCGGCGGCGAGGGAGCG
DENND1A.V3          CGCGCGCCGGGCACGCGCGCCGGCGACCATGGCGTTCGCCGGGCTGGAGCGAGTACATTAACCCCTGGAGGCGGCGGCGGCGGCGAGGGAGCG
DENND1A.V4          CGCGCGCCGGGCACGCGCGCCGGCGACCATGGCGTTCGCCGGGCTGGAGCGAGTACATTAACCCCTGGAGGCGGCGGCGGCGGCGAGGGAGCG
DENND1A.V1,3,4_F    ------------------------------------------------------------------------------------------------
DENND1A.V1,3,4_R    ------------------------------------------------------------------------------------------------

DENND1A.V1          AGCCTCGAGCGGGCGGGCCCCAGCCTGAGGGAAGGGAGGAAGGGGCGGGGAGAGCGCCAGAGGGAGGCCGGTCGGCCGCGGGCGGGCGGGCAG
DENND1A.V3          AGCCTCGAGCGGGCGGGCCCCAGCCTGAGGGAAGGGAGGAAGGGGCGGGGAGAGCGCCAGAGGGAGGCCGGTCGGCCGCGGGCGGGCGGGCAG
DENND1A.V4          AGCCTCGAGCGGGCGGGCCCCAGCCTGAGGGAAGGGAGGAAGGGGCGGGGAGAGCGCCAGAGGGAGGCCGGTCGGCCGCGGGCGGGCGGGCAG
DENND1A.V1,3,4_F    ------------------------------------------------------------------------------------------------
DENND1A.V1,3,4_R    ------------------------------------------------------------------------------------------------

DENND1A.V1          CGCAGCGCCGAGCGGGGCCCGCGGGCCCATGAGGAGGCCTGGGGACCATGGGCTCCAGGATCAAgtgagtgcggcc.....gtttcttttgtag
DENND1A.V3          CGCAGCGCCGAGCGGGGCCCGCGGGCCCATGAGGAGGCCTGGGGACCATGGGCTCCAGGATCAA
DENND1A.V4          CGCAGCGCCGAGCGGGGCCCGCGGGCCCATGAGGAGGCCTGGGGACCATGGGCTCCAGGATCAA----------------------------
DENND1A.V1,3,4_F    ------------------------------------------------------------------------------------------------
DENND1A.V1,3,4_R    ------------------------------------------------------------------------------------------------

DENND1A.V1          GCAGAATCCAGAGACCACATTTGAAGTATATGTTGAAGTGGCCTATCCCAGGACAGGTGGCACTCTTTCAGgtacttt.....ttatttacag
DENND1A.V3          GCAGAATCCAGAGACCACATTTGAAGTATATGTTGAAGTGGCCTATCCCAGGACAGGTGGCACTCTTTCAG
DENND1A.V4          ------------------------------------------------------------------------------------------------
DENND1A.V1,3,4_F    ------------------------------------------------------------------------------------------------
DENND1A.V1,3,4_R    ------------------------------------------------------------------------------------------------

DENND1A.V1          ATCCTGAGGTGCAGAGGCAATTCCCGGAGGACTACAGTGACCAGgttcggaatgcgt.....tctttctctccacag
DENND1A.V3          ATCCTGAGGTGCAGAGGCAATTCCCGGAGGACTACAGTGACCAG----------------------------------------------------
DENND1A.V4          ------------------------------------------------------------------------------------------------
DENND1A.V1,3,4_F    ------------------------------------------------------------------------------------------------
DENND1A.V1,3,4_R    ------------------------------------------------------------------------------------------------

DENND1A.V1          GAAGTATCTACAGACTTTGACCAAGTTTTGTTTCCCCTTCTATGTGGACAGgtagtgtcagattttcaaa.....gtagtgtcagattttcaaa
DENND1A.V3          GAAGTATCTACAGACTTTGACCAAGTTTTGTTTCCCCTTCTATGTGGACAG----------------------------------------------
DENND1A.V4          GAAGTATCTACAGACTTTGACCAAGTTTTGTTTCCCCTTCTATGTGGACAG----------------------------------------------
DENND1A.V1,3,4_F    ------------------------------------------------------------------------------------------------
DENND1A.V1,3,4_R    ------------------------------------------------------------------------------------------------

DENND1A.V1          CCTCACAGTTAGCCAAGTTGGCCAGAACTTCACATTCGTGCTCACTGCATTGACAGCAAACAGAGATTCGGGTTCTGCCGCTTATCTTCAGGA
DENND1A.V3          CCTCACAGTTAGCCAAGTTGGCCAGAACTTCACATTCGTGCTCACTGCATTGACAGCAAACAGAGATTCGGGTTCTGCCGCTTATCTTCAGGA
DENND1A.V4          CCTCACAGTTAGCCAAGTTGGCCAGAACTTCACATTCGTGCTCACTGCATTGACAGCAAACAGAGATTCGGGTTCTGCCGCTTATCTTCAGGA
DENND1A.V1,3,4_F    ------------------------------------------------------------------------------------------------
DENND1A.V1,3,4_R    ------------------------------------------------------------------------------------------------

DENND1A.V1          GCGAAGAGCTGCTTCTGTATCTTAAGgtaagggagaaggcttgggctgt.....tttcctcttcttcctccag
DENND1A.V3          GCGAAGAGCTGCTTCTGTATCTTAAG----------------------------------------------------------------------
DENND1A.V4          GCGAAGAGCTGCTTCTGTATCTTAAG----------------------------------------------------------------------
DENND1A.V1,3,4_F    ------------------------------------------------------------------------------------------------
DENND1A.V1,3,4_R    ------------------------------------------------------------------------------------------------
```

Exon 1 Exon 2 Exon 3 Exon 4 Exon 5

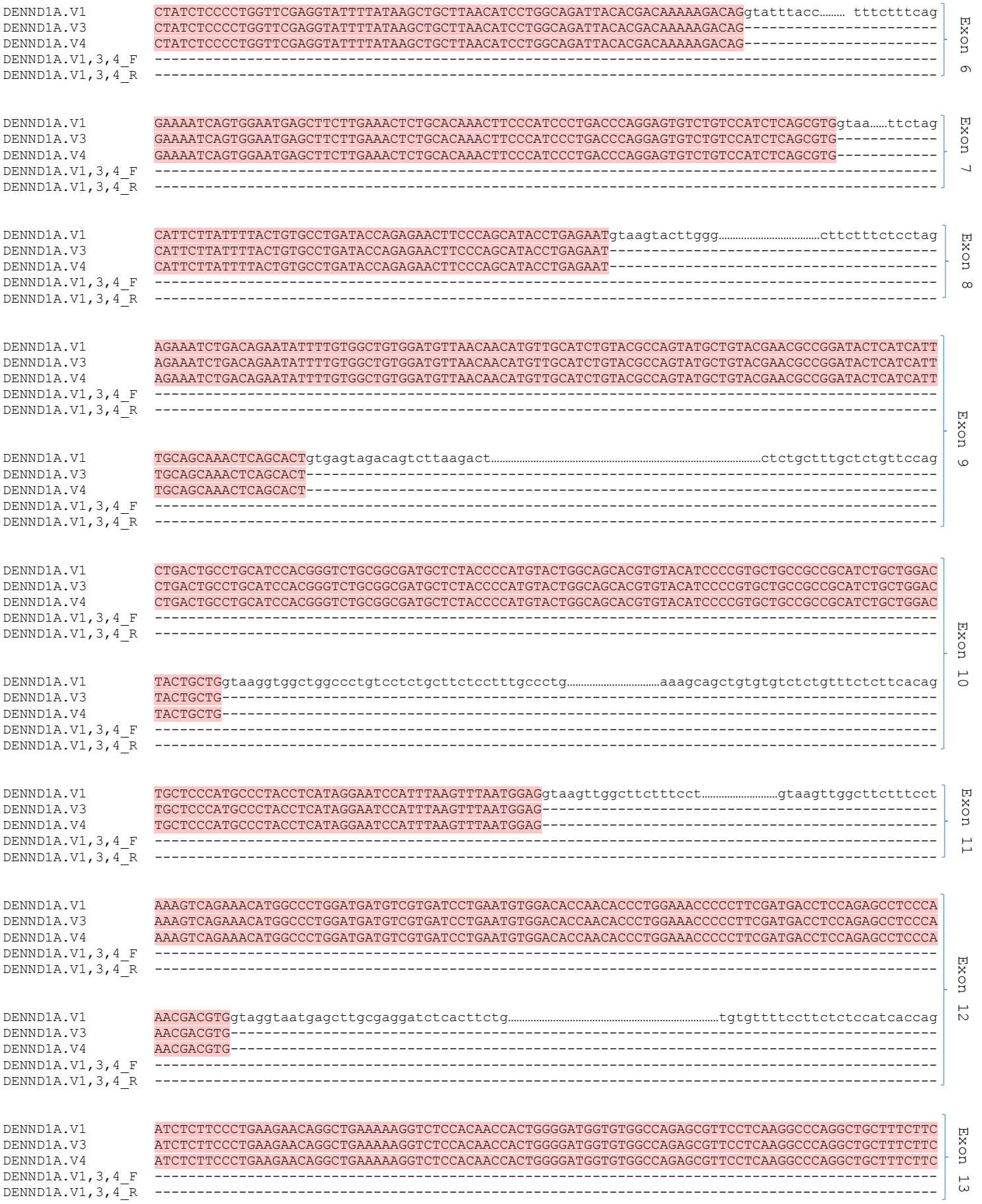
DENND1A.V1 CTATCTCCCCTGGTTCGAGGTATTTTATAAGCTGCTTAACATCCTGGCAGATTACACGACAAAAAGACAGgtatttacc..... tttctttcag
DENND1A.V3 CTATCTCCCCTGGTTCGAGGTATTTTATAAGCTGCTTAACATCCTGGCAGATTACACGACAAAAAGACAG----------
DENND1A.V4 CTATCTCCCCTGGTTCGAGGTATTTTATAAGCTGCTTAACATCCTGGCAGATTACACGACAAAAAGACAG----------
DENND1A.V1,3,4_F ----------
DENND1A.V1,3,4_R ----------
Exon 6
DENND1A.V1 GAAAATCAGTGGAATGAGCTTCTTGAAACTCTGCACAAACTTCCCATCCCTGACCCAGGAGTGTCTGTCCATCTCAGCGTGgtaa.....ttctag
DENND1A.V3 GAAAATCAGTGGAATGAGCTTCTTGAAACTCTGCACAAACTTCCCATCCCTGACCCAGGAGTGTCTGTCCATCTCAGCGTG----------
DENND1A.V4 GAAAATCAGTGGAATGAGCTTCTTGAAACTCTGCACAAACTTCCCATCCCTGACCCAGGAGTGTCTGTCCATCTCAGCGTG----------
DENND1A.V1,3,4_F ----------
DENND1A.V1,3,4_R ----------
Exon 7
DENND1A.V1 CATTCTTATTTTACTGTGCCTGATACCAGAGAACTTCCCAGCATACCTGAGAATgtaagtacttggg.....cttctttctcctag
DENND1A.V3 CATTCTTATTTTACTGTGCCTGATACCAGAGAACTTCCCAGCATACCTGAGAAT----------
DENND1A.V4 CATTCTTATTTTACTGTGCCTGATACCAGAGAACTTCCCAGCATACCTGAGAAT----------
DENND1A.V1,3,4_F ----------
DENND1A.V1,3,4_R ----------
Exon 8
DENND1A.V1 AGAAATCTGACAGAATATTTTGTGGCTGTGGATGTTAACAACATGTTGCATCTGTACGCCAGTATGCTGTACGAACGCCGGATACTCATCATT
DENND1A.V3 AGAAATCTGACAGAATATTTTGTGGCTGTGGATGTTAACAACATGTTGCATCTGTACGCCAGTATGCTGTACGAACGCCGGATACTCATCATT
DENND1A.V4 AGAAATCTGACAGAATATTTTGTGGCTGTGGATGTTAACAACATGTTGCATCTGTACGCCAGTATGCTGTACGAACGCCGGATACTCATCATT
DENND1A.V1,3,4_F ----------
DENND1A.V1,3,4_R ----------
DENND1A.V1 TGCAGCAAACTCAGCACTgtgagtagacagtcttaagact.....ctctgctttgctctgttccag
DENND1A.V3 TGCAGCAAACTCAGCACT----------
DENND1A.V4 TGCAGCAAACTCAGCACT----------
DENND1A.V1,3,4_F ----------
DENND1A.V1,3,4_R ----------
Exon 9
DENND1A.V1 CTGACTGCCTGCATCCACGGGTCTGCGGCGATGCTCTACCCCATGTACTGGCAGCACGTGTACATCCCCGTGCTGCCGCCGCATCTGCTGGAC
DENND1A.V3 CTGACTGCCTGCATCCACGGGTCTGCGGCGATGCTCTACCCCATGTACTGGCAGCACGTGTACATCCCCGTGCTGCCGCCGCATCTGCTGGAC
DENND1A.V4 CTGACTGCCTGCATCCACGGGTCTGCGGCGATGCTCTACCCCATGTACTGGCAGCACGTGTACATCCCCGTGCTGCCGCCGCATCTGCTGGAC
DENND1A.V1,3,4_F ----------
DENND1A.V1,3,4_R ----------
DENND1A.V1 TACTGCTGgtaaggtggctggccctgtcctctgcttctcctttgccctg.....aaagcagctgtgtgtctctgtttctcttcacag
DENND1A.V3 TACTGCTG----------
DENND1A.V4 TACTGCTG----------
DENND1A.V1,3,4_F ----------
DENND1A.V1,3,4_R ----------
Exon 10
DENND1A.V1 TGCTCCCATGCCCTACCTCATAGGAATCCATTTAAGTTTAATGGAGgtaagttggcttctttcct.....gtaagttggcttctttcct
DENND1A.V3 TGCTCCCATGCCCTACCTCATAGGAATCCATTTAAGTTTAATGGAG----------
DENND1A.V4 TGCTCCCATGCCCTACCTCATAGGAATCCATTTAAGTTTAATGGAG----------
DENND1A.V1,3,4_F ----------
DENND1A.V1,3,4_R ----------
Exon 11
DENND1A.V1 AAAGTCAGAAACATGGCCCTGGATGATGTCGTGATCCTGAATGTGGACACCAACACCCTGGAAACCCCCTTCGATGACCTCCAGAGCCTCCCA
DENND1A.V3 AAAGTCAGAAACATGGCCCTGGATGATGTCGTGATCCTGAATGTGGACACCAACACCCTGGAAACCCCCTTCGATGACCTCCAGAGCCTCCCA
DENND1A.V4 AAAGTCAGAAACATGGCCCTGGATGATGTCGTGATCCTGAATGTGGACACCAACACCCTGGAAACCCCCTTCGATGACCTCCAGAGCCTCCCA
DENND1A.V1,3,4_F ----------
DENND1A.V1,3,4_R ----------
DENND1A.V1 AACGACGTGgtaggtaatgagcttgcgaggatctcacttctg.....tgtgttttccttctctccatcaccag
DENND1A.V3 AACGACGTG----------
DENND1A.V4 AACGACGTG----------
DENND1A.V1,3,4_F ----------
DENND1A.V1,3,4_R ----------
Exon 12
DENND1A.V1 ATCTCTTCCCTGAAGAACAGGCTGAAAAAGGTCTCCACAACCACTGGGGATGGTGTGGCCAGAGCGTTCCTCAAGGCCCAGGCTGCTTTCTTC
DENND1A.V3 ATCTCTTCCCTGAAGAACAGGCTGAAAAAGGTCTCCACAACCACTGGGGATGGTGTGGCCAGAGCGTTCCTCAAGGCCCAGGCTGCTTTCTTC
DENND1A.V4 ATCTCTTCCCTGAAGAACAGGCTGAAAAAGGTCTCCACAACCACTGGGGATGGTGTGGCCAGAGCGTTCCTCAAGGCCCAGGCTGCTTTCTTC
DENND1A.V1,3,4_F ----------
DENND1A.V1,3,4_R ----------
Exon 13

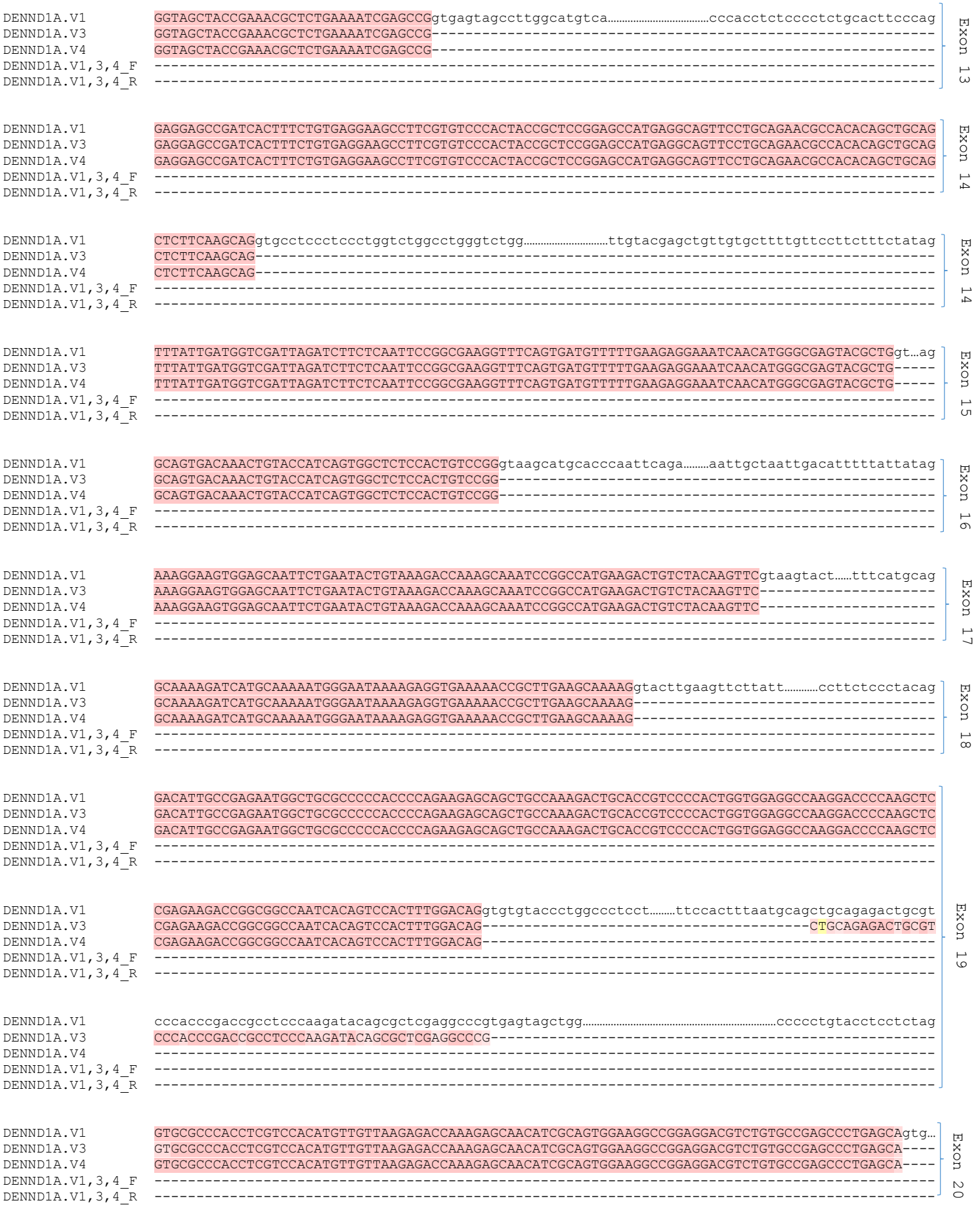
DENND1A.V1
DENND1A.V3
DENND1A.V4
DENND1A.V1,3,4_F
DENND1A.V1,3,4_R
Exon 13
Exon 14
Exon 14
Exon 15
Exon 16
Exon 17
Exon 18
Exon 19
Exon 20


DENND1A.V1 ccccagcctggtaaagcccttgcgacactatgcggtcttcctctccgaagactcctctgatgatgaatgccagcgggaagagggcccgagctc
DENND1A.V3 ------CCTGGTAAAGCCCTTGCGACACTATGCGGTCTTCCTCTCCGAAGACTCCTCTGATGATGAATGCCAGCGGGAAGAGGGCCCGAGCTC
DENND1A.V4 ------CCTGGTAAAGCCCTTGCGACACTATGCGGTCTTCCTCTCCGAAGACTCCTCTGATGATGAATGCCAGCGGGAAGAGGGCCCGAGCTC
DENND1A.V1,3,4_F ----------
DENND1A.V1,3,4_R ----------
Exon 20
DENND1A.V1 tggcttcaccgagagctttttcttctccgctccctttgaatggtctctccttcc……cctgctctgtccccgacag
DENND1A.V3 TGGCTTCACCGAGAGCTTTTTCTTCTCCGCTCCCTTTGAATGG----------
DENND1A.V4 TGGCTTCACCGAGAGCTTTTTCTTCTCCGCTCCCTTTGAATGG----------
DENND1A.V1,3,4_F ----------
DENND1A.V1,3,4_R ----------
DENND1A.V1 GCCGCAGCCGTATCGGACACTCAGGGAGTCAGACAGCGCGGAAGGCGACGAGGCAGAGAGTCCAGAGCAGCAAGTGCGGAAGTCCACAGGCCC
DENND1A.V3 GCCGCAGCCGTATCGGACACTCAGGGAGTCAGACAGCGCGGAAGGCGACGAGGCAGAGAGTCCAGAGCAGCAAGTGCGGAAGTCCACAGGCCC
DENND1A.V4 GCCGCAGCCGTATCGGACACTCAGGGAGTCAGACAGCGCGGAAGGCGACGAGGCAGAGAGTCCAGAGCAGCAAGTGCGGAAGTCCACAGGCCC
DENND1A.V1,3,4_F ----------
DENND1A.V1,3,4_R ----------
Exon 21
DENND1A.V1 TGTCCCAGCTCCCCCTGACCGGGCTGCCAGCATCGACCTTCTGGAAGACGTCTTCAGCAACCTGGACATGGAGGCCGCACTGCAGCCACTGGG
DENND1A.V3 TGTCCCAGCTCCCCCTGACCGGGCTGCCAGCATCGACCTTCTGGAAGACGTCTTCAGCAACCTGGACATGGAGGCCGCACTGCAGCCACTGGG
DENND1A.V4 TGTCCCAGCTCCCCCTGACCGGGCTGCCAGCATCGACCTTCTGGAAGACGTCTTCAGCAACCTGGACATGGAGGCCGCACTGCAGCCACTGGG
DENND1A.V1,3,4_F ----------
DENND1A.V1,3,4_R ----------
DENND1A.V1 CCAGGCCAAGAGCTTAGAGGACCTTCGTGCCCCCAAAGACCTGAGGGAGCAGCCAGGGACCTTTGACTATCAGgtatggc……ccaacag
DENND1A.V3 CCAGGCCAAGAGCTTAGAGGACCTTCGTGCCCCCAAAGACCTGAGGGAGCAGCCAGGGACCTTTGACTATCAG----------
DENND1A.V4 CCAGGCCAAGAGCTTAGAGGACCTTCGTGCCCCCAAAGACCTGAGGGAGCAGCCAGGGACCTTTGACTATCAG----------
DENND1A.V1,3,4_F ----------CAGCCAGGGACCTTTGACTA----------
DENND1A.V1,3,4_R ----------
Exon 21
DENND1A.V1 AGGCTGGATCTGGGCGGGAGTGAGAGGAGCCGCGGGGTGACAGTGGCCTTGAAGCTTACCCACCCGTACAACAAGCTCTGGAGCCTGGGCCAG
DENND1A.V3 AGGCTGGATCTGGGCGGGAGTGAGAGGAGCCGCGGGGTGACAGTGGCCTTGAAGCTTACCCACCCGTACAACAAGCTCTGGAGCCTGGGCCAG
DENND1A.V4 AGGCTGGATCTGGGCGGGAGTGAGAGGAGCCGCGGGGTGACAGTGGCCTTGAAGCTTACCCACCCGTACAACAAGCTCTGGAGCCTGGGCCAG
DENND1A.V1,3,4_F ----------
DENND1A.V1,3,4_R ----------CACCCGTACAACAAGCTCTG----------
DENND1A.V1 GACGACATGGCCATCCCCAGCAAGCCCCCAGCTGCCTCCCCTGAGAAGCCCTCGGCCCTGCTCGGGAACTCCCTGGCCCTGCCTCGAAGGCCC
DENND1A.V3 GACGACATGGCCATCCCCAGCAAGCCCCCAGCTGCCTCCCCTGAGAAGCCCTCGGCCCTGCTCGGGAACTCCCTGGCCCTGCCTCGAAGGCCC
DENND1A.V4 GACGACATGGCCATCCCCAGCAAGCCCCCAGCTGCCTCCCCTGAGAAGCCCTCGGCCCTGCTCGGGAACTCCCTGGCCCTGCCTCGAAGGCCC
DENND1A.V1,3,4_F ----------
DENND1A.V1,3,4_R ----------
DENND1A.V1 CAGAACCGGGACAGCATCCTGAACCCCAGTGACAAGGAGGAGGTGCCCACCCCTACTCTGGGCAGCATCACCATCCCCCGGCCCCAAGGCAG
DENND1A.V3 CAGAACCGGGACAGCATCCTGAACCCCAGTGACAAGGAGGAGGTGCCCACCCCTACTCTGGGCAGCATCACCATCCCCCGGCCCCAAGGCAG
DENND1A.V4 CAGAACCGGGACAGCATCCTGAACCCCAGTGACAAGGAGGAGGTGCCCACCCCTACTCTGGGCAGCATCACCATCCCCCGGCCCCAAGGCAG
DENND1A.V1,3,4_F ----------
DENND1A.V1,3,4_R ----------
Exon 22
DENND1A.V1 GAAGACCCCAGAGCTGGGCATCGTGCCTCCACCGCCCATTCCCCGCCCGGCCAAGCTCCAGGCTGCCGGCGCCGCACTTGGTGACGTCTCAGA
DENND1A.V3 GAAGACCCCAGAGCTGGGCATCGTGCCTCCACCGCCCATTCCCCGCCCGGCCAAGCTCCAGGCTGCCGGCGCCGCACTTGGTGACGTCTCAGA
DENND1A.V4 GAAGACCCCAGAGCTGGGCATCGTGCCTCCACCGCCCATTCCCCGCCCGGCCAAGCTCCAGGCTGCCGGCGCCGCACTTGGTGACGTCTCAGA
DENND1A.V1,3,4_F ----------
DENND1A.V1,3,4_R ----------
DENND1A.V1 GCGGCTGCAGACGGATCGGGACAGGCGAGCTGCCCTGAGTCCAGGGCTCCTGCCTGGTGTTGTCCCCCAAGGCCCCACTGAACTGCTCCAGCC
DENND1A.V3 GCGGCTGCAGACGGATCGGGACAGGCGAGCTGCCCTGAGTCCAGGGCTCCTGCCTGGTGTTGTCCCCCAAGGCCCCACTGAACTGCTCCAGCC
DENND1A.V4 GCGGCTGCAGACGGATCGGGACAGGCGAGCTGCCCTGAGTCCAGGGCTCCTGCCTGGTGTTGTCCCCCAAGGCCCCACTGAACTGCTCCAGCC
DENND1A.V1,3,4_F ----------
DENND1A.V1,3,4_R ----------
DENND1A.V1 GCTCAGCCCTGGCCCCGGGGCTGCAGGCACGAGCAGTGACGCCCTGCTCGCCCTCCTGGACCCGCTCAGCACAGCCTGGTCAGGCAGCACCCT
DENND1A.V3 GCTCAGCCCTGGCCCCGGGGCTGCAGGCACGAGCAGTGACGCCCTGCTCGCCCTCCTGGACCCGCTCAGCACAGCCTGGTCAGGCAGCACCCT
DENND1A.V4 GCTCAGCCCTGGCCCCGGGGCTGCAGGCACGAGCAGTGACGCCCTGCTCGCCCTCCTGGACCCGCTCAGCACAGCCTGGTCAGGCAGCACCC
DENND1A.V1,3,4_F ----------
DENND1A.V1,3,4_R ----------


DENND1A.V1 CCCGTCACGCCCCGCCACCCCGAATGTAGCCACCCCATTCACCCCCCAATTCAGCTTCCCCCCTGCAGGGACACCCACCCCATTCCCACAGCC
DENND1A.V3 CCCGTCACGCCCCGCCACCCCGAATGTAGCCACCCCATTCACCCCCCAATTCAGCTTCCCCCCTGCAGGGACACCCACCCCATTCCCACAGCC
DENND1A.V4 CCCGTCACGCCCCGCCACCCCGAATGTAGCCACCCCATTCACCCCCCAATTCAGCTTCCCCCCTGCAGGGACACCCACCCCATTCCCACAGCC
DENND1A.V1,3,4_F ----------
DENND1A.V1,3,4_R ----------
DENND1A.V1 ACCACTCAACCCCTTTGTCCCATCCATGCCAGCAGCCCCACCCACCCTGCCCCTGGTCTCCACACCAGCCGGGCCTTTCGGGGCCCCTCCAGC
DENND1A.V3 ACCACTCAACCCCTTTGTCCCATCCATGCCAGCAGCCCCACCCACCCTGCCCCTGGTCTCCACACCAGCCGGGCCTTTCGGGGCCCCTCCAGC
DENND1A.V4 ACCACTCAACCCCTTTGTCCCATCCATGCCAGCAGCCCCACCCACCCTGCCCCTGGTCTCCACACCAGCCGGGCCTTTCGGGGCCCCTCCAGC
DENND1A.V1,3,4_F ----------
DENND1A.V1,3,4_R ----------
DENND1A.V1 TTCCCTGGGGCCGGCTTTTGCGTCCGGCCTCCTGCTGTCCAGTGCTGGCTTCTGTGCCCCTCACAGGTCTCAGCCCAACCTCTCCGCCCTCTC
DENND1A.V3 TTCCCTGGGGCCGGCTTTTGCGTCCGGCCTCCTGCTGTCCAGTGCTGGCTTCTGTGCCCCTCACAGGTCTCAGCCCAACCTCTCCGCCCTCTC
DENND1A.V4 TTCCCTGGGGCCGGCTTTTGCGTCCGGCCTCCTGCTGTCCAGTGCTGGCTTCTGTGCCCCTCACAGGTCTCAGCCCAACCTCTCCGCCCTCTC
DENND1A.V1,3,4_F ----------
DENND1A.V1,3,4_R ----------
DENND1A.V1 CATGCCCAACCTCTTTGGCCAGATGCCCATGGGCACCCACACGAGCCCCCTACAGCCGCTGGGTCCCCCAGCAGTTGCCCCGTCGAGGATCCG
DENND1A.V3 CATGCCCAACCTCTTTGGCCAGATGCCCATGGGCACCCACACGAGCCCCCTACAGCCGCTGGGTCCCCCAGCAGTTGCCCCGTCGAGGATCCG
DENND1A.V4 CATGCCCAACCTCTTTGGCCAGATGCCCATGGGCACCCACACGAGCCCCCTACAGCCGCTGGGTCCCCCAGCAGTTGCCCCGTCGAGGATCCG
DENND1A.V1,3,4_F ----------
DENND1A.V1,3,4_R ----------
DENND1A.V1 AACGTTGCCCCTGGCCCGCTCAAGTGCCAGGGCTGCTGAGACCAAGCAGGGGCTGGCCCTGAGGCCTGGAGACCCCCCGCTTCTGCCTCCCAG
DENND1A.V3 AACGTTGCCCCTGGCCCGCTCAAGTGCCAGGGCTGCTGAGACCAAGCAGGGGCTGGCCCTGAGGCCTGGAGACCCCCCGCTTCTGCCTCCCAG
DENND1A.V4 AACGTTGCCCCTGGCCCGCTCAAGTGCCAGGGCTGCTGAGACCAAGCAGGGGCTGGCCCTGAGGCCTGGAGACCCCCCGCTTCTGCCTCCCAG
DENND1A.V1,3,4_F ----------
DENND1A.V1,3,4_R ----------
DENND1A.V1 GCCCCCTCAAGGCCTGGAGCCAACACTGCAGCCCTCTGCTCCTCAACAGGCCAGAGACCCCTTTGAGGATTTGTTACAGAAAACCAAGCAAGA
DENND1A.V3 GCCCCCTCAAGGCCTGGAGCCAACACTGCAGCCCTCTGCTCCTCAACAGGCCAGAGACCCCTTTGAGGATTTGTTACAGAAAACCAAGCAAGA
DENND1A.V4 GCCCCCTCAAGGCCTGGAGCCAACACTGCAGCCCTCTGCTCCTCAACAGGCCAGAGACCCCTTTGAGGATTTGTTACAGAAAACCAAGCAAGA
DENND1A.V1,3,4_F ----------
DENND1A.V1,3,4_R ----------
DENND1A.V1 CGTGAGCCCGAGTCCGGCCCTGGCCCCGGCCCCAGACTCGGTGGAGCAGCTCAGGAAGCAGTGGGAGACCTTCGAGTGAGCCGGGCCCTGAGG
DENND1A.V3 CGTGAGCCCGAGTCCGGCCCTGGCCCCGGCCCCAGACTCGGTGGAGCAGCTCAGGAAGCAGTGGGAGACCTTCGAGTGAGCCGGGCCCTGAGG
DENND1A.V4 CGTGAGCCCGAGTCCGGCCCTGGCCCCGGCCCCAGACTCGGTGGAGCAGCTCAGGAAGCAGTGGGAGACCTTCGAGTGAGCCGGGCCCTGAGG
DENND1A.V1,3,4_F ----------
DENND1A.V1,3,4_R ----------
DENND1A.V1 GTGGGGGATGCACCGAGGCCCGAGGGTCCGTCCACTGCTGCGGTTCCGAGGCTCCCCCGCCACTCTCTCTCTGCCCAGGTTCTGCTGGTGGGA
DENND1A.V3 GTGGGGGATGCACCGAGGCCCGAGGGTCCGTCCACTGCTGCGGTTCCGAGGCTCCCCCGCCACTCTCTCTCTGCCCAGGTTCTGCTGGTGGGA
DENND1A.V4 GTGGGGGATGCACCGAGGCCCGAGGGTCCGTCCACTGCTGCGGTTCCGAGGCTCCCCCGCCACTCTCTCTCTGCCCAGGTTCTGCTGGTGGGA
DENND1A.V1,3,4_F ----------
DENND1A.V1,3,4_R ----------
DENND1A.V1 AGGGATGGGACCCCTCTCTGCTGCCCCCTCCTCCCCTCCACACTGCCCATCTCTGATGTCTGGCCCTGGGGAATGGCACCAGTTCCAGCCTGG
DENND1A.V3 AGGGATGGGACCCCTCTCTGCTGCCCCCTCCTCCCCTCCACACTGCCCATCTCTGATGTCTGGCCCTGGGGAATGGCACCAGTTCCAGCCTGG
DENND1A.V4 AGGGATGGGACCCCTCTCTGCTGCCCCCTCCTCCCCTCCACACTGCCCATCTCTGATGTCTGGCCCTGGGGAATGGCACCAGTTCCAGCCTGG
DENND1A.V1,3,4_F ----------
DENND1A.V1,3,4_R ----------
DENND1A.V1 GAATCAACCCAGTTCCTGAGTGCCCATCCCACCCCGCGGTTGCCTCTCCTCGGCACCCTTGATTGGGTTTTGCACTAAAGAGGTCAGCTGGGC
DENND1A.V3 GAATCAACCCAGTTCCTGAGTGCCCATCCCACCCCGCGGTTGCCTCTCCTCGGCACCCTTGATTGGGTTTTGCACTAAAGAGGTCAGCTGGGC
DENND1A.V4 GAATCAACCCAGTTCCTGAGTGCCCATCCCACCCCGCGGTTGCCTCTCCTCGGCACCCTTGATTGGGTTTTGCACTAAAGAGGTCAGCTGGGC
DENND1A.V1,3,4_F ----------
DENND1A.V1,3,4_R ----------
DENND1A.V1 CAATGATATTGCTCCAGACCGAGTCCTACCCACCTTCCCCCGGAAGTGTCCCAAGAGGCTCCGAAGGCCTCCCCTCCGAGCCCAGCTCTCCTG
DENND1A.V3 CAATGATATTGCTCCAGACCGAGTCCTACCCACCTTCCCCCGGAAGTGTCCCAAGAGGCTCCGAAGGCCTCCCCTCCGAGCCCAGCTCTCCTG
DENND1A.V4 CAATGATATTGCTCCAGACCGAGTCCTACCCACCTTCCCCCGGAAGTGTCCCAAGAGGCTCCGAAGGCCTCCCCTCCGAGCCCAGCTCTCCTG
DENND1A.V1,3,4_F ----------
DENND1A.V1,3,4_R ----------
Exon 22

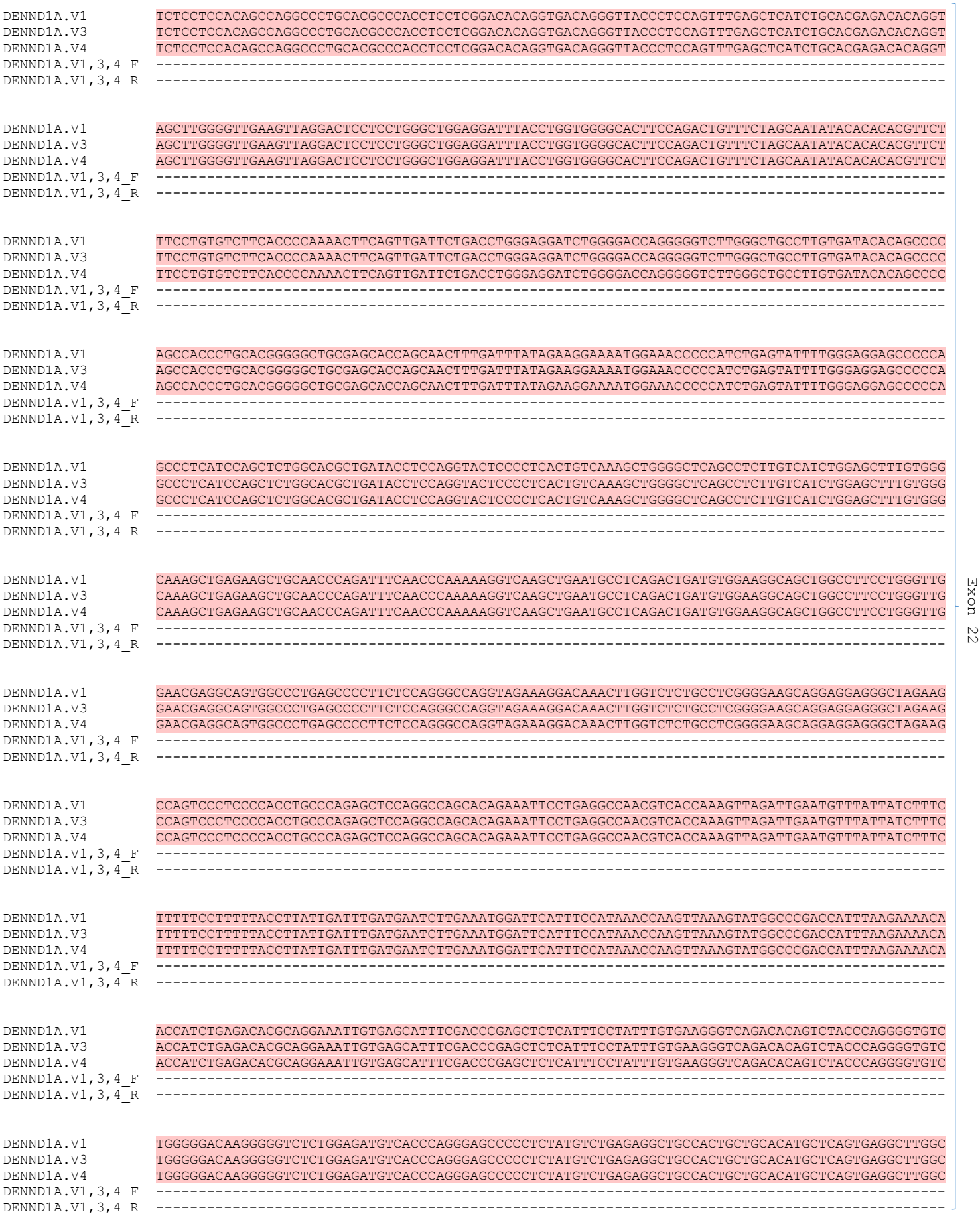
DENND1A.V1 TCTCCTCCACAGCCAGGCCCTGCACGCCCACCTCCTCGGACACAGGTGACAGGGTTACCCTCCAGTTTGAGCTCATCTGCACGAGACACAGGT
DENND1A.V3 TCTCCTCCACAGCCAGGCCCTGCACGCCCACCTCCTCGGACACAGGTGACAGGGTTACCCTCCAGTTTGAGCTCATCTGCACGAGACACAGGT
DENND1A.V4 TCTCCTCCACAGCCAGGCCCTGCACGCCCACCTCCTCGGACACAGGTGACAGGGTTACCCTCCAGTTTGAGCTCATCTGCACGAGACACAGGT
DENND1A.V1,3,4_F ----------
DENND1A.V1,3,4_R ----------
DENND1A.V1 AGCTTGGGGTTGAAGTTAGGACTCCTCCTGGGCTGGAGGATTTACCTGGTGGGGCACTTCCAGACTGTTTCTAGCAATATACACACACGTTCT
DENND1A.V3 AGCTTGGGGTTGAAGTTAGGACTCCTCCTGGGCTGGAGGATTTACCTGGTGGGGCACTTCCAGACTGTTTCTAGCAATATACACACACGTTCT
DENND1A.V4 AGCTTGGGGTTGAAGTTAGGACTCCTCCTGGGCTGGAGGATTTACCTGGTGGGGCACTTCCAGACTGTTTCTAGCAATATACACACACGTTCT
DENND1A.V1,3,4_F ----------
DENND1A.V1,3,4_R ----------
DENND1A.V1 TTCCTGTGTCTTCACCCCAAAACTTCAGTTGATTCTGACCTGGGAGGATCTGGGGACCAGGGGGTCTTGGGCTGCCTTGTGATACACAGCCCC
DENND1A.V3 TTCCTGTGTCTTCACCCCAAAACTTCAGTTGATTCTGACCTGGGAGGATCTGGGGACCAGGGGGTCTTGGGCTGCCTTGTGATACACAGCCCC
DENND1A.V4 TTCCTGTGTCTTCACCCCAAAACTTCAGTTGATTCTGACCTGGGAGGATCTGGGGACCAGGGGGTCTTGGGCTGCCTTGTGATACACAGCCCC
DENND1A.V1,3,4_F ----------
DENND1A.V1,3,4_R ----------
DENND1A.V1 AGCCACCCTGCACGGGGGCTGCGAGCACCAGCAACTTTGATTTATAGAAGGAAAATGGAAACCCCCATCTGAGTATTTTGGGAGGAGCCCCCA
DENND1A.V3 AGCCACCCTGCACGGGGGCTGCGAGCACCAGCAACTTTGATTTATAGAAGGAAAATGGAAACCCCCATCTGAGTATTTTGGGAGGAGCCCCCA
DENND1A.V4 AGCCACCCTGCACGGGGGCTGCGAGCACCAGCAACTTTGATTTATAGAAGGAAAATGGAAACCCCCATCTGAGTATTTTGGGAGGAGCCCCCA
DENND1A.V1,3,4_F ----------
DENND1A.V1,3,4_R ----------
DENND1A.V1 GCCCTCATCCAGCTCTGGCACGCTGATACCTCCAGGTACTCCCCTCACTGTCAAAGCTGGGGCTCAGCCTCTTGTCATCTGGAGCTTTGTGGG
DENND1A.V3 GCCCTCATCCAGCTCTGGCACGCTGATACCTCCAGGTACTCCCCTCACTGTCAAAGCTGGGGCTCAGCCTCTTGTCATCTGGAGCTTTGTGGG
DENND1A.V4 GCCCTCATCCAGCTCTGGCACGCTGATACCTCCAGGTACTCCCCTCACTGTCAAAGCTGGGGCTCAGCCTCTTGTCATCTGGAGCTTTGTGGG
DENND1A.V1,3,4_F ----------
DENND1A.V1,3,4_R ----------
DENND1A.V1 CAAAGCTGAGAAGCTGCAACCCAGATTTCAACCCAAAAAGGTCAAGCTGAATGCCTCAGACTGATGTGGAAGGCAGCTGGCCTTCCTGGGTTG
DENND1A.V3 CAAAGCTGAGAAGCTGCAACCCAGATTTCAACCCAAAAAGGTCAAGCTGAATGCCTCAGACTGATGTGGAAGGCAGCTGGCCTTCCTGGGTTG
DENND1A.V4 CAAAGCTGAGAAGCTGCAACCCAGATTTCAACCCAAAAAGGTCAAGCTGAATGCCTCAGACTGATGTGGAAGGCAGCTGGCCTTCCTGGGTTG
DENND1A.V1,3,4_F ----------
DENND1A.V1,3,4_R ----------
DENND1A.V1 GAACGAGGCAGTGGCCCTGAGCCCCTTCTCCAGGGCCAGGTAGAAAGGACAAACTTGGTCTCTGCCTCGGGGAAGCAGGAGGAGGGCTAGAAG
DENND1A.V3 GAACGAGGCAGTGGCCCTGAGCCCCTTCTCCAGGGCCAGGTAGAAAGGACAAACTTGGTCTCTGCCTCGGGGAAGCAGGAGGAGGGCTAGAAG
DENND1A.V4 GAACGAGGCAGTGGCCCTGAGCCCCTTCTCCAGGGCCAGGTAGAAAGGACAAACTTGGTCTCTGCCTCGGGGAAGCAGGAGGAGGGCTAGAAG
DENND1A.V1,3,4_F ----------
DENND1A.V1,3,4_R ----------
DENND1A.V1 CCAGTCCCTCCCCACCTGCCCAGAGCTCCAGGCCAGCACAGAAATTCCTGAGGCCAACGTCACCAAAGTTAGATTGAATGTTTATTATCTTTC
DENND1A.V3 CCAGTCCCTCCCCACCTGCCCAGAGCTCCAGGCCAGCACAGAAATTCCTGAGGCCAACGTCACCAAAGTTAGATTGAATGTTTATTATCTTTC
DENND1A.V4 CCAGTCCCTCCCCACCTGCCCAGAGCTCCAGGCCAGCACAGAAATTCCTGAGGCCAACGTCACCAAAGTTAGATTGAATGTTTATTATCTTTC
DENND1A.V1,3,4_F ----------
DENND1A.V1,3,4_R ----------
DENND1A.V1 TTTTTCCTTTTTACCTTATTGATTTGATGAATCTTGAAATGGATTCATTTCCATAAACCAAGTTAAAGTATGGCCCGACCATTTAAGAAAACA
DENND1A.V3 TTTTTCCTTTTTACCTTATTGATTTGATGAATCTTGAAATGGATTCATTTCCATAAACCAAGTTAAAGTATGGCCCGACCATTTAAGAAAACA
DENND1A.V4 TTTTTCCTTTTTACCTTATTGATTTGATGAATCTTGAAATGGATTCATTTCCATAAACCAAGTTAAAGTATGGCCCGACCATTTAAGAAAACA
DENND1A.V1,3,4_F ----------
DENND1A.V1,3,4_R ----------
DENND1A.V1 ACCATCTGAGACACGCAGGAAATTGTGAGCATTTCGACCCGAGCTCTCATTTCCTATTTGTGAAGGGTCAGACACAGTCTACCCAGGGGTGTC
DENND1A.V3 ACCATCTGAGACACGCAGGAAATTGTGAGCATTTCGACCCGAGCTCTCATTTCCTATTTGTGAAGGGTCAGACACAGTCTACCCAGGGGTGTC
DENND1A.V4 ACCATCTGAGACACGCAGGAAATTGTGAGCATTTCGACCCGAGCTCTCATTTCCTATTTGTGAAGGGTCAGACACAGTCTACCCAGGGGTGTC
DENND1A.V1,3,4_F ----------
DENND1A.V1,3,4_R ----------
DENND1A.V1 TGGGGGACAAGGGGGTCTCTGGAGATGTCACCCAGGGAGCCCCCTCTATGTCTGAGAGGCTGCCACTGCTGCACATGCTCAGTGAGGCTTGGC
DENND1A.V3 TGGGGGACAAGGGGGTCTCTGGAGATGTCACCCAGGGAGCCCCCTCTATGTCTGAGAGGCTGCCACTGCTGCACATGCTCAGTGAGGCTTGGC
DENND1A.V4 TGGGGGACAAGGGGGTCTCTGGAGATGTCACCCAGGGAGCCCCCTCTATGTCTGAGAGGCTGCCACTGCTGCACATGCTCAGTGAGGCTTGGC
DENND1A.V1,3,4_F ----------
DENND1A.V1,3,4_R ----------
Exon 22


DENND1A.V1 GGCCATCCTGGCACATGGCTCTTCCTGGGTCAACCGTGACCTGTCTGGCTCAGGAATGGGCTCTGGCTGCTGGGGGAGCCGTGTCACTCCTGG
DENND1A.V3 GGCCATCCTGGCACATGGCTCTTCCTGGGTCAACCGTGACCTGTCTGGCTCAGGAATGGGCTCTGGCTGCTGGGGGAGCCGTGTCACTCCTGG
DENND1A.V4 GGCCATCCTGGCACATGGCTCTTCCTGGGTCAACCGTGACCTGTCTGGCTCAGGAATGGGCTCTGGCTGCTGGGGGAGCCGTGTCACTCCTGG
DENND1A.V1,3,4_F ----------
DENND1A.V1,3,4_R ----------
DENND1A.V1 GCCATGGGGGCACCTCCTGGGCACTTAGGTGTTTCAGCATAGATTCCAGTTTCGCACCCTGGGCAGACCCCCAGGCCCCATCCGGGATAGGGC
DENND1A.V3 GCCATGGGGGCACCTCCTGGGCACTTAGGTGTTTCAGCATAGATTCCAGTTTCGCACCCTGGGCAGACCCCCAGGCCCCATCCGGGATAGGGC
DENND1A.V4 GCCATGGGGGCACCTCCTGGGCACTTAGGTGTTTCAGCATAGATTCCAGTTTCGCACCCTGGGCAGACCCCCAGGCCCCATCCGGGATAGGGC
DENND1A.V1,3,4_F ----------
DENND1A.V1,3,4_R ----------
DENND1A.V1 AGAGGAGGTGCTGGCGGCCCCAGGGAAGGAGGGTGTGTACCCCAAGGCCCCCTGGCTGTGCTGAGGGGCTGGGGTGAGCGCTCCATGTTCACA
DENND1A.V3 AGAGGAGGTGCTGGCGGCCCCAGGGAAGGAGGGTGTGTACCCCAAGGCCCCCTGGCTGTGCTGAGGGGCTGGGGTGAGCGCTCCATGTTCACA
DENND1A.V4 AGAGGAGGTGCTGGCGGCCCCAGGGAAGGAGGGTGTGTACCCCAAGGCCCCCTGGCTGTGCTGAGGGGCTGGGGTGAGCGCTCCATGTTCACA
DENND1A.V1,3,4_F ----------
DENND1A.V1,3,4_R ----------
DENND1A.V1 TGAGCACTGCTGCCTCTTCACTTGTGGGACTTTTTGCAAACCCAAGGATGAACTTTGTGTGCATTCAATAAAATCATCTTGGGGAAGAGG
DENND1A.V3 TGAGCACTGCTGCCTCTTCACTTGTGGGACTTTTTGCAAACCCAAGGATGAACTTTGTGTGCATTCAATAAAATCATCTTGGGGAAGAGG
DENND1A.V4 TGAGCACTGCTGCCTCTTCACTTGTGGGACTTTTTGCAAACCCAAGGATGAACTTTGTGTGCATTCAATAAAATCATCTTGGGGAAGAGG
DENND1A.V1,3,4_F ----------
DENND1A.V1,3,4_R ----------
Exon 22

Supplemental Fig. S4. Alignment of human *DENND1A.V2*; bovine *DENND1A*; and predicted bovine *DENND1A.V2* primer sequences. Alignment was generated with CLUSTAL multiple sequence alignment by Kalign (2.0) based on sequences available at Ensembl Asia with transcript ID: human *DENND1A.V2* (ENST00000373620.7) and bovine *DENND1A* (ENSBTAG00000003610). Uppercase letters represent the exons, whereas lowercase letters represent the introns and only the sequence encompassing the exons is shown. Highlighted areas represent the primer sequences. ..... represent areas of intronic sequence that are not illustrated in order to reduce the size of this file.

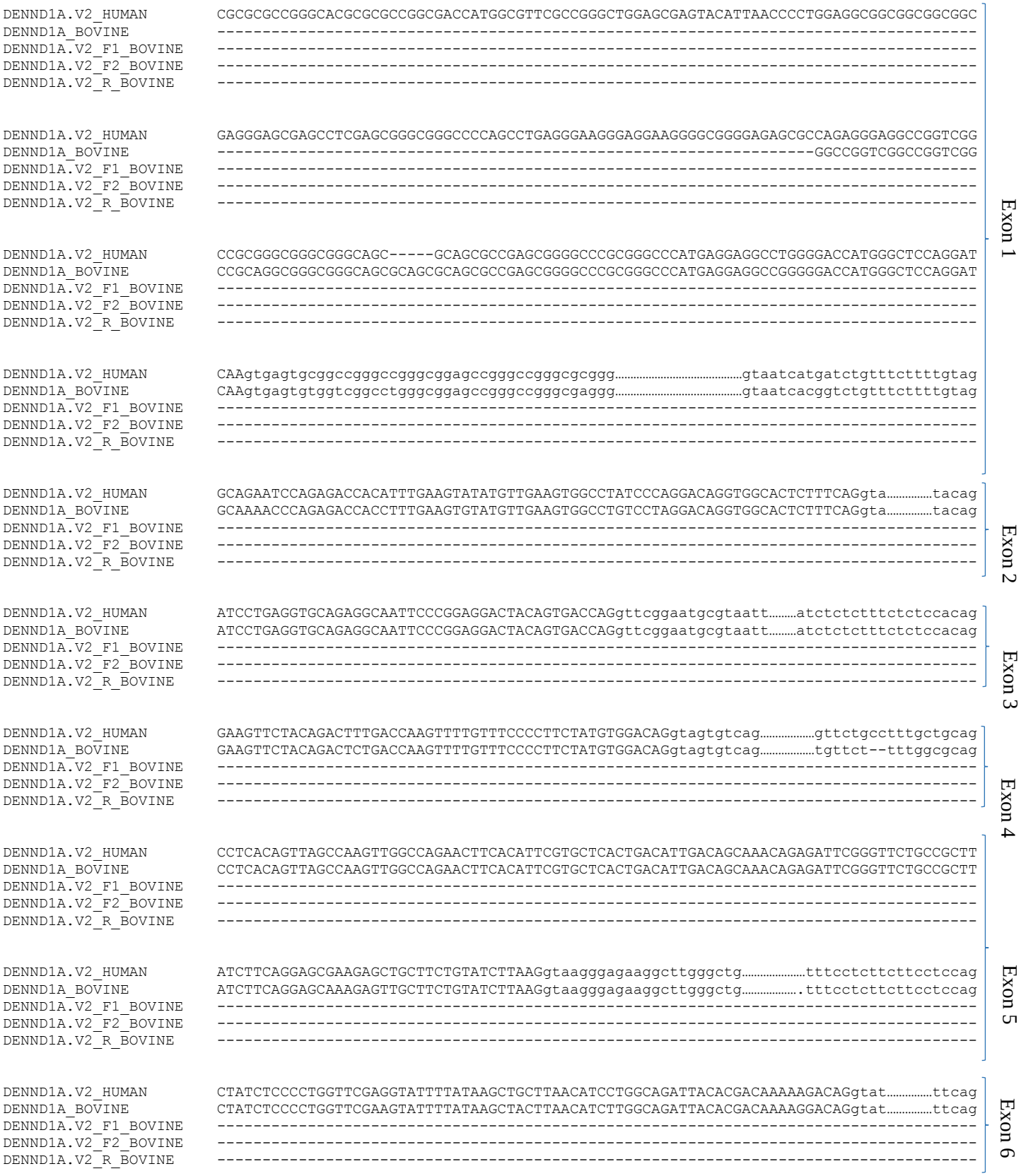

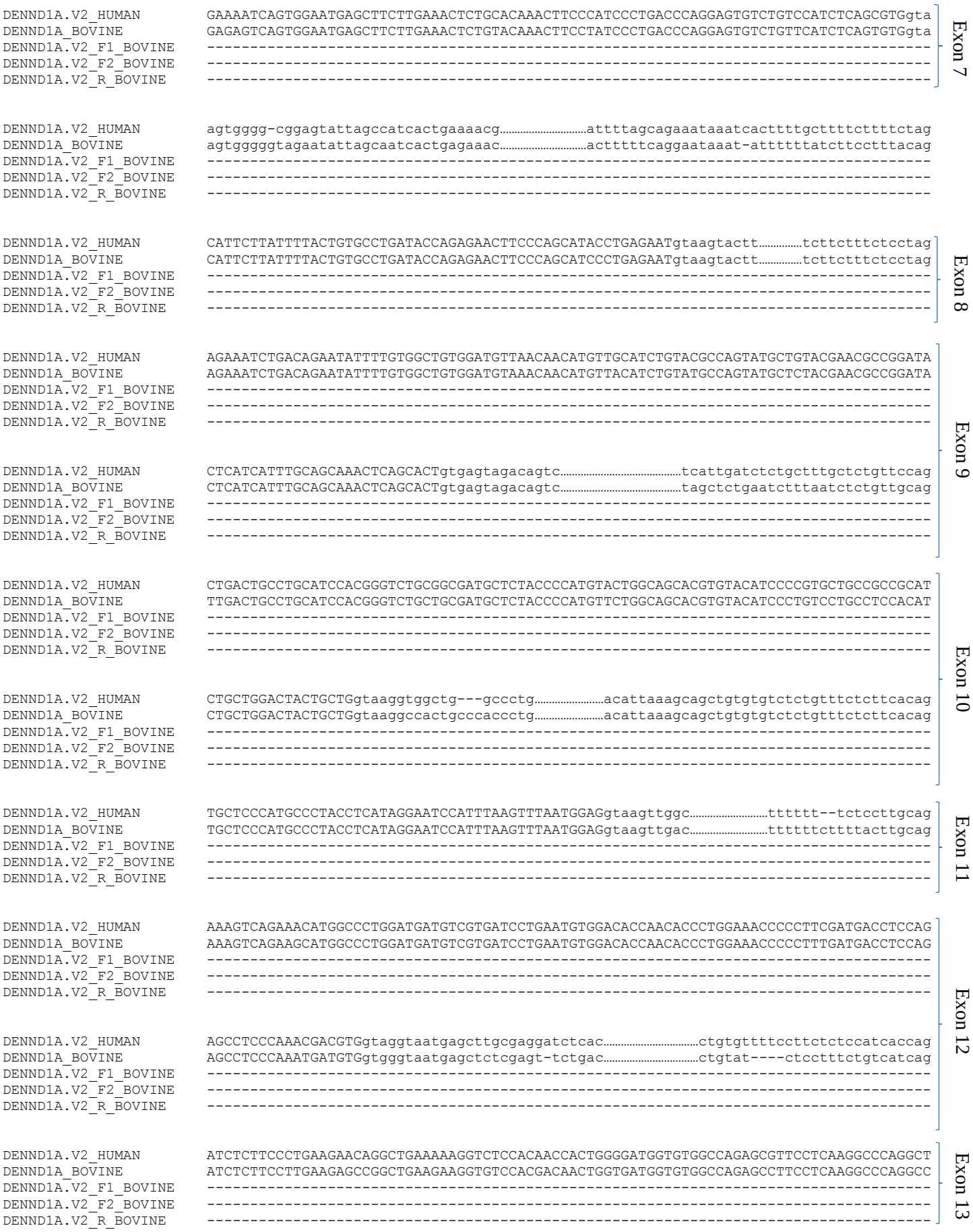
DENND1A.V2_HUMAN GAAAATCAGTGGAATGAGCTTCTTGAAACTCTGCACAAACTTCCCATCCCTGACCCAGGAGTGTCTGTCCATCTCAGCGTGgta
DENND1A_BOVINE GAGAGTCAGTGGAATGAGCTTCTTGAAACTCTGTACAAACTTCCTATCCCTGACCCAGGAGTGTCTGTTCATCTCAGTGTGgta
DENND1A.V2_F1_BOVINE
DENND1A.V2_F2_BOVINE
DENND1A.V2_R_BOVINE
Exon 7
DENND1A.V2_HUMAN agtgggg-cggagtattagccatcactgaaaacg.....attttagcagaaataaatcacttttgcttttcttttctag
DENND1A_BOVINE agtgggggtagaatattagcaatcactgagaaac.....acttttttcaggaataaat-attttttatcttcctttacag
DENND1A.V2_F1_BOVINE
DENND1A.V2_F2_BOVINE
DENND1A.V2_R_BOVINE
DENND1A.V2_HUMAN CATTCTTATTTTACTGTGCCTGATACCAGAGAACTTCCCAGCATACCTGAGAATgtaagtactt.....tcttctttctcctag
DENND1A_BOVINE CATTCTTATTTTACTGTGCCTGATACCAGAGAACTTCCCAGCATCCCTGAGAATgtaagtactt.....tcttctttctcctag
DENND1A.V2_F1_BOVINE
DENND1A.V2_F2_BOVINE
DENND1A.V2_R_BOVINE
Exon 8
DENND1A.V2_HUMAN AGAAATCTGACAGAATATTTTGTGGCTGTGGATGTTAACAACATGTTGCATCTGTACGCCAGTATGCTGTACGAACGCCGGATA
DENND1A_BOVINE AGAAATCTGACAGAATATTTTGTGGCTGTGGATGTAAACAACATGTTACATCTGTATGCCAGTATGCTCTACGAACGCCGGATA
DENND1A.V2_F1_BOVINE
DENND1A.V2_F2_BOVINE
DENND1A.V2_R_BOVINE
DENND1A.V2_HUMAN CTCATCATTTGCAGCAAACTCAGCACTgtgagtagacagtc.....tcattgatctctgctttgctctgttccag
DENND1A_BOVINE CTCATCATTTGCAGCAAACTCAGCACTgtgagtagacagtc.....tagctctgaatctttaatctctgttgcag
DENND1A.V2_F1_BOVINE
DENND1A.V2_F2_BOVINE
DENND1A.V2_R_BOVINE
Exon 9
DENND1A.V2_HUMAN CTGACTGCCTGCATCCACGGGTCTGCGGCGATGCTCTACCCCATGTACTGGCAGCACGTGTACATCCCCGTGCTGCCGCCGCAT
DENND1A_BOVINE TTGACTGCCTGCATCCACGGGTCTGCTGCGATGCTCTACCCCATGTTCTGGCAGCACGTGTACATCCCTGTCCTGCCTCCACAT
DENND1A.V2_F1_BOVINE
DENND1A.V2_F2_BOVINE
DENND1A.V2_R_BOVINE
DENND1A.V2_HUMAN CTGCTGGACTACTGCTGgtaaggtggctg---gccctg.....acattaaagcagctgtgtgtctctgtttctcttcacag
DENND1A_BOVINE CTGCTGGACTACTGCTGgtaaggccactgcccaccctg.....acattaaagcagctgtgtgtctctgtttctcttcacag
DENND1A.V2_F1_BOVINE
DENND1A.V2_F2_BOVINE
DENND1A.V2_R_BOVINE
Exon 10
DENND1A.V2_HUMAN TGCTCCCATGCCCTACCTCATAGGAATCCATTTAAGTTTAATGGAGgtaagttggc.....tttttt--tctccttgcag
DENND1A_BOVINE TGCTCCCATGCCCTACCTCATAGGAATCCATTTAAGTTTAATGGAGgtaagttgac.....ttttttctttttacttgcag
DENND1A.V2_F1_BOVINE
DENND1A.V2_F2_BOVINE
DENND1A.V2_R_BOVINE
Exon 11
DENND1A.V2_HUMAN AAAGTCAGAAACATGGCCCTGGATGATGTCGTGATCCTGAATGTGGACACCAACACCCTGGAAACCCCCTTCGATGACCTCCAG
DENND1A_BOVINE AAAGTCAGAAGCATGGCCCTGGATGATGTCGTGATCCTGAATGTGGACACCAACACCCTGGAAACCCCCTTTGATGACCTCCAG
DENND1A.V2_F1_BOVINE
DENND1A.V2_F2_BOVINE
DENND1A.V2_R_BOVINE
DENND1A.V2_HUMAN AGCCTCCCAAACGACGTGgtaggtaatgagcttgcgaggatctcac.....ctgtgttttccttctctccatcaccag
DENND1A_BOVINE AGCCTCCCAAATGATGTGgtgggtaatgagctctcgagt-tctgac.....ctgtat----ctcctttctgtcatcag
DENND1A.V2_F1_BOVINE
DENND1A.V2_F2_BOVINE
DENND1A.V2_R_BOVINE
Exon 12
DENND1A.V2_HUMAN ATCTCTTCCCTGAAGAACAGGCTGAAAAAGGTCTCCACAACCACTGGGGATGGTGTGGCCAGAGCGTTCCTCAAGGCCCAGGCT
DENND1A_BOVINE ATCTCTTCCTTGAAGAGCCGGCTGAAGAAGGTGTCCACGACAACTGGTGATGGTGTGGCCAGAGCCTTCCTCAAGGCCCAGGCC
DENND1A.V2_F1_BOVINE
DENND1A.V2_F2_BOVINE
DENND1A.V2_R_BOVINE
Exon 13

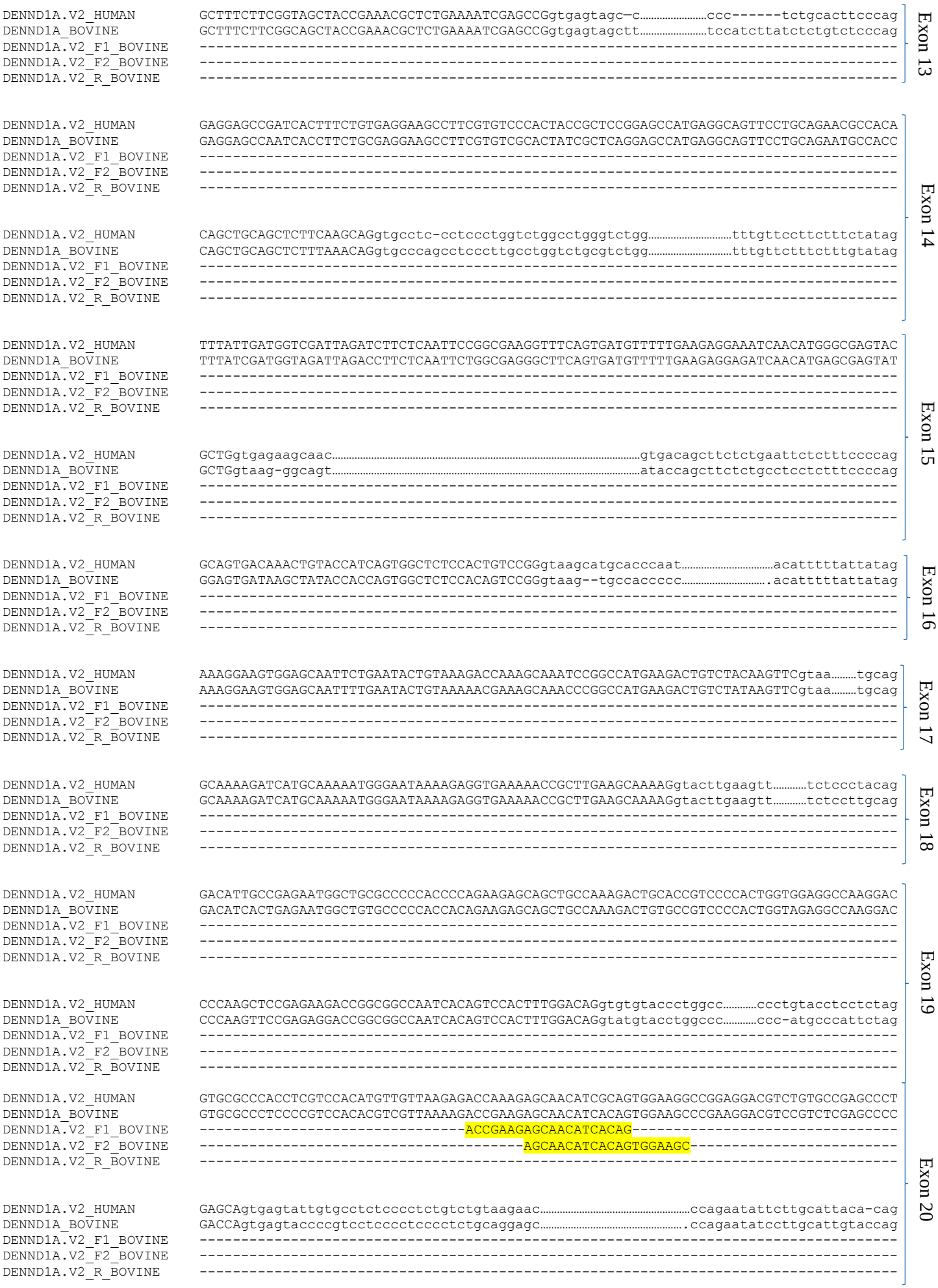
DENND1A.V2_HUMAN
DENND1A_BOVINE
DENND1A.V2_F1_BOVINE
DENND1A.V2_F2_BOVINE
DENND1A.V2_R_BOVINE
Exon 13
Exon 14
Exon 15
Exon 16
Exon 17
Exon 18
Exon 19
Exon 20


DENND1A.V2_HUMAN AAACACCATTGCAACACCAGCTACACTCCACATCCTACAGAAAAGCATTACCCATTTTGCGGCCAAGTTCCCGACGAGAGGCTG
DENND1A_BOVINE aaaca----------caccaacacttgccagtctaccgaaaagcattgcccat-ttgtggccaagtccccgattagagcttg
DENND1A.V2_F1_BOVINE ----------
DENND1A.V2_F2_BOVINE ----------
DENND1A.V2_R_BOVINE ----------
DENND1A.V2_HUMAN GACCTCTTCATCACATTGACTTACGCCGTTGCTTTTCCAGACTGGGCAGAGGGGCTGACTTCG-CAGTGTGTGCCAAAGAGCCG
DENND1A_BOVINE Gacctccccaccacacgtgtttatgctgttgcttttccagccccgtgataggagattgctgcgtcagtgtatg-caaagagcca
DENND1A.V2_F1_BOVINE ----------
DENND1A.V2_F2_BOVINE ----------
DENND1A.V2_R_BOVINE ----------GATAGGAGATTGCTGCGTCA----------
DENND1A.V2_HUMAN GTGTCTGATAATCCCATTTTCCTGCTTATCACCTGAACTGTGTCAGTATCACTTTTAGTTTTGTTGGTTGGTTGGTTTGTTGTT
DENND1A_BOVINE gggtctggcacccccatcattctggtggttaccagagctgggtcggtaccactttg--------tgcgggttttgttttgtttt
DENND1A.V2_F1_BOVINE ----------
DENND1A.V2_F2_BOVINE ----------
DENND1A.V2_R_BOVINE ----------
DENND1A.V2_HUMAN TGTTTAATATGCCCTGTTTTCTACTTCTGTTGGA-AAATATTTGGGGTTGAAATAAACCAGTGGGAGCATGGG-AGCCAGTTTG
DENND1A_BOVINE attgcattatgccttgttatggatttctttgggggaaacatttgaggttgaaatgaaccggtgggagcagggttggctagttta
DENND1A.V2_F1_BOVINE ----------
DENND1A.V2_F2_BOVINE ----------
DENND1A.V2_R_BOVINE ----------
DENND1A.V2_HUMAN GTGG-TTGGCAAACTACCAGTGATAGAAAACAAATGACAGGTTTTCTGTGAGCGTACGTCACAGTGGCTCG---------GGCC
DENND1A_BOVINE Gtgggctggcacactggcagttatagaagacaaatgacaggttctctgtgatcacgcataacagtgctccaccgtacagtggcc
DENND1A.V2_F1_BOVINE ----------
DENND1A.V2_F2_BOVINE ----------
DENND1A.V2_R_BOVINE ----------
DENND1A.V2_HUMAN CACAAGGAGACAGAGGGGTACGTTTCAGGACATCATTCCAAGGGTTTCTGTTCACGTTTGTTTAAC----------GAGGAAG
DENND1A_BOVINE caccaggagatagggaggtacattttagaacatcattccaagagtttctgttcacttctttttttttttatggggtgagggaag
DENND1A.V2_F1_BOVINE ----------
DENND1A.V2_F2_BOVINE ----------
DENND1A.V2_R_BOVINE ----------
DENND1A.V2_HUMAN GGGAAGTTGTTCTCCCATAATACCAGTGGTATTTCTAGTGCAACCCGGGTGTTTTTCTACGCCTCTTCCCATGCTGCTTCCCCA
DENND1A_BOVINE gcagggctgtattcctataacgccagtgacatttctggtgtaacccgggtgtttccctgcgtctcttcccatgctgccttctcc
DENND1A.V2_F1_BOVINE ----------
DENND1A.V2_F2_BOVINE ----------
DENND1A.V2_R_BOVINE ----------
DENND1A.V2_HUMAN C-----CCCCCCACTGTGCTCCGCCCCTTCCAAATGCCATGTCACAACAGCACTTGGATGTGTTTTTCTCAACTGTCATCAGCT
DENND1A_BOVINE ctgcccccaccccctgttgtgctccacttccaaatgccatgtcacaacagcacttggatgtgtttttctcaactgtcatcagct
DENND1A.V2_F1_BOVINE ----------
DENND1A.V2_F2_BOVINE ----------
DENND1A.V2_R_BOVINE ----------
DENND1A.V2_HUMAN CCAGCTGGCAGGACCAACTTCTTGAAACACAGGAAGCATCCAGCGGAAAATATTTTAATAAAACAGACTCCTCATAAAATATT
DENND1A_BOVINE ccagctggcaagaccaacttcttgaaacacaggaagcatccagcggaaaatattttaataaaacagactcctcataaaatgtt
DENND1A.V2_F1_BOVINE ----------
DENND1A.V2_F2_BOVINE ----------
DENND1A.V2_R_BOVINE ----------
DENND1A.V2_HUMAN GTTCGGGGGAGGGGGAAGAAACCGGCTC-CACCAATCTGTCGGCATTGTATTGGGAGATGTGAGAAGCCAGGCTGGCAG-CAGG
DENND1A_BOVINE gttttgggg----ggaagaacccgcccctccccagtctgtcagcattgtgtcgggagacacgagaagacaagccggcgggcagg
DENND1A.V2_F1_BOVINE ----------
DENND1A.V2_F2_BOVINE ----------
DENND1A.V2_R_BOVINE ----------
DENND1A.V2_HUMAN GGCCCGATCCTAATGGGCCTTTGTCAGGTGGTGGTTCCGTGTTGGGCACACGGACTTGGTGCCTGGCCCTTTAATCTGGCCTGG
DENND1A_BOVINE agccacatcctaatggggctttgttgcg-ggtggttcagtgctgggcacgcggactcggtgcctggccctttaatctggcctgg
DENND1A.V2_F1_BOVINE ----------
DENND1A.V2_F2_BOVINE ----------
DENND1A.V2_R_BOVINE ----------
Exon 21

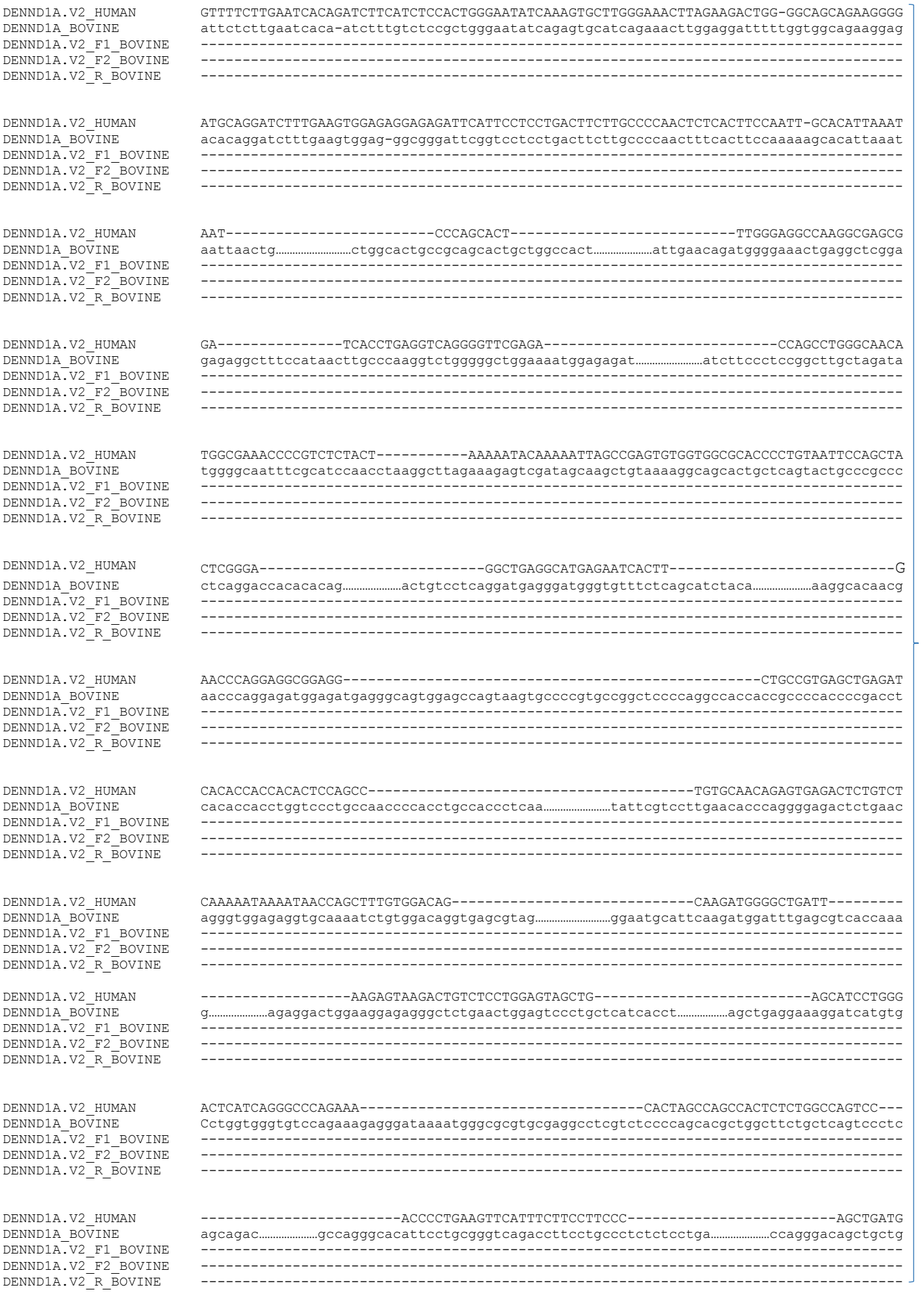
DENND1A.V2_HUMAN GTTTTCTTGAATCACAGATCTTCATCTCCACTGGGAATATCAAAGTGCTTGGGAAACTTAGAAGACTGG-GGCAGCAGAAGGGG
DENND1A_BOVINE attctcttgaatcaca-atctttgtctccgctgggaatatcagagtgcatcagaaacttggaggatttttggtggcagaaggag
DENND1A.V2_F1_BOVINE
DENND1A.V2_F2_BOVINE
DENND1A.V2_R_BOVINE
DENND1A.V2_HUMAN ATGCAGGATCTTTGAAGTGGAGAGGAGAGATTCATTCCTCCTGACTTCTTGCCCCAACTCTCACTTCCAATT-GCACATTAAAT
DENND1A_BOVINE acacaggatctttgaagtggag-ggcgggattcggtcctcctgacttcttgccccaactttcacttccaaaaagcacattaaat
DENND1A.V2_F1_BOVINE
DENND1A.V2_F2_BOVINE
DENND1A.V2_R_BOVINE
DENND1A.V2_HUMAN AAT----------CCCAGCACT----------TTGGGAGGCCAAGGCGAGCG
DENND1A_BOVINE aattaactg……ctggcactgccgcagcactgctggccact……attgaacagatggggaaactgaggctcgga
DENND1A.V2_F1_BOVINE
DENND1A.V2_F2_BOVINE
DENND1A.V2_R_BOVINE
DENND1A.V2_HUMAN GA----------TCACCTGAGGTCAGGGGTTCGAGA----------CCAGCCTGGGCAACA
DENND1A_BOVINE gagaggctttccataacttgcccaaggtctgggggctggaaaatggagagat……atcttccctccggcttgctagata
DENND1A.V2_F1_BOVINE
DENND1A.V2_F2_BOVINE
DENND1A.V2_R_BOVINE
DENND1A.V2_HUMAN TGGCGAAACCCCGTCTCTACT----------AAAAATACAAAAATTAGCCGAGTGTGGTGGCGCACCCCTGTAATTCCAGCTA
DENND1A_BOVINE tggggcaatttcgcatccaacctaaggcttagaaagagtcgatagcaagctgtaaaaggcagcactgctcagtactgcccgccc
DENND1A.V2_F1_BOVINE
DENND1A.V2_F2_BOVINE
DENND1A.V2_R_BOVINE
DENND1A.V2_HUMAN CTCGGGA----------GGCTGAGGCATGAGAATCACTT----------G
DENND1A_BOVINE ctcaggaccacacacag……actgtcctcaggatgagggatgggtgtttctcagcatctaca……aaggcacaacg
DENND1A.V2_F1_BOVINE
DENND1A.V2_F2_BOVINE
DENND1A.V2_R_BOVINE
DENND1A.V2_HUMAN AACCCAGGAGGCGGAGG----------CTGCCGTGAGCTGAGAT
DENND1A_BOVINE aacccaggagatggagatgagggcagtggagccagtaagtgccccgtgccggctccccaggccaccaccgccccaccccgacct
DENND1A.V2_F1_BOVINE
DENND1A.V2_F2_BOVINE
DENND1A.V2_R_BOVINE
DENND1A.V2_HUMAN CACACCACCACACTCCAGCC----------TGTGCAACAGAGTGAGACTCTGTCT
DENND1A_BOVINE cacaccacctggtccctgccaaccccacctgccaccctcaa……tattcgtccttgaacacccaggggagactctgaac
DENND1A.V2_F1_BOVINE
DENND1A.V2_F2_BOVINE
DENND1A.V2_R_BOVINE
DENND1A.V2_HUMAN CAAAAATAAAATAACCAGCTTTGTGGACAG----------CAAGATGGGGCTGATT----------
DENND1A_BOVINE agggtggagaggtgcaaaatctgtggacaggtgagcgtag……ggaatgcattcaagatggatttgagcgtcaccaaa
DENND1A.V2_F1_BOVINE
DENND1A.V2_F2_BOVINE
DENND1A.V2_R_BOVINE
DENND1A.V2_HUMAN ----------AAGAGTAAGACTGTCTCCTGGAGTAGCTG----------AGCATCCTGGG
DENND1A_BOVINE g……agaggactggaaggagagggctctgaactggagtccctgctcatcacct……agctgaggaaaggatcatgtg
DENND1A.V2_F1_BOVINE
DENND1A.V2_F2_BOVINE
DENND1A.V2_R_BOVINE
DENND1A.V2_HUMAN ACTCATCAGGGCCCAGAAA----------CACTAGCCAGCCACTCTCTGGCCAGTCC---
DENND1A_BOVINE Cctggtgggtgtccagaaagagggataaaatgggcgcgtgcgaggcctcgtctccccagcacgctggcttctgctcagtccctc
DENND1A.V2_F1_BOVINE
DENND1A.V2_F2_BOVINE
DENND1A.V2_R_BOVINE
DENND1A.V2_HUMAN ----------ACCCCTGAAGTTCATTTCTTCCTTCCC----------AGCTGATG
DENND1A_BOVINE agcagac……gccagggcacattcctgcgggtcagaccttcctgccctctctcctga……ccagggacagctgctg
DENND1A.V2_F1_BOVINE
DENND1A.V2_F2_BOVINE
DENND1A.V2_R_BOVINE
Exon 21

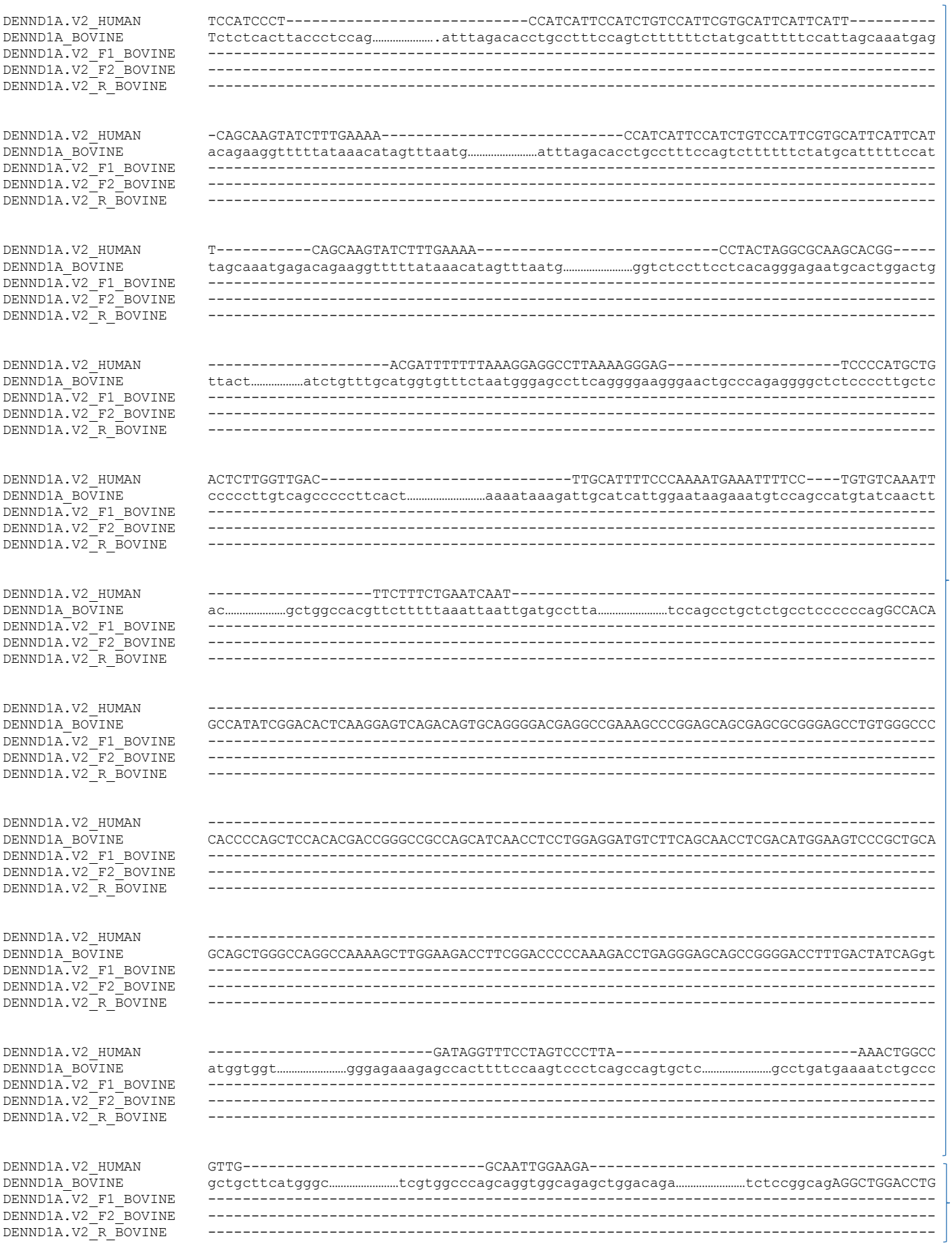
DENND1A.V2_HUMAN TCCATCCCT----------CCATCATTCCATCTGTCCATTCGTGCATTCATTCATT----------
DENND1A_BOVINE Tctctcacttaccctccag.....atttagacacctgcctttccagtctttttttctatgcatttttccattagcaaatgag
DENND1A.V2_F1_BOVINE ----------
DENND1A.V2_F2_BOVINE ----------
DENND1A.V2_R_BOVINE ----------
DENND1A.V2_HUMAN -CAGCAAGTATCTTTGAAAA----------CCATCATTCCATCTGTCCATTCGTGCATTCATTCAT
DENND1A_BOVINE acagaaggtttttataaacatagtttaatg.....atttagacacctgcctttccagtctttttttctatgcatttttccat
DENND1A.V2_F1_BOVINE ----------
DENND1A.V2_F2_BOVINE ----------
DENND1A.V2_R_BOVINE ----------
DENND1A.V2_HUMAN T----------CAGCAAGTATCTTTGAAAA----------CCTACTAGGCGCAAGCACGG-----
DENND1A_BOVINE tagcaaatgagacagaaggtttttataaacatagtttaatg.....ggtctccttcctcacagggagaatgcactggactg
DENND1A.V2_F1_BOVINE ----------
DENND1A.V2_F2_BOVINE ----------
DENND1A.V2_R_BOVINE ----------
DENND1A.V2_HUMAN ----------ACGATTTTTTTAAAGGAGGCCTTAAAAGGGAG----------TCCCCATGCTG
DENND1A_BOVINE ttact.....atctgtttgcatggtgtttctaatgggagccttcaggggaagggaactgcccagaggggctctccccttgctc
DENND1A.V2_F1_BOVINE ----------
DENND1A.V2_F2_BOVINE ----------
DENND1A.V2_R_BOVINE ----------
DENND1A.V2_HUMAN ACTCTTGGTTGAC----------TTGCATTTTCCCAAAATGAAATTTTCC----TGTGTCAAATT
DENND1A_BOVINE ccccctttgtcagcccccttcact.....aaaataaagattgcatcattggaataagaaatgtccagccatgtatcaacttt
DENND1A.V2_F1_BOVINE ----------
DENND1A.V2_F2_BOVINE ----------
DENND1A.V2_R_BOVINE ----------
DENND1A.V2_HUMAN ----------TTCTTTCTGAATCAAT----------
DENND1A_BOVINE ac.....gctggccacgttctttttaaattaattgatgcctta.....tccagcctgctctgcctccccccagGCCACA
DENND1A.V2_F1_BOVINE ----------
DENND1A.V2_F2_BOVINE ----------
DENND1A.V2_R_BOVINE ----------
DENND1A.V2_HUMAN ----------
DENND1A_BOVINE GCCATATCGGACACTCAAGGAGTCAGACAGTGCAGGGGACGAGGCCGAAAGCCCGGAGCAGCGAGCGCGGGAGCCTGTGGGCCC
DENND1A.V2_F1_BOVINE ----------
DENND1A.V2_F2_BOVINE ----------
DENND1A.V2_R_BOVINE ----------
DENND1A.V2_HUMAN ----------
DENND1A_BOVINE CACCCCAGCTCCACACGACCGGGCCGCCAGCATCAACCTCCTGGAGGATGTCTTCAGCAACCTCGACATGGAAGTCCCGCTGCA
DENND1A.V2_F1_BOVINE ----------
DENND1A.V2_F2_BOVINE ----------
DENND1A.V2_R_BOVINE ----------
DENND1A.V2_HUMAN ----------
DENND1A_BOVINE GCAGCTGGGCCAGGCCAAAAGCTTGGAAGACCTTCGGACCCCCAAAGACCTGAGGGAGCAGCCGGGGACCTTTGACTATCAGgt
DENND1A.V2_F1_BOVINE ----------
DENND1A.V2_F2_BOVINE ----------
DENND1A.V2_R_BOVINE ----------
DENND1A.V2_HUMAN ----------GATAGGTTTCCTAGTCCCTTA----------AAACTGGCC
DENND1A_BOVINE atggtggt.....gggagaaagagccacttttccaagtccctcagccagtgctc.....gcctgatgaaaatctgccc
DENND1A.V2_F1_BOVINE ----------
DENND1A.V2_F2_BOVINE ----------
DENND1A.V2_R_BOVINE ----------
DENND1A.V2_HUMAN GTTG----------GCAATTGGAAGA----------
DENND1A_BOVINE gctgcttcatgggc.....tcgtggcccagcaggtggcagagctggacaga.....tctccggcagAGGCTGGACCTG
DENND1A.V2_F1_BOVINE ----------
DENND1A.V2_F2_BOVINE ----------
DENND1A.V2_R_BOVINE ----------
Exon 21
Exon 22 bovine

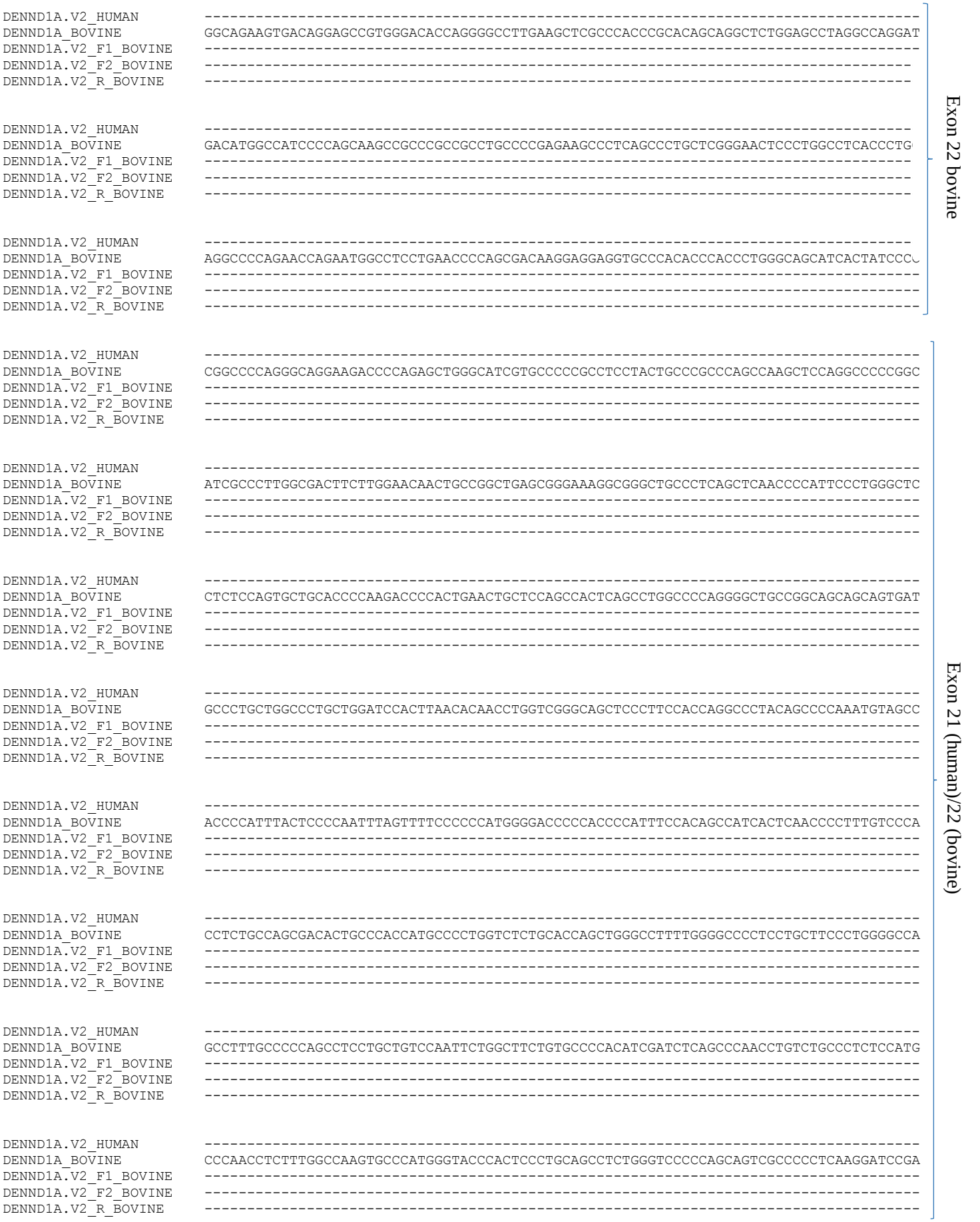
DENND1A.V2_HUMAN ----------
DENND1A_BOVINE GGCAGAAGTGACAGGAGCCGTGGGACACCAGGGGCCTTGAAGCTCGCCCACCCGCACAGCAGGCTCTGGAGCCTAGGCCAGGAT
DENND1A.V2_F1_BOVINE ----------
DENND1A.V2_F2_BOVINE ----------
DENND1A.V2_R_BOVINE ----------
DENND1A.V2_HUMAN ----------
DENND1A_BOVINE GACATGGCCATCCCCAGCAAGCCGCCCGCCGCCTGCCCCGAGAAGCCCTCAGCCCTGCTCGGGAACTCCCTGGCCTCACCCTG
DENND1A.V2_F1_BOVINE ----------
DENND1A.V2_F2_BOVINE ----------
DENND1A.V2_R_BOVINE ----------
DENND1A.V2_HUMAN ----------
DENND1A_BOVINE AGGCCCCAGAACCAGAATGGCCTCCTGAACCCCAGCGACAAGGAGGAGGTGCCCACACCCACCCTGGGCAGCATCACTATCCCC
DENND1A.V2_F1_BOVINE ----------
DENND1A.V2_F2_BOVINE ----------
DENND1A.V2_R_BOVINE ----------
DENND1A.V2_HUMAN ----------
DENND1A_BOVINE CGGCCCCAGGGCAGGAAGACCCCAGAGCTGGGCATCGTGCCCCCGCCTCCTACTGCCCGCCCAGCCAAGCTCCAGGCCCCCGGC
DENND1A.V2_F1_BOVINE ----------
DENND1A.V2_F2_BOVINE ----------
DENND1A.V2_R_BOVINE ----------
DENND1A.V2_HUMAN ----------
DENND1A_BOVINE ATCGCCCTTGGCGACTTCTTGGAACAACTGCCGGCTGAGCGGGAAAGGCGGGGCTGCCCTCAGCTCAACCCCATTCCCTGGGCTC
DENND1A.V2_F1_BOVINE ----------
DENND1A.V2_F2_BOVINE ----------
DENND1A.V2_R_BOVINE ----------
DENND1A.V2_HUMAN ----------
DENND1A_BOVINE CTCTCCAGTGCTGCACCCCAAGACCCCACTGAACTGCTCCAGCCACTCAGCCTGGCCCCAGGGGCTGCCGGCAGCAGCAGTGAT
DENND1A.V2_F1_BOVINE ----------
DENND1A.V2_F2_BOVINE ----------
DENND1A.V2_R_BOVINE ----------
DENND1A.V2_HUMAN ----------
DENND1A_BOVINE GCCCTGCTGGCCCTGCTGGATCCACTTAACACAACCTGGTCGGGCAGCTCCCTTCCACCAGGCCCTACAGCCCCAAATGTAGCC
DENND1A.V2_F1_BOVINE ----------
DENND1A.V2_F2_BOVINE ----------
DENND1A.V2_R_BOVINE ----------
DENND1A.V2_HUMAN ----------
DENND1A_BOVINE ACCCCATTTACTCCCCAATTTAGTTTTCCCCCCATGGGGACCCCCACCCCATTTCCACAGCCATCACTCAACCCCTTTGTCCCA
DENND1A.V2_F1_BOVINE ----------
DENND1A.V2_F2_BOVINE ----------
DENND1A.V2_R_BOVINE ----------
DENND1A.V2_HUMAN ----------
DENND1A_BOVINE CCTCTGCCAGCGACACTGCCCACCATGCCCCTGGTCTCTGCACCAGCTGGGCCTTTTGGGGCCCCTCCTGCTTCCCTGGGGCCA
DENND1A.V2_F1_BOVINE ----------
DENND1A.V2_F2_BOVINE ----------
DENND1A.V2_R_BOVINE ----------
DENND1A.V2_HUMAN ----------
DENND1A_BOVINE GCCTTTGCCCCCAGCCTCCTGCTGTCCAATTCTGGCTTCTGTGCCCCACATCGATCTCAGCCCAACCTGTCTGCCCTCTCCATG
DENND1A.V2_F1_BOVINE ----------
DENND1A.V2_F2_BOVINE ----------
DENND1A.V2_R_BOVINE ----------
DENND1A.V2_HUMAN ----------
DENND1A_BOVINE CCCAACCTCTTTGGCCAAGTGCCCATGGGTACCCACTCCCTGCAGCCTCTGGGTCCCCCAGCAGTCGCCCCCTCAAGGATCCGA
DENND1A.V2_F1_BOVINE ----------
DENND1A.V2_F2_BOVINE ----------
DENND1A.V2_R_BOVINE ----------
Exon 22 bovine
Exon 21 (human)/22 (bovine)

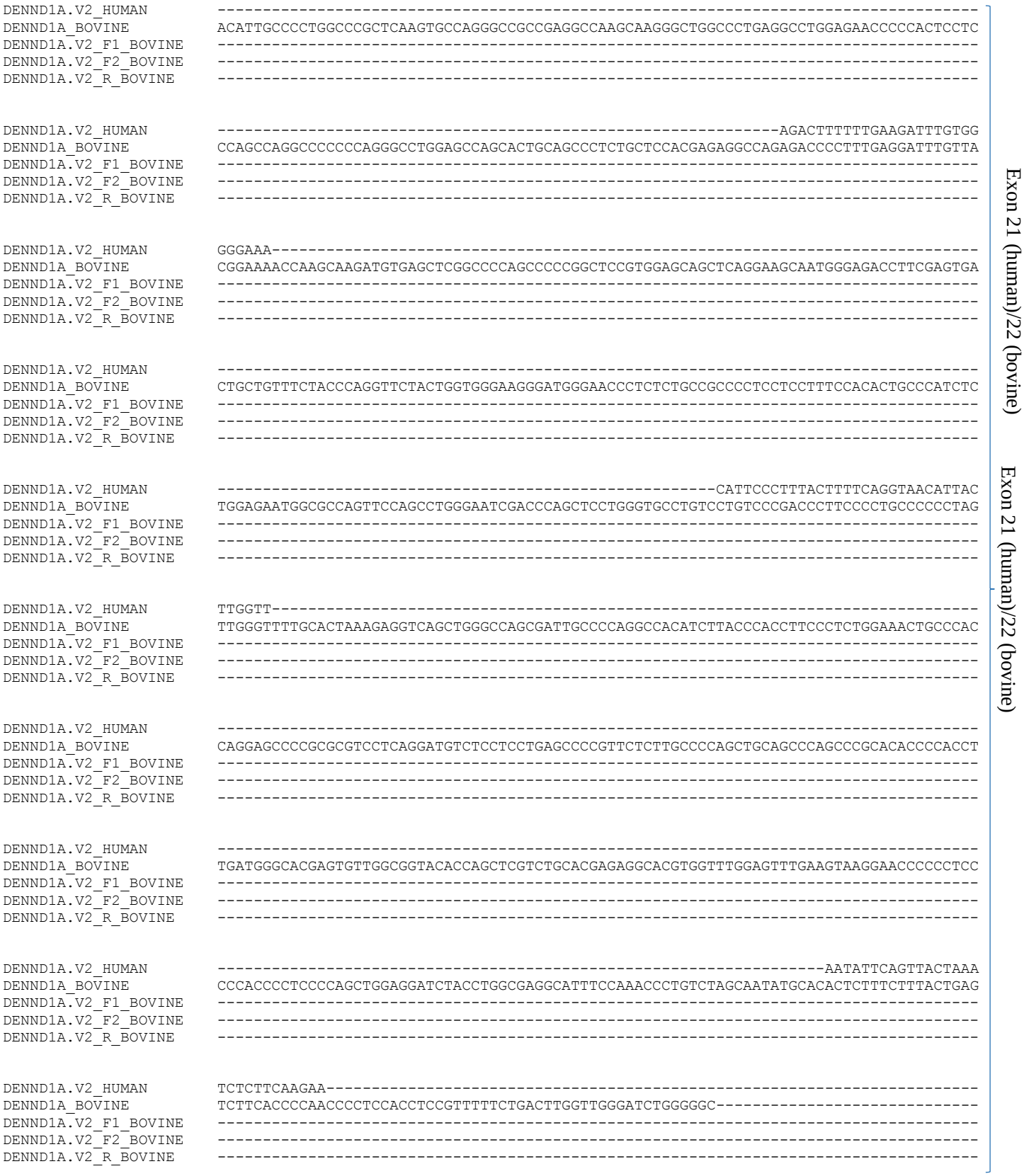
DENND1A.V2_HUMAN
DENND1A_BOVINE
DENND1A.V2_F1_BOVINE
DENND1A.V2_F2_BOVINE
DENND1A.V2_R_BOVINE
Exon 21 (human)/22 (bovine)
Exon 21 (human)/22 (bovine)

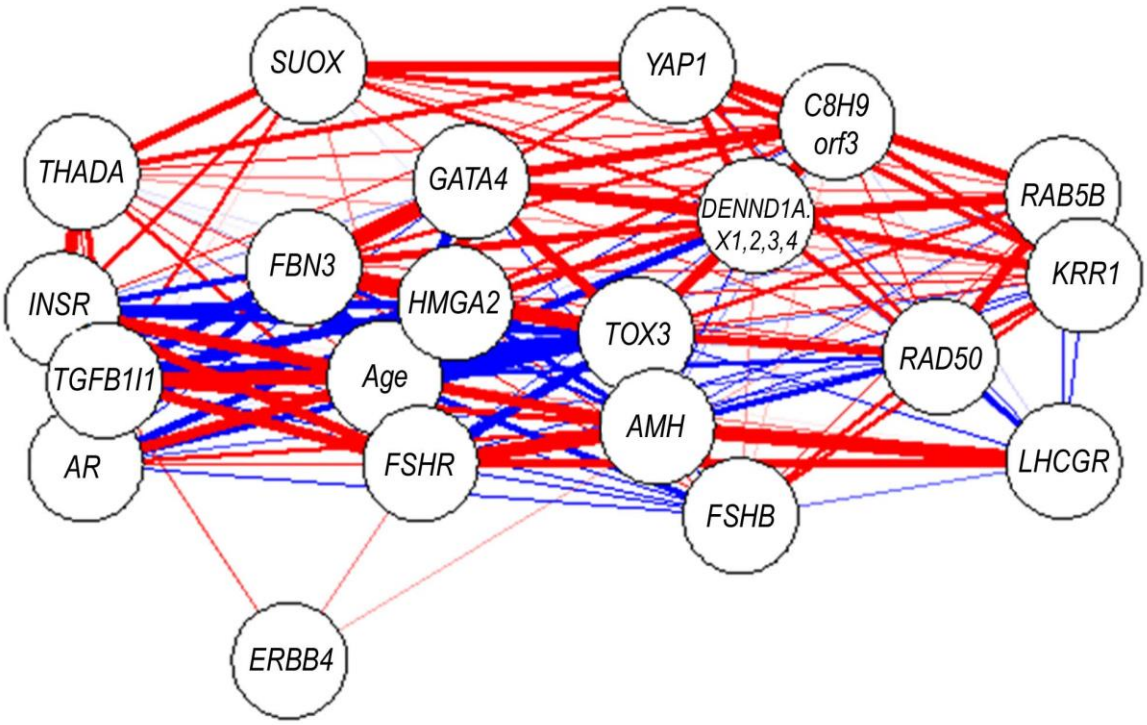

Supplemental Fig. 5. An adjacent matrix network graph of bovine gene expression using correlation coefficients from Tables II generated with R-program. The closeness of the genes and the thickness of the interconnecting lines indicate the strength of the correlations between genes. Red and blue lines represent positive and negative correlation, respectively. Age is gestational age.

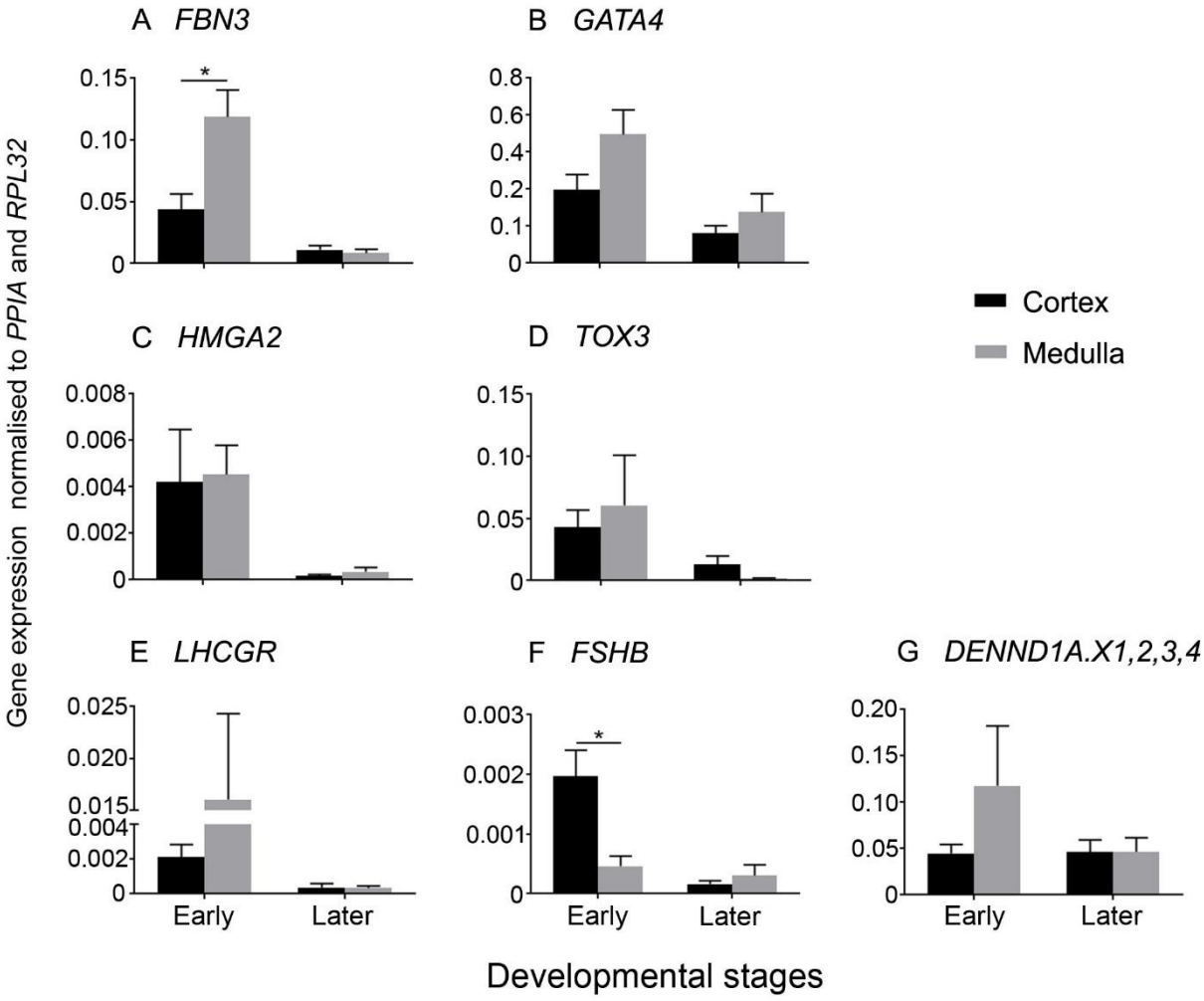

Supplemental Fig. 6. Differential mRNA expression levels of PCOS candidate genes which are highly expressed during early gestation in the cortex and medulla of bovine fetal ovaries. Samples were grouped into early (n = 5, 10 – 17 weeks of gestation) and later (n= 5, 36 – 39 weeks of gestation) time of gestation. Data are presented as mean ± s.e.m. (normalised to *PPIA* and *RPL32*). Black and grey bars represent cortex and medulla, respectively. Unpaired t-test were applied to analyse the data. **P* < 0.05.

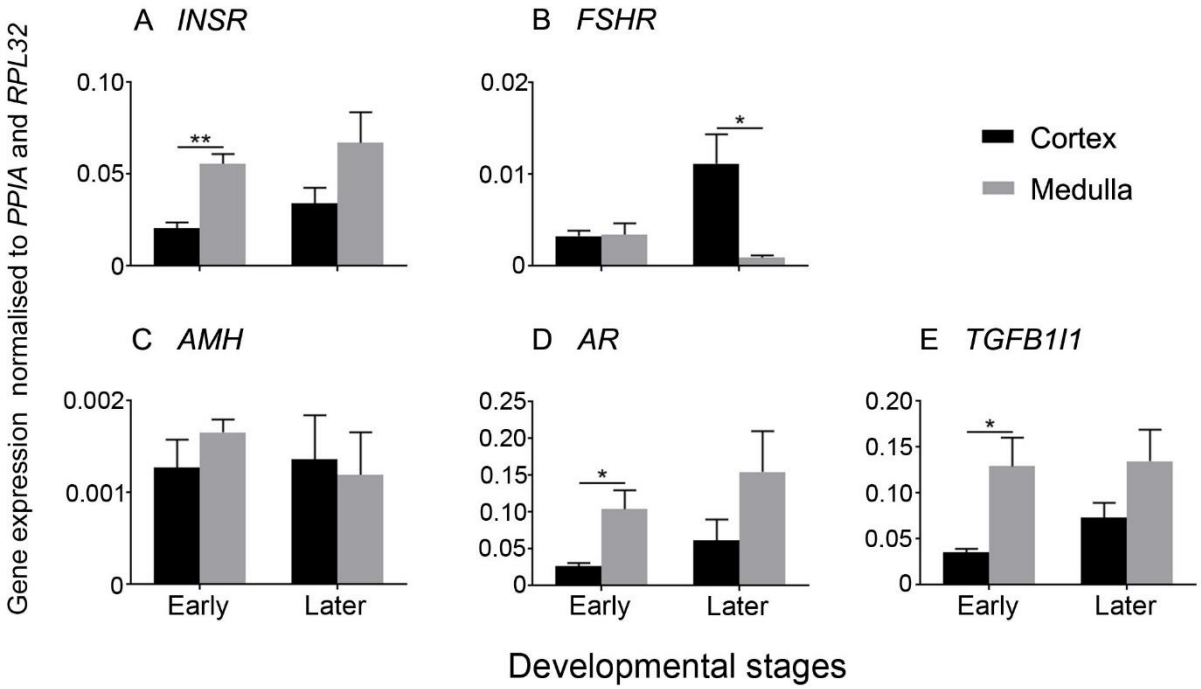

Supplemental Fig. 7. Differential mRNA expression levels of genes which are highly expressed late in gestation in the cortex and medulla of bovine fetal ovaries. Samples were grouped into early (n = 5, 10 – 17 weeks of gestation) and later (n= 5, 36 – 39 weeks of gestation) stages of gestation. Data are presented as mean ± s.e.m. (normalised to *PPIA* and *RPL32*). Black and grey bars represent cortex and medulla, respectively. Unpaired t-test were applied to analyse the data. **P* < 0.05, ***P* < 0.01.

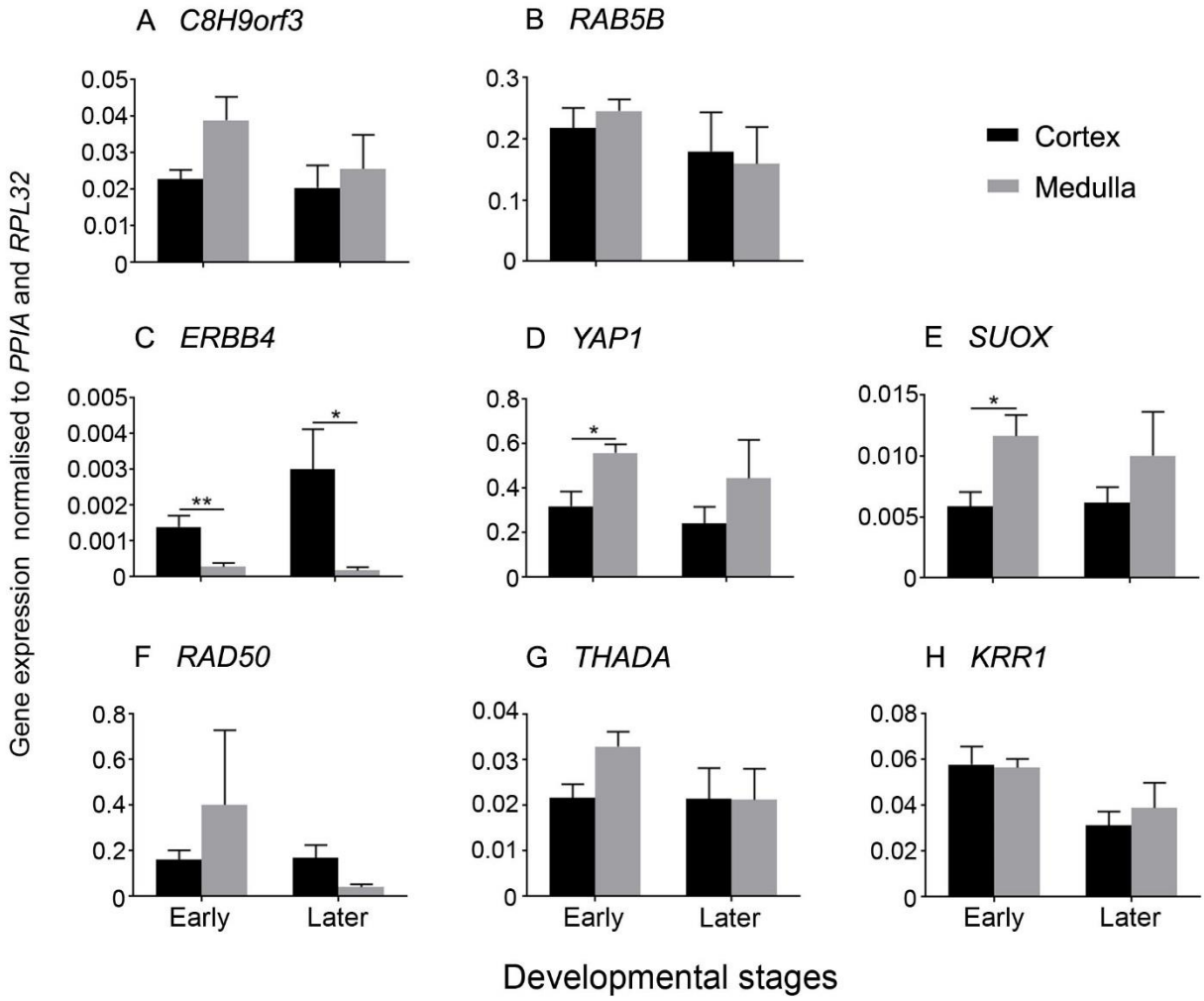

Supplementary Figure 8. Differential mRNA expression levels of PCOS candidate genes which are evenly expressed throughout gestation in the cortex and medulla of bovine fetal ovaries. Samples were grouped into early (n = 5, 10 – 17 weeks of gestation) and late (n= 5, 36 – 39 weeks of gestation) stages of gestation. Data are presented as mean ± s.e.m. (normalised to *PPIA* and *RPL32*). Black and grey bars represent cortex and medulla, respectively. Unpaired t-test were applied to analyse the data. **P* < 0.05.

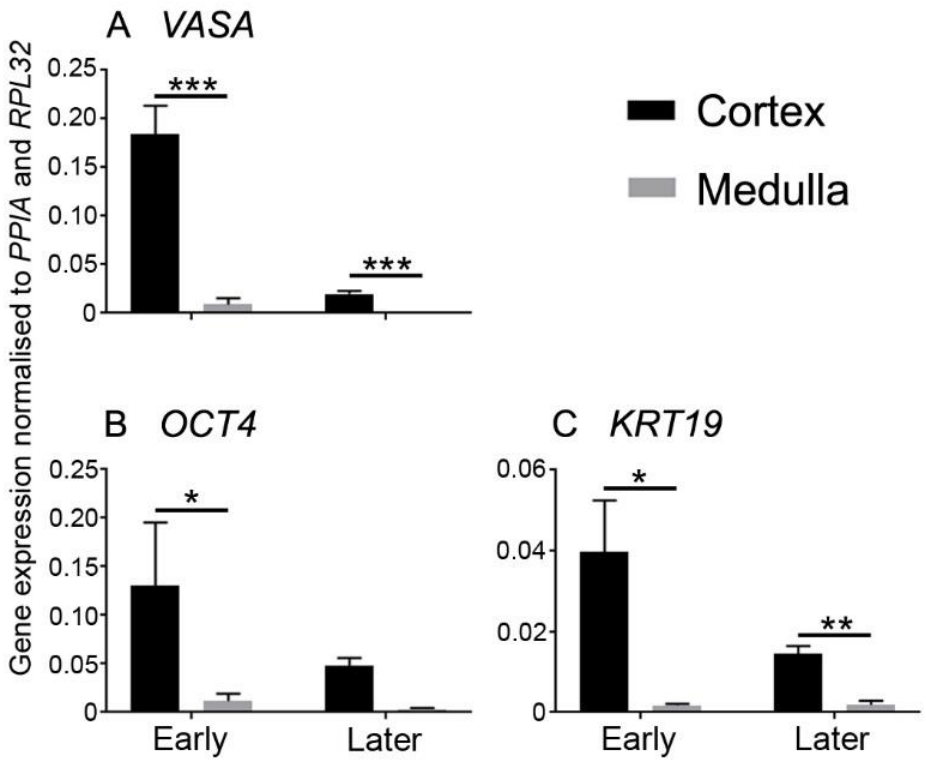

Supplemental Fig. 9. Differential mRNA expression levels of (A) *VASA*, (B) *OCT4* and (C) *KRT19* throughout gestation in the cortex and medulla of bovine fetal ovaries. Samples were grouped into early (n = 5, 10 – 17 weeks of gestation) and late (n= 5, 36 – 39 weeks of gestation) stages of gestation. Data are presented as mean ± s.e.m. (normalised to *PPIA* and *RPL32*). Black and grey bars represent cortex and medulla, respectively. Unpaired t-test were applied to analyse the data. **P* < 0.05, ***P* < 0.01, ****P* < 0.001.

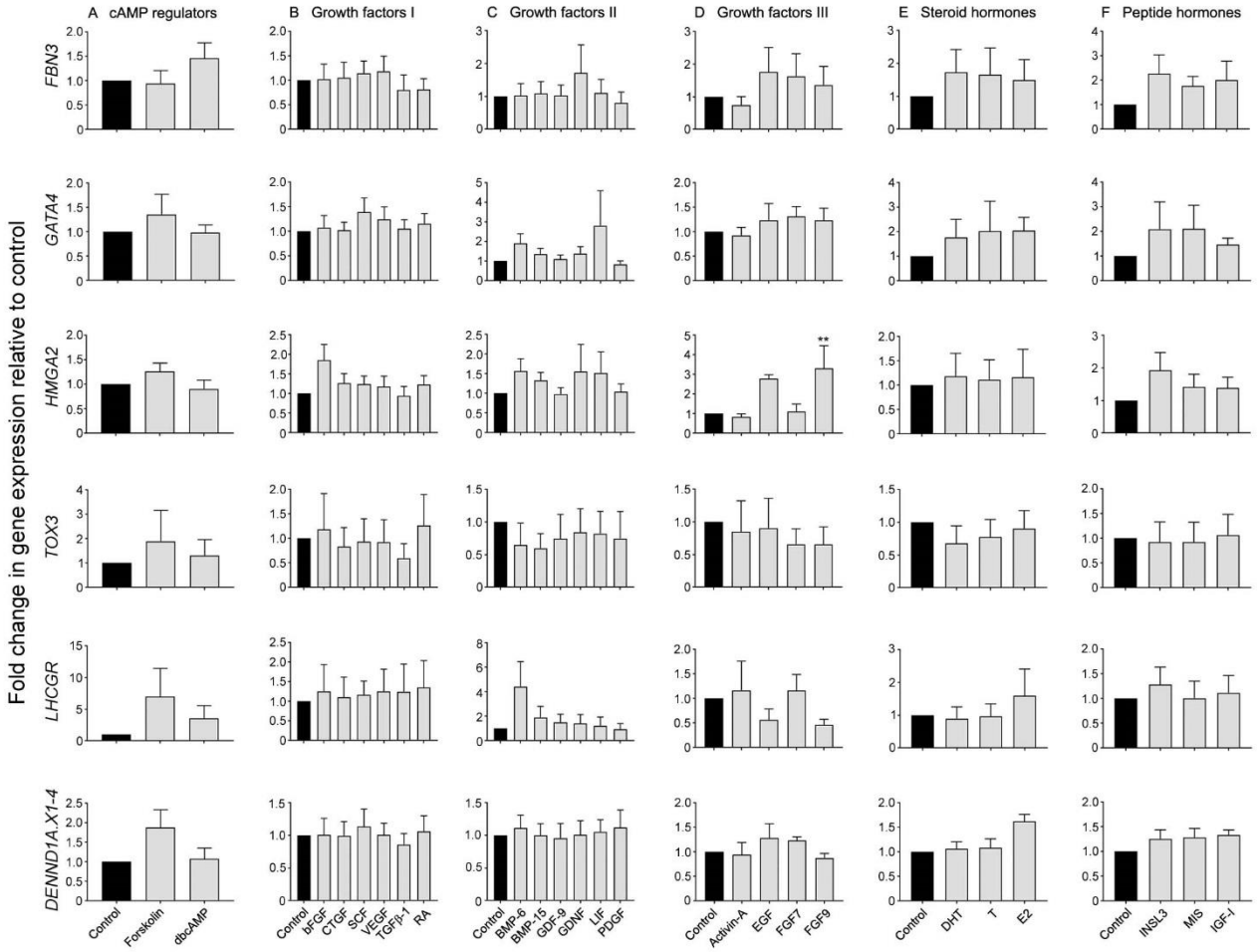

Supplemental Fig. 10. Differential mRNA expression levels of PCOS candidate genes which are highly expressed during early gestation in bovine fetal fibroblasts from less than 150 days of gestation cultured for 18 h in the presence of 24 different hormones and growth factors as indicated (A to F). Data are represented as mean ± s.e.m. of fold change in expression relative to the untreated control (n = 4 ovaries, each from 13, 14, 17 and 19 weeks of gestation). One-way ANOVA with Dunnet's *post hoc* test were used to analyse the data. Asterisk symbols indicates statistically significant different form the control. **P<0.01.

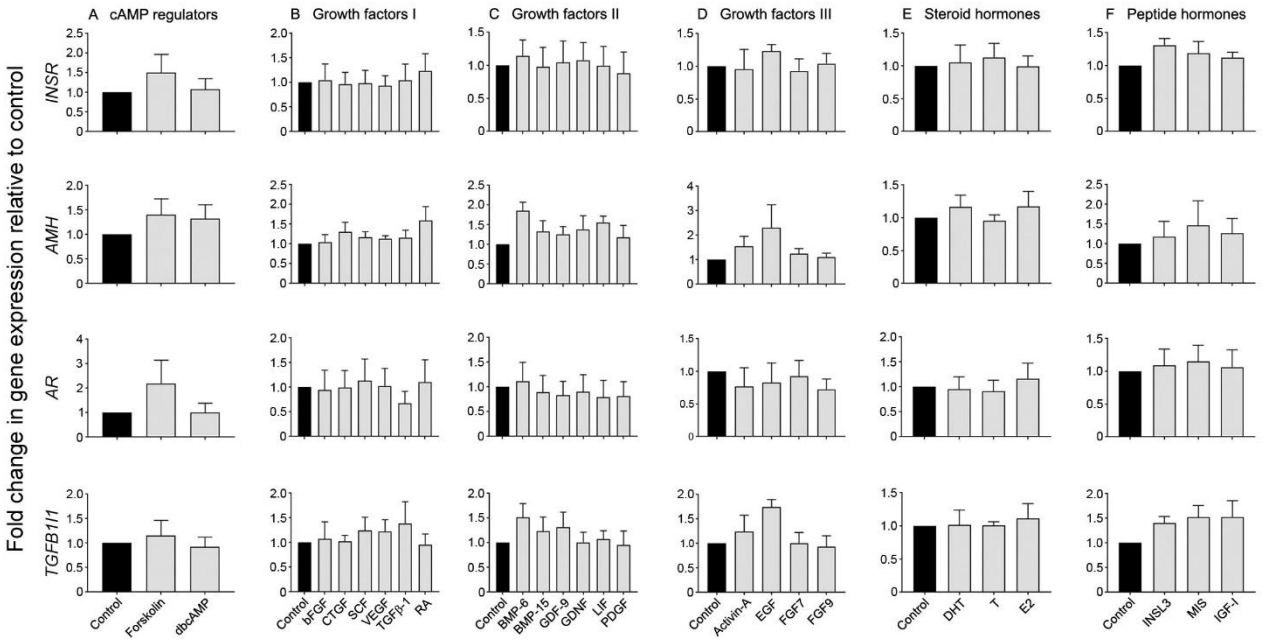

Supplemental Fig. 11. Differential mRNA expression levels of PCOS candidate genes which are highly expressed late during gestation in bovine fetal fibroblasts from less than 150 days of gestation cultured for 18 h in the presence of 24 different hormones and growth factors as indicated (A to F). Data are represented as mean ± s.e.m. of fold change in expression relative to the untreated control (n = 4 ovaries, each from 13, 14, 17 and 19 weeks of gestation). One-way ANOVA with Dunnet's *post hoc* test were used to analyse the data. Asterisk symbols indicates statistically significant different form the control.

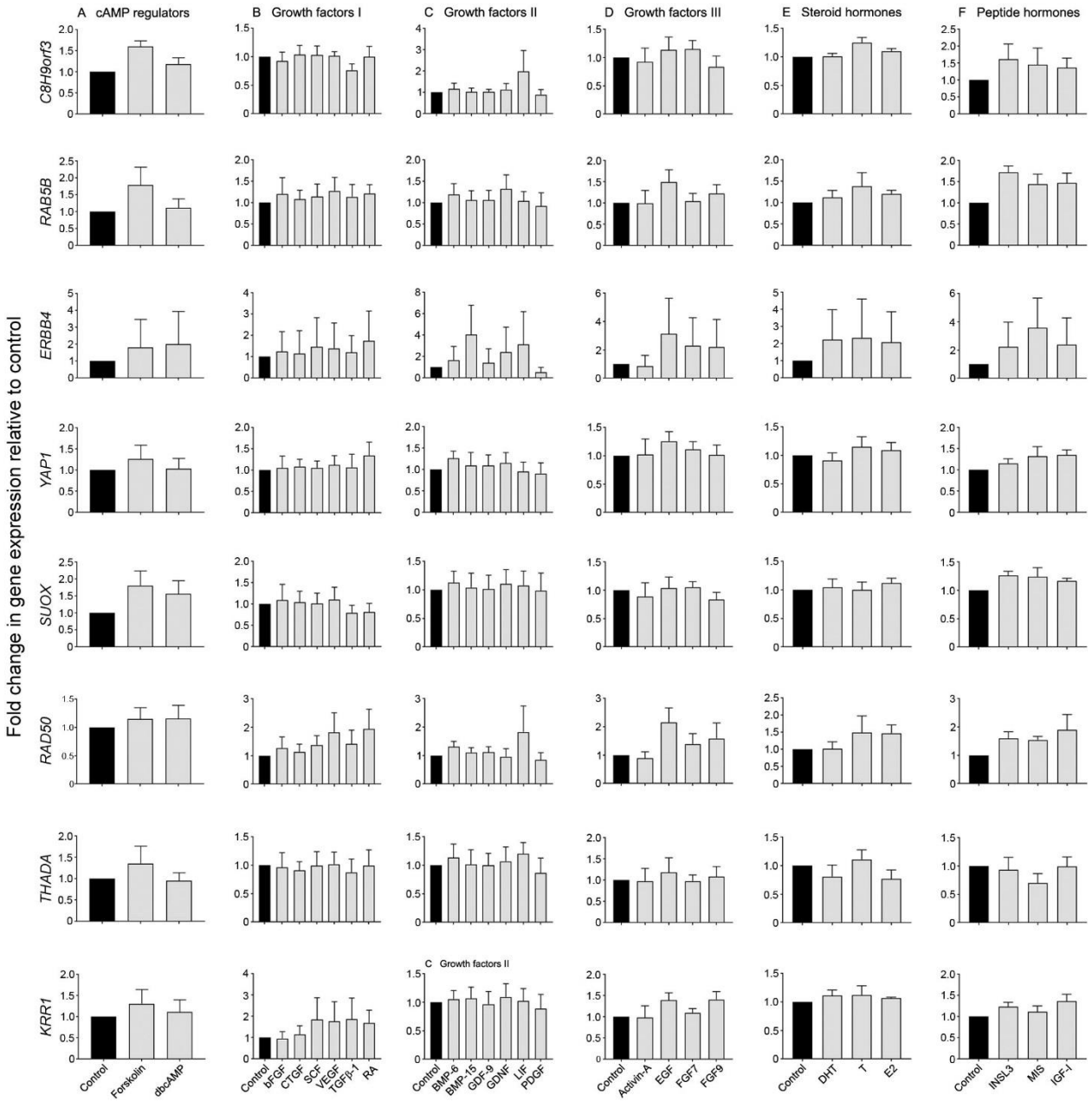

Supplemental Fig. 12. Differential mRNA expression levels of PCOS candidate genes which are evenly expressed throughout gestation in bovine fetal fibroblasts from less than 150 days of gestation cultured for 18 h in the presence of 24 different hormones and growth factors as indicated (A to F). Data are represented as mean ± s.e.m. of fold change in expression relative to the untreated control (n = 4 ovaries, each from 13, 14, 17 and 19 weeks of gestation). One-way ANOVA with Dunnet's *post hoc* test were used to analyse the data. Asterisk symbols indicates statistically significant different form the control.

Chapter IV:

Morphometric analyses and gene expression related to germ cells, gonadal ridge epithelial-like cells and granulosa cells during development of the bovine fetal ovary

Introduction to chapter IV

The development of fetal ovary begins at the surface of mesonephros, a temporary kidney during fetal life. The mesonephric epithelial cells differentiate into GREL cells and then proliferate, forming the developing ovary along with germ cells. Once the mesonephric stroma penetrates and branches, some GREL cells and germ cells are clustered into ovigerous cords. GREL cells give rise to granulosa cells, forming primordial follicles first located in the inner ovarian cortex. In this publication, my contribution was 15%, morphometrically analysing the non-stroma component of ovarian cortex morphometrically throughout gestation. My aim for this publication is to analyse the behaviour of GREL and germ cells during bovine fetal ovarian development, in relation with the changes in the stromal-areas. The non-stromal areas containing GREL cells and germ cells were morphometrically analysed across gestation. Using a stromal marker, collagen type I, and proliferation marker, Ki67, the non-stromal area was identified by subtracting the total cortical area with the stromal area. The total volume, volume density, proliferation index and numerical density of proliferating cells as well as all cells in the non-stromal area were counted and analysed in the five different stages of development, based on the morphological characteristics. The total volume of non-stromal areas in the ovarian cortex inclined significantly, however the volume density of non-stromal areas declined significantly throughout gestation. This study was conducted by Monica Dwi Hartanti.

For publication purposes, we combined these results with another gene expression study done by our group, analysing germ cell, stem cell, GREL cell and granulosa markers throughout gestations. We concluded that these genes had a relationships between each other and might indicate their parts in critical points during ovarian development, such as differentiation of GREL cells to granulosa cells. We managed to produce one paper published in PLos One and I am the co-author in this paper.

Statement of Authorship

Title of Paper	**Morphometric analyses and gene expression related to germ cells, gonadal ridge epithelial-like cells and granulosa cells during development of the bovine fetal ovary**
Publication Status	☑ Published ☐ Accepted for Publication ☐ Submitted for Publication ☐ Unpublished and Unsubmitted work written in manuscript style
Publication Details	Katja Hummitzsch, Nicholas Hatzirodos, Helen F. Irving-Rodgers, **Monica D. Hartanti**, Viv E.A. Perry, Richard A. Anderson and Raymond J. Rodgers; Morphometric analyses and gene expression related to germ cells, gonadal ridge epithelial-like cells and granulosa cells during development of the bovine fetal ovary; *PLoS One*; 2019, 14(3):e0214130.

Co-Author

Name of Co-Author (Candidate)	**Monica Dwi Hartanti**		
Contribution to the Paper	**Planned and developed work, performed analysis on some samples, interpreted data, and revised the manuscript.**		
Overall percentage (%)	**15 %**		
Certification:	**This paper reports on original research I conducted during the period of my Higher Degree by Research candidature and is not subject to any obligations or contractual agreements with a third party that would constrain its inclusion in this thesis. I am the co-author of this paper.**		
Signature		**Date**	**07/04/2019**

Author Contributions

By signing the Statement of Authorship, each author certifies that:

i. **the candidate's stated contribution to the publication is accurate (as detailed above);**

ii. **permission is granted for the candidate in include the publication in the thesis; and**

Principal Author

Name of Principal Author	**Katja Hummitzsch**		
Contribution to the Paper	**Planned and developed work, performed analysis on some samples, interpreted data, drafted, wrote and revised the manuscript.**		
Signature		**Date**	24/05/2019

Name of Co-Author	Nicholas Hatzirodos		
Contribution to the Paper	Planned work of cultured bovine samples.		
Signature		Date	24/05/2019

Name of Co-Author	Helen F Irving-Rodgers		
Contribution to the Paper	Supervised development of work and manuscript evaluation.		
Signature		Date	24/05/2019

Name of Co-Author	Viv E A Perry		
Contribution to the Paper	Developing of experiment tissues.		
Signature		Date	24/5/19

Name of Co-Author	Richard A Anderson		
Contribution to the Paper	Manuscript evaluation.		
Signature		Date	24 May 2019

Name of Co-Author	Raymond J Rodgers		
Contribution to the Paper	Supervised development of work, manuscript evaluation and acted as corresponding author.		
Signature		Date	24 May, 2019

PLOS ONE

RESEARCH ARTICLE

Morphometric analyses and gene expression related to germ cells, gonadal ridge epithelial-like cells and granulosa cells during development of the bovine fetal ovary

Katja Hummitzsch[1], Nicholas Hatzirodos[1], Helen F. Irving-Rodgers[1,2], Monica D. Hartanti[1], Viv E. A. Perry[3], Richard A. Anderson[4], Raymond J. Rodgers[1]*

1 Discipline of Obstetrics and Gynaecology, School of Medicine, Robinson Research Institute, University of Adelaide, Adelaide, South Australia, Australia, **2** School of Medical Science, Griffith University, Gold Coast Campus, Gold Coast, Queensland, Australia, **3** School of Veterinary Medicine and Science, University of Nottingham, Sutton Bonington, Leicestershire, United Kingdom, **4** Medical Research Council Centre for Reproductive Health, University of Edinburgh, Queen's Medical Research Institute, Edinburgh, United Kingdom

* ray.rodgers@adelaide.edu.au

Citation: Hummitzsch K, Hatzirodos N, Irving-Rodgers HF, Hartanti MD, Perry VEA, Anderson RA, et al. (2019) Morphometric analyses and gene expression related to germ cells, gonadal ridge epithelial-like cells and granulosa cells during development of the bovine fetal ovary. PLoS ONE 14(3): e0214130. https://doi.org/10.1371/journal.pone.0214130

Editor: Yang Yu, Peking University Third Hospital, CHINA

Received: September 5, 2018

Accepted: March 7, 2019

Published: March 22, 2019

Data Availability Statement: All relevant data are within the manuscript and its Supporting Information files.

Funding: Funding support for this research was obtained from the National Health and Medical Research Council of Australia, the University of Adelaide, and the Australian Research Council. The funder had no role in study design, data collection

Abstract

Cells on the surface of the mesonephros give rise to replicating Gonadal Ridge Epithelial-Like (GREL) cells, the first somatic cells of the gonadal ridge. Later germ cells associate with the GREL cells in the ovigerous cords, and the GREL cells subsequently give rise to the granulosa cells in follicles. To examine these events further, 27 bovine fetal ovaries of different gestational ages were collected and prepared for immunohistochemical localisation of collagen type I and Ki67 to identify regions of the ovary and cell proliferation, respectively. The non-stromal cortical areas (collagen-negative) containing GREL cells and germ cells and later in development, the follicles with oocytes and granulosa cells, were analysed morphometrically. Another set of ovaries (n = 17) were collected and the expression of genes associated with germ cell lineages and GREL/granulosa cells were quantitated by RT-PCR. The total volume of non-stromal areas in the cortex increased significantly and progressively with ovarian development, plateauing at the time the surface epithelium developed. However, the proportion of non-stromal areas in the cortex declined significantly and progressively throughout gestation, largely due to a cessation in growth of the non-stroma cells and the continued growth of stroma. The proliferation index in the non-stromal area was very high initially and then declined substantially at the time follicles formed. Thereafter, it remained low. The numerical density of the non-stromal cells was relatively constant throughout ovarian development. The expression levels of a number of genes across gestation either increased (*AMH*, *FSHR*, *ESR1*, *INHBA)*, declined (*CYP19A1*, *ESR2*, *ALDH1A1*, *DSG2*, *OCT4*, *LGR5*) or showed no particular pattern (*CCND2*, *CTNNB1*, *DAZL*, *FOXL2*, *GATA4*, *IGFBP3*, *KRT19*, *NR5A1*, *RARRES1*, *VASA*, *WNT2B*). Many of the genes whose expression changed across gestation, were positively or negatively correlated with each other. The relationships between these genes may reflect their roles in the important events

and analysis, decision to publish, or preparation of the manuscript.

Competing interests: The authors have declared that no competing interests exist.

such as the transition of ovigerous cords to follicles, oogonia to oocytes or GREL cells to granulosa cells.

Introduction

The ovary development starts with the formation of the genital ridge formed by increased proliferation of the surface epithelium on the ventromedial side of the mesonephros. These proliferating cells are now termed the gonadal ridge epithelial-like (GREL) cells [1] and express cytokeratin 19 (*KRT19*) and desmosomal proteins such as desmoglein-2 (*DSG2*) and plakophilin-2. Later in development the GREL cells differentiate into pre-granulosa or surface epithelial cells. The formation of the genital ridge requires the expression of empty spiracles homeobox protein 2 (*EMX2*), LIM homeobox protein 9 (*LHX9*), Wilms Tumor 1 (*WT1*), steroidogenic factor (*SF1*/*NR5A1*) [2, 3] and GATA binding protein 4 (*GATA4*) [4]. The absence of sex determining region Y (*SRY*) results in the bipotential gonad committing to the ovary-determining pathway. This is accompanied by the expression of Wingless-related MMTV integration site family member 4 (*Wnt4*) [5], β-catenin (*CTNNB1*) [6], R-spondin 1 (*Rspo1*) [7] and Forkhead box L2 (*FOXL2*) [8, 9] [10].

The primordial germ cells arise from the yolk sac and migrate under the influence of kit ligand and its receptor towards the gonad. After colonising the developing gonad composed of GREL cells, the primordial germ cells start proliferating and express pluripotency markers such as octamer binding protein 4 (*OCT4*) [11]. Later in the developing ovary the mitotically active germ cells, termed oogonia, become oocytes after entering meiosis. The entry into meiosis is accompanied by expression of deleted in azoospermia-like (*DAZL*) and induced by retinoic acid, which is synthesised by aldehyde dehydrogenases (*ALDH1-3*) [12]. Subsequently germ cells switch from expressing *DAZL* to *VASA* [11]. Oocytes arrest in the dictyate phase of meiosis I until shortly before ovulation when meiosis is resumed.

The ovarian stroma arises from the mesonephric connective tissue after breakdown of the basal lamina underlying the surface epithelium [1]. This stroma, including its vasculature, penetrates the mass of GREL cells and PGCs/oogonia, branching as it does and so corralling the GREL and germ cells into forming the ovigerous cords [1]. Subsequently the continued expansion of the stroma [13] likely separates the ovigerous cords into smaller cords until the first primordial follicles are formed, consisting of one layer of flattened pre-granulosa cells and a meiotically-arrested oocyte [1, 14, 15]. In the mouse, two different populations of primordial follicles have been identified [16]. Medullary follicles are activated shortly after birth, while cortically located follicles activate gradually throughout life. In addition, medullary pre-granulosa cells express *FOXL2* while cortical pre-granulosa cells express Leucine Rich Repeat Containing G Protein-Coupled Receptor 5 (*LGR5*) [17].

Lateral spread of the stroma below the surface of the ovary partitions some GRELs to the surface, which become the surface epithelial cells. Fibroblasts, the major cell type of the stroma, express Nuclear Receptor Subfamily 2 Group F Member 2 (*NR2F2/COUP-TFII*) and produce fibrillar extracellular matrix components, such as collagen type I (*COL1A1*), collagen type III (*COL3A1*) and fibrillins (*FBN1-3*) [1, 18]. Members of the TGFβ-superfamily have important roles during oogenesis and folliculogenesis [19–22]. Activin or inhibin (*INHBA*), anti-Mullerian hormone (*AMH*) and FSH receptor (*FSHR*) are involved in granulosa cell proliferation and differentiation [19].

Many of the recent discoveries of the developing ovary come from studies of mice using lineage tracing techniques and manipulation of gene expression during development. Whilst these have helped to make substantial gains on our knowledge, these studies generally have not fully assessed the behaviours of the different somatic cell types, such as GREL cells and fibroblasts, and the processes that these can undertake in unison at different stages of ovarian development. To address this, the current study first examined replication of non-stromal cells and the changes in their volume during gestation and compares this with changes in the stromal compartments [13]. The expression patterns of genes related to germ and stem cells, and GREL and granulosa cells in fetal ovaries across gestation were also examined and discussed in relation to changes occurring in the ovary at those times. Genes related to stromal cells and the extracellular matrix have been discussed in a companion publication [23].

Materials and methods

Tissues

Fetuses of pregnant *Bos taurus* cows were collected at T&R Pastoral abattoir at Murray Bridge, SA, Australia and then transported on ice to the laboratory. Crown-rump length was measured to estimate gestational age [24]. Some ovaries were fixed in 4% paraformaldehyde (Merck Pty Ltd, Kilsyth, VIC, Australia) in 0.1 M phosphate buffer (pH 7.4) for immunohistochemistry and morphometric analyses (n = 27) and others from different animals were frozen at -80˚C for subsequent RNA analyses (n = 17).

Gender determination

To confirm the gender of young fetuses (smaller than 8 cm), genomic DNA was extracted from the tail samples using the Wizard SV Genomic DNA Purification System (Promega Australia, Alexandria, NSW, Australia) according to the manufacturer's instructions. Genomic DNA was amplified with a primer pair (sense primer: `5′-TCACTCCTGCAAAAGGAGCA-3′`, antisense primer: `5′-TTATTGTGGCCCAGGCTTG-3′`), specific for a region in the SRY-determining sequence, and primers specific for the 18S ribosomal RNA gene sequence [25] in separate reactions. SRY product sequences were verified by automated sequencing (3730 DNA analyser; Applied Biosystems, Mulgrave, VIC, Australia).

Histology and immunohistochemistry

Fixed ovaries, as used previously [13] were embedded in paraffin using a Leica EG 1140H (Leica Microsystems, Nussloch, Germany). Six-μm sections were cut using a CM1850 V2.2 Leica microtome (Leica Microsystems), mounted on Superfrost glass slides (HD Scientific Supplies, Wetherill Park, NSW, Australia) and stored at RT until used for haematoxylin-eosin (H&E) staining and immunohistochemistry. H&E-stained sections were used for sample grouping based on histological morphology: stage 1—ovigerous cord formation (n = 7, 79 ± 6 days of gestation), stage 2—ovigerous cord breakdown (n = 4, 127 ± 6 days), stage 3—follicle formation (n = 3, 173 ± 12 days), stage 4—ovarian surface epithelium formation (n = 8, 234 ± 9 days) and stage 5—tunica albuginea formation (n = 5, 264 ± 6 days)] [13].

An indirect immunofluorescence method was used for colocalisation of Ki-67 and collagen type I as previously described in detail previously [13] and illustrated in Fig 1. Primary antibodies were mouse anti-human Ki67 (1:800; M7240/MIB-1; DAKO Australia Pty Ltd, Botany, NSW, Australia) to identify proliferating cells in combination with rabbit anti-human collagen type I (1:400; 20μg/ml; ab34710; Abcam, Sapphire Bioscience Pty Ltd., Waterloo, NSW, Australia) to identify the stroma. Secondary antibodies were donkey anti-mouse IgG conjugated

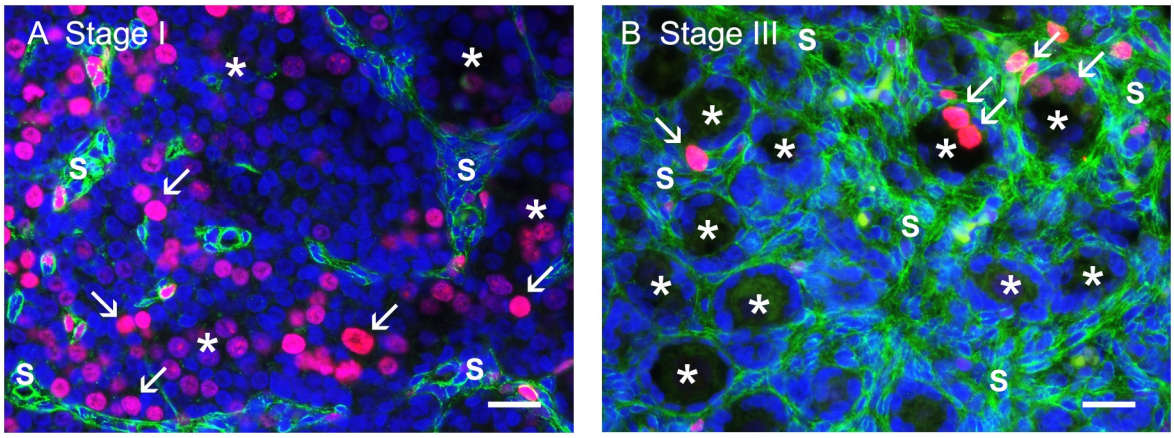

Fig 1. Representative photographs from stage I (the formation of ovigerous cords) (A) and stage III (the formation of follicles) (B). Collagen type I (green) is colocalised with the proliferation marker Ki67 (red, marked with arrow). Nuclei are counterstained with DAPI. Scale bar: 25 μm. * ovigerous cords/ primordial follicles, S stroma.

https://doi.org/10.1371/journal.pone.0214130.g001

to Cy3 (1:100; 715-166-151) and biotin-SP-conjugated AffiniPure donkey anti-rabbit IgG (1:100; 711-066-152) followed by fluorescein DTAF-conjugated streptavidin (1:100; 016-010-084). All secondary antibodies and conjugated streptavidin were from Jackson ImmunoResearch Laboratories Inc. (West Grove, PA, USA). Cell nuclei were counterstained with 4',6'-diamidino-2-phenylindole dihydrochloride (DAPI) solution (Molecular Probes, Eugene, OR, USA). Non-immune mouse and rabbit sera (Sigma-Aldrich, New South Wales, Australia) were used as negative controls. All sections were photographed with an Olympus BX50 microscope (Olympus, Tokyo, Japan) with an epifluorescence attachment and a Spot RT digital camera (Diagnostic Instruments, Sterling Heights, MI, USA) at a magnification of 40x.

Image analyses

Fluorescence images were analysed with ImageJ software. For this purpose, the cortical region of the largest section from each ovary was examined morphometrically. Ten fields of view were analysed for ovaries from fetuses with CRL < 50 cm (182 days of gestation) and 20 fields of view (0.06 mm^2) for a CRL > 50 cm. The image analysis procedure has been described in detail by Hartanti et al. [13]. To identify the amount of non-stromal compartment in the cortex containing the ovigerous cords and follicles, the stromal area identified by collagen type I staining was subtracted from the total cortical area. The proportion of non-stromal in the cortex (volume density) was calculated as the ratio between the non-stromal area and the total cortical area. The ovarian volume was estimated using the ovarian weight and assuming a density of 1g/cm^3. The volume of the cortex was then derived from the volume of the ovary and the volume density of the cortex. Similarly, the non-stromal volume was calculated from the volume of cortex and the volume density of non-stroma in the cortex. The number of proliferating cells (KI-67 positive) in ovigerous cords or follicles and the total number of non-stromal cells (DAPI positive) in a field of view were counted. Results of proliferating cells were presented as a proliferation index and as a numerical density in the non-stromal area.

RNA extraction, cDNA synthesis and quantitative real time PCR

All fetal ovary samples for RNA sample extraction were homogenised with 1 ml of Trizol (Cat # 15596–026, Thermo Fisher Scientific, Waltham, MA, USA) each for two 10 s cycles at 3,500 rpm in a PowerLyzer 24 Bench Top Bead-Based Homogeniser (MoBio, Carlsbad, Ca, USA).

The samples were then processed according to the standard Trizol protocol and resuspended in 30 μl of nuclease free H_2O. Ten μg or less of each sample was treated with 2 U of DNAse 1 for 20 min at 37˚ C and the enzyme removed using DNAse inactivation reagent (Thermo Fisher Scientific). Two hundred ng of DNAse-treated RNA was used for reverse transcription reactions with or without Superscript RT III (Thermo Fisher Scientific) to generate cDNA or negative control to detect genomic contaminant, respectively.

PCR primers pairs were designed where possible to span intron-exon junctions or from different exons for quantitative real time PCR (qRT-PCR) using the free web-based software programs, Primer3 plus (Rozen and Skaletsky) and Net primer (PREMIER Biosoft, Palo Alto, CA, USA), based on the Reference RNA sequences available in NCBI (Table 1). The cDNA was diluted from 1 in 4 to 1in 1000 and pooled from 10 samples to generate 5 standards which were used to establish a standard curve for testing primer combinations for quantitative real time PCR. Only those assays which gave a single sharp peak by melt curve analysis and achieved an amplification efficiency of 0.9–1.1 and an R^2 value $\geq$ 0.98 were used for quantitation of gene expression.

The reactions were performed in duplicate on a Fluidigm Biomark HD instrument (San Francisco, CA, USA) using the following protocol. The reaction started with a pre-amplification step consisting of a 95˚C hold for 10 min, followed by 12 cycles of 95˚C for 15 s and 60˚C for 4 min each using 50 nM of each primer and 2.5 μl of cDNA in 10 μl. The amplified product was then diluted 1 in 5 and added in 0.05 μl to the final reaction volume of 0.1 μl in a 48 x 48 plate which contained 500 nM of each primer per assay. The final amplification conditions were a 60 s activation step at 95˚C, followed by 30 cycles of 96˚C denaturation for 5 s and 60˚C annealing/extension for 20 s using SsoFast EvaGreen Supermix with Low ROX (Biorad, Hercules, Ca, USA) which contained a fluorescent intercalating agent for measuring amplification. The expression values for each gene were determined as the mean of the ratio of $2^{-\Delta Ct}$ for the target gene to the mean of *RPL32* and *PPIA* because this gene combination was determined to be the most stable across all samples out of *RPL32*, *PPIA*, *ACTB* and *GAPDH* with a value of 0.056 using the Normfinder program.

Statistical analyses

ANOVA and post-hoc statistical calculations using Tukey's test were performed using GraphPad Prism version 6.00 (GraphPad Software Inc., La Jolla, CA, USA) following log transformation where appropriate to normalise the raw data distribution. Pearson's correlations across all target genes and samples were performed on the data in Partek Genomics Suite (St Louis, MI, USA). Hierarchical clustering by gene only was also performed on the data using the Euclidian algorithm for dissimilarity with average linkage in Partek to generate a heatmap of relative gene expression. Prior to clustering, the raw data were first normalised by adjusting the mean expression across all samples for each gene to zero and the standard deviation to one.

Results and discussion

Morphometric analyses of non-stromal component of the ovarian cortex

The non-stromal area of the cortex includes ovigerous cords at early stages (stages I and II) and follicles at later stages (stages III to V) (Fig 1). Its total volume increased significantly and progressively with ovarian development but plateaued at stage IV (Fig 2A). However the proportion of non-stroma in the cortex (volume density) declined significantly and progressively throughout gestation (Fig 2B), largely due to a cessation at stage III as indicated by the plateauing in its volume, and the continued growth of stroma after stage III [13].

Table 1. List of genes and primers used for qRT-PCR.

Gene name	Gene Symbol	GenBank Accession No.	Primers (5'-3')	Size (bp)
Aldehyde dehydrogenase 1 family, member A1	*ALDH1A1*	NM_174239.2	F: GCGGAAACACAGTGGTTGTC	150
			R: GAGAAGAAATGGCTGCCCCT	
Anti Mullerian Hormone	*AMH*	NM_173890.1	F: ACACCGGCAAGCTCCTCAT	67
			R: CACCATGTTTGGGACGTGG	
Cyclin D2	*CCND2*	NM_001076372.1	F: GGTGGATCTCCTGGCAAAGA	98
			R: ACGGTACTGCTGCAGGCTATTC	
Catenin (cadherin-associated protein), beta 1, 88kDa	*CTNNB1*	NM_001076141	F: GAATTGACAAAACTGCTGAATGATG	102
			R: GATGGCGTGTCTCGAAGCTT	
Cytochrome P450 family 19 subfamily A, member 1	*CYP19A1*	NM_174305.1	F: ATGCTTTTGGAAGTGCTG	143
			R: TTAGCGCTCGAGGCAC	
Deleted in azoospermia-like	*DAZL*	NM_001081725.1	F: ACGTTTTGCCCAGTGAATGC	98
			R: TACCACCGTCTGTATGCTTCTG	
Desmoglein 2	*DSG2*	NM_001192172.2	F: AAGACCCTCGCTGAAGTTTG	84
			R: TGCTTCTCTTGCGGGTTTTG	
Estrogen receptor 1	*ESR1*	NM_001001443.1	F: GTCCACCTTTTGGAATGTGC	124
			R: ATTTTCCCTGGTTCCTGTCC	
Estrogen receptor 2	*ESR2*	NM_174051.3	F: TCGACTTCGGAAGTGCTATGAG	136
			R: ACCGTTCCTCTTGGTTTTGC	
Forkhead box L2	*FOXL2*	NM_001031750.1	F: AGAATAGCATCCGCCACAAC	127
			R: CCCTTCTCGAACATGTCCTC	
Follicle stimulating hormone receptor (FSHR)	*FSHR*	NM_174061.1	F: GACCCTGATGCCTTCCAGA	74
			R: TGGCAAGTGCTTAATACCTGTGTT	
Glyceraldehyde 3-phosphate dehydrogenase	*GAPDH*	NM_001034034.2	F: ACCACTTTGGCATCGTGGAG	76
			R: GGGCCATCCACAGTCTTCTG	
GATA binding protein 4	*GATA4*	NM_001192877.1	F: CAGGAGGCAAAAATGCTAGG	82
			R: ATCACCCGTCGTCTTTCTTC	
Inhibin, beta A	*INHBA*	NM_174363.2	F: ATCATCACGTTCGCGGAATC	144
			R: ACTTTGCTCCGGGTCCTGTT	
Keratin 19	*KRT19*	NM_001015600.3	F: AAGCTTTGCGCATGAGTGTG	97
			R: TCAATCTGCATCTCCAGGTCAG	
Leucine-rich repeat containing G protein-coupled receptor 5	*LGR5*	NM_001277226	F: TTGGGAGATCTGCTTTTCAACA	64
			R: TGTGAGGCGCCATTCAAA	
Nuclear receptor subfamily 5, group A, member 1	*NR5A1*	NM_174403.2	F: CAGACCTTCATCTCCATCGTG	147
			R: CTTGCCATGCTGAATCTGAC	
POU class 5 homeobox 1	*OCT4*	NM_174580.2	F: AGGCTTTGCAGCTCAGTTTC	79
			R: TTGTTGTCAGCTTCCTCCAC	
Ribosomal protein L19	*RPL19*	NM_001040516.1	F: GATCCGGAAGCTGATCAAAG	113
			R: TACCCATATGCCTGCCTTTC	
DEAD (Asp-Glu-Ala-Asp) box polypeptide 4	*VASA*	NM_001007819.1	F: ATGAAGCTGATCGCATGCTG	91
			R: TGACGCTGTTCCTTTGATGG	
Wingless-type MMTV integration site family, member 2B	*WNT2B*	NM_001099363	F: CGGACTGACCTGGTCTACTTTG	67
			R: AGGGAACCTGCAGCCTTGT	

F is forward and R is the reverse primer sequence.

https://doi.org/10.1371/journal.pone.0214130.t001

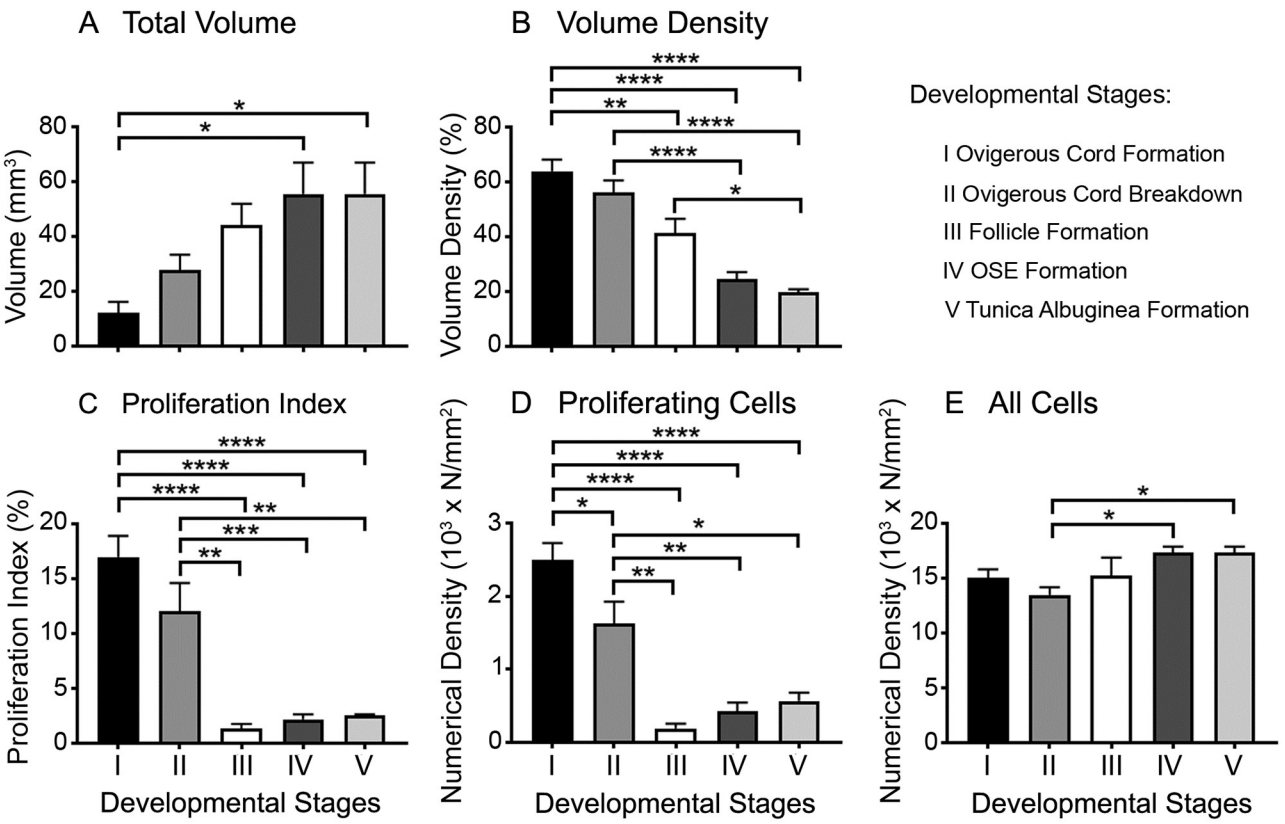

Fig 2. Morphometric analyses of the non-stromal component of the ovarian cortex during bovine fetal ovarian development. Data are presented as means ± SEM. Samples were grouped into 5 stages of ovarian development based on their histological morphology: ovigerous cord formation (n = 7, stage I), ovigerous cord breakdown (n = 4, stage II), follicle formation (n = 3, stage III), ovarian surface epithelium (OSE) formation (n = 8, stage IV) and tunica albuginea formation (n = 5, stage V). One-way ANOVA with post hoc Tuckey's test were used to analyse the data. * $P < 0.05$, ** $P < 0.01$, *** $P < 0.001$, **** $P < 0.0001$. Volume density is the percentage of cortex that is the non-stromal compartment.

https://doi.org/10.1371/journal.pone.0214130.g002

Expression of Ki67 was used to estimate the percentage of proliferating cells at different developmental stages. The proliferation index of the non-stromal area was highest at stages I and II, declining substantially at stage III and remaining very low thereafter (Fig 2C). Furthermore, we calculated the numerical density of proliferating cells and all cells in the non-stromal compartment. The numerical density of proliferating cells also significantly declined at stage III and then remained low (Fig 2D). The observed high proliferation in the early stages of ovarian development relates mainly to the germ cells (identified based on their morphology), which show high mitotic activity after settling in the genital ridge and differentiation into oogonia [26, 27]. The decline in proliferation at stage III was, however, accompanied by an increase of the total volume of non-stroma and further small percentage increases in stages IV and V. These were presumably due to increases in the volumes of germ cells from oogonia to oocytes and at the very latter stages activation of follicles.

The highest number of ovarian germ cells is reached around day 90 in the bovine [28] and 182 days in human gestation [29]. The oogonia start to enter meiosis between weeks 10–11 in human [29] and arrest in prophase I until puberty. However in the human fetal ovary, mitotic oogonia occur simultaneously to meiotic oocytes until five months of gestation [29, 30], which is the time point after stage II in our study when the proliferation drops drastically. This is the time when the first primordial follicles are formed, between days 90–140 in the bovine [31] and days 126–133 in the human [32]. However, the numerical density of proliferating cells did

slightly increase from stage III to stage IV but not significantly. This is consistent with the activation of primordial follicles toward differentiation into primary follicles, which occurs in the human between 238–266 days [33] and in the bovine between 140–210 days of gestation [31], corresponding to stage III and IV in our study. The subsequent differentiation of the primary follicles to secondary follicles is accompanied by granulosa cell proliferation to form the multiple layers of granulosa cells in more mature follicles. The first secondary follicles have been observed in the bovine fetal ovary after day 210 of gestation [31], which corresponds with stage IV in our study. The numerical density of all the non-stromal cells appeared relatively stable throughout ovarian development (Fig 2E).

Germ cell markers

The pluripotency marker *OCT4* was highly expressed in early ovarian development and then declined rapidly by 120 days of gestation at stage II (Fig 2A and S1A Fig). This is expected as germ cells first undergo mitosis and then differentiate and enter meiosis I after colonising the developing ovary. *DAZL* and *VASA* levels were very low at 58 and 66 days, with higher but variable levels during the rest of gestation (Fig 3B and 3D and S1B–S1D Fig). As we observed previously in early gestation in particular [1] the developmental stage of ovaries can differ from one animal to another at the same age. This variability might be caused by environmental effects such as nutrition during gestation [34]. We therefore devised a classification system of developmental stages I to V for the morphometric analysis instead of using gestational age. However, for the RNA analyses the ovaries were not collected for histological classification and so we have analysed those data by age of the fetus as determined by the crown-rump length [24], which could contribute to some variability.

In species with long gestations and large ovaries, like the bovine, different portions of the ovary can be at different developmental stages, especially since follicle formation commences

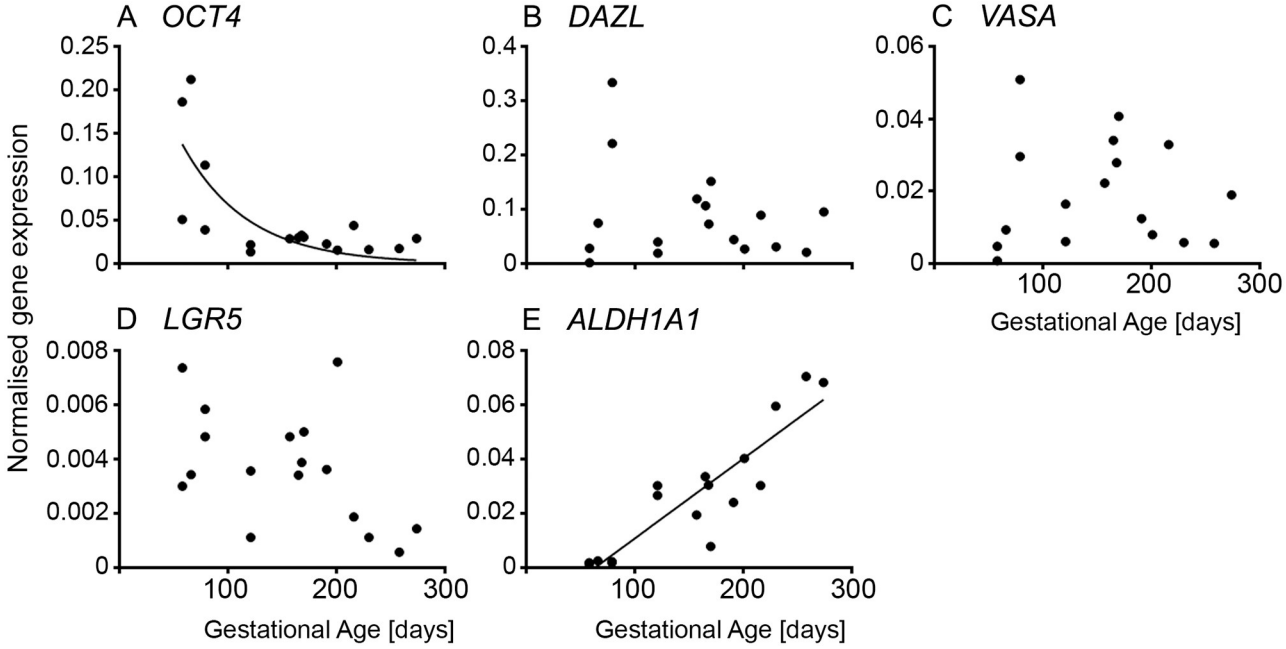

Fig 3. Germ and stem cell-specific genes in fetal ovarian development. Expression levels of genes for each animal are plotted against gestational age in days (n = 16 or 17).

https://doi.org/10.1371/journal.pone.0214130.g003

at the medullary-cortical interface and progresses over time in the direction of the surface. Thus it is not unusual to have follicles near the medulla that have not only formed but have commenced growing whilst at the same time ovigerous cords are still present near the surface of the ovary (Fig 3K of [1]). Consequently, although individual germ cells sequentially express *OCT4*, *DAZL* and then *VASA* [1], this does not necessarily occur with RNA analyses of whole ovaries as the isolated RNA from whole ovaries reflects the total of all the developmental stages of germ cells at any one time in each ovary.

Stem cell markers

Whilst *LGR5* and *ALDH1A1* are stem cell markers, their expression could indicate development of either germ cells or somatic stem cells that exist in the ovary [15]. The stem cell marker *LGR5* declined throughout gestation to low levels in the third trimester (Fig 2B–2D and S1B–S1D Fig). A recent study in human fetal ovaries reported an initial decline in *LGR5* expression levels from 8–11 weeks to 14–16 weeks, but then no further change towards 17–21 weeks [35]. Furthermore, treatment with BMP-4 of cultured fetal cells (~ 14 weeks) increased the expression of *LGR5*. In the mouse, *lgr5* expression first occurs at E13.5 in cells on the surface and subsurface. The subsurface expression declines towards postnatal day 1 and is diminished by postnatal day 7. The *lgr5*-positive cells in the subsurface express *foxl2*, a granulosa cell marker, and the *lgr5*-positive cells on the surface express cytokeratin 8, a surface epithelial marker [36]. *lgr5*-positive cells are also involved in the rapid remodelling of the surface epithelial layer after ovulation, suggesting that they have stem cell properties [36]. On the other hand, Rastetter *et al*. [17] found that *lgr5* is expressed in somatic cells, which neither express *foxl2* nor *nr2f2* (*coup-tfII*), and that *lgr5* expression increases after sex determination in the fetal mouse ovary until birth.

The expression of *ALDH1A1*, another stem cell marker, is barely detectable prior to day 79 but increased significantly and linearly thereafter (Fig 2E and S1E Fig). *ALDH1A1*, encodes retinaldehyde dehydrogenase, and is involved in the last step of the synthesis of retinoic acid, which is crucial for entry of germ cells into meiosis. This would explain the observed increase in the bovine as the entry of oogonia into meiosis occurs around 80 to 130 days of gestation [37]. In contrast, a study in the human fetal ovary analysing the mRNA levels of *ALDH1A1* at 8–9 weeks (undifferentiated primordial germ cells), 14–16 weeks (meiotic entry) and 17–20 weeks (primordial follicle formation), reported a trend of declining expression [12]. The significance of *ALDH1A1* expression in the bovine ovary is yet to be determined.

GREL cell markers

KRT19 has been shown to be expressed in GREL cells [1]. Later in development when the surface epithelium has formed it is more highly expressed in the ovarian surface epithelial cells [1]. *KRT19* expression was highest at mid gestation (Fig 4A and S2A Fig). Cytokeratin 19 has been previously detected in the undifferentiated gonadal blastemal, in the somatic cells of ovigerous cords and early follicle stages in the mice [38] and in the rat [39] as well as in the ovigerous cords and primordial, primary and preovulatory follicles in human [40]. *DSG2* is a desmosomal protein also expressed in GREL cells and later in the ovarian surface epithelial cells [1]. It was more highly expressed in early gestation and then declined steadily across gestation (Fig 4B and S2B Fig). This expression pattern can be explained by the differentiation of GREL cells into either surface epithelial cells or granulosa cells with the latter not expressing desmosomes [41].

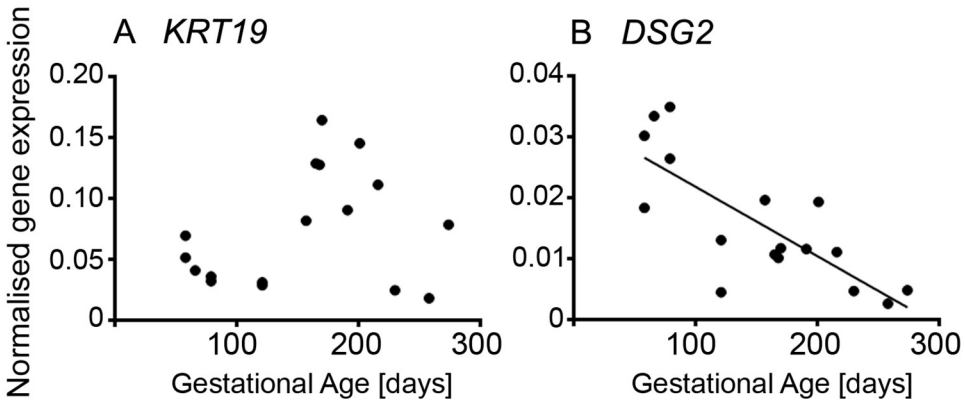

Fig 4. Genes specific for GREL cells in fetal ovarian development. Expression levels of genes for each animal are plotted against gestational age in days (n = 16 or 17).

https://doi.org/10.1371/journal.pone.0214130.g004

Granulosa cell markers

The genes analysed in this section were chosen based on knowledge of either direct expression in fetal ovaries or in some cases inferred from expression observed in adult ovarian granulosa cells, such as *CYP19A1*. Analysing the expression of genes specific for granulosa cells revealed three patterns (Fig 4 and S3 Fig). Firstly, genes which increased throughout gestation and these include: *AMH* (Fig 5B and S3B Fig), *FSHR* (Fig 5C and S3C Fig), *ESR1* (Fig 5E and S3E Fig) and *INHBA* (Fig 5G and S3G Fig). *AMH* and *FSHR* have low expression in early and mid-gestation and then a rapid increase towards the end of gestation, whereas the expression of *ESR1* and *INHBA* increased steadily across gestation. The increase in *AMH* as well as *FSHR* is consistent with follicle activation and growth, which commences around day 180 of gestation in the bovine [42]. *AMH* is expressed by granulosa cells from preantral and small antral follicles [43] in women. *FSHR* is expressed in the granulosa cells of primary and secondary follicles with greater expression at antral stages in the bovine fetus [42]. Similar to our findings in this study, *INHBA* increases in second trimester human ovaries [44]. In rodents, *inhba* is expressed at low levels in the fetal ovary [45, 46], which might be due to follicle formation occurring mostly after birth. There is no detectable *INHBA* expression in ovine fetal ovaries throughout gestation [47]. However, the activin/inhibin βA subunit has been immunolocalised to clusters of maturing oocytes in the fetal human ovary (18 weeks) prior to primordial follicle formation, suggesting a role of activin A in the proliferation and survival of germ cells at this stage [44]. Activin-βA mRNA is expressed in the goat from 36 dpc until adulthood and has been considered to be a candidate co-factor for the action of FOXL2 on *CYP19A1* [48]. Treatment of fetal human ovary transplants with activin A increased proliferation of oogonia [44], and in neonatal mice the number of primordial follicles [49]. The corresponding receptors; ActRIIA, ActRIIB and ALK4 (ActRIB) are expressed by germ cells and the latter two additionally in stromal cells or other somatic cells amongst germ cell nests. The signalling targets of activin, Smad 2 and 3, have been localised to the nuclei of stromal cells and other somatic cells between germ cells nests and also to pre-granulosa cells of primordial follicles in human fetal ovaries between 14 and 20 weeks [50]. The expression of *INHBA* is increased in fetal human ovary transplants treated with prostaglandin E2, which in vivo is synthesised by germ cells [51]. Activins not only affect germ cell proliferation and survival, but are also involved in the later stages of follicle differentiation, granulosa cell proliferation and oocyte maturation [reviewed in [52, 53]].

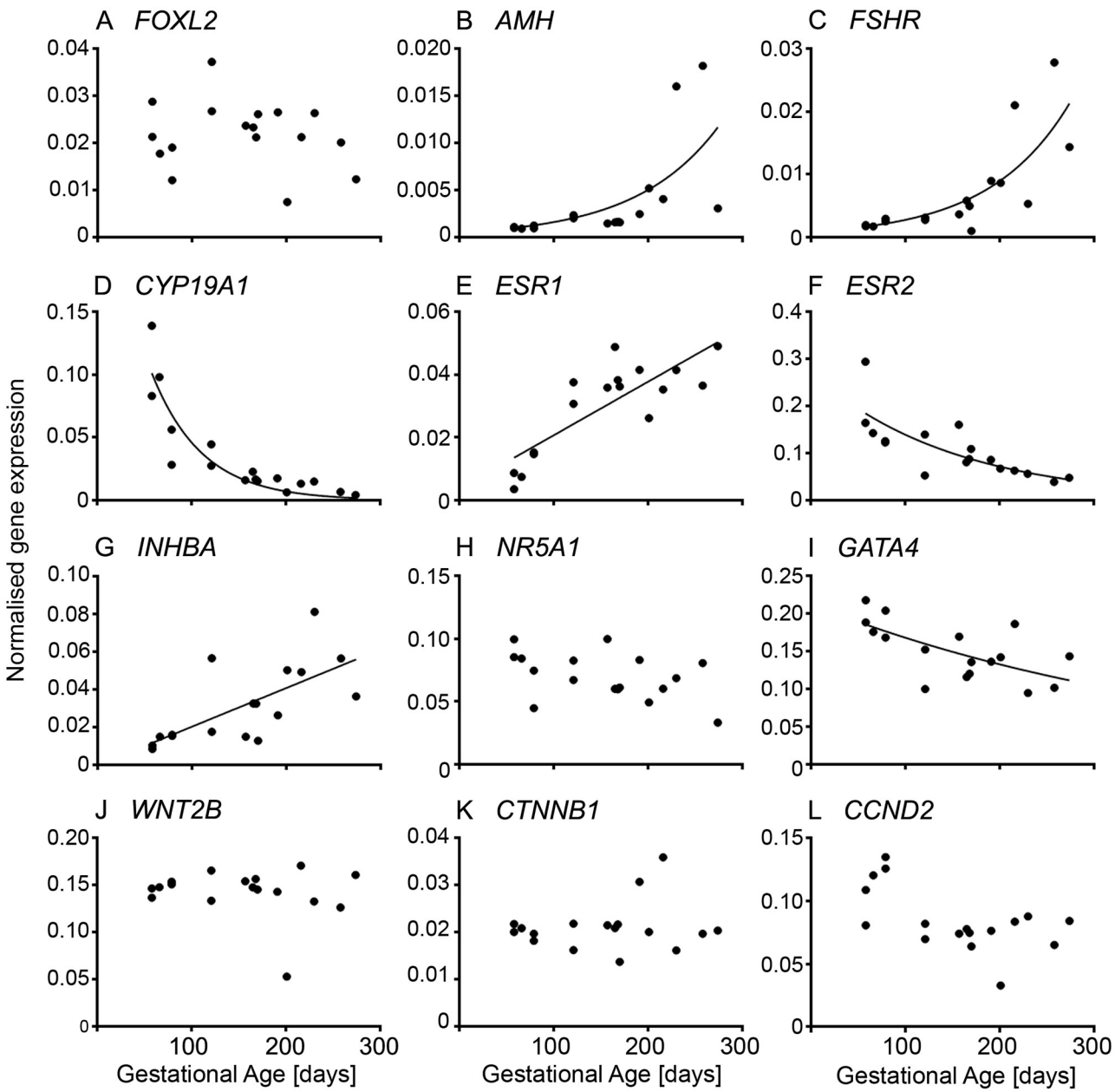

Fig 5. Granulosa cell-specific genes in fetal ovarian development. Expression levels of genes for each animal are plotted against gestational age in days (n = 16 or 17).

https://doi.org/10.1371/journal.pone.0214130.g005

Genes whose expression declined with gestational age included: *CYP19A1* (Fig 5D and S3D Fig), *ESR2* (Fig 5F and S3F Fig), *GATA4* (Fig 5I and S3I Fig) and the cell cycle gene *CCND2* (Fig 5L and S3L Fig). Previous studies in cattle focusing on the expression of P450arom (encoded by *CYP19A1*) and the two oestrogen receptors, ERα (*ESR1*) and ERβ (*ESR2*), throughout gestation, found no decline in the expression of P450arom and ERβ. The results were determined by in situ hybridisation and immunolocalisation [54, 55], neither of which is as accurate as the quantitative RT-PCR used in the current study. Both mRNAs and proteins were expressed by surface epithelial cells, pre-granulosa cells, granulosa cells and cells in the

medulla, which are likely stromal cells [54, 55]. On the other hand, it has been reported that oestradiol is produced early in ovarian development and declines when follicle growth occurs later in gestation [31, 56], which could explain the high expression levels we observed in the first trimester and the following observed decline in *CYP19A1* and *ESR2* throughout gestation. In the goat, *CYP19A1* and *ESR2* expression has been detected from 36 dpc and *ESR1* from 40 dpc until adulthood [48, 57]. P450arom is localised to somatic cells, which express *FOXL2*, in the medullar region, whereas ERβ is also localised to germ cells [48]. In mice, *ESR1* is mainly expressed in interstitial (stromal) cells, whereas *ESR2* is expressed in granulosa cells [58]. So, the observed increase of *ESR1* could be due to the expansion of the stromal compartment [13] throughout ovarian development. We previously found that a high cell proliferation rate occurs in stromal and non-stromal compartments early in ovarian development which then declines towards mid- and late gestation [13], which would also explain the higher expression levels of *CCND2* observed early in gestation.

GATA-4 plays an important role during formation of the genital ridge and sex determination [59, 60]. Down-stream targets of GATA-4 are *AMH* [60, 61], *SF1* (alias *NR5A1*), *STAR* (steroidogenic acute regulatory protein), *CYP19A1* [62, 63], *INHA* and *INHBB* [64] and *FOXL2* [65, 66]. It is constantly expressed in the bipotential gonad and after sex differentiation in the ovary in fetal mice [67] and pigs [68]. In the postnatal mice, GATA-4 is found in the granulosa and thecal cells of growing follicles and stromal cells, but not in luteal cells [67], in contrast to the human adult ovary [69]. In human fetal ovaries, *GATA4* is expressed in stromal and pre-granulosa cells and later in granulosa cells with the highest expression occurring early in development (~ 14 weeks) [70]–similar to our findings. Downregulation or loss of GATA-4 caused interruptions in folliculogenesis and recruitment of granulosa and thecal cells resulting in lower numbers of primary follicles and activated follicles, and increased follicular atresia in the existing follicles in adult mouse ovaries [59, 71]. GATA-4 appears to have an anti-apoptotic effect on granulosa cells [70]. A more recent study in the developing mouse ovary suggests that cells expressing *gata4* are precursor cells of granulosa cells and that there are two populations; one which additionally expresses p27, and one which is not expressing p27 and which is therefore highly proliferative [72]. The latter gives rise to the granulosa cells, which will form the so-called cortical follicles from E18.5 to postnatal day 5, whereas the other population is involved in the formation of the medullar follicles between E12.5 and E14.5 [17, 72].

FOXL2 (Fig 5A and S3A Fig), *NR5A1* (Fig 5H and S3H Fig), *WNT2B* (Fig 5J and S3J Fig) and *CTNNB1* (Fig 5K and S3K Fig) are constitutively expressed throughout gestation. FOXL2 has been described as a female-specific marker from sex differentiation until adulthood [73, 74] and has been shown to be expressed early in bovine ovarian development in the GREL cells which are enclosed together with the germ cells in the ovigerous cords, and in the granulosa cells later in development after follicle formation and growth occur [1]. In the human fetal ovary, *FOXL2* expression increases from 9 weeks to 18 weeks, when the first follicles are formed [32]. The protein localises to the somatic cells streams in the ovarian stroma and the somatic cells intermingled with germ cells, which will become pre-granulosa cells, as well as pre-granulosa cells of primordial follicles. In goats, FOXL2 directly activates *CYP19A1* by binding to its promotor 2 [48] but in the current study no correlation between *FOXL2* and *CYP19A1* was observed, suggesting that there could be differences between species in the regulation of *CYP19A1*. *NR5A1* has been shown to be expressed in the fetal bovine ovary in the cells of the ovigerous cords and on the ovarian surface and later in development in the granulosa cells of growing follicles [1]. In the adult bovine ovary, *NR5A1* (alias *SF-1*) is expressed by granulosa and thecal cells [75]. In contrast to the bovine fetal ovary, *NR5A1* is expressed in the genital ridge of mice and rats until sex determination and then declines in the female until late in gestation in the mice (E18.5) [76] or until after birth in the rat [77] when primordial follicle

formation occurs. In the human fetal ovary, persistent *NR5A1* expression has been shown from the point of genital ridge formation up to week 15 of gestation [78] while expression later than this is unclear. Little is known about the expression of *WNT2B* in the ovary. In the immature rat, *WNT2B* has been localised to the ovarian surface epithelium by in situ hybridisation and has also been shown to be expressed in ovarian cancer cell lines [79]. Previously, Hatziros et al. [80] found in the bovine adult ovary that *WNT2B* is downregulated in the theca interna of large (9–12 mm) compared to small (3–5 mm) healthy follicles, whereas the Wnt inhibitor *FRZB* was upregulated.

Relationships between cell markers

Pearson correlation analyses (Tables 2 and 3) of genes expressed in germ and stem cells show a very strong positive correlation between *DAZL* and *VASA*, which both are reported to induce meiotic progression in germ cells [81]. *OCT4* and *LGR5* show both a negative correlation with *ALDH1A1* but a strong positive correlation with the GREL cell marker *DSG2*. *ALDH1A1* was negatively correlated with *DSG2*. There were also correlations between germ cell markers and granulosa cell markers. *OCT4* positively correlated with *CYP19A1* and *CCDN2*, and negatively with *ESR1* and *INHBA*. *DAZL* showed a positive correlation with *CCDN2* and *VASA* but was negatively correlated with *NR5A1*. The stem cell marker *LGR5* correlated negatively with *AMH*, *FSHR* and *INHBA* but positively with *DSG2*. The other stem cell-specific marker, *ALDH1A1*, appears to be strongly correlated with many granulosa cell-specific genes; positively with *AMH*, *FSHR*, *ESR1* and *INHBA*, and negatively with *CYP19A1*, *ESR2*, *GATA4* and *CCDN2*. This is interesting as retinoic acid signalling appears to be essential for induction of meiosis of germ cells but not for granulosa cell specification, at least in mice [82]. On the other

Table 2. Pearson's correlation coefficients between markers for germ and stem cells and all genes examined and gestational age. The intensity of the background colour indicates the strength of the significance of the correlation. Blue is a negative correlation and red is a positive correlation. ($^{a}P < 0.05$, $^{b}P < 0.01$, $^{c}P < 0.01$; n = 17).

		Germ and stem cell markers				
		OCT4	***DAZL***	***VASA***	***LGR5***	***ALDH1A1***
Gestational age		**-0.620[b]**	-0.242	-0.022	-0.479	**0.897[d]**
Germ and stem cell markers	***OCT4***		0.055	-0.162	0.375	**-0.560[a]**
	DAZL	0.055		**0.858[c]**	0.284	-0.388
	VASA	-0.162	**0.858[c]**		0.191	-0.267
	LGR5	0.375	0.284	0.191		**-0.603[a]**
	ALDH1A1	**-0.560[a]**	-0.388	-0.267	**-0.603[a]**	
GREL cell markers	***KRT19***	-0.197	0.003	0.368	0.394	-0.042
	DSG2	**0.779[c]**	0.429	0.131	**0.714[b]**	**-0.789[c]**
Granulosa cell markers	***FOXL2***	-0.160	-0.368	-0.196	-0.297	-0.137
	AMH	-0.319	-0.332	-0.367	**-0.506[a]**	**0.737[c]**
	FSHR	-0.314	-0.215	-0.093	**-0.499[a]**	**0.702[b]**
	CYP19A1	**0.651[b]**	-0.155	-0.360	0.188	**-0.645[b]**
	ESR1	**-0.695[b]**	-0.14	0.171	-0.476	**0.729[c]**
	ESR2	0.378	0.008	-0.137	0.351	**-0.712[b]**
	INHBA	**-0.486[a]**	-0.375	-0.292	**-0.573[a]**	**0.795[c]**
	NR5A1	0.315	-0.381	**-0.487[a]**	0.053	-0.380
	GATA4	0.474	0.346	0.178	0.432	**-0.701[c]**
	WNT2B	0.169	0.319	0.415	-0.322	-0.212
	CTNNB1	-0.039	-0.138	0.011	-0.204	0.011
	CCND2	**0.633[b]**	**0.597[a]**	0.301	0.098	**-0.512[a]**

https://doi.org/10.1371/journal.pone.0214130.t002

Table 3. Pearson's correlation coefficients between markers for GREL and granulosa cells and all genes examined and gestational age. The intensity of the background colour indicates the strength of the significance of the correlation. Blue is a negative correlation and red is a positive correlation. ($^{a}P < 0.05$, $^{b}P < 0.01$, $^{c}P < 0.01$; n = 17).

		GREL cell marker		Granulosa cell markers											
		KRT19	*DSG2*	*FOXL2*	*AMH*	*FSHR*	*CYP19A1*	*ESR1*	*ESR2*	*INHBA*	*NR5A1*	*GATA4*	*WNT2B*	*CTNNB1*	*CCND2*
Gestational age		0.276	**-0.775^{c}**	-0.180	**0.618^{b}**	**0.733^{c}**	**-0.794^{c}**	**0.822^{c}**	**-0.744^{c}**	**0.687^{b}**	-0.441	**-0.622^{b}**	-0.156	0.175	**-0.587^{a}**
Germ and stem cell markers	***DAZL***	0.003	0.429	-0.368	-0.332	-0.215	-0.155	-0.140	0.008	-0.375	-0.381	0.346	0.319	-0.138	**0.597^{a}**
	VASA	0.368	0.131	-0.196	-0.367	-0.093	-0.360	0.171	-0.137	-0.292	**-0.487^{a}**	0.178	0.415	0.011	0.301
	OCT4	-0.197	**0.779^{c}**	-0.16	-0.319	-0.314	**0.651^{b}**	**-0.695^{b}**	0.378	**-0.486^{a}**	0.315	0.474	0.169	-0.039	**0.633^{b}**
	LGR5	0.394	**0.714^{b}**	-0.297	**-0.506^{a}**	**-0.499^{a}**	0.188	-0.476	0.351	**-0.573^{a}**	0.053	0.432	-0.322	-0.204	0.098
	ALDH1A1	-0.042	**-0.789^{c}**	-0.137	**0.737^{c}**	**0.702^{b}**	**-0.645^{b}**	**0.729^{c}**	**-0.712^{b}**	**0.795^{c}**	-0.38	**-0.701^{b}**	-0.212	0.011	**-0.512^{a}**
GREL cell markers	***KRT19***		-0.123	-0.208	-0.323	-0.018	-0.34	0.333	-0.146	-0.107	-0.343	-0.076	-0.204	0.171	**-0.525^{a}**
	DSG2	-0.123		-0.277	**-0.517^{a}**	**-0.507^{a}**	**0.587^{a}**	**-0.820^{c}**	**0.549^{a}**	**-0.673^{b}**	0.27	**0.705^{b}**	0.011	-0.100	**0.647^{b}**
Granulosa cell markers	***FOXL2***	-0.208	-0.277		-0.019	-0.248	0.24	0.11	0.306	-0.101	**0.598^{a}**	-0.137	0.418	-0.062	-0.092
	AMH	-0.323	**-0.517^{a}**	-0.019		**0.624^{b}**	-0.368	0.317	-0.481	**0.766^{c}**	-0.011	**-0.563^{a}**	-0.305	-0.130	-0.277
	FSHR	-0.018	**-0.507^{a}**	-0.248	**0.624^{b}**		-0.472	0.408	**-0.548^{a}**	**0.520^{a}**	-0.211	-0.259	-0.057	0.447	-0.314
	CYP19A1	-0.34	**0.587^{a}**	0.24	-0.368	-0.472		**-0.832^{c}**	**0.853^{c}**	**-0.549^{a}**	**0.581^{a}**	**0.632^{b}**	0.111	-0.085	0.439
	ESR1	0.333	**-0.820^{c}**	0.11	0.317	0.408	**-0.832^{c}**		-0.733	**0.550^{a}**	-0.410	**-0.754^{c}**	0.089	0.121	**-0.531^{a}**
	ESR2	-0.146	**0.549^{a}**	0.306	-0.481	**-0.548^{a}**	**0.853^{c}**	**-0.733^{c}**		**-0.721^{b}**	**0.626^{b}**	**0.748^{c}**	0.152	-0.122	0.297
	INHBA	-0.107	**-0.673^{b}**	-0.101	**0.766^{c}**	**0.520^{a}**	**-0.549^{a}**	**0.550^{b}**	**-0.721^{b}**		-0.339	**-0.699^{b}**	-0.360	0.120	-0.424
	NR5A1	-0.343	0.270	**0.598^{a}**	-0.011	-0.211	**0.581^{a}**	-0.410	**0.626^{b}**	-0.339		0.240	0.118	0.036	0.068
	GATA4	-0.076	**0.705^{b}**	-0.137	**-0.563^{a}**	-0.259	**0.632^{b}**	**-0.754^{c}**	**0.748^{c}**	**-0.699^{b}**	0.240		0.238	0.223	**0.512^{a}**
	WNT2B	-0.204	0.011	0.418	-0.305	-0.057	0.111	0.089	0.152	-0.360	0.118	0.238		0.185	**0.555^{a}**
	CTNNB1	0.171	-0.100	-0.062	-0.130	0.447	-0.085	0.121	-0.122	0.120	0.036	0.223	0.185		-0.052
	CCND2	**-0.525^{a}**	**0.647^{b}**	-0.092	-0.277	-0.314	0.439	**-0.531^{a}**	0.297	-0.424	0.068	**0.512^{a}**	**0.555^{a}**	-0.052	

https://doi.org/10.1371/journal.pone.0214130.t003

hand, *DSG2* was positively correlated with *CYP19A1*, *ESR2*, *GATA4* and *CCDN2*, and negatively with *AMH*, *FSHR*, *ESR1* and *INHBA* and additionally negatively with *ALDH1A1*.

Surprisingly, no correlation existed between *KRT19* and *DSG2*. Furthermore, *KRT19* was only correlated to *CCDN2*. Correlation analysis of the genes within the group of granulosa cell-specific markers, revealed a positive correlation between *FOXL2* and *NR5A1*, between *AMH*, *FSHR* and *INHBA*, between *FSHR* and *ESR2*, and between *WNT2B* and *CCDN2*. *CYP19A1* correlated positively with *ESR2*, *NR5A1* and *GATA4*, but negatively with *ESR1* and *INHBA*. As expected, *ESR1* was positively correlated with *INHBA*, but negatively with *ESR2*, *GATA4* and *CCDN2*. *ESR2* showed a positive correlation with *GATA4*, whereas *INHBA* was negatively correlated with *GATA4*. Additionally, *GATA4* was positively correlated with *CCDN2*. Interestingly, *CTNNB1* showed no correlation with any of the germ, stem, GREL or granulosa cell markers.

The multitude of both negative and positive correlations, therefore, in expression of genes in germ and somatic cells, and the correlations amongst genes expressed within a cell lineage, suggest a degree of co-regulation or coordination of behaviours of different cells. Since many of these genes either increase or decrease during gestation, the relationships between these genes may reflect their physiological role in the transition of ovigerous cords to follicles, oogonia to oocytes or GREL cells to granulosa cells.

Gene expression and ovarian development. The early cortex is characterised by formation and growth of the ovigerous cords which occurs by replication of GREL and germ cells. It is characterised by high proliferation indices (Fig 2) and high expression of *CCND2* (Fig 5).

The germ cells are less mature and there is high expression of *OCT4* and *DAZL*. GREL cells are present at that stage and they have extensive cell junctions and express *DSG2* which is elevated at these early stages (Fig 4). *CYP19* and *ESR2* are also highly expressed at these early stages suggesting that oestradiol might have a role then. Subsequently the cords begin to break into smaller clusters of cells (stage II) and *ESR1* and *ALDH1* are upregulated. The change in *ESR1* probably reflects maturation of oogonia into oocytes. As development continues and follicles are being formed (stage III), cell replication declines and *CYP19A1*, *ESR2* and *OCT4* are down regulated. This, in conjunction with continued expansion of stroma [13], may have led to a decline in the proportion of the non-stromal compartments in the cortex. The changes in *OCT4* signal maturation of the germ cells. At later stages follicle activation commences and expression of genes in growing follicles, *FSHR*, *AMH* and *INHBA*, is increased. *KRT19* is expressed in the surface epithelium [1] and its expression is increased as the surface epithelium is formed (stage IV).

Conclusions

The expression of many genes increased across gestation matched by a concomitant decline in others, with many being positively or negatively correlated, even when potentially not expressed in the same cell type. These relationships between genes may reflect their roles in the transition of ovigerous cords to follicles, oogonia to oocytes, or GREL cells to granulosa cells. Further work is now underway to identify genes that act as regulators and those that are regulated.

Supporting information

S1 Fig. Expression of germ and stem cell markers. Measurement of gene expression of germ and stem cell markers in fetal ovaries by q-PCR graphed by trimester (1st, 2nd and 3rd trimesters have n = 5, n = 7 and n = 5 animals, respectively). Mean ± SEM are shown and statistical differences between trimesters are shown as **, or ****, indicating $P < 0.01$ or $P < 0.0001$, respectively.
(TIF)

S2 Fig. Expression GREL cell markers. Measurement of gene expression of GREL cell markers in fetal ovaries by q-PCR graphed by trimester (1st, 2nd and 3rd trimesters have n = 5, n = 7 and n = 5 animals, respectively). Mean ± SEM are shown and statistical differences between trimesters are shown as ***, indicating $P < 0.001$, respectively.
(TIF)

S3 Fig. Expression of granulosa cell markers. Measurement of gene expression of granulosa cell markers in fetal ovaries by q-PCR graphed by trimester (1st, 2nd and 3rd trimesters have n = 5, n = 7 and n = 5 animals, respectively). Mean ± SEM are shown and statistical differences between trimesters are shown as *, **, ***, or ****, indicating $P < 0.05$, $P < 0.01$, $P < 0.001$ or $P < 0.0001$, respectively.
(TIF)

Acknowledgments

We would like to thank Thomas Foods International, Murray Bridge, SA for the supply of fetal bovine ovaries and Mrs. Wendy Bonner for the collection of these tissues from the abattoir.

Author Contributions

Conceptualization: Katja Hummitzsch, Nicholas Hatzirodos, Helen F. Irving-Rodgers, Richard A. Anderson, Raymond J. Rodgers.

Data curation: Helen F. Irving-Rodgers, Monica D. Hartanti.

Formal analysis: Katja Hummitzsch, Nicholas Hatzirodos, Monica D. Hartanti, Viv E. A. Perry.

Funding acquisition: Viv E. A. Perry, Richard A. Anderson, Raymond J. Rodgers.

Investigation: Katja Hummitzsch, Nicholas Hatzirodos, Helen F. Irving-Rodgers, Monica D. Hartanti.

Methodology: Katja Hummitzsch, Nicholas Hatzirodos, Helen F. Irving-Rodgers, Monica D. Hartanti.

Project administration: Helen F. Irving-Rodgers, Raymond J. Rodgers.

Supervision: Raymond J. Rodgers.

Writing – original draft: Katja Hummitzsch, Nicholas Hatzirodos, Monica D. Hartanti.

Writing – review & editing: Helen F. Irving-Rodgers, Viv E. A. Perry, Richard A. Anderson, Raymond J. Rodgers.

References

1. Hummitzsch K, Irving-Rodgers HF, Hatzirodos N, Bonner W, Sabatier L, Reinhardt DP, et al. A new model of development of the mammalian ovary and follicles. PLoS One. 2013; 8(2):e55578. https://doi.org/10.1371/journal.pone.0055578 PMID: 23409002.
2. Eggers S, Ohnesorg T, Sinclair A. Genetic regulation of mammalian gonad development. Nat Rev Endocrinol. 2014; 10(11):673–83. Epub 2014/09/24. https://doi.org/10.1038/nrendo.2014.163 PMID: 25246082.
3. She ZY, Yang WX. Molecular mechanisms involved in mammalian primary sex determination. J Mol Endocrinol. 2014; 53(1):R21–37. Epub 2014/06/15. https://doi.org/10.1530/JME-14-0018 PMID: 24928207.
4. Hu YC, Okumura LM, Page DC. Gata4 is required for formation of the genital ridge in mice. PLoS genetics. 2013; 9(7):e1003629. Epub 2013/07/23. https://doi.org/10.1371/journal.pgen.1003629 PMID: 23874227.
5. Vainio S, Heikkila M, Kispert A, Chin N, McMahon AP. Female development in mammals is regulated by Wnt-4 signalling. Nature. 1999; 397(6718):405–9. Epub 1999/02/16. https://doi.org/10.1038/17068 PMID: 9989404.
6. Maatouk DM, DiNapoli L, Alvers A, Parker KL, Taketo MM, Capel B. Stabilization of beta-catenin in XY gonads causes male-to-female sex-reversal. Hum Mol Genet. 2008; 17(19):2949–55. Epub 2008/07/12. https://doi.org/10.1093/hmg/ddn193 PMID: 18617533.
7. Tomizuka K, Horikoshi K, Kitada R, Sugawara Y, Iba Y, Kojima A, et al. R-spondin1 plays an essential role in ovarian development through positively regulating Wnt-4 signaling. Hum Mol Genet. 2008; 17(9):1278–91. Epub 2008/02/06. https://doi.org/10.1093/hmg/ddn036 PMID: 18250097.
8. Ottolenghi C, Omari S, Garcia-Ortiz JE, Uda M, Crisponi L, Forabosco A, et al. Foxl2 is required for commitment to ovary differentiation. Hum Mol Genet. 2005; 14(14):2053–62. Epub 2005/06/10. https://doi.org/10.1093/hmg/ddi210 PMID: 15944199.
9. Uhlenhaut NH, Jakob S, Anlag K, Eisenberger T, Sekido R, Kress J, et al. Somatic sex reprogramming of adult ovaries to testes by FOXL2 ablation. Cell. 2009; 139(6):1130–42. Epub 2009/12/17. https://doi.org/10.1016/j.cell.2009.11.021 PMID: 20005806.
10. Pannetier M, Chassot AA, Chaboissier MC, Pailhoux E. Involvement of FOXL2 and RSPO1 in Ovarian Determination, Development, and Maintenance in Mammals. Sex Dev. 2016; 10(4):167–84. Epub 2016/09/21. https://doi.org/10.1159/000448667 PMID: 27649556.
11. Anderson RA, Fulton N, Cowan G, Coutts S, Saunders PT. Conserved and divergent patterns of expression of DAZL, VASA and OCT4 in the germ cells of the human fetal ovary and testis. BMC Dev Biol. 2007; 7:136. https://doi.org/10.1186/1471-213X-7-136 PMID: 18088417.

12. Childs AJ, Cowan G, Kinnell HL, Anderson RA, Saunders PT. Retinoic Acid signalling and the control of meiotic entry in the human fetal gonad. PLoS One. 2011; 6(6):e20249. Epub 2011/06/16. https://doi.org/10.1371/journal.pone.0020249 PMID: 21674038.

13. Hartanti MD, Hummitzsch K, Irving-Rodgers HF, Bonner WM, KJ C, Anderson RA, et al. Morphometric and gene expression analyses of stromal expansion during bovine fetal ovarian development. Reprod Fert Devel (in press). 2018:(in press).

14. Hummitzsch K, Irving-Rodgers HF, Schwartz J, Rodgers RJ. Development of the Mammalian Ovary and Follicles. In: Leung PCK, Adashi E, editors. The Ovary. 3 ed: Academic Press; 2018.

15. Hummitzsch K, Anderson RA, Wilhelm D, Wu J, Telfer EE, Russell DL, et al. Stem cells, progenitor cells, and lineage decisions in the ovary. Endocr Rev. 2015; 36(1):65–91. Epub 2014/12/30. https://doi.org/10.1210/er.2014-1079 PMID: 25541635.

16. Mork L, Maatouk DM, McMahon JA, Guo JJ, Zhang P, McMahon AP, et al. Temporal differences in granulosa cell specification in the ovary reflect distinct follicle fates in mice. Biol Reprod. 2012; 86(2):37. Epub 2011/10/07. https://doi.org/10.1095/biolreprod.111.095208 PMID: 21976597.

17. Rastetter RH, Bernard P, Palmer JS, Chassot AA, Chen H, Western PS, et al. Marker genes identify three somatic cell types in the fetal mouse ovary. Dev Biol. 2014; 394(2):242–52. Epub 2014/08/27. https://doi.org/10.1016/j.ydbio.2014.08.013 PMID: 25158167.

18. Hatzirodos N, Bayne RA, Irving-Rodgers HF, Hummitzsch K, Sabatier L, Lee S, et al. Linkage of regulators of TGF-beta activity in the fetal ovary to polycystic ovary syndrome. FASEB J. 2011; 25(7):2256–65. Epub 2011/03/18. https://doi.org/10.1096/fj.11-181099 PMID: 21411746.

19. Knight PG, Glister C. TGF-beta superfamily members and ovarian follicle development. Reproduction. 2006; 132(2):191–206. Epub 2006/08/04. https://doi.org/10.1530/rep.1.01074 PMID: 16885529.

20. Drummond AE. TGFbeta signalling in the development of ovarian function. Cell Tissue Res. 2005; 322 (1):107–15. Epub 2005/06/29. https://doi.org/10.1007/s00441-005-1153-1 PMID: 15983782.

21. Field SL, Dasgupta T, Cummings M, Orsi NM. Cytokines in ovarian folliculogenesis, oocyte maturation and luteinisation. Mol Reprod Dev. 2014; 81(4):284–314. https://doi.org/10.1002/mrd.22285 PMID: 24273059 Epub 2013 Dec 13.

22. Rossi RO, Costa JJ, Silva AW, Saraiva MV, Van den Hurk R, Silva JR. The bone morphogenetic protein system and the regulation of ovarian follicle development in mammals. Zygote. 2016; 24(1):1–17. https://doi.org/10.1017/S096719941400077X PMID: 25613521 Epub 2015 Jan 23.

23. Hatzirodos N, Hummitzsch K, Irving-Rodgers HF, Breen J, Perry VEA, Anderson RA, et al. Transcript abundance of stromal and thecal cell related genes during bovine ovarian development. PLoS One. 2019; 14(3):e0213575. https://doi.org/10.1371/journal.pone.0213575 PMID: 30856218 eCollection 2019.

24. Russe I. Oogenesis in cattle and sheep. Bibl Anat. 1983; 24:77–92. PMID: 6847603.

25. Irving-Rodgers HF, Harland ML, Sullivan TR, Rodgers RJ. Studies of granulosa cell maturation in dominant and subordinate bovine follicles: novel extracellular matrix focimatrix is co-ordinately regulated with cholesterol side-chain cleavage CYP11A1. Reproduction. 2009; 137(5):825–34. Epub 2009/03/06. https://doi.org/10.1530/REP-08-0485 PMID: 19261832.

26. De Felici M. Origin, Migration, and Proliferation of Human Primordial Germ Cells. In: Coticchio GA, Coticchio D.F.; De Santis L., editor. Oogenesis. XII 2013. p. 364.

27. Findlay JK, Hutt KJ, Hickey M, Anderson RA. How Is the Number of Primordial Follicles in the Ovarian Reserve Established? Biol Reprod. 2015; 93(5):111. Epub 2015/10/02. https://doi.org/10.1095/biolreprod.115.133652 PMID: 26423124.

28. Tanaka Y, Nakada K, Moriyoshi M, Sawamukai Y. Appearance and number of follicles and change in the concentration of serum FSH in female bovine fetuses. Reproduction. 2001; 121(5):777–82. Epub 2001/06/28. PMID: 11427166.

29. Kurilo LF. Oogenesis in antenatal development in man. Hum Genet. 1981; 57(1):86–92. Epub 1981/01/01. PMID: 7262874.

30. Baker TG. A quantitative and cytological study of germ cell in human ovaries. Proc R Soc Lond B Biol Sci. 1963; 158:417–33. Epub 1963/10/22. https://doi.org/10.1098/rspb.1963.0055 PMID: 14070052.

31. Yang MY, Fortune JE. The capacity of primordial follicles in fetal bovine ovaries to initiate growth in vitro develops during mid-gestation and is associated with meiotic arrest of oocytes. Biol Reprod. 2008; 78(6):1153–61. https://doi.org/10.1095/biolreprod.107.066688 PMID: 18305225.

32. Duffin K, Bayne RA, Childs AJ, Collins C, Anderson RA. The forkhead transcription factor FOXL2 is expressed in somatic cells of the human ovary prior to follicle formation. Mol Hum Reprod. 2009; 15 (12):771–7. Epub 2009/08/27. https://doi.org/10.1093/molehr/gap065 PMID: 19706741.

33. Forabosco A, Sforza C. Establishment of ovarian reserve: a quantitative morphometric study of the developing human ovary. Fertil Steril. 2007; 88(3):675–83. Epub 2007/04/17. https://doi.org/10.1016/j.fertnstert.2006.11.191 PMID: 17434504.

34. Copping KJ, Ruiz-Diaz MD, Rutland CS, Mongan NP, Callaghan MJ, McMillen IC, et al. Peri-conception and first trimester diet modifies reproductive development in bulls. Reprod Fertil Dev. 2017. Epub 2017/11/16. https://doi.org/10.1071/rd17102 PMID: 29141178.

35. Bayne RA, Donnachie DJ, Kinnell HL, Childs AJ, Anderson RA. BMP signalling in human fetal ovary somatic cells is modulated in a gene-specific fashion by GREM1 and GREM2. Mol Hum Reprod. 2016; 22(9):622–33. https://doi.org/10.1093/molehr/gaw044 PMID: 27385727.

36. Ng A, Tan S, Singh G, Rizk P, Swathi Y, Tan TZ, et al. Lgr5 marks stem/progenitor cells in ovary and tubal epithelia. Nature cell biology. 2014; 16(8):745–57. Epub 2014/07/07. https://doi.org/10.1038/ncb3000 PMID: 24997521.

37. Lavoir MC, Basrur PK, Betteridge KJ. Isolation and identification of germ cells from fetal bovine ovaries. Mol Reprod Dev. 1994; 37(4):413–24. Epub 1994/04/01. https://doi.org/10.1002/mrd.1080370408 PMID: 8011326.

38. Appert A, Fridmacher V, Locquet O, Magre S. Patterns of keratins 8, 18 and 19 during gonadal differentiation in the mouse: sex- and time-dependent expression of keratin 19. Differentiation. 1998; 63(5):273–84. Epub 1998/11/12. https://doi.org/10.1046/j.1432-0436.1998.6350273.x PMID: 9810706.

39. Fridmacher V, Locquet O, Magre S. Differential expression of acidic cytokeratins 18 and 19 during sexual differentiation of the rat gonad. Development. 1992; 115(2):503–17. PMID: 1385062

40. Loffler S, Horn LC, Weber W, Spanel-Borowski K. The transient disappearance of cytokeratin in human fetal and adult ovaries. Anat Embryol (Berl). 2000; 201(3):207–15. Epub 2000/02/09. PMID: 10664181.

41. Mora JM, Fenwick MA, Castle L, Baithun M, Ryder TA, Mobberley M, et al. Characterization and significance of adhesion and junction-related proteins in mouse ovarian follicles. Biol Reprod. 2012; 86(5):153, 1–14. Epub 2012/02/11. https://doi.org/10.1095/biolreprod.111.096156 PMID: 22321830.

42. Wandji SA, Pelletier G, Sirard MA. Ontogeny and cellular localization of 125I-labeled insulin-like growth factor-I, 125I-labeled follicle-stimulating hormone, and 125I-labeled human chorionic gonadotropin binding sites in ovaries from bovine fetuses and neonatal calves. Biol Reprod. 1992; 47(5):814–22. PMID: 1477207.

43. Visser JA, de Jong FH, Laven JS, Themmen AP. Anti-Mullerian hormone: a new marker for ovarian function. Reproduction. 2006; 131(1):1–9. Epub 2006/01/03. https://doi.org/10.1530/rep.1.00529 PMID: 16388003.

44. Martins da Silva SJ, Bayne RA, Cambray N, Hartley PS, McNeilly AS, Anderson RA. Expression of activin subunits and receptors in the developing human ovary: activin A promotes germ cell survival and proliferation before primordial follicle formation. Dev Biol. 2004; 266(2):334–45. Epub 2004/01/24. PMID: 14738881.

45. Roberts VJ, Sawchenko PE, Vale W. Expression of inhibin/activin subunit messenger ribonucleic acids during rat embryogenesis. Endocrinology. 1991; 128(6):3122–9. Epub 1991/06/01. https://doi.org/10.1210/endo-128-6-3122 PMID: 2036981.

46. Mendis SH, Meachem SJ, Sarraj MA, Loveland KL. Activin A balances Sertoli and germ cell proliferation in the fetal mouse testis. Biol Reprod. 2011; 84(2):379–91. Epub 2010/10/12. https://doi.org/10.1095/biolreprod.110.086231 PMID: 20926807.

47. Engelhardt H, Harkness LM, Thomas GB, Brooks AN, McNeilly AS, Baird DT. Expression of inhibin alpha- and beta A-subunit mRNA and protein in the fetal sheep ovary throughout gestation. Mol Cell Endocrinol. 1995; 107(2):141–7. Epub 1995/02/01. PMID: 7768325.

48. Pannetier M, Fabre S, Batista F, Kocer A, Renault L, Jolivet G, et al. FOXL2 activates P450 aromatase gene transcription: towards a better characterization of the early steps of mammalian ovarian development. J Mol Endocrinol. 2006; 36(3):399–413. Epub 2006/05/25. https://doi.org/10.1677/jme.1.01947 PMID: 16720712.

49. Bristol-Gould SK, Kreeger PK, Selkirk CG, Kilen SM, Cook RW, Kipp JL, et al. Postnatal regulation of germ cells by activin: the establishment of the initial follicle pool. Dev Biol. 2006; 298(1):132–48. Epub 2006/08/26. https://doi.org/10.1016/j.ydbio.2006.06.025 PMID: 16930587.

50. Coutts SM, Childs AJ, Fulton N, Collins C, Bayne RA, McNeilly AS, et al. Activin signals via SMAD2/3 between germ and somatic cells in the human fetal ovary and regulates kit ligand expression. Dev Biol. 2008; 314(1):189–99. Epub 2008/01/02. https://doi.org/10.1016/j.ydbio.2007.11.026 PMID: 18166170.

51. Bayne RA, Eddie SL, Collins CS, Childs AJ, Jabbour HN, Anderson RA. Prostaglandin E2 as a regulator of germ cells during ovarian development. J Clin Endocrinol Metab. 2009; 94(10):4053–60. Epub 2009/07/16. https://doi.org/10.1210/jc.2009-0755 PMID: 19602557.

52. de Kretser DM, Hedger MP, Loveland KL, Phillips DJ. Inhibins, activins and follistatin in reproduction. Hum Reprod Update. 2002; 8(6):529–41. Epub 2002/12/25. PMID: 12498423.

53. Phillips DJ. Activins, inhibins and follistatins in the large domestic species. Domestic animal endocrinology. 2005; 28(1):1–16. Epub 2004/12/29. https://doi.org/10.1016/j.domaniend.2004.05.006 PMID: 15620803.

54. Burkhart MN, Juengel JL, Smith PR, Heath DA, Perry GA, Smith MF, et al. Morphological development and characterization of aromatase and estrogen receptors alpha and beta in fetal ovaries of cattle from days 110 to 250. Anim Reprod Sci. 2010; 117(1–2):43–54. Epub 2009/03/21. https://doi.org/10.1016/j.anireprosci.2009.02.010 PMID: 19299095.

55. Garverick HA, Juengel JL, Smith P, Heath DA, Burkhart MN, Perry GA, et al. Development of the ovary and ontongeny of mRNA and protein for P450 aromatase (arom) and estrogen receptors (ER) alpha and beta during early fetal life in cattle. Anim Reprod Sci. 2010; 117(1–2):24–33. Epub 2009/06/09. https://doi.org/10.1016/j.anireprosci.2009.05.004 PMID: 19501990.

56. Shemesh M. Estradiol-17 beta biosynthesis by the early bovine fetal ovary during the active and refractory phases. Biol Reprod. 1980; 23(3):577–82. Epub 1980/10/01. PMID: 6256013.

57. Pailhoux E, Vigier B, Vaiman D, Servel N, Chaffaux S, Cribiu EP, et al. Ontogenesis of female-to-male sex-reversal in XX polled goats. Dev Dyn. 2002; 224(1):39–50. Epub 2002/05/02. https://doi.org/10.1002/dvdy.10083 PMID: 11984872.

58. Jefferson WN, Couse JF, Banks EP, Korach KS, Newbold RR. Expression of estrogen receptor beta is developmentally regulated in reproductive tissues of male and female mice. Biol Reprod. 2000; 62 (2):310–7. Epub 2000/01/22. PMID: 10642567.

59. Heikinheimo M, Ermolaeva M, Bielinska M, Rahman NA, Narita N, Huhtaniemi IT, et al. Expression and hormonal regulation of transcription factors GATA-4 and GATA-6 in the mouse ovary. Endocrinology. 1997; 138(8):3505–14. Epub 1997/08/01. https://doi.org/10.1210/endo.138.8.5350 PMID: 9231805.

60. Viger RS, Mertineit C, Trasler JM, Nemer M. Transcription factor GATA-4 is expressed in a sexually dimorphic pattern during mouse gonadal development and is a potent activator of the Mullerian inhibiting substance promoter. Development. 1998; 125(14):2665–75. Epub 1998/06/24. PMID: 9636081.

61. Tremblay JJ, Viger RS. Transcription factor GATA-4 enhances Mullerian inhibiting substance gene transcription through a direct interaction with the nuclear receptor SF-1. Mol Endocrinol. 1999; 13(8):1388–401. Epub 1999/08/14. https://doi.org/10.1210/mend.13.8.0330 PMID: 10446911.

62. Tremblay JJ, Viger RS. GATA factors differentially activate multiple gonadal promoters through conserved GATA regulatory elements. Endocrinology. 2001; 142(3):977–86. Epub 2001/02/22. https://doi.org/10.1210/endo.142.3.7995 PMID: 11181509.

63. Monga R, Ghai S, Datta TK, Singh D. Involvement of transcription factor GATA-4 in regulation of CYP19 gene during folliculogenesis and luteinization in buffalo ovary. J Steroid Biochem Mol Biol. 2012; 130(1–2):45–56. https://doi.org/10.1016/j.jsbmb.2011.12.010 PMID: 22245270 Epub 2 Jan 9.

64. Feng ZM, Wu AZ, Zhang Z, Chen CL. GATA-1 and GATA-4 transactivate inhibin/activin beta-B-subunit gene transcription in testicular cells. Mol Endocrinol. 2000; 14(11):1820–35. Epub 2000/11/15. https://doi.org/10.1210/mend.14.11.0549 PMID: 11075815.

65. Manuylov NL, Smagulova FO, Leach L, Tevosian SG. Ovarian development in mice requires the GATA4-FOG2 transcription complex. Development. 2008; 135(22):3731–43. https://doi.org/10.1242/dev.024653 PMID: 18927154.

66. Padua MB, Fox SC, Jiang T, Morse DA, Tevosian SG. Simultaneous gene deletion of gata4 and gata6 leads to early disruption of follicular development and germ cell loss in the murine ovary. Biol Reprod. 2014; 91(1):24. Epub 2014/06/06. https://doi.org/10.1095/biolreprod.113.117002 PMID: 24899573.

67. Anttonen M, Ketola I, Parviainen H, Pusa AK, Heikinheimo M. FOG-2 and GATA-4 Are coexpressed in the mouse ovary and can modulate mullerian-inhibiting substance expression. Biol Reprod. 2003; 68 (4):1333–40. https://doi.org/10.1095/biolreprod.102.008599 PMID: 12606418.

68. McCoard SA, Wise TH, Fahrenkrug SC, Ford JJ. Temporal and spatial localization patterns of Gata4 during porcine gonadogenesis. Biol Reprod. 2001; 65(2):366–74. Epub 2001/07/24. PMID: 11466202.

69. Laitinen MP, Anttonen M, Ketola I, Wilson DB, Ritvos O, Butzow R, et al. Transcription factors GATA-4 and GATA-6 and a GATA family cofactor, FOG-2, are expressed in human ovary and sex cord-derived ovarian tumors. J Clin Endocrinol Metab. 2000; 85(9):3476–83. Epub 2000/09/22. https://doi.org/10.1210/jcem.85.9.6828 PMID: 10999851.

70. Vaskivuo TE, Anttonen M, Herva R, Billig H, Dorland M, te Velde ER, et al. Survival of human ovarian follicles from fetal to adult life: apoptosis, apoptosis-related proteins, and transcription factor GATA-4. J Clin Endocrinol Metab. 2001; 86(7):3421–9. Epub 2001/07/10. https://doi.org/10.1210/jcem.86.7.7679 PMID: 11443219.

71. Efimenko E, Padua MB, Manuylov NL, Fox SC, Morse DA, Tevosian SG. The transcription factor GATA4 is required for follicular development and normal ovarian function. Dev Biol. 2013; 381(1):144–58. https://doi.org/10.1016/j.ydbio.2013.06.004 PMID: 23769843.

72. Gustin SE, Hogg K, Stringer JM, Rastetter RH, Pelosi E, Miles DC, et al. WNT/beta-catenin and p27/FOXL2 differentially regulate supporting cell proliferation in the developing ovary. Dev Biol. 2016; 412(2):250–60. https://doi.org/10.1016/j.ydbio.2016.02.024 PMID: 26939755.

73. Cocquet J, Pailhoux E, Jaubert F, Servel N, Xia X, Pannetier M, et al. Evolution and expression of FOXL2. J Med Genet. 2002; 39(12):916–21. Epub 2002/12/10. https://doi.org/10.1136/jmg.39.12.916 PMID: 12471206.

74. Loffler KA, Zarkower D, Koopman P. Etiology of ovarian failure in blepharophimosis ptosis epicanthus inversus syndrome: FOXL2 is a conserved, early-acting gene in vertebrate ovarian development. Endocrinology. 2003; 144(7):3237–43. Epub 2003/06/18. https://doi.org/10.1210/en.2002-0095 PMID: 12810580.

75. Murayama C, Miyazaki H, Miyamoto A, Shimizu T. Involvement of Ad4BP/SF-1, DAX-1, and COUP-TFII transcription factor on steroid production and luteinization in ovarian theca cells. Molecular and cellular biochemistry. 2008; 314(1–2):51–8. Epub 2008/04/15. https://doi.org/10.1007/s11010-008-9764-y PMID: 18409030.

76. Ikeda Y, Shen WH, Ingraham HA, Parker KL. Developmental expression of mouse steroidogenic factor-1, an essential regulator of the steroid hydroxylases. Mol Endocrinol. 1994; 8(5):654–62. Epub 1994/05/01. https://doi.org/10.1210/mend.8.5.8058073 PMID: 8058073.

77. Hatano O, Takayama K, Imai T, Waterman MR, Takakusu A, Omura T, et al. Sex-dependent expression of a transcription factor, Ad4BP, regulating steroidogenic P-450 genes in the gonads during prenatal and postnatal rat development. Development. 1994; 120(10):2787–97. Epub 1994/10/01. PMID: 7607070.

78. Hanley NA, Ball SG, Clement-Jones M, Hagan DM, Strachan T, Lindsay S, et al. Expression of steroidogenic factor 1 and Wilms' tumour 1 during early human gonadal development and sex determination. Mech Dev. 1999; 87(1–2):175–80. Epub 1999/09/24. PMID: 10495282.

79. Ricken A, Lochhead P, Kontogiannea M, Farookhi R. Wnt signaling in the ovary: identification and compartmentalized expression of wnt-2, wnt-2b, and frizzled-4 mRNAs. Endocrinology. 2002; 143(7):2741–9. https://doi.org/10.1210/endo.143.7.8908 PMID: 12072409.

80. Hatzirodos N, Hummitzsch K, Irving-Rodgers HF, Rodgers RJ. Transcriptome profiling of the theca interna in transition from small to large antral ovarian follicles. PLoS One. 2014; 9(5):e97489. https://doi.org/10.1371/journal.pone.0097489 PMID: 24830430.

81. Medrano JV, Ramathal C, Nguyen HN, Simon C, Reijo Pera RA. Divergent RNA-binding proteins, DAZL and VASA, induce meiotic progression in human germ cells derived in vitro. Stem Cells. 2012; 30(3):441–51. Epub 2011/12/14. https://doi.org/10.1002/stem.1012 PMID: 22162380.

82. Minkina A, Lindeman RE, Gearhart MD, Chassot AA, Chaboissier MC, Ghyselinck NB, et al. Retinoic acid signaling is dispensable for somatic development and function in the mammalian ovary. Dev Biol. 2017; 424(2):208–20. https://doi.org/10.1016/j.ydbio.2017.02.015 PMID: 28274610 Epub Mar 6.

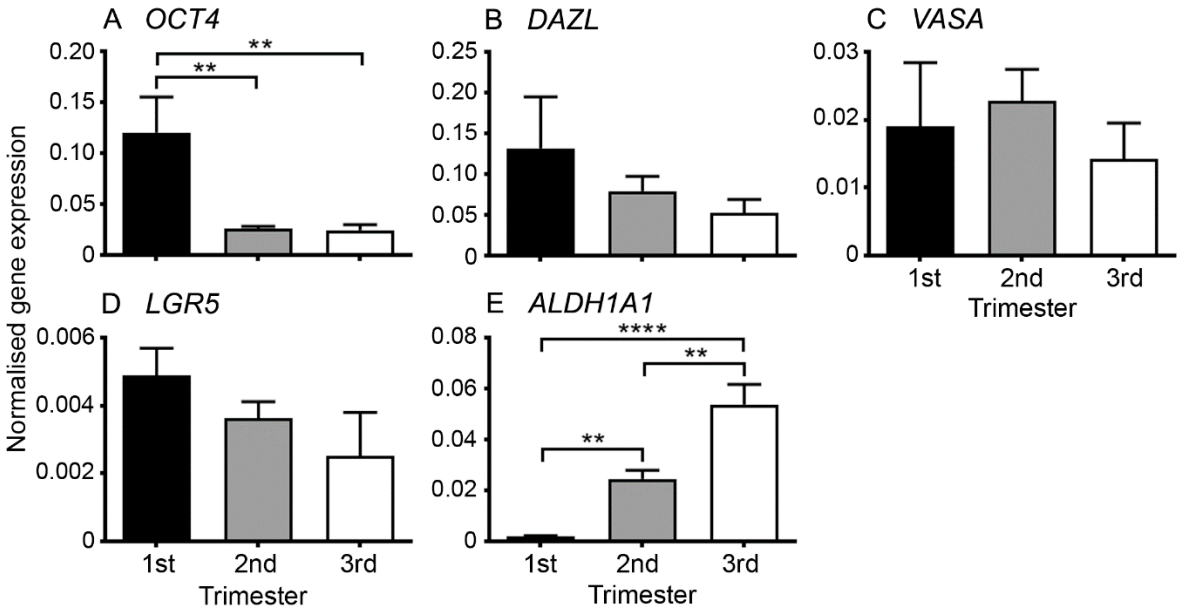

S1 Fig. Germ and stem cell marker expression. Measurement of gene expression of germ and stem cell markers in fetal ovaries by q-PCR graphed by trimester (1st, 2nd and 3rd trimesters have n = 5, n = 7 and n = 5 animals, respectively). Mean ± SEM are shown and statistical differences between trimesters are shown as **, or ****, indicating $P < 0.01$ or $P < 0.0001$, respectively.

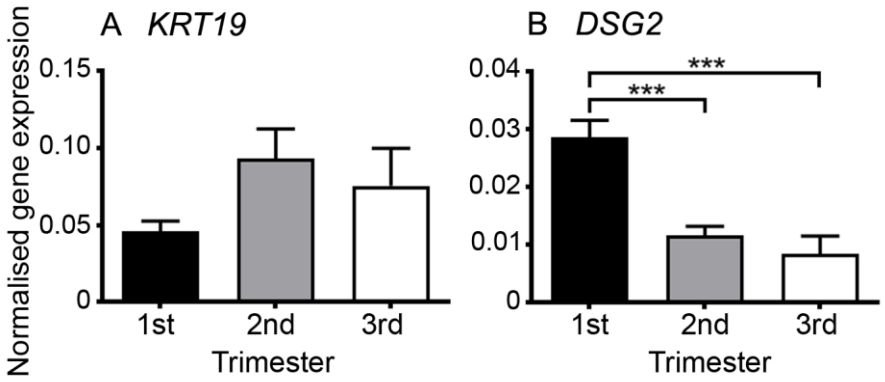

S2 Fig. GREL cell marker expression. Measurement of gene expression of GREL cell markers in fetal ovaries by q-PCR graphed by trimester (1st, 2nd and 3rd trimesters have n = 5, n = 7 and n = 5 animals, respectively). Mean ± SEM are shown and statistical differences between trimesters are shown as ***, indicating $P < 0.001$, respectively.

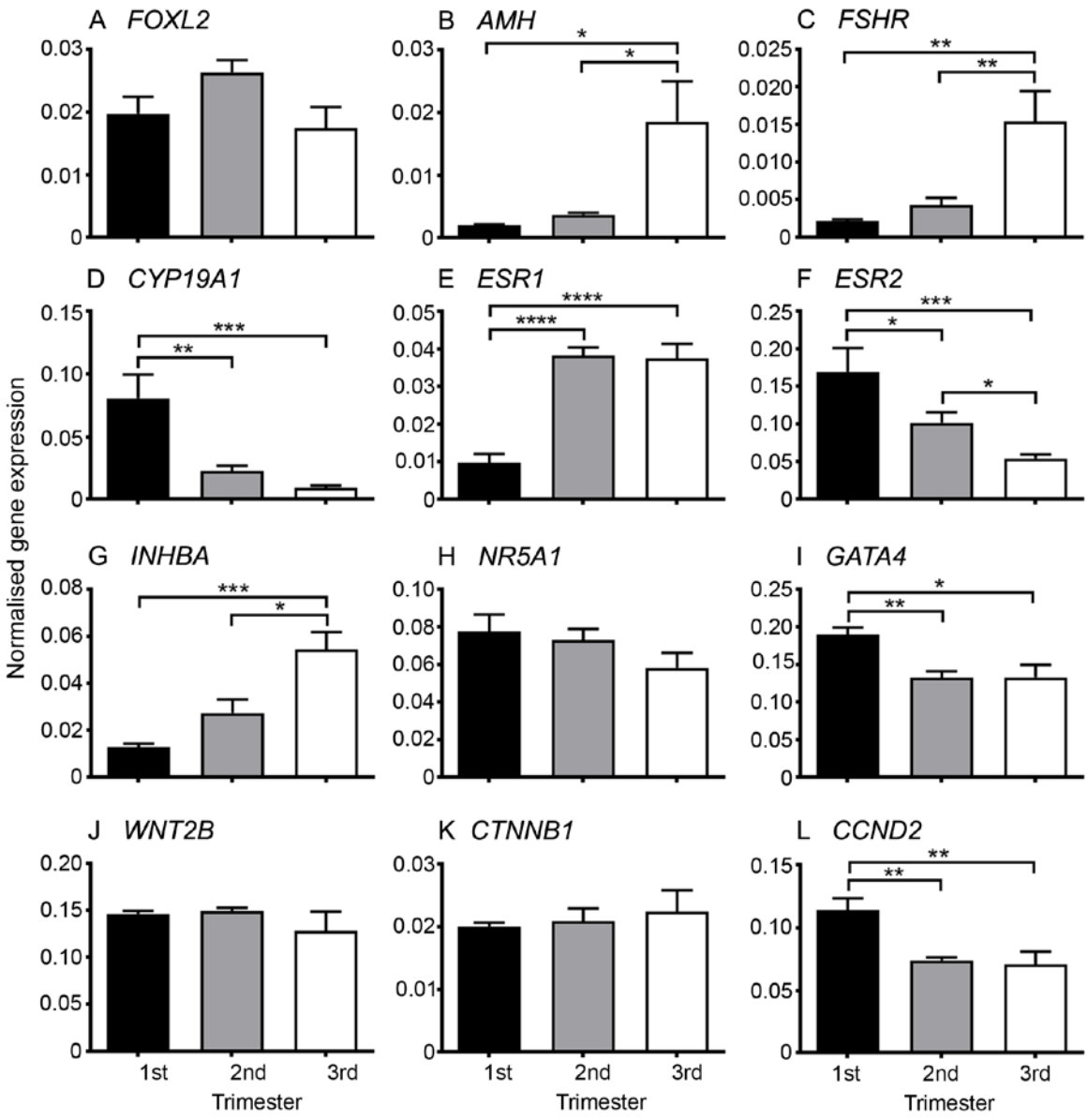

S3 Fig. Granulosa cell marker expression. Measurement of gene expression of granulosa cell markers in fetal ovaries by q-PCR graphed by trimester (1st, 2nd and 3rd trimesters have n = 5, n = 7 and n = 5 animals, respectively). Mean ± SEM are shown and statistical differences between trimesters are shown as *, **, ***, or ****, indicating $P < 0.05$, $P < 0.01$, $P < 0.001$ or $P < 0.0001$, respectively.

Chapter V:

Formation of the Bovine Ovarian Surface Epithelium during Fetal Development

This chapter is based on the following article that was submitted to Journal of Histochemistry and Cytochemistry:

Monica D. Hartanti, Katja Hummitzsch, Wendy M. Bonner, Nicole A Bastian, Helen F. Irving-Rodgers and Raymond J. Rodgers, "Formation of the Bovine Ovarian Surface Epithelium during Fetal Development"

Statement of Authorship

Title of Paper	**Formation of the Bovine Ovarian Surface Epithelium during fetal development.**
Publication Status	☐ Published ☐ Accepted for Publication ☑ Submitted for Publication ☐ Unpublished and Unsubmitted work written in manuscript style
Publication Details	**Hartanti, M.D., Hummitzsch, K., Bonner, W.M., Bastian, N.A., Irving-Rodgers, H.F., Rodgers, R.J.; Formation of the bovine ovarian surface epithelium during fetal development; Journal of Histochemistry & Cytochemistry**

Principal Author

Name of Principal Author (Candidate)	**Monica Dwi Hartanti**		
Contribution to the Paper	**Planned and developed work of bovine samples, performed analysis on all samples, interpreted data, drafted, wrote and revised the manuscript.**		
Overall percentage (%)	**75 %**		
Certification:	**This paper reports on original research I conducted during the period of my Higher Degree by Research candidature and is not subject to any obligations or contractual agreements with a third party that would constrain its inclusion in this thesis. I am the primary author of this paper.**		
Signature		**Date**	**21/12/2018**

Co-Author Contributions

By signing the Statement of Authorship, each author certifies that:

i. **the candidate's stated contribution to the publication is accurate (as detailed above);**
ii. **permission is granted for the candidate in include the publication in the thesis; and**
iii. **the sum of all co-author contributions is equal to 100% less the candidate's stated contribution.**

Name of Co-Author	**Katja Hummitzach**		
Contribution to the Paper	**Supervised development of work, provided samples and manuscript evaluation.**		
Signature		**Date**	**21/12/2018**

Name of Co-Author	Wendy M Bonner		
Contribution to the Paper	Provided samples and conducted some of lab work.		
Signature		Date	9/7/19.

Name of Co-Author	Nicole A Bastian		
Contribution to the Paper	Provided samples.		
Signature		Date	9/7/2019

Name of Co-Author	Helen F Irving-Rodgers		
Contribution to the Paper	Supervised development of work and manuscript evaluation.		
Signature		Date	21/12/2018

Name of Co-Author	Raymond J Rodgers		
Contribution to the Paper	Supervised development of work, manuscript evaluation and acted as corresponding author.		
Signature		Date	9/7/2019

Formation of the Bovine Ovarian Surface Epithelium during Fetal Development

Monica D. Hartanti, Katja Hummitzsch, Wendy M. Bonner, Nicole A Bastian, Helen F. Irving-Rodgers and Raymond J. Rodgers

Discipline of Obstetrics and Gynaecology, School of Medicine, Robinson Research Institute, The University of Adelaide, SA 5005, Australia (MDH, KH, WMB, NAB, HFI-R, RJR); Faculty of Medicine, Trisakti University, Jakarta, Indonesia (MDH) and School of Medical Science, Griffith University, Gold Coast Campus, Qld 4222, Australia (HFI-R)

*Corresponding author: Raymond J. Rodgers, The University of Adelaide, AHMS, Level 5, North Terrace/ George Street, Adelaide, SA 5005; +6188313 3932. Email ray.rodgers@adelaide.edu.au

Short title: Development of the Ovarian Surface

Summary (200 words)

When first formed the ovary has an established epithelium only at its base or hilum. Later, an epithelium is established around the rest of the ovary. To examine this further we conducted scanning electron microscopy of the surface of bovine fetal ovaries and immunohistochemistry of ovarian cross-sections. From the earliest time point, the cells on the surface of the base or hilum of the ovary were cuboidal. On the remainder of the ovary, the surface was more irregular. By mid-development, the surface was covered completely with either a stratified or simple epithelium of cuboidal cells. Clefts were observed in the surface and appeared to form due to the expansion of stroma surrounding each open ovigerous cord, elevating the areas surrounding each cord, whilst leaving the opening of the cord to form the base of each cleft. The continued expansion of the surrounding stroma below the surface appeared not only to close the ovigerous cords from the surface but to compress the clefts into the shape of a groove. Later, most of the ovarian surface was covered with a simple cuboidal epithelium. The changes to the ovarian surface during fetal development coincide with the remodeling of the stroma and cords below.

Keywords

fetal ovary, surface epithelium, scanning electron microscopy, ovigerous cords, stroma, development

Introduction

The mature ovary is covered by a predominantly single layer of flat to cuboidal epithelial cells. This surface epithelium is rich in keratins 7, 8, 18 and 19, and has intercellular desmosomes and incomplete tight junctions (Auersperg et al. 2001; Zhu et al. 2004). The sub-epithelial basal lamina is underlain by the stromal fibrous tunica albuginea (Hummitzsch et al. 2013; Zhu et al. 2004). Interestingly, the surface epithelium in the mature ovary is extremely dynamic. Continued expansion and contraction of the surface occurs as follicles and corpora lutea grow and regress beneath it. Additionally, cell death and the repair of the tunica and surface epithelium at the point of rupture of the follicle wall occurs during the event of ovulation (Murdoch 1994; Nicosia et al. 1991). It is assumed that stem cells in the remaining surface epithelium proliferate and differentiate, to restore the surface damaged at ovulation. Until recently, little was known about the surface epithelial stem cells (Flesken-Nikitin et al. 2013; Ng et al. 2014; Rastetter et al. 2014) with the first study to identify possible stem/progenitor cells in mice (Szotek et al. 2008). The ovarian surface epithelium is also potentially a major contributor to the incidence of ovarian cancers. Ovarian epithelial carcinomas represent around 90% of ovarian malignant neoplasms (Torre et al. 2018). However, there is good evidence to suggest that at least the high grade serous ovarian carcinomas and not derived from the ovarian surface epithelium but could arise from the secretory cells of the oviduct (Kroeger and Drapkin 2017; Labidi-Galy et al. 2017).

The ovarian surface epithelium is also dynamic during fetal development. Earlier literature identified that the surface epithelium originates from the mesoderm-derived epithelial layer, which lines the intra-embryonic coelom and the area on the ventral surface of the mesonephros where the gonad is subsequently formed (Byskov 1986; Fröjdman and Pelliniemi 1995). The mesonephric surface is covered by a simple epithelium, except where gonadal thickening occurs (Kenngott et al. 2013). This thickening is due to proliferation of the surface cells which we have termed as gonadal ridge epithelial-like (GREL) cells (Hummitzsch et al. 2013). We observed that when the bovine fetal ovary is first formed, it is not covered by an established surface epithelium underlain by a basal lamina at the interface with stroma except at the base or hilum of the ovary (Hummitzsch et al. 2015; Hummitzsch et al. 2013; Rodgers and Hummitzsch 2014). The base or hilum of the ovary is in fact a protrusion of the mesonephros and it is covered by an established surface epithelium with a sub-epithelial basal lamina and epithelial-stromal interface. The remaining part of the ovary is composed of primordial germ cells interspersed in a cluster of GREL cells, which arise from the mesonephric surface epithelium through proliferation in a process that is also associated with degradation of the sub-epithelial basal lamina. Subsequently, the stroma from the

mesonephros, with its leading edge basal lamina, penetrates into the ovarian primordium towards its surface; branching as it does so. This branching process gives rise to alternating areas of stroma and GREL cells/primordial germ cells, known as ovigerous cords. Eventually the stroma expands to just below the GREL cells on the surface of the ovary and spreads laterally, closing off the ovigerous cords from the surface and trapping GREL cells on the surface (Hummitzsch et al. 2013). These GREL cells on the surface eventually develop an epithelial phenotype rich in cell junctions, as identified by immunostaining for plakophilin-2 and desmoglein-2, and with a sub-epithelial basal lamina (Hummitzsch et al. 2013). The cells of the surface epithelium of the adult mouse ovary are also not uniform in their phenotype and gene expression (Flesken-Nikitin et al. 2013; Ng et al. 2014). Thus, the different developmental pathways for ovarian surface epithelial cells could be important in causing the heterogeneity of ovarian surface epithelial cells.

Since the surface epithelium of the ovary has heterogeneous cellular origins, undergoes continual death and renewal in adult life, and could be important in ovarian cancer, we examined the surface of the developing ovary using scanning electron microscopy (SEM). To interpret the features that we observed with SEM, we identified cytokeratin 19 (CK19) in epithelial cells and laminin 111 in basal laminas using immunohistochemistry on ovarian cross sections. We also performed morphometric analysis of the proportions of cells on the surface that had different shapes.

Materials and Methods

Bovine Ovaries

Pairs of bovine fetal ovaries from different developmental stages were collected from pregnant *Bos taurus* cows processed at an abattoir (Midfield Meat International, Warrnambool, Victoria, Australia). To estimate the gestational age, the crown-rump length (CRL) was measured (Russe 1983). One ovary from each pair was fixed with 2.5% glutaraldehyde (ProSciTech, Thuringowa, Queensland, Australia) in 0.1 M phosphate buffer solution (PBS; Merck Pty Ltd, Victoria, Australia) for subsequent SEM (n = 11 were used for SEM), whereas the corresponding ovary was embedded in O.C.T. compound (ProSciTech, Thuringowa, Queensland, Australia) and stored in dry ice for subsequent histology and immunohistochemistry. All samples were then transported to the laboratory. DNA was extracted from tail samples from fetuses with CRL < 10 cm to determine the fetal sex using PCR of the SRY gene, as previously described (Hummitzsch et al. 2013). The samples were grouped into three developmental stages; early stage (SEM n = 3, IHC n = 2, <100 days of

gestation), mid stage (SEM n = 5, IHC n = 8, 100-170 days of gestation) and late stage (SEM n = 3, IHC n = 4, >170 days of gestation). Furthermore, the age of each fetus was estimated from the CRL [$y = -0.0103x^2 + 3.4332x + 36.08$; where y is the age in days and x is the CRL in cm, determined using Russe's method (1983)].

Histology

O.C.T. embedded blocks were cut using a Leica CM3050S Cryostat (Leica Biosystems, Victoria, Australia) into serial sections of 8 µm thickness. The sections were then mounted on Superfrost glass slides (HD Scientific Supplies, Wetherill Park, NSW, Australia), transported in dry ice, then stored at -20 C until used for hematoxylin-eosin staining and immunohistochemistry.

Immunohistochemistry

An indirect immunofluorescence method was used for dual localization of CK19 and laminin 111. The primary antibodies used were mouse anti-human CK19 (0.25 µg/ml; Boehringer Ingelheim GmbH, Ingelheim am Rhein, Germany) to identify epithelial cells in combination with rabbit anti-mouse laminin 111, (L9393, from the basement membrane of an EHS mouse tumour, 5 µg/ml; Sigma Chemical Co, St Louis, MO, USA) to localize the basal lamina. The secondary antibodies were Biotin-(SP)-conjugated AffiniPure donkey anti-mouse IgG (1:100; #711 066 152) and donkey anti-rabbit IgG conjugated to Cy3 (1:100; #715 166 151) followed by dichlorotriazinylamino fluorescein (DTAF)-conjugated streptavidin (1:100; #016 010 084). All the secondary antibodies and conjugated streptavidin were from Jackson ImmunoResearch Laboratories Inc (West Grove, PA, USA). The cell nuclei were counterstained with a 4',6'-diamidino-2-phenylindole dihydrochloride (DAPI) solution (Molecular Probes, Fisher Scientific, Hampton, NH, USA). The bovine adult ovary was used as a positive control. Nonimmune mouse and rabbit sera (Sigma-Aldrich, St. Louis, MO, USA) were used as negative controls. All sections were photographed with an Olympus BX51 microscope with an epifluorescence attachment and a Spot RT digital camera (Diagnostic Instruments, Meyer Instrument, Houston, TX, USA).

Morphometric Analyses

Morphometric analyses were conducted on the largest cross-section from each ovary, determined by hematoxylin-eosin staining for every 10^{th} section. To analyse the ovarian surface, mid and late stage samples were used, and the surface was identified based on the positive CK19 and laminin 111 staining. Using ImageJ software (Schindelin et al. 2012), the ovarian epithelial perimeter was determined from the combined images taken from the

ovarian surface as a CK19 positive area at x20 magnification. The proportions of the perimeter of the surface covered by multi- or single- layered cuboidal cells, or squamous cells, or that which was denuded were measured. No columnar-shaped cells were observed.

Scanning Electron Microscopy

The fixed bovine fetal ovaries were washed 3 times with 0.1 M PBS pH 7.25 (Merck Pty Ltd, Victoria, Australia). The samples were then transported to Adelaide Microscopy and postfixed with 2% osmium tetroxide in PBS for 1 hour. After washing twice for 5 mins with PBS containing 4% sucrose, the samples were then dehydrated in a graded series of ethanol (2 x 10 min each in 70, 90, and 100%). The samples were incubated in 1:1 100% ethanol:hexamethyldisilazane (HMDS) for 10 mins, then 2 x 10 mins in 100% HMDS, air dried and mounted on aluminium stubs with sticky tabs. A thin layer of dabs of paint was applied around the samples and dried. The stubs were then placed under vacuum in a 208 High Resolution Sputter Coater (Cressington Scientific Instruments, Watford, UK). After choosing the correct positions, the stubs were metallized with platinum using high vacuum systems and then stored in SEM storage boxes until examination. The processed samples were examined with a Philips XL30 SEM (North Billerica, MA, USA) operated at 10 kV.

Statistical Analyses

All statistical analyses were carried out using Microsoft Office Excel 2010 and GraphPad Prism Version 7.00 for Windows (GraphPad Software Inc., La Jolla, CA, USA). The morphometric data were statistically compared using *t*-tests.

Results

Immunohistochemical Changes

The early ovarian primordium developed on the ventral side of the mesonephros. As observed previously (Hummitzsch et al. 2013) the mesonephros was covered by a simple single-layered surface epithelium which stained strongly for CK19 (Fig. 1). The same surface epithelium was observed at the base or hilum of the developing ovarian primordium (Figs. 1A and B). These simple surface epithelial cells of the mesonephros and the hilum of the ovary were underlain by a basal lamina, identified by localizing laminin 111 (Fig. 1B). The rest of the ovarian surface, not at the base or hilum of the ovary, was not covered by a surface epithelium underlain by a basal lamina. Instead GREL cells, which also expressed lower levels of CK19 and formed the main body of the ovarian primordium, formed the outmost layer of cells on

this part of the ovary (Fig. 1C). They appeared to be relatively tightly connected to each other (Fig. 1C). Laminin 111 fibres of basal lamina fragments were observed inside the developing ovary, where the mesonephric stroma had penetrated. At the end of the first trimester, the stroma had expanded towards the ovarian surface (Fig. 1D). This resulted in the formation of ovigerous cords, which contained both germ and GREL cells. The ovigerous cords were separated from the stromal compartments by a basal lamina. The GREL cells on the surface stained more strongly for CK19 than the GREL cells deeper in the ovary.

In the second trimester, the stroma had penetrated further towards the ovarian surface and had commenced expanding laterally below the surface (Fig. 2A). A basal lamina formed below some layers of GREL cells on the surface (Fig. 2B) and continued to separate the stroma from the ovigerous cords. GREL cells on the surface began to stain more strongly for CK19. The staining across the surface was uneven (Fig. 2A). The surface appeared to be physically uneven and was sporadically punctuated with deep clefts containing strongly CK19-positive GREL cells on the surface of the clefts (Fig. 2C). At this stage, some of the ovigerous cords were still open towards the surface (Figs 2A, D and E) and, in some instances, the openings were below the level of the surrounding surface, suggesting that the clefts might be formed at the openings of the ovigerous cords by expansion of the stroma below the surface and around the cleft. Numerous GREL cells at the opening of the ovigerous cords were staining more strongly for CK19 (Figs 2E and D).

At the medullary end of the ovigerous cords, the expansion of the stroma resulted in the breakdown of the ovigerous cords, firstly into smaller cords and then into primordial follicles (Figs 2E and F). Some of these follicles were activated and had begun to differentiate into primary follicles. The stroma became denser, especially below the surface (Fig. 2F). At the beginning of the mid-stage, the cells on the surface formed multiple layers (Figs. 2A, B, D and E). However, at the end of the second trimester, more areas of the surface had become single-layered (Figs 2F, G and H). The surface cells in the single layers had either flattened (Fig. 2G) or cuboidal shapes (Fig. 2H).

At the late stage of ovarian development, the surface of the ovary was still very irregular with clefts and grooves (Fig. 3A). The surface cells were tightly packed but some denuded areas were observed (Fig. 3B). Areas of multi-layered surface epithelium were also found, especially in the clefts (Fig. 3C), but the majority of the surface at this stage appeared to be single-layered (Fig. 3D).

Morphometric Changes

We analysed the proportions of cuboidal (single- or multi-layered) and flattened squamous cells in the ovarian surface throughout mid and late development (Table 1). There was no

significant difference between the proportions of the single-layered cuboidal cells between the two developmental stages examined (Fig. 4A); with this cell type making up approximately 85 % of the ovarian surface cover. Multilayered cuboidal cells covered around 10% of the surface during mid and late development (Fig. 4B). The percentage of flat squamous cells per surface epithelial perimeter was higher at the late stage, with approximately 7%, compared with the mid stage with around 2.5% (Fig. 4C). We rarely observed areas of the ovary which were not covered by an epithelium (very small areas in 2 of the 14 ovaries examined). We assumed these denuded areas were probably artefacts (Fig. 3B) resulting from the sample processing and excluded them from the analyses.

Ultrastructural Changes

SEM of the ovarian primordium revealed a very uneven surface with clefts and grooves (Fig. 5A). The cells on the surface were either squamous with an extracellular matrix between the cells (Fig. 5B), or they were round in shape (Fig. 5C, D). Microvilli (Fig. 5E) and isolated cilia (Fig. 5F) were visible on the surface of the cells. Infrequently, germ cells which were larger than the surface cells and had a round shape with smooth appearance, were observed on the surface (Fig. 5G).

The surface of the ovary appeared even more irregular at mid-stage than at earlier stages. SEM showed clefts and grooves (Fig. 6). The surface cells appear more rounded in shape in areas that were less uneven (Fig. 6B). The stroma was visible in areas where the surface had been denuded during processing (Fig. 6B). In areas further away from the hilum, flat deep clefts covered the surface (Fig. 6C). The cells between the clefts appeared flat and the cell borders were indistinct (Fig. 6C)and gaps between the surface cells were filled with an extracellular matrix (Fig. 6D).

At the late stages, the ovary still had an uneven surface (Fig. 7A). There appeared to be two types of cell shape: rounded cells (Figs 7B and C) and more spindle-shaped cells (Figs 7B and C). Some shallow clefts were observed on the surface (Fig. 7D). The surface cells had microvilli (Fig. 7E), but there were also areas where the surface of the cells was covered by blebs (Fig. 7F).

Discussion

This study identified detailed changes occurring on the surface of the ovary throughout gestation by using SEM of the ovarian surface and immunohistochemistry of ovarian cross sections. Immunostaining for CK19 identified the formation of epithelial cells. CK19 is a

member of a large family of epithelial keratins, which form cytoskeletal intermediate filaments (Turner and Milliken 2000) and CK19 is generally expressed in simple epithelia (Ordonez 2013), as occurs on the ovarian surface. CK19 has been observed at low levels in GREL cells in the early stages of ovarian development and at high levels in surface epithelial cells later in development of bovine ovaries (Hummitzsch et al. 2013), in adult human ovaries (Auersperg and Maines-Bandiera 2000; Matei et al. 2002; Ramayya et al. 2010) and in neonatal and adult ovine ovaries (Logan et al. 2002). Polyclonal antiserum to laminin 111 was used to visualize the basal laminas in the developing ovary. Basal laminas, when newly formed during fetal development, are often rich in laminins, which are less rigid than later in development when they become cross-linked to type IV collagens via nidogens (Miner et al. 2004). The reduced rigidity of laminin-rich basal laminas enables early basal lamina to expand easily during growth. Of the laminin chains, α1, β1 and γ1 are also common in fetal basal laminas (Miner et al. 2004). In the fetal ovary, basal laminas occur at the interface of ovigerous cords and surrounding stroma. They also develop beneath the surface epithelium at the interface with stroma. Previously, we identified a number of other components of basal lamina in fetal ovaries, including collagen type IV α1, collagen XVIII, perlecan and nidogens 1 and 2, and observed the sub-epithelial basal lamina by transmission electron microscopy (Hummitzsch et al. 2013). The immunohistochemistry of ovarian cross-sections that we undertook was valuable in identifying and interpreting the SEM changes in surface topology that occurred during development of the ovary.

As observed here and previously, when the bovine fetal ovary is first formed it is not covered by an established surface epithelium underlain by a basal lamina at an interface with stroma, as observed in adult ovaries, except at the base or hilum of the ovary (Hummitzsch et al. 2015; Hummitzsch et al. 2013; Rodgers and Hummitzsch 2014). The base or hilum of the ovary is a protrusion of the mesonephros. That part of the ovary is covered by an established classic surface epithelium with a sub-epithelial basal lamina and epithelial-stromal interface and is derived directly from the mesonephros. The remaining major apical part of the ovary is composed of a cluster of GREL cells, which arise from the mesonephric surface epithelium through proliferation in a process that is also associated with degradation of the sub-epithelial basal lamina on the surface of the mesonephros. It is this non hilum apical part of the ovary that undergoes many changes during fetal development and as reported here.

In the current study, in the early stages of ovarian development, GREL cells on the non-hilum surface formed the outmost layer of cells. They formed a compact layer. In an earlier study of bovine fetal ovaries, we showed by electron microscopy that the GREL cells of the outermost layer were connected to each other by adherens junctions (Hummitzsch et al. 2013). At the mid-stage of ovarian development, germ cells had migrated into the ovary and

started proliferating. At the same time, the penetrating stroma, also originating from the mesonephros, started to spread laterally below the ovarian surface. At this point, some germ cells were then trapped on the surface (Hummitzsch et al. 2013). Germ cells were therefore observed by SEM on the ovarian surface, as had also been observed previously in bovine (Hummitzsch et al. 2013), human (Motta and Makabe 1986) and murine ovaries (Kerr et al. 2006). The penetrating stroma did not reach and spread out onto the surface of the ovary but rather spread laterally below and it could also be speculated that this because the GREL cells on the surface had formed a barrier as a compact layer of cells connected by adherens junctions.

Clefts and grooves were present on the surface of the ovary, as observed here by SEM and previously in the human developing ovary (Motta and Makabe 1982). The clefts and grooves are probably the same structures, but one is more rounded and the other more elongated. We prefer to use the terms 'cleft', defined as a hollow area or indentation, and 'groove', defined as a long, narrow cut or depression, as these descriptors do not readily imply assumptions about how they are formed. Some other terms, such as 'invagination', 'folds', 'furrows' or 'sulci', have previously been used but they imply some mechanism as to how these structures are formed that may not be correct. We observed that the clefts and grooves developed at the opening of the ovigerous cords to the surface of the ovary. We interpret that clefts first develop, not by invagination of the surface, but rather by stroma, which surrounds the open cords, expanding and thus lifting the surface around each open cord and thus forming a cleft as stylized in Fig 8. The areas surrounding the clefts then appeared as ridges or papillae under SEM, and as also observed in the developing human ovary (Motta and Makabe 1982). This description is supported by the localization of stroma around the cords and the known substantial expansion that the stroma undergoes during early fetal development of the ovary (Hartanti et al. 2018).

During development, the GREL cells on the surface of the ovary began to epithelialize, as seen by the increased intensity of staining for CK19. This occurred once the stroma had penetrated to below the surface and there was then a sub-epithelial basal lamina and epithelial-stromal interface. At the top of the ovigerous cords open to the surface where clefts formed, the GREL cells inside the clefts and grooves also epithelialized with increased staining for CK19. However, these cells were not in a single layer, as the GREL cells on the wall of the clefts near their opening to the surface also epithelialized. Eventually the clefts appeared to be compressed from their sides as the surrounding stroma expanded, turning them into fissure-shaped grooves, lined with epithelial cells that stained strongly for CK19. Eventually, some of these clusters of epithelial cells appeared to be internalized, as the stroma expanded laterally below the surface leaving a single layer of epithelial cells on the surface

underlain by stroma and some islets of epithelial cells surrounded by stroma, situated below the surface. The ultimate fate of these structures is unknown.

The shape of epithelial cells (squamous, cuboidal or columnar) and type of epithelium (simple or stratified) is of interest. Variation of cell shapes has been reported in adult ovarian surfaces of humans (Blaustein 1984; Gillett et al. 1991) and other mammals (Motta and Van Blerkom 1980). It has been suggested that this variation is due to a result of mechanical deformation of normal cells during ovulation. It is observed that, during ovulation, mouse ovarian surface epithelial cells undergo active proliferation (Singavarapu et al. 2010), which is also likely to alter the cell shape. We observed that the GREL cells covering the ovarian surface differentiated into a simple surface epithelium (Hummitzsch et al. 2013), with most of the surface covered by single layers of cuboidal (80%) or squamous (5%) cells. In the current study, only two ovaries out of the fourteen examined by immunohistochemistry were missing small proportions (< 3%) of surface epithelium and this is regarded as an artefact. In some cross-sections this was confirmed, as surface cells were observed to be detaching. It has been reported that denuding of the surface epithelium of the human ovary is due to tissue handling (Gillett 1991; Kruk et al. 1990). Cells on the surface were also observed to have an ECM deposited continuously around each cell and between each other. The cells had microvilli, cilia and blebs on their antral sides. At this stage, we are not sure if the blebs are real or artefacts, as they were not observed consistently.

In summary, the surface topology of the ovary is largely governed by cellular activities beneath the surface. In adults, the surface is continually altered by expansion and contraction of the follicles and corpora lutea, and cell death and the repair of the tunica and surface epithelium occurs at the point of rupture of the follicle wall during ovulation. In the developing fetal ovary, many of the changes in surface topology also appear to arise by rearrangement of cells below the surface. The penetration of stroma into the ovarian primordium and the lateral expansion of stroma beneath the surface contribute to the formation of an established surface epithelium with a sub-epithelial basal lamina and an epithelial-stromal interface. The early formation of clefts on the ovarian surface appears due to the expansion of stroma surrounding each open ovigerous cord, elevating the areas surrounding each cord, whilst leaving the opening of the cord to form the base of each cleft. Then the continued expansion of the surrounding stroma below the surface not only closes the ovigerous cords from the surface but appears to compress the clefts into the shape of a groove on the surface. In some cases this separates the epithelial cells on the walls of the clefts and grooves from the surface entirely to produce a structure similar to an inclusion cyst. Clearly these studies indicate that the role of stroma may be far more important the hitherto realized.

Acknowledgements

The authors would like to thank Midfield Meat International for providing the bovine tissues for this research. We are also grateful to Ms Lisa Donovan and Ms Ruth Williams of Adelaide Microscopy for providing training and expertise on the processing of samples for SEM and the use of the Philips XL30 Scanning Electron Microscope.

Competing Interests

The author(s) declare they have no competing interests.

Author Contributions

MDH, KH, HFI-R and RJR designed the study on bovine samples. KH, HFI-R, WMB and NAB collected the bovine samples. MDH carried out the SEM tissue preparation and analyses and MDH KH, HFI-R, and WMB carried out the immunohistochemistry. MDH, KH, HFI-R and RJR carried out the data analysis of the bovine samples. MDH drafted the manuscript. KH, HFI-R and RJR critically revised and approved the final version of the manuscript.

Funding

The research was funded by an Australia Awards Scholarship from the Australian Government, The University of Adelaide, the National Health and Medical Research Council of Australia, the NHMRC Centre for Research Excellence in the Evaluation, Management and Health Care Needs of Polycystic Ovary Syndrome.

References

Auersperg N, Maines-Bandiera SL (2000) Culture and characterization of human ovarian surface epithelium. In Bartlett JMS, ed. Ovarian cancer: methods and protocols. Totowa, New Jersey, USA, Humana Press

Auersperg N, Wong AST, Choi K-C, Kang SK, Leung PCK (2001) Ovarian surface epithelium: biology, endocrinology, and pathology. Endocr Rev 22:255-288

Blaustein A (1984) Peritoneal mesothelium and ovarian surface cells shared characteristics. Int J Gynecol Pathol 3:361-375

Byskov AG (1986) Differentiation of mammalian embryonic gonad. Physiol Rev 66:71-117

Flesken-Nikitin A, Hwang CI, Cheng CY, Michurina TV, Enikolopov G, Nikitin AY (2013) Ovarian surface epithelium at the junction area contains a cancer-prone stem cell niche. Nature 495:241-245

Fröjdman K, Pelliniemi LJ (1995) α6 subunit of integrins in the development and sex differentiation of the mouse ovary. Dev Dyn 202:397-404

Gillett WR (1991) Artefactual loss of human ovarian surface epithelium: potential clinical significance. Reprod Fertil Dev 3:93-98

Gillett WR, Mitchell A, Hurst PR (1991) A scanning electron microscopic study of the human ovarian surface epithelium: characterization of two cell types. Hum Reprod 6:645-650

Hartanti MD, Hummitzsch K, Irving-Rodgers HF, Bonner WM, KJ C, Anderson RA, McMillen IC, Perry VE, Rodgers RJ (2018) Morphometric and gene expression analyses of stromal expansion during bovine fetal ovarian development. Reprod Fert Devel:(in press)

Hummitzsch K, Anderson RA, Wu J, Telfer EE, Russell DL, Robertson SA, Rodgers RJ (2015) Stem cells, progenitor cells and lineage decisions in the ovary. Endocrine Rev 36:65-91

Hummitzsch K, Irving-Rodgers HF, Hatzirodos N, Bonner W, Sabatier L, Reinhardt DP, Sado Y, Ninomiya Y, Wilhelm D, Rodgers RJ (2013) A new model of development of the mammalian ovary and follicles. PLoS One 8:e55578

Kenngott RA, Vermehren M, Ebach K, Sinowatz F (2013) The role of ovarian surface epithelium in folliculogenesis during fetal development of the bovine ovary: a histological and immunohistochemical study. Sex Dev 7:180-195

Kerr JB, Duckett R, Myers M, Britt KL, Mladenovska T, Findlay JK (2006) Quantification of healthy follicles in the neonatal and adult mouse ovary: evidence for maintenance of primordial follicle supply. Reproduction 132:95-109

Kroeger PT, Jr., Drapkin R (2017) Pathogenesis and heterogeneity of ovarian cancer. Curr Opin Obstet Gynecol 29:26-34. doi: 10.1097/GCO.0000000000000340.

Kruk PA, Maines-Bandiera SL, Auersperg N (1990) A simplified method to culture human ovarian surface epithelium. Lab Invest 63:132-136

Labidi-Galy SI, Papp E, Hallberg D, Niknafs N, Adleff V, Noe M, Bhattacharya R, Novak M, Jones S, Phallen J, Hruban CA, Hirsch MS, Lin DI, Schwartz L, Maire CL, Tille JC, Bowden M, Ayhan A, Wood LD, Scharpf RB, Kurman R, Wang TL, Shih IM, Karchin R, Drapkin R, Velculescu VE (2017) High grade serous ovarian carcinomas originate in the fallopian tube. Nat Commun 8:1093. doi: 1010.1038/s41467-41017-00962-41461.

Logan KA, Juengel JL, McNatty KP (2002) Onset of Steroidogenic Enzyme Gene Expression During Ovarian Follicular Development in Sheep1. Biology of Reproduction 66:906-916

Matei D, Graeber TG, Baldwin RL, Karlan BY, Rao J, Chang DD (2002) Gene expression in epithelium ovarian carcinoma. Oncogene 21:6289-6298

Miner JH, Li C, Mudd JL, Go G, Sutherland AE (2004) Compositional and structural requirements for laminin and basement membranes during mouse embryo implantation and gastrulation. Development 131:2247-2256. doi: 2210.1242/dev.01112. Epub 02004 Apr 01121.

Motta PM, Makabe S (1986) Germ cells in the ovarian surface during fetal development in humans. A three-dimensional microanatomical study by scanning and transmission electron microscopy. J Submicrosc Cytol 18:271-290
Motta PM, Makabe S (1982) Development of the ovarian surface and associated germ cells in the human fetus. Cell Tissue Res 226:493-510
Motta PM, Van Blerkom J (1980) Scanning electron microscopy of the mammalian ovary. In Motta PM, Hafez ESE, eds. Biology of the ovary. Netherlands, Martinus Nijhoff Publisher
Murdoch WJ (1994) Ovarian surface epithelium during ovulatory and anovulatory ovine estrous cycles. Anat Rec 240:322-326
Ng A, Tan S, Singh G, Rizk P, Swathi Y, Tan TZ, Huang RY, Leushacke M, Barker N (2014) Lgr5 marks stem/progenitor cells in ovary and tubal epithelia. Nat Cell Biol 16:745-757
Nicosia SV, Saunders BO, Acevedo-Duncan ME, Setrakian S, Degregorio R (1991) Biopathology of ovarian mesothelium. In Familiari G, Makabe S, Motta PM, eds. Ultrastructure of the ovary. New York, USA, Springer Science+Business Media
Ordonez NG (2013) Broad-spectrum immunohistochemical epithelial markers: a review. Hum Pathol 44:1195-1215. doi: 1110.1016/j.humpath.2012.1111.1016. Epub 2013 Feb 1118.
Ramayya MS, Sheng M, Moroz K, Hill SM, Rowan BG (2010) Human steroidogenic factor-1 (hSF-1) regulates progesterone biosynthesis and growth of ovarian surface epithelial cancer cells. J Steroid Biochem Mol Biol 119:14-25
Rastetter RH, Bernard P, Palmer JS, Chassot AA, Chen H, Western PS, Ramsay RG, Chaboissier MC, Wilhelm D (2014) Marker genes identify three somatic cell types in the fetal mouse ovary. Dev Biol (in press)
Rodgers RJ, Hummitzsch K (2014) Formation of the Ovary at http://www.youtube.com/watch?v=1O97DtAyaDc. In, YouTube
Russe I (1983) Oogenesis in cattle and sheep. Bibl Anat 24:77-92
Schindelin J, Arganda-Carreras I, Frise E, Kaynig V, Longair M, Pietzsch T, Preibisch S, Rueden C, Saalfeld S, Schmid B, Tinevez JY, White DJ, Hartenstein V, Eliceiri K, Tomancak P, Cardona A (2012) Fiji: an open-source platform for biological-image analysis. Nat Methods 9:676-682
Singavarapu R, Buchinsky N, Cheon D-J, Orsulic S (2010) Whole ovary immunohistochemistry for monitoring cell proliferation and ovulatory
wound repair in the mouse. Reprod Biol Endocrinol 8:98
Szotek PP, Chang HL, Brennand K, Fujino A, Pieretti-Vanmarcke R, Lo Celso C, Dombkowski D, Preffer F, Cohen KS, Teixeira J, Donahoe PK (2008) Normal ovarian surface epithelial label-retaining cells exhibit stem/progenitor cell characteristics. Proc Natl Acad Sci U S A 105:12469-12473
Torre LA, Trabert B, DeSantis CE, Miller KD, Samimi G, Runowicz CD, Gaudet MM, Jemal A, Siegel RL (2018) Ovarian cancer statistics, 2018. CA Cancer J Clin 68:284-296. doi: 210.3322/caac.21456. Epub 22018 May 21429.
Turner JJ, Milliken S (2000) A case of keratin-positive acute myeloid leukemia: a possible role for cytokeratin 19 as a specific epithelial marker. Pathology 32:98-101
Zhu Y, Maric J, Nilsson M, Brannstrom M, Janson PO, Sundfeldt K (2004) Formation and barrier function of tight junctions in human ovarian surface epithelium. Biol Reprod 71:53-59

Figures

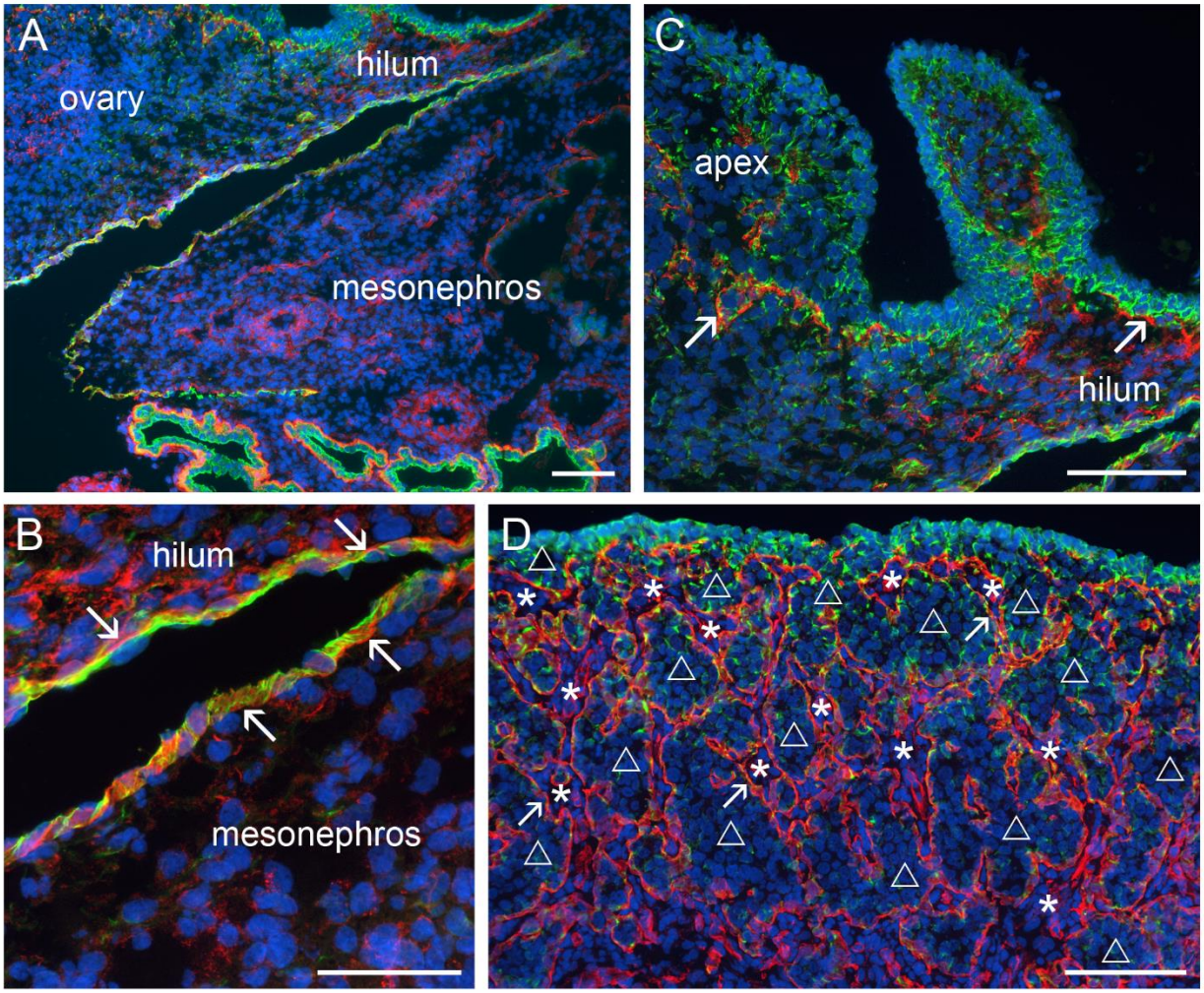

Figure 1. Fluorescence micrographs of the ovary and mesonephros during early stages of development [cytokeratin 19 (CK19) in green; laminin 111 in red]. (A) The fetal ovary (top left) developed on the ventral surface of the mesonephros (bottom right). (B) The hilum area of the developing ovary and the mesonephros were covered by single-layered surface epithelium, strongly positive for CK19 and underlain by a basal lamina (laminin 111 positive, arrows). (C) The remaining ovary/apex surface at this stage of development was not covered by a surface epithelial layer underlain by a basal lamina, rather it is covered by somatic GREL cells, which also expressed CK19 and fragments of basal lamina observed throughout the ovary (arrows). (D) Penetration of mesonephric stroma into the developing ovary resulted in the formation of ovigerous cords (unfilled triangle), which contain germ and GREL cells, separated from the stroma (asterisk) by a basal lamina (arrows). The GREL cells at this later stage and closer to the surface strongly expressed CK19. Nuclei were counterstained with DAPI (blue). (A) - (C) 53 days and (D) 76 days of gestation. Scale bars: (A), (C) and (D) 100 μm, (B) 50 μm.

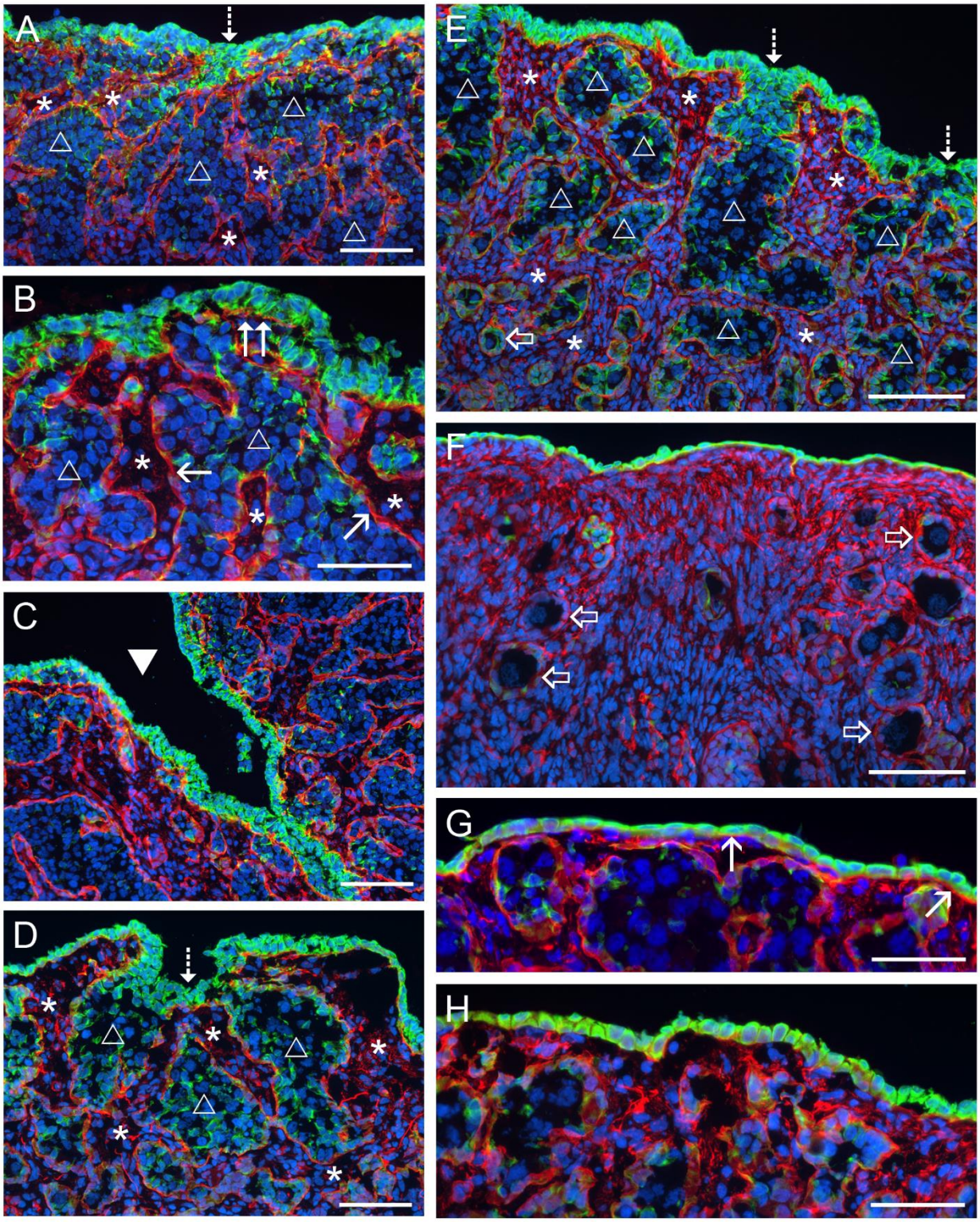

Figure 2. Fluorescence micrographs of the ovary during mid stages of development (CK19 is green; laminin 111 is red). (A) Stroma has penetrated further towards the surface and then spread laterally below layers of GREL cells on the surface. The staining of CK19 showed a gradient – strong in GREL cells on the surface and in GREL cells clustering at the opening to the ovarian surface of the ovigerous cords. The weakest staining was in GREL cells deeper in the cords in the ovary. Basal lamina (laminin 111 positive) separated the ovigerous cords (unfilled triangle) and stromal compartments (asterisk). The ovigerous cords were still open at the surface (dotted-line arrow) in some areas and strongly positive GREL cells were observed clustered at the openings. (B) A basal lamina formed below the surface cells (double arrow) and started to close the ovigerous cords (unfilled triangle) from outside the ovary. The surface

of the developing ovary was very uneven; (C) deep clefts (filled triangle) and (D) shallow clefts in areas of ovigerous cords being open to the surface (dotted-line arrow) were visible and again strongly CK19 positive, clustered at the opening. (E) The stroma expanded and laminin 111 fibres (red) were visible in the stromal compartments (asterisk). The expansion caused the breakdown of ovigerous cords (unfilled triangle) into smaller cords and finally into the smaller primordial follicles (block arrow) closer to the medulla. GREL cells differentiated into pre-granulosa cells of primordial follicles and weakly stained for CK19. Additionally, fewer ovigerous cords were still open to the surface (dotted-line arrow). (F) Later in development, all ovigerous cords were broken down into follicles (block arrow) and a proper surface epithelium was separated from the stroma below by a basal lamina. The surface epithelium changed from multi-layered to single-layered, with areas of (G) flattened cells or (H) cuboidal cells. Nuclei were counterstained in DAPI (blue). (A) 124 days, (B) and (C) 107 days, (D) 146 days, (E) 144 days, (F) 180 days, (G) and (H) 135 days of gestation. Scale bars: (A), (C), (D) – (F) 100 μm, (B), (G) and (H) 50 μm.

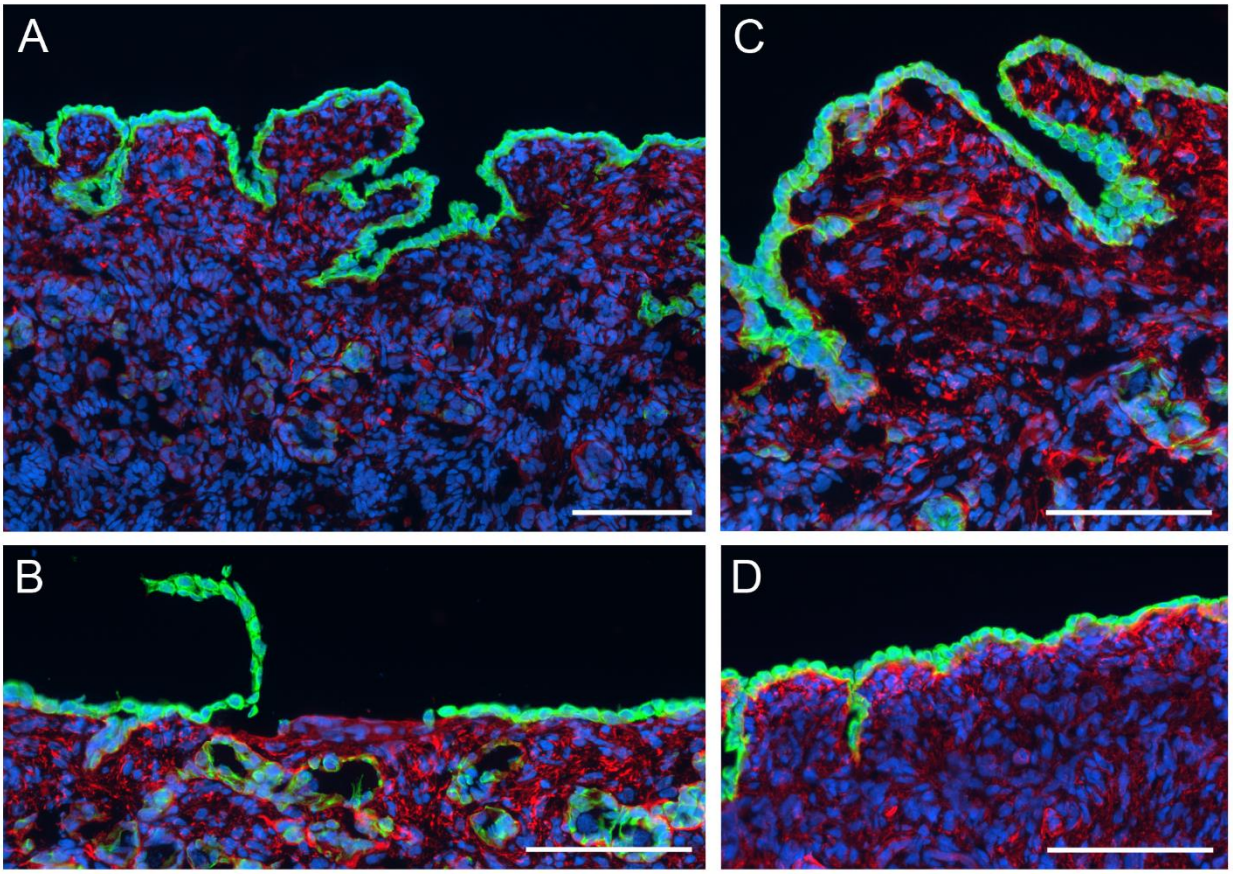

Figure 3. Fluorescence micrographs of the ovarian surface during late stages of development. (A) The surface of the late stage ovary remained uneven, showing folds and deep clefts. The surface epithelial cells stained strongly for CK19 (green). Below the surface epithelium, the stroma was now denser (red, stained for laminin 111) and had formed the tunica albuginea. (B) The surface epithelial cells were tightly connected with each other and easily shed as layer. (C) Even the fully developed ovary had areas with multi-layered surface epithelium, but most of the surface cover was (D) single layered. Nuclei were counterstained in blue. (A) 214 days, (B) and (C) 205 days and (D) 243 days of gestation. Scale bars: (A) – (D) 100 μm.

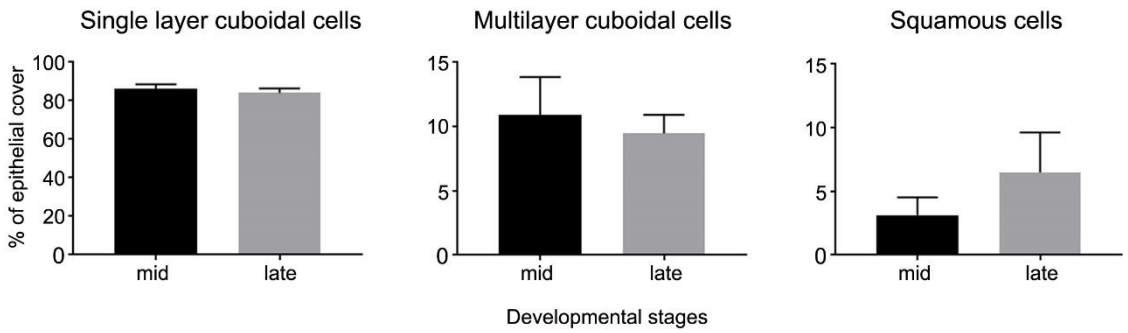

Figure 4. Morphometric analyses of the ovarian surface epithelial cells during bovine fetal development. Data are presented as mean ± s.e.m. Samples were grouped into two stages of ovarian development: mid (n = 4, 100-170 days of gestation) and late (n = 4, >170 days of gestation) stages. (A) The proportion of the area of the ovarian surface occupied by multilayer cuboidal epithelial cells, (B) The proportion of the area of the ovarian surface occupied by single-layered cuboidal epithelial cells and (C) The proportion of the area of the ovarian surface occupied by squamous epithelial cells. One-way ANOVA with post hoc Tuckey's tests were used to analyse the data.

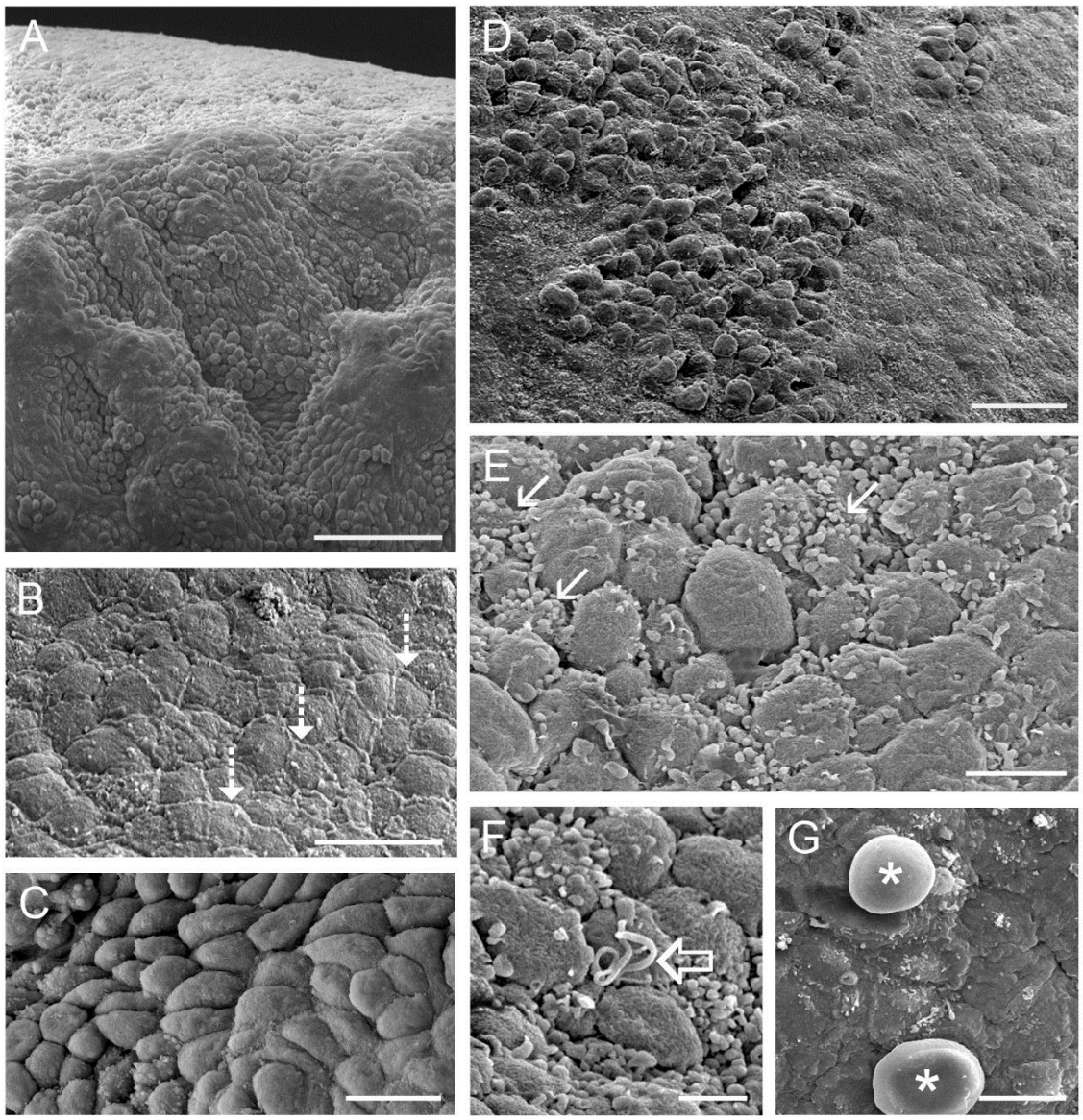

Figure 5. Scanning electron micrographs of the ovarian surface during early stages of development. (A) The surface of the developing ovary appeared uneven and furrowed. It was covered by areas of flattened cells (B), whose intercellular gaps were filled with extracellular matrix material (dotted arrow), and rounded cells (C) close to each other (D). The surface cells had microvilli (E, arrow) and single cilia (F, unfilled arrow). Sporadically, germ cells were visible on the surface (G, asterisk). (A), (C) and (G) 76 days, (B) and (D) 53 days, (E) and (F) 66 days of gestation. Scale bars: (A) 50 μm, (B) and (C) 10 μm, (D) 20 μm, (E) and (G) 5 μm, and (F) 2.5 μm.

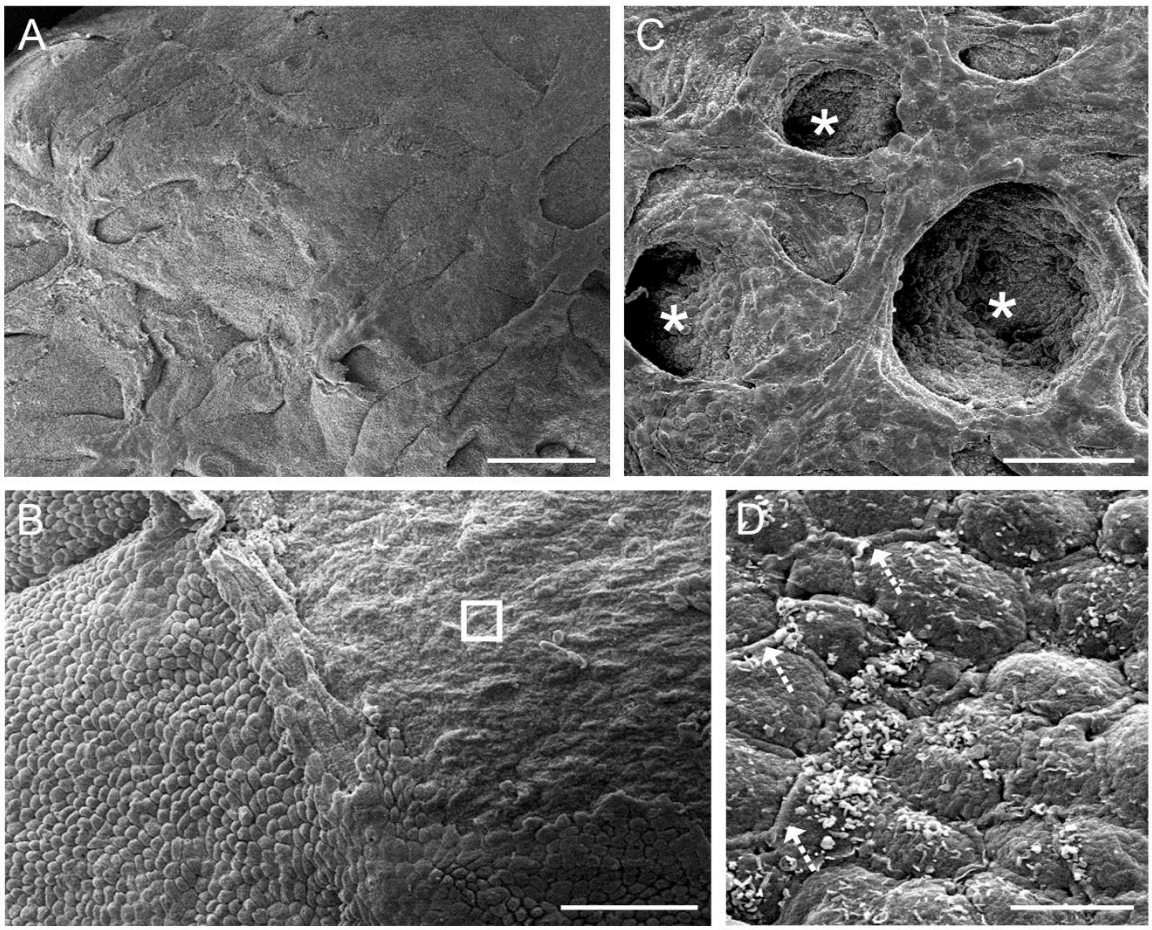

Figure 6. Scanning electron micrographs of the ovarian surface during mid stages of development. (A) The surface of the mid-stage ovary appeared more uneven than in the early stages, with tissue strands and furrows. (B) Most of the ovary was covered by rounded cells and, sporadically, denuded areas were visible (unfilled square). (C) Flat and deep clefts (asterisk) populated the surface. (D) Extracellular matrix material filled the gaps between cells (dotted line). (A) 144 days, (B) 107 days, (C) 124 days and (D) 101 days of gestation. Scale bars: (A) 200 μm, (B) and (C) 50 μm and (D) 5 μm.

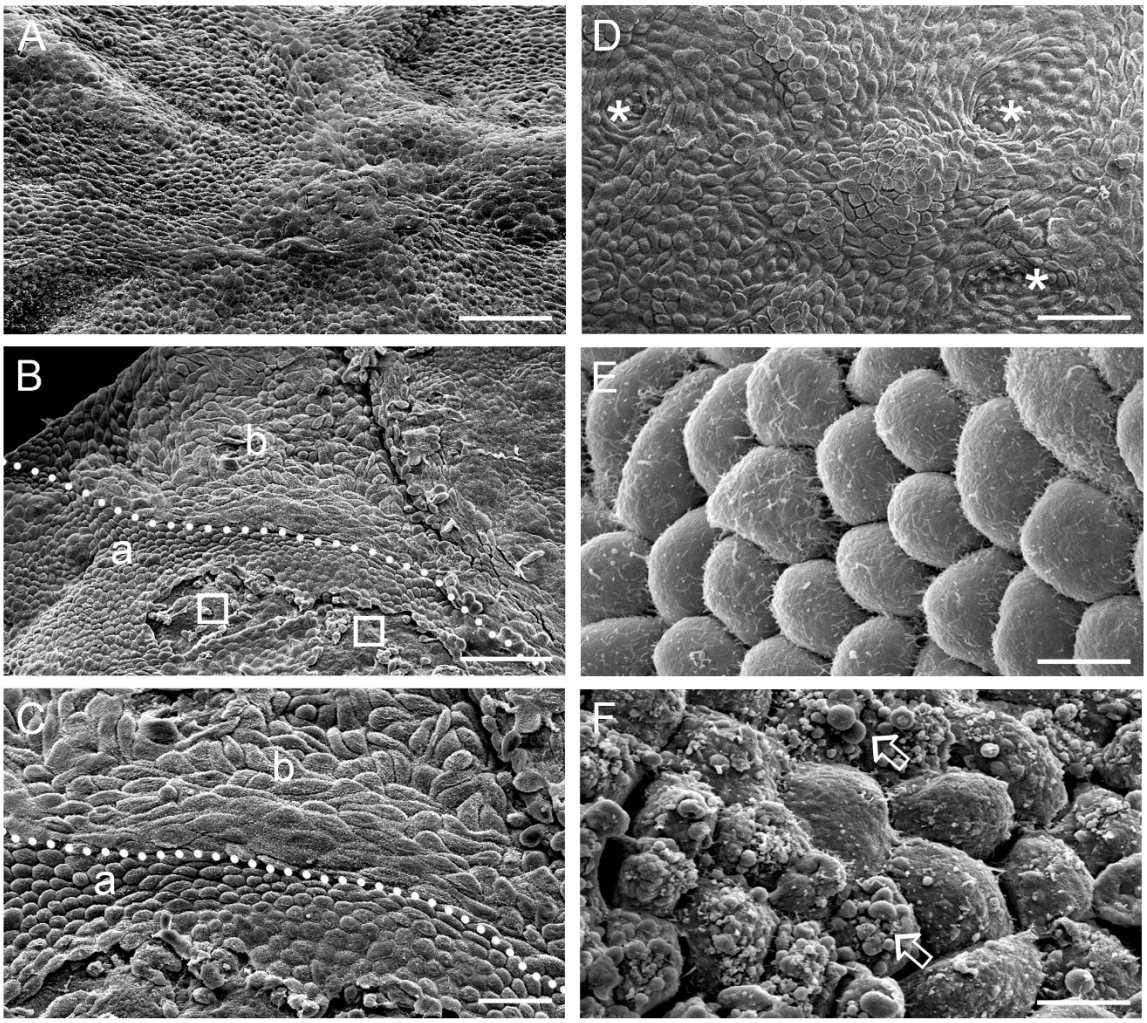

Figure 7. Scanning electron micrographs of ovarian surface during late stages of development. (A) There were fewer clefts/furrows covering the surface at the late stages. (B) The surface cells appeared to have different shapes, with areas with rounded cells (a) and more spindle-shaped cells (b). Denuded areas were sporadically visible (unfilled square). (C) Different cell shapes at higher magnification. (D) Shallow clefts were found in some areas. (E) Microvilli were visible on the surface of cells. (F) In some areas, the surface cells were covered by blebs (block arrow). (A) and (F) 214 days, (B) - (E) 243 days of gestation. Scale bars: (A), (B) and (D) 50 μm, (C) 20 μm, (E) and (F) 5 μm.

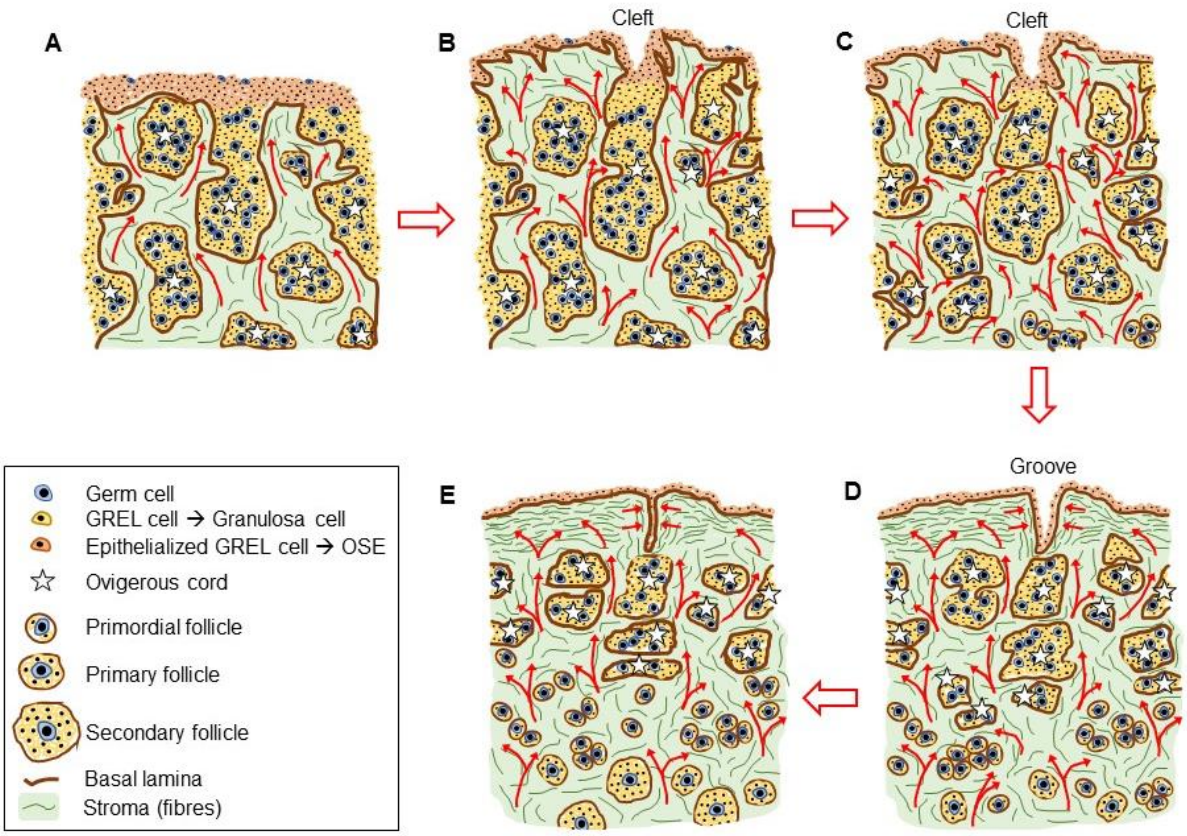

Figure 8. Schematic diagram showing the formation of clefts and grooves on the surface of the ovary. This diagram was assembled from the current data and that published previously (Hummitzsch et al. 2013). (A) GREL cells form the outermost layers of cells on the non-hilum surface of the ovary. Germ cells have migrated into the ovary and started proliferating. Penetrating stroma (arrows) originating from the mesonephros has penetrated the ovary and branched as it did so. This branching process gave rise to alternating areas of stroma and GREL cells/primordial germ cells, with the later known as ovigerous cords (*). (B) The penetrating stroma did not reach the surface of the ovary, rather, to just below it. It began to spread laterally below the surface, except where the ovigerous cords are open to the surface at this stage. The expansion of stroma surrounding open ovigerous cords (arrows) raised the surface surrounding the openings of ovigerous cords and thus created clefts, each with an opening of a cord at its base. (C) The continued expansion of the stroma leads to a single layer of GREL cells on the surface between the clefts. These cells have epithelized. GREL cells on the sides and bottom of the clefts are epithelized. (D) Continued expansion of the stroma compresses the clefts into the shapes of grooves. (E) Eventually the grooves become separated from the surface by the laterally spreading of stroma. This produces a structure similar to an inclusion cyst. What happens to these subsequently is not known but they are rare in adult ovaries.

Table 1. Surface characteristics of mid and late stages of bovine fetal ovaries.

Sample No.	Gestational age (days)	* Length of ovarian surface epithelium (mm)	* Length of single layered cuboidal cells (mm)	* Length of multilayered cuboidal cells (mm)	* Length of flat squamous cells (mm)
1	101	2.85	2.25	0.52	0.07
2	107	3.48	2.76	0.54	0.17
3	144	5.34	4.08	1.01	0.25
4	160	4.86	3.86	0.29	0.71
5	180	5.07	3.89	0.40	0.78
6	205	4.22	3.58	0.40	0.24
7	214	3.81	3.26	0.46	0.09
8	243	7.72	6.57	0.67	0.48

* Length is the perimenter of the ovary measured using a histologial cross section of the ovary.

Chapter VI:

General discussion and future research directions

6.1.General discussion

This thesis consists of four interconnected studies examining the development of the bovine fetal ovary and its potential links with reproductive disorders. The first study in this thesis identified the changes in stromal behaviour during bovine fetal ovary development. The second study connected the ovarian development with PCOS, one of the reproductive disorders in which the stroma in the adult ovary is grossly fibrous and extensive. The third study analysed the portrait of changes in GREL cells, granulosa cells and oogonium/oocytes during bovine fetal ovarian development. The last study described the changes to the ovarian surface during bovine fetal development, linking them with the remodelling of the stroma and ovigerous cords.

The important role of stroma during fetal ovarian development has been shown recently. It is believed that the stroma has critical roles in the formation of ovigerous cords, follicles, surface epithelium and tunica albuginea (Hummitzsch, et al. 2013). Early in the development of the ovary, the stroma from the mesonephros penetrates the developing ovary. It branches as it does so. The stroma continues to penetrate the ovary primordium towards the ovarian surface, grouping the primordial germ cells and some GREL cells into ovigerous cords. Once the stroma reaches to just below the surface of the ovary, it spreads laterally, causing the ovigerous cords to become smaller and eventually become follicles (Sarraj and Drummond 2012, Smith, et al. 2014). GREL cells on the ovarian surface then differentiate into surface epithelium and the stroma beneath the surface changes its phenotype into tunica albuginea (Hummitzsch, et al. 2013).

Morphometric analyses were used to analyse the developmental changes in the ovary. Since there is variation in the developmental stage between ovaries of the same age in cattle (Hummitzsch, et al. 2013), we grouped our bovine fetal ovaries into five different stages: Stage I, ovigerous cord formation; Stage II, ovigerous cord breakdown; Stage III, follicle formation; Stage IV, ovarian surface epithelium formation and Stage V, tunica albuginea formation. Using cortical stroma of bovine fetal ovaries, we were able to analyse the developing ovary morphometrically and demonstrate that the ovarian stroma expands throughout gestation and the expansion is at its greatest during early development, due to cell proliferation.

The movement of ovarian stroma during fetal development is believed to be regulated by many genes, such as fibrillin 1-3 (*FBN1-3*), *TGFB1-3*, decorin (*DCN*), and versican

(*VCAN*) (Hummitzsch, et al. 2013, Prodoehl, et al. 2009). To correlate the histological changes in the stroma with gene expression, we analysed 18 genes that are known to be correlated with the extracellular matrix, such as asporin (*ASPN*), biglycan (*BGN*), lumican (*LUM*), fibromodulin (*FMOD*), fibronectin (FN) and osteoglycin (*OGN*). These genes were highly expressed later in gestation and their expression levels correlated with each other, confirming our observation about stromal expansion during fetal ovarian development.

Abnormal stromal growth has been linked to reproductive disorders, such as PCOS (Abbott, et al. 2006, Li and Huang 2008). Working together with our international collaborators, we were able to show that most of the PCOS candidate genes studied in recent GWAS papers were expressed during fetal ovarian development. The expression levels of these genes can be categorised into 3 groups: early, late and constant expression. Our outcomes also suggested the possibility of TGFβ regulation in the expression of some of the PCOS candidate genes. TGFβ has been known to stimulate stromal expansion and collagen deposition. This study highlighted the possibility of predisposition to the development of the PCOS phenotype in adulthood arising during fetal development.

Using the cortical non-stromal area, consisting of germ cells, GREL cells and granulosa cells, and the same classification stages, we conducted a morphometric analysis and were able to describe how the volume of the non-stromal areas progressively increased during ovarian development, then levelled off during the formation of the surface epithelium. Additionally, the proportion of non-stromal areas in the ovarian cortex decreased throughout gestation. This could be due to an interruption in the growth of the non-stroma cells and the continued growth of stroma. Our study showed that the proliferation index in the non-stromal area was very high initially and then declined substantially at the time follicles formed, which is stage III of development. Thereafter, it remained low. This is consistent with the proliferation of oogonia, which occurs until 5 months of gestation in the human fetal ovary, the time when the primordial follicles begin to form at 90-140 days (Yang and Fortune 2008) and 126-133 days (Duffin, et al. 2009) of gestation in cattle and humans, respectively. The numerical density of the non-stromal cells was relatively constant throughout ovarian development.

In early ovarian development, proliferation of GREL cells is observed at the genital ridge at the ventral side of mesonephros (Hummitzsch, et al. 2013). At this stage, a true classical surface epithelium can only be seen at the base of the ovarian primordium, which is

really a protruding mesonephros. After the stroma reaches to just below the ovarian surface, the GREL cells on the surface differentiate into a classical surface epithelium, covering the rest of the fetal ovary (Hummitzsch, et al. 2013). In adult life, the ovarian surface consists of two different shapes of cells: cuboidal and squamous cells. It is believed that these two cell types have a critical role during the post-ovulation repair of ovarian surface (Flesken-Nikitin, et al. 2013, Ng, et al. 2014). We carefully examined the ovarian surface using SEM throughout fetal development and divided the samples into three groups: the early, mid and late stages of development. The early stage ovary has a group of cuboidal cells near the base of the ovary, whereas the rest of the ovarian surface has an irregular surface with invaginations. This is consistent with our previous finding that in early development, the developing ovary is not covered by a classical epithelium, except at the ovarian base. The rest of the ovarian surface consists of GREL cells and germ cells (Hummitzsch, et al. 2013). The mid stage ovarian surface consists of cuboidal cells near the base of the ovary, with involutions occurring across the rest of the ovarian surface. At this stage, the stroma has penetrated the developing ovary towards the ovarian surface and has enclosed some GREL cells and oogonia into ovigerous cords, which are open to the surface. Some GREL cells at the ovarian surface have commenced differentiating into a surface epithelium (Hummitzsch, et al. 2013). It has been suggested that the stroma has an important role in the formation of the ovarian surface epithelium. We believe that the involutions represent the open ovigerous cords and the protrusions around the involutions represent the areas where the stroma has penetrated to just below the ovarian surface, as shown in our immunohistochemistry of ovarian cross sections. At a late stage, the ovarian surface consisted of two types of cells: cuboidal cells and squamous cells. Involutions were still observed in this stage, however, they were wider and the invaginations deeper than the mid stage ovarian surface, as shown by our immunohistochemistry.

The ovarian surface epithelium consists of two different shapes of cell: cuboidal and squamous cells. In the human fetal ovary, the surface epithelium is observed to be changed from a flat to a cuboidal simple epithelium at around 10-20 weeks of gestation (Motta, et al. 1997). Our immunohistochemistry results showed that mid and late stage ovaries consist of multi and single layered cuboidal cells, as well as single layered squamous cells. Although we did not find any significant differences between mid and late stage ovaries, we observed that late stage ovaries had more areas with squamous cells when compared with mid stage

ovaries. This could be due to the different stages of the follicles in the cortex of the late stage ovary and might be related to preparation for the ovulation process in the adult ovary.

Collectively, this thesis provides further evidence of the importance of stromal changes during fetal ovarian development. Additionally, this thesis substantiates a linkage between PCOS-candidate genes and ovarian development and this could improve our understanding of the origin(s) of PCOS. The outcomes of this thesis provide a foundation for promising future research directions, highlighting that understanding fetal ovary development is imperative.

6.2. Future Directions

This thesis offers outcomes that can be used to inform future studies related to ovarian development. It is clearly shown that the stroma has a critical role in the development of the ovary. Investigating the function and mechanism of stromal related genes during fetal ovarian development is imperative, given the growing evidence about the important of stroma in the formation of ovigerous cords, follicles, surface epithelium and tunica albuginea.

Analysing the PCOS candidate genes during fetal ovarian development is also important. We have shown that some PCOS candidate genes were highly expressed during early ovarian development, the time when the stromal development is observed to be at its greatest. One of these genes is HMGA2, which was recently shown to affect leanness in pigs (Chung, et al. 2018), suggesting that HMGA2 might be related to the proliferation of pre-adipocytes cells. One of PCOS' complications is obesity, reported in 61 to 76% of patients with PCOS in the United States and Australia (Fauser, et al. 2012). Future research should examine the role and regulation of this gene further in the fetal ovary.

Recently, THADA has been shown to be an important cause of obesity. A knockout THADA study in *Drosophila* found that THADA knockout mutants were characterised by obesity and reduced thermogenesis, as well as a higher lipid storage in fat body compared to wild type (Moraru, et al. 2017). It will be interesting to study this gene analysing its role and regulation in the fetal ovary, as well as in the adult PCOS ovary and fat cells.

Recent studies have linked PCOS with inflammation. Women with PCOS have higher levels of inflammatory cytokines (IL6, IL18, and TNF alpha) and Th1 subsets (Al-Musawy, et al. 2018, Qin, et al. 2016). TOX has been shown to play a critical role in the development of the immune system (Aliahmad, et al. 2010, Aliahmad and Kaye 2008, Aliahmad, et al.

2012). We also observed that TOX3 was highly expressed at the time the ovarian stroma penetrates the developing ovary, suggesting that TOX3 might be related to stromal behaviour during ovarian development. It would be interesting to study the role and regulation of TOX3 further, especially in the ovarian stroma where immune cells reside.

The adult ovarian surface changes its morphology and this is thought to be related to the ovulation process. Our observations on the fetal ovarian surface suggest a role of stroma in the formation of the ovarian surface epithelium. The fetal ovarian surface epithelium is believed to originate from the mesonephric epithelium at the base of the ovary and from GREL cells for the rest of the ovarian surface. Future study should target the relationship between stromal expansion and surface epithelial morphology.

6.3. References

Abbott, DH, V Padmanabhan, and DA Dumesic 2006 Contributions of androgen and estrogen to fetal programming of ovarian dysfunction. *Reprod Biol Endocrinol* **4** 17.

Al-Musawy, S, I Al-Saimary, and M Flaifil 2018 Levels of cytokines profile in polycystic ovary syndrome. *Medical Journal of Babylon* **15** 124-128.

Aliahmad, P, B de la Torre, and J Kaye 2010 Shared dependence on the DNA-binding factor TOX for the development of lymphoid tissue-inducer cell and NK cell lineages. *Nat Immunol* **11** 945-952.

Aliahmad, P, and J Kaye 2008 Development of all CD4 T lineages requires nuclear factor TOX. *J Exp Med* **205** 245-256.

Aliahmad, P, A Seksenyan, and J Kaye 2012 The many roles of TOX in the immune system. *Current opinion in immunology* **24** 173-177.

Chung, J, X Zhang, B Collins, RB Sper, K Gleason, S Simpson, S Koh, J Sommer, WL Flowers, RM Petters, and JA Piedrahita 2018 High mobility group A2 (HMGA2) deficiency in pigs leads to dwarfism, abnormal fetal resource allocation, and cryptorchidism. *Proc Natl Acad Sci U S A* **115** 5420-5425.

Duffin, K, RA Bayne, AJ Childs, C Collins, and RA Anderson 2009 The forkhead transcription factor FOXL2 is expressed in somatic cells of the human ovary prior to follicle formation. *Mol Hum Reprod* **15** 771-777.

Fauser, BC, BC Tarlatzis, RW Rebar, RS Legro, AH Balen, R Lobo, E Carmina, J Chang, BO Yildiz, JS Laven, J Boivin, F Petraglia, CN Wijeyeratne, RJ Norman, A Dunaif, S Franks, RA Wild, D Dumesic, and K Barnhart 2012 Consensus on women's health aspects of polycystic ovary syndrome (PCOS): the Amsterdam ESHRE/ASRM-Sponsored 3rd PCOS Consensus Workshop Group. *Fertil Steril* **97** 28-38 e25.

Flesken-Nikitin, A, CI Hwang, CY Cheng, TV Michurina, G Enikolopov, and AY Nikitin 2013 Ovarian surface epithelium at the junction area contains a cancer-prone stem cell niche. *Nature* **495** 241-245.

Hummitzsch, K, HF Irving-Rodgers, N Hatzirodos, W Bonner, L Sabatier, DP Reinhardt, Y Sado, Y Ninomiya, D Wilhelm, and RJ Rodgers 2013 A new model of development of the mammalian ovary and follicles. *PLoS One* **8** e55578.

Li, Z, and H Huang 2008 Epigenetic abnormality: a possible mechanism underlying the fetal origin of polycystic ovary syndrome. *Med Hypotheses* **70** 638-642.

Moraru, A, G Cakan-Akdogan, K Strassburger, M Males, S Mueller, M Jabs, M Muelleder, M Frejno, BP Braeckman, M Ralser, and AA Teleman 2017 THADA Regulates the Organismal Balance between Energy Storage and Heat Production. *Developmental cell* **41** 72-81.e76.

Motta, PM, S Makabe, and SA Nottola 1997 The ultrastructure of human reproduction. I. The natural history of the female germ cell: origin, migration and differentiation inside the developing ovary. *Hum Reprod Update* **3** 281-295.

Ng, A, S Tan, G Singh, P Rizk, Y Swathi, TZ Tan, RY Huang, M Leushacke, and N Barker 2014 Lgr5 marks stem/progenitor cells in ovary and tubal epithelia. *Nat Cell Biol* **16** 745-757.

Prodoehl, MJ, HF Irving-Rodgers, WM Bonner, TM Sullivan, GC Micke, MA Gibson, VE Perry, and RJ Rodgers 2009 Fibrillins and latent TGFbeta binding proteins in bovine ovaries of offspring following high or low protein diets during pregnancy of dams. *Mol Cell Endocrinol* **307** 133-141.

Qin, L, W Xu, X Li, W Meng, L Hu, Z Luo, Y Wang, S Luo, and S Li 2016 Differential Expression Profile of Immunological Cytokines in Local Ovary in Patients with Polycystic Ovarian Syndrome: analysis by Flow Cytometry. *European Journal of Obstetrics and Gynecology and Reproductive Biology* **197** 136-141.

Sarraj, MA, and AE Drummond 2012 Mammalian foetal ovarian development: consequences for health and disease. *Reproduction* **143** 151-163.

Smith, P, D Wilhelm, and RJ Rodgers 2014 Development of mammalian ovary. *J Endocrinol* **221** R145-161.

Yang, MY, and JE Fortune 2008 The capacity of primordial follicles in fetal bovine ovaries to initiate growth in vitro develops during mid-gestation and is associated with meiotic arrest of oocytes. *Biol Reprod* **78** 1153-1161.

Chapter VII:

Concluding remarks

Concluding remarks

This present thesis highlights the critical role of stroma during fetal ovarian development, especially in the formation of ovarian surface epithelium as well as the fetal predisposition of PCOS. However, there are many aspects that still need to be investigated, such as the factors that regulate the differentiation of GREL cells into surface epithelial cells and its relationship with stromal penetration. The discovery of advance technology in genetic and molecular biology provides the possibility of revealing the complex process of gene expression and regulation during fetal ovarian development. The ultimate goals would be to determine and understand the underlying mechanism of fetal ovarian development to understand the pathogenesis of reproductive disorders, such as PCOS, leading to the discovery of screening and prevention methods.